UAB
Universitat Autònoma de Barcelona

IMMUNE CHARACTERIZATION OF MULTISYSTEM INFLAMMATORY SYNDROME IN CHILDREN (MIS-C)

Tetyana Pidkova

ADVERTIMENT. L'accés als continguts d'aquesta tesi queda condicionat a l'acceptació de les condicions d'ús establertes per la següent llicència Creative Commons: https://creativecommons.org/licenses/?lang=ca

ADVERTENCIA. El acceso a los contenidos de esta tesis queda condicionado a la aceptación de las condiciones de uso establecidas por la siguiente licencia Creative Commons: https://creativecommons.org/licenses/?lang=es

WARNING. The access to the contents of this doctoral thesis it is limited to the acceptance of the use conditions set by the following Creative Commons license: https://creativecommons.org/licenses/?lang=en

UAB
Universitat Autònoma
de Barcelona

IMMUNE CHARACTERIZATION OF MULTISYSTEM INFLAMMATORY SYNDROME IN CHILDREN (MIS-C)

Tetyana Pidkova

PhD programme in Advanced Immunology
Department of Cellular Biology, Physiology, and Immunology
Universitat Autònoma de Barcelona

IMMUNE CHARACTERIZATION OF MULTISYSTEM INFLAMMATORY SYNDROME IN CHILDREN (MIS-C)

Thesis presented by Tetyana Pidkova to qualify for the PhD degree in Advanced Immunology by the Universitat Autònoma de Barcelona.

The presented work has been performed in the Cell Virology and Immunology (VIC) group, at IrsiCaixa, directed by Dr Julià Blanco Arbués and Dr Benjamin Trinité, and tutored by Dr Julià Blanco Arbués.

Tetyana Pidkova	Julià Blanco Arbués, PhD	Benjamin Trinité, PhD
PhD candidate	Thesis director & tutor	Thesis director

Badalona, June 2026

The author of this thesis has been supported by a predoctoral grant from the Fundació Autònoma Solidària, Programa Acollida (Universitat Autònoma de Barcelona).

Unrelated to this work, Dr. Julià Blanco Arbués is founder and shareholder of the spin-off AlbaJuna Therapeutics S.L and reports institutional grants from HIPRA and MSD. The author of this thesis declares no conflicts of interest.

The printing of this thesis was fully funded by Fundació Privada Institut de Recerca sobre Immunopatologies-Caixa IrsiCaixa.

Images and graphs were created using Biorender, R or GraphPad Prism.

El Dr. Julià Blanco Arbués, investigador d'IrsiCaixa, de la Fundació Institut d'Investigació en Ciències de la Salut Germans Trias i Pujol (IGTP), del CIBERINFEC i professor de la Universitat de Vi-Universitat Central de Catalunya, i el Dr. Benjamin Trinité, investigador d'IrsiCaixa,

fan constar

que el treball experimental i la redacció de la memòria de la Tesi Doctoral titulada "**IMMUNE CHARACTERIZATION OF MULTISYSTEM INFLAMMATORY SYNDROME IN CHILDREN (MIS-C)**" han estat realitzats per la Tetyana Pidkova sota llur direcció, i que

consideren

que és apte per a ser presentat i optar al grau de Doctora en Immunologia Avançada per la Universitat Autònoma de Barcelona.

I per que quedi constància, signen aquest document a

Badalona, el 30 de juny de 2026

Dr. Julià Blanco Arbués **Dr. Benjamin Trinité**

«Сміливі завжди мають щастя».

— Іван Багряний, «Тигролови»

Acknowledgments

First, I would like to express my deepest gratitude to my thesis directors, Ben and Julià. Throughout this journey, you have been an enormous source of support and guidance, helping me believe in myself as a scientist. I could not have dreamed of better mentors, and I truly believe that all of us in the VIC team are very lucky to have you both. Julià, although my arrival was like "unexpected child", you welcomed me into the VIC family with huge kindness and made me feel part of the team from the very beginning. Your unconditional support, kindness, and trust on me have meant so much to me, as has your unforgettable fig jam. Ben, thanks a lot for your patience in explaining things repeatedly when needed. Thank you for all the knowledge you shared with me, for your unfailing dedication, and for always being there whenever I needed help or advice, whether it was related to work or personal. Also, for teaching me that good results come with patience, and, of course, for always being my coffee supporter.

També voldria agrair a Ventura l'oportunitat de formar part d'IrsiCaixa i el fet d'haver estat sempre disponible quan he necessitat ajuda. Un agraïment especial a la Lidia i la Lourdes, que em van cuidar des del principi i em van fer sentir acompanyada durant tot aquest procés. També a l'Alejandro i la Judith, per gestionar tots els meus problemes burocràtics.

A huge thanks goes to all the VIC people who made my PhD and laboratory experience warm and full of good memories: Francesc, Carmen, Carla, Edwards, Ferran T., Anna B., Raquel, and Esther, whose positive energy can motivate everyone around her. To Víctor, whom I probably made very tired with all my analyses, but without whom my work would not look nearly as amazing. Un agradecimiento muy especial a Silvia, quien siempre estuvo ahí para cuidarme en esos pequeños detalles que, en realidad, son muy importantes. To Júlia, my desk companion, with whom I could talk about everything and nothing. Huge thanks to my Annas for guiding me through the "catalanization" and for becoming such great and reliable friends. To Amaya, my soulmate, who, despite coming from faraway origins, shares so much in common with me. Ferran deserves a special line here for the valuable contribution he made to this thesis, for his help, patience, and support, even while writing his own.

Special thanks to Sara for our morning routines and for making every day at IrsiCaixa brighter. I also do not want to forget Gooya and Maria, who were also part of this important chapter. And to all the PhD students with whom I shared this meaningful path.

A huge thank you also goes to Itziar and Nuria, who helped me overcome my doubts and made me believe that I truly belong as a scientist. An additional thank you to Itziar for turning on Spice Girls during my P3 work just to make me happier, and to everyone who supported me throughout my laboratory adventures.

And finally, thanks to all the IrsiCaixa people from whom I ever asked for milk for my coffee. There were many of you, and I am very grateful.

I would also like to thank the ISGlobal team, Ruth, Marta, Carlota, Gemma, and Diana, for their valuable contribution to our research. A special thank you to Marta, who taught me so much and with whom I share much in common.

I would also like to thank the SJD team, Rosa and Claudia, without whom this project would not have been possible. Thank you for your help and dedication throughout these four years, and for being an important part of this work. I am also very grateful to Jordi and his team for providing the samples and for always being available whenever questions arose.

Звісно, без моєї мами я б не була тією, ким є сьогодні. Я безмежно вдячна тобі за кожне рішення,яке ти приймала, щоб я виросла саме такою якою я. Дякую за твою підтримку, любов і віру в мене, а також за те, що ти завжди підтримувала мене у всіх моїх рішеннях, навіть тоді, коли шлях був непростим. Окрема подяка дідові Васі. Без нього я б не змогла досягти багатьох своїх звершень, адже саме він казав, що треба прагнути кращого, не зупинятися на досягнутому і ставати кращою версією себе. Також я хочу подякувати Андрію за його самовідданість, доброту і постійну присутність і турботу протягом усіх років моїх безкінечних навчань. Я вас дуже люблю і вдячна вам більше, ніж можуть висловити слова.

Finalment, voldria donar les gràcies a la meva família catalana — Ferran, Elena, Miquel, Mar i Mel — amb qui aquest capítol temporal, anomenat “doctorat a Barcelona”, es va convertir en una segona llar permanent. Gràcies per acollir-me, donar-me suport i fer-me sentir estimada aquí. Us estimo molt i us agraeixo més del que les paraules poden expressar.

Моїм друзям — Славі, Назару, Вікторії, Міці, Марті, Леву й Анничці — дякую за те, що попри відстань ви завжди залишалися поруч. Ваша дружба допомагали мені відчувати дім навіть далеко від нього. Звісно, я також хочу подякувати моїм кумам — Галі та Віталіку — і маленькому Маркусику, які стали для мене важливою частинкою України далеко від дому.

Als meus amics catalans, gràcies per haver esdevingut una part tan important del meu sentiment de confort, pertinença i certesa que era exactament on havia de ser: a la Judith i el Ferran; al Jordi i la Júlia; l’Ainoa i el Miquel; i a l’Estella, la Laia.

Us ho agraeixo molt! Una abraçada.

Abbreviations

ACE2	Angiotensin-converting enzyme 2
ADCC	Antibody-dependent cellular cytotoxicity
ALC	Absolute lymphocyte count
ALT	Alanine aminotransferase
AST	Aspartate aminotransferase
C-GAS / cGAS	Cyclic GMP-AMP synthase
CC	Convalescent COVID-19
CCL	C-C motif chemokine ligand
CD	Cluster of differentiation
CD40L	CD40 ligand
CD8α	CD8 alpha chain
CDC	Centers for Disease Control and Prevention
CDCP1	CUB domain-containing protein 1
COVID-19	Coronavirus disease 2019
CRP	C-reactive protein
CX3CL	C-X3-C motif chemokine ligand; fractalkine
CX3CR	C-X3-C motif chemokine receptor
CXCL	C-X-C motif chemokine ligand
DCs	Dendritic cells
DNA	Deoxyribonucleic acid
DNER	Delta/Notch-like epidermal growth factor-related receptor
EBV	Epstein-Barr virus
ECMO	Extracorporeal membrane oxygenation
EN-RAGE	Extracellular newly identified RAGE-binding protein; S100A12
ENE-COVID	Spanish National Seroepidemiological Study of SARS-CoV-2 Infection
ESR	Erythrocyte sedimentation rate
EULAR/ACR	European League Against Rheumatism / American College of Rheumatology
PRINTO	Paediatric Rheumatology International Trials Organisation
Fc	Fragment crystallizable region
FlexMAP	Luminex/FlexMAP multiplex assay platform
g/dL	Grams per deciliter
GISAID	Global Initiative on Sharing All Influenza Data
hACE2	Human angiotensin-converting enzyme 2
Hb	Hemoglobin
HC	Healthy children
HCoV	Human coronavirus
HEK293T	Human embryonic kidney 293T cell line
HGF	Hepatocyte growth factor
HIV-1	Human immunodeficiency virus type 1
HLH	Hemophagocytic lymphohistiocytosis
IC50	Half-maximal inhibitory concentration

ICU	Intensive care unit
ID50	50% inhibitory dilution
IDSA	Infectious Diseases Society of America
IFN	Interferon
Ig	Immunoglobulin
IL	Interleukin
IL22RA2	Interleukin 22 receptor subunit alpha 2
IQR	Interquartile range
ISCIII	Instituto de Salud Carlos III
ISGlobal	Barcelona Institute for Global Health
IVIG	Intravenous immunoglobulin
JIA	Juvenile idiopathic arthritis
KD	Kawasaki disease
LAP TGF-β1	Latency-associated peptide of transforming growth factor beta 1
LDG	Lactate dehydrogenase; likely document variant/typo of LDH
LDH	Lactate dehydrogenase
LLOQ	Lower limit of quantification
LVEF	Left ventricular ejection fraction
LYST	Lysosomal trafficking regulator
MAS	Macrophage activation syndrome
MCP-1, -2, -3	Monocyte chemoattractant protein 1, 2, 3
MERS-CoV	Middle East respiratory syndrome coronavirus
MFI	Median fluorescence intensity
mg/dL	Milligrams per deciliter
mg/kg	Milligrams per kilogram
MHC	Major histocompatibility complex
microg/L	Micrograms per liter
MIS	Multisystem inflammatory syndrome
MIS-A	MIS in adults
MIS-C	MIS syndrome in children
MIS-N	MIS in neonates
MIS-V	MIS after vaccination
MMP	Matrix metalloproteinase
mRNA	Messenger ribonucleic acid
NAAT	Nucleic acid amplification test
NETs	Neutrophil extracellular traps
NF-κB	Nuclear factor kappa-light-chain-enhancer of activated B cells
ng/L	Nanograms per liter
ng/mL	Nanograms per milliliter
NIBSC	National Institute for Biological Standards and Control
NK	Natural killer
NPX	Normalized Protein eXpression
NSP	Non-structural protein
NT-3	Neurotrophin 3
NT-proBNP	N-terminal prohormone of brain natriuretic peptide

NTD	N-terminal domain
OOB	Out-of-bag
ORF	Open reading frame
OSI	Organ system involvement
OSM	Oncostatin M
p-value	Probability value
PBS	Phosphate-buffered saline
PCA	Principal component analysis
PCC	Post-COVID-19 condition
PCR	Polymerase chain reaction
PCT	Procalcitonin
PD-L1	Programmed death-ligand 1
PE	Phycoerythrin
PEA	Proximity extension assay
pH	Potential of hydrogen
PICU	Pediatric intensive care unit
PIMS-TS	Pediatric inflammatory multisystem syndrome temporally associated with SARS-CoV-2
pp1a, b	Polyprotein 1a, b
PRR	Pattern-recognition receptor
PT	Prothrombin time
PTT	Partial thromboplastin time
qPCR	Quantitative PCR
RBD	Receptor-binding domain
RCPCH	Royal College of Paediatrics and Child Health
RENAVE	Red Nacional de Vigilancia Epidemiológica
RNA	Ribonucleic acid
RNase L	Ribonuclease L
rpm	Revolutions per minute
RT-qPCR	Reverse transcription quantitative PCR
S	Spike protein
S1/S2	Spike protein subunits 1 and 2
SARS-CoV	Severe acute respiratory syndrome coronavirus
SARS-CoV-2	Severe acute respiratory syndrome coronavirus 2
SCF	Stem cell factor
SctΔ19	SARS-CoV-2 spike construct with 19-amino-acid cytoplasmic tail deletion
SD	Still disease
sJIA	Systemic juvenile idiopathic arthritis
STING	Stimulator of interferon genes
STRING	Search Tool for the Retrieval of Interacting Genes/Proteins database
TCID50	50% tissue culture infectious dose
TCR	T-cell receptor
TGF-β	Transforming growth factor beta
Th1, 2	T helper 1, 2
TLR	Toll-like receptor

TMEM154	Transmembrane protein 154
TMPRSS2	Transmembrane serine protease 2
TNF	Tumor necrosis factor
TNFRSF9	TNF receptor superfamily member 9
TRANCE	TNF-related activation-induced cytokine
TRBV11-2	T-cell receptor beta variable 11-2
TWEAK	TNF-related weak inducer of apoptosis
U/L	Units per liter
ULOQ	Upper limit of quantification
Vβ21.3	T-cell receptor beta variable 21.3
VCAp18	Epstein-Barr virus viral capsid antigen p18
VEGF	Vascular endothelial growth factor
VIC	Cell Virology and Immunology group
VOC	Variant of concern
VSV-G	Vesicular stomatitis virus glycoprotein
WHO	World Health Organization
xMAP	Multi-analyte profiling technology
xPONENT	Luminex data acquisition/analysis software
ZEBRA	BamHI Z Epstein-Barr replication activator
µg/mL	Micrograms per milliliter

Table of contents

SUMMARY **21**

INTRODUCTION **29**

Overview of COVID-19 pandemic **31**

1. SARS-CoV-2 virology 32
   - 1.1. The virion 32
   - 1.2. Viral entry 34
2. Immune Response (Adults vs Children) 36
   - 2.1. Innate immune response 36
   - 2.2. Adaptive immune response 38
3. Genetic evolution and variants of SARS-CoV-2 43
4. Immune escape 45
5. Immune imprinting and hybrid immunity 46
6. Epidemiology in Spain 47
7. Acute disease in adults and children 49
8. Clinical management and long-term consequences of COVID-19 51
   - 8.1. Diagnosis 51
   - 8.2. Treatment 52
   - 8.3. Vaccines 54
   - 8.4. Post COVID-19 condition (long COVID) 55

Multisystem inflammatory syndrome after SARS-CoV-2 ..... **57**

9. Multisystem inflammatory syndrome in neonates 57
10. Multisystem inflammatory syndrome in adults 59
11. Multisystem inflammatory syndrome after SARS-CoV-2 vaccination 60
12. Multisystem inflammatory syndrome in children 61
    - 12.1. Case definition 61
    - 12.2. Risk factors 64
    - 12.3. Epidemiology 65

13. Elements of Pathogenesis of MIS-C 67
13.1. Innate response 67
13.2. Cellular response 68
13.3. Humoral response 69
13.4. The main current hypotheses for the origine of MIS-C pathogenesis 69
13.5. The Role of the Immune System in the Change in MIS-C Epidemiology ... 72

14. Diagnostic comparison with the pediatric inflammatory conditions 74
14.1. Other inflammatory conditions 74
14.2. Challenges of diagnostic criteria 76

15. Clinical management 78
15.1. Initial therapy 78
15.2. Advanced therapy 80

HYPOTHESES AND OBJECTIVES 81

METHODS 87

1. Study cohort 89
1.1. Study Approval 89
1.2. Sample processing and storage 89
1.3. Cohort description 89

2. Total antibody quantification 91
3. Neutralization activity 92
4. Measurement of antigen-specific antibodies 94
5. Proteomic analysis of inflammatory biomarkers 96
6. Statistical analysis 97

RESULTS 101

1. Cohort description 103
1.1. Convalescent COVID-19 103
1.2. Participants COVID-19 onset distribution 104
1.3. Healthy children participants 105
1.4. MIS-C participants 105
1.5. Kawasaki disease participants 109
1.6. Still disease participants 110
1.7. Total immunoglobulin levels 113

2. Humoral response in MIS-C and CC 114

2.1. SARS-CoV-2-specific humoral immune responses 114
2.2. Neutralizing anti-SARS-CoV-2 humoral immune responses 115
2.3. SARS-CoV-2-specific IgA and IgG subclasses 118
2.4. Antibody isotype/Subclass ratios 120
2.5. Correlation analysis of SARS-CoV-2-specific markers 122
2.6. Biomarker selection and participants classification 124

3. Characterization of the antibody reactivity against common cold coronaviruses and EBV in MIS-C, KD, and control groups. 127

3.1. Humoral responses against common cold coronaviruses 127
3.2. Humoral responses against Epstein–Barr virus 132
3.3. Biomarker selection and participants classification 133

4. Inflammatory response associated with MIS-C 138

4.1. Inflammatory biomarkers associated with acute MIS-C 138
4.2. Severity-associated inflammatory biomarkers in MIS-C 143
4.3. Co-associations between inflammatory biomarkers and clinical parameters in MIS-C 146
4.4. Longitudinal Stabilization of Biomarker Profiles Post-MIS-C Treatment .148

5. Comparative inflammatory profiling of MIS-C, Kawasaki disease, and childhood-onset Still's disease 150

5.1. Inflammatory biomarkers of the acute phase of MIS-C, SD, and KD 150
5.2. Inflammatory biomarkers differentiating MIS-C, SD, and KD 154
5.3. Pairwise associations within top inflammatory biomarkers and clinical parameters. 158

DISCUSSION 161

CONCLUSIONS 177

BIBLIOGRAPHY 181

ANNEX 208

SUMMARY

Although acute COVID-19 is usually milder in children than in adults, a small proportion of pediatric patients develop Multisystem Inflammatory Syndrome in Children (MIS-C), a severe post-infectious hyperinflammatory condition that appears several weeks after infection. So far, the immune mechanisms underlying MIS-C remain incompletely understood.

We hypothesized that MIS-C results from an altered immune response after SARS-CoV-2 infection, characterized by changes in antibody responses and a specific inflammatory biomarker profile. This work aimed to characterize humoral and inflammatory immune responses in untreated acute MIS-C, using convalescent COVID-19 (CC) children as a matched control group. MIS-C was also compared with Kawasaki disease (KD) and Still's disease (SD) to identify shared and disease-specific inflammatory signatures. MIS-C patients were followed at 2 and 18 months.

We analyzed immunoglobulin isotypes, and IgG and IgA subclass usage of antigen-specific SARS-CoV-2 responses using Luminex, along with their neutralizing activity. Antibody reactivity against common cold coronaviruses and EBV was also assessed. Olink-based profiling was used to characterize inflammatory signatures, severity-associated biomarkers, and longitudinal changes.

MIS-C patients showed antibody levels and neutralizing activity largely comparable to CC children, but with clear differences in antibody isotype and subclass distribution. MIS-C was characterized by increased SARS-CoV-2-specific IgG2 responses, generally lower IgG3 responses except against S2, and increased S2-specific IgA, IgA1, and IgA2 responses. These findings suggest selective dysregulation of class-switching in humoral immunity. Differences in the contribution of IgA responses to the neutralizing antibody profile were also observed compared with CC.

Common cold coronavirus antibody responses were increased in both MIS-C and CC children, suggesting cross-reactivity. MIS-C patients also showed increased EBV ZEBRA-specific IgG2, IgG3, and IgG4 responses, suggesting possible EBV reactivation-associated humoral responses.

Inflammatory analysis showed that MIS-C has a distinct soluble biomarker profile compared with CC children, characterized by IFN-γ-related chemokines, endothelial activation, immune-cell recruitment, and systemic inflammation. Several biomarkers, including soluble TNFRSF9, soluble CD8α, IL-33, IL-2, CD244, and SCF, were associated with ICU admission or more severe presentation. Longitudinal follow-up showed that this profile normalized after recovery, with biomarker levels comparable to CC children at 2 and 18 months.

Comparison of MIS-C with KD and SD showed shared inflammatory and vascular pathways but also distinct immune signatures. MIS-C is characterized by an IFNy signature, while KD was characterized by markers linked to vascular inflammation and remodeling, and SD showed a strong IL-18/IL-6-associated autoinflammatory pattern.

In conclusion, data suggests that MIS-C is a distinct post-infectious immune syndrome characterized by altered humoral immunity and a transient but intense inflammatory response. The findings highlight selective antibody subclass dysregulation, increased responses to EBV reactivation-associated antigens, IFN-γ-driven endothelial inflammation, and severity-associated soluble biomarkers as features of MIS-C immunopathology.

RESUM

Tot i que la COVID-19 és més lleu en infants que en adults, una petita proporció de pacients pediàtrics desenvolupa la Síndrome Inflamatòria Multisistèmica en Infants (MIS-C), una condició hiperinflamatòria postinfecciosa greu que apareix setmanes després de la infecció. Fins ara, els mecanismes immmunològics del MIS-C no han estat completament definits.

Hipotetizant que el MIS-C deriva d'una resposta immunitària alterada després de la infecció per SARS-CoV-2, amb canvis en les respostes d'anticossos i un perfil inflamatori específic; en aquest treball hem caracteritzat les respostes humorals i inflamatòries en MIS-C, utilitzant infants recuperats de COVID-19 (CC) com a control. També es comprà el MIS-C amb la malaltia de Kawasaki (KD) i la malaltia de Still (SD), i es va seguir un subgrup de pacients amb MIS-C als 2 i 18 mesos.

Mitjançant Luminex, es van analitzar diferents isotips d'immunoglobulines i llurs subclases contra antígens de SARS-CoV-2, incloent-hi l'anàlisi de la capacitat de neutralització. També es va estudiar la reactivitat contra coronavirus del refredat comú i EBV. MItjançant Olink es caracteritzaren les signatures inflamatòries, els biomarcadors associats a la gravetat i els canvis longitudinals.

Els pacients amb MIS-C van mostrar nivells d'anticossos i activitat neutralitzant comparables als infants CC, però amb diferències clares en la distribució d'isotips i subclasses. El grup MIS-C es caracteritzà per elevades respostes IgG2 específiques contra SARS-CoV-2, respostes IgG3 generalment més baixes excepte contra S2, i un augment de respostes IgA, IgA1 i IgA2 específiques contra S2. Aquests resultats suggereixen una desregulació del canvi de classe de la immunitat humoral, observant-se també diferències en la contribució de les respostes IgA al perfil neutralitzant respecte als controls.

Les respostes contra coronavirus del refredat comú van ser més elevades en MIS-C i en CC, suggerint reactivitat creuada dels anticossos. Els grup MIS-C també mostrà un augment de respostes IgG2, IgG3 i IgG4 específiques contra EBV ZEBRA, compatible anb una reactivació d'EBV.

L'anàlisi de marcadors inflamatoris mostrà que el MIS-C presenta un perfil de biomarcadors diferent als infants CC, caracteritzat per quimiocines relacionades amb IFN-γ, activació endotelial, reclutament immunitari i inflamació sistèmica. Amés, TNFRSF9 soluble, CD8α soluble, IL-33, IL-2, CD244 i SCF es van associar amb l'ingrés a la UCI o amb una presentació més greu. El seguiment longitudinal mostrà que aquest perfil es normalitzava amb la recuperació, amb nivells comparables als infants CC als 2 i 18 mesos.

La comparació dels pacients MIS-C amb KD i SD va mostrar vies inflamatòries i vasculars compartides, però diferents signatures immunitàries. MIS-C es caracterizava per l'activació d'IFNy, mentre que KD es caracterizava per inflamació i remodelació vascular, i SD mostravaun patró autoinflamatori associat amb IL-18/IL-6.

En conclusió, les dades suggereixen que MIS-C és una síndrome postinfecciosa distintiva, caracteritzada per una immunitat humoral alterada i una resposta inflamatòria transitòria però intensa. Els resultats destaquen una desregulació selectiva de subclasses d'anticossos, una resposta elevada contra antígens associats a la reactivació d'EBV, una inflamació mediada per IFN-γ i la existencia de biomarcadors de gravetat, com a elements definitoris de la immunopatologia del MIS-C.

RESUMEN

Aunque la COVID-19 es más leve en niños que en adultos, una pequeña proporción de pacientes pediátricos desarrolla el Síndrome Inflamatorio Multisistémico en Niños (MIS-C), una condición hiperinflamatoria postinfecciosa grave que aparece semanas después de la infección. Hasta ahora, los mecanismos inmunológicos del MIS-C no han sido completamente definidos.

Hipotetizando que el MIS-C deriva de una respuesta inmunitaria alterada tras la infección por SARS-CoV-2, con cambios en las respuestas de anticuerpos y un perfil inflamatorio específico; en este trabajo hemos caracterizado las respuestas humorales e inflamatorias en MIS-C, utilizando niños recuperados de COVID-19 (CC) como control. También se comparó el MIS-C con la enfermedad de Kawasaki (KD) y la enfermedad de Still (SD), y se siguió a un subgrupo de pacientes con MIS-C a los 2 y 18 meses.

Mediante Luminex, se analizaron diferentes isotipos de inmunoglobulinas y sus subclases contra antígenos de SARS-CoV-2, incluyendo el análisis de la capacidad neutralizante. También se estudió la reactividad contra coronavirus del resfriado común y EBV. Mediante Olink se caracterizaron las firmas inflamatorias, los biomarcadores asociados a la gravedad y los cambios longitudinales.

Los pacientes con MIS-C mostraron niveles de anticuerpos y actividad neutralizante comparables al grupo CC, pero con diferencias claras en la distribución de isotipos y subclases. El MIS-C se caracterizó por elevadas respuestas IgG2 específicas contra SARS-CoV-2, respuestas IgG3 generalmente más bajas excepto contra S2, y un aumento de respuestas IgA, IgA1 e IgA2 específicas contra S2. Estos resultados sugieren una desregulación del cambio de clase de la inmunidad humoral, observándose también diferencias en la contribución de las IgA al perfil neutralizante respecto a los controles. Las respuestas contra coronavirus del resfriado común fueron más elevadas en MIS-C y en CC, sugiriendo reactividad cruzada de los anticuerpos. El grupo MIS-C también mostró un aumento de respuestas IgG2, IgG3 e IgG4 específicas contra EBV ZEBRA, compatible con una reactivación de EBV.

El análisis de marcadores inflamatorios mostró que MIS-C presenta un perfil de biomarcadores diferente al grupo control, caracterizado por quimiocinas relacionadas con IFN-γ, activación endotelial, reclutamiento inmunitario e inflamación sistémica. Además, TNFRSF9 soluble, CD8α soluble, IL-33, IL-2, CD244 y SCF se asociaron con el ingreso en la UCI o con una presentación más grave. El seguimiento longitudinal mostró que este perfil se normalizaba con la recuperación, con niveles comparables a los niños CC a los 2 y 18 meses.

La comparación los grupos MIS-C con KD y SD mostró vías inflamatorias y vasculares compartidas, pero diferentes firmas inmunitarias. MIS-C se caracteriza por activación de IFNy, mientras que KD se caracteriza por inflamación y remodelación vascular, y SD muestra un patrón autoinflamatorio asociado con IL-18/IL-6.

En conclusión, los datos sugieren que MIS-C es un síndrome postinfeccioso distintivo, caracterizado por una inmunidad humoral alterada y una respuesta inflamatoria transitoria pero intensa. Los resultados destacan una desregulación selectiva de subclases de anticuerpos, una respuesta elevada contra antígenos asociados a la reactivación de EBV, una inflamación mediada por IFN-γ y la existencia de biomarcadores de gravedad, como elementos definitorios de la inmunopatología del MIS-C.

РЕЗЮМЕ

Пандемія COVID-19 показала, що інфекція SARS-CoV-2 може мати різні клінічні наслідки у дорослих і дітей. Хоча гострий COVID-19 у дітей зазвичай перебігає легше, у невеликої частки педіатричних пацієнтів розвивається мультисистемний запальний синдром у дітей (MIS-C) — тяжкий постінфекційний гіперзапальний стан, який зазвичай виникає через кілька тижнів після інфекції. Імунні механізми, що лежать в основі MIS-C, досі залишаються не повністю з'ясованими.

Ми припустили, що MIS-C може бути наслідком зміненої імунної відповіді після інфекції SARS-CoV-2, яка характеризується порушеннями у відповідях антитіл та специфічним запальним профілем. Метою цієї роботи було охарактеризувати гуморальну та запальну імунну відповідь при гострому нелікованому MIS-C, використовуючи дітей, які одужали після COVID-19 (CC), як контрольну групу. Крім того, MIS-C порівнювали з хворобою Кавасакі (KD) та хворобою Стілла (SD), а підгрупу пацієнтів із MIS-C спостерігали через 2 та 18 місяців.

Було проаналізовано SARS-CoV-2-специфічні відповіді антитіл, включаючи нейтралізацію, ізотипи імуноглобулінів та підкласи IgG і IgA. Також оцінювали реактивність антитіл проти коронавірусів звичайної застуди та EBV за допомогою технології Luminex. Профілювання Olink використовували для характеристики запальних сигнатур, біомаркерів тяжкості та змін під час подальшого спостереження.

У пацієнтів з MIS-C загальні рівні антитіл і нейтралізувальна активність були подібними до показників у дітей із групи CC, але профіль антитіл відрізнявся за розподілом ізотипів і підкласів. MIS-C характеризувався підвищеними IgG2 проти SARS-CoV-2, загалом нижчими IgG3, за винятком S2, а також підвищеними IgA, IgA1 та IgA2 проти S2. Ці результати свідчать про вибіркове порушення перемикання класів гуморального імунітету. Крім того, у пацієнтів з MIS-C спостерігався більший внесок IgA-відповідей у нейтралізувальний профіль порівняно з контрольною групою.

Відповіді антитіл проти коронавірусів звичайної застуди були підвищені як у пацієнтів із MIS-C, так і в дітей CC, що свідчить про можливу перехресну

реактивність. Пацієнти з MIS-C також мали підвищені відповіді IgG2, IgG3 та IgG4 проти EBV ZEBRA, що може вказувати на гуморальні відповіді, пов'язані з реактивацією EBV.

Аналіз запального профілю дозволив виявити відмінний набір біомаркерів у пацієнтів з MIS-C порівняно з дітьми CC. Він характеризувався хемокінами, пов'язаними з IFN-γ, активацією ендотелію, рекрутуванням імунних клітин та системним запаленням. TNFRSF9, CD8α, IL-33, IL-2, CD244 і SCF були пов'язані з госпіталізацією у відділення інтенсивної терапії або тяжчим клінічним перебігом. Подальше спостереження показало, що після одужання цей профіль нормалізувався, а рівні біомаркерів стали подібними до таких у дітей із групи CC через 2 та 18 місяців.

Порівняння з KD і SD показало, що ці педіатричні гіперзапальні захворювання мають частково подібні профілі експресії запальних і судинних біомаркерів, однак водночас характеризуються власними відмінними імунними профілями. KD характеризувалася переважно судинним запаленням і ремоделюванням, тоді як SD мала виражений аутозапальний профіль, пов'язаний з IL-18/IL-6.

Отже, ця дисертація демонструє, що MIS-C є окремим постінфекційним імунним синдромом, який характеризується зміненою гуморальною імунною відповіддю та транзиторною, але інтенсивною запальною реакцією.

INTRODUCTION

Overview of COVID-19 pandemic

Despite substantial advances in healthcare, medical treatments, and overall quality of life worldwide, infectious disease outbreaks remain among the most difficult public-health threats to predict, prevent, contain, and control. The coronavirus disease 2019 (COVID-19), caused by severe acute respiratory syndrome coronavirus 2 (SARS-CoV-2), was a major reminder of this challenge. The disease was first recognized in December 2019 in a cluster of patients with atypical pneumonia of unknown cause in Wuhan, China[1,2]. The World Health Organization (WHO) declared a Public Health Emergency of International Concern on January 30th, 2020, and characterized COVID-19 as a global pandemic on March 11th 2020[3]. The acute global emergency phase ended on 5 May 2023[4] after 3 years, 4 months, and 5 days. SARS-CoV-2 has continued to circulate globally, but the epidemiological situation is more stable, with generally lower severity than during the earlier pandemic waves, mainly because of high acquired immunity and vaccination at the population level, better clinical management, and the fact that currently circulating variants have not shown higher pathogenicity than earlier Omicron lineages. As of March 27th, 2026, there are no SARS-CoV-2 variants currently meeting the criteria for a Variant of Concern[5].

By the end of December 2025, more than 779 million confirmed cases and over 7 million confirmed deaths had been reported globally[6]. In addition, the WHO documented more than 28.1 million COVID-19-associated hospitalizations across 172 countries until November 2024, confirming the enormous burden of severe disease presentations on the healthcare systems worldwide[7]. Individuals younger than 25 years accounted for 22.6% of global reported cases, but only around 0.6% of reported deaths, underscoring low fatality associated with COVID-19 in this age group[8]. Although acute SARS-CoV-2 infection in children and adolescents is generally less severe than in adults, pediatric COVID-19 cannot be evaluated only through mortality rates[9,10]. A small but clinically important proportion of children develop severe acute disease or delayed immune-mediated complications after infection[11,12]. Among these, Multisystem Inflammatory Syndrome in Children (MIS-C) became one of the most important pediatric complications of the pandemic characterizing as a serious

hyperinflammatory condition that usually appears several weeks after SARS-CoV-2 infection[13]. The emergence of MIS-C showed that, despite the relatively low fatality of acute COVID-19 in children, SARS-CoV-2 could trigger severe post-infectious immune dysregulation in the pediatric population[14,15].

According to WHO's February 2026 Global Risk Assessment, the global public health risk at the end of 2025 remained moderate[16]. COVID-19 can also be regarded as one of the most intensively documented and globally coordinated infectious disease emergencies in modern medicine. The WHO together with clinicians and scientists rapidly issued strategic preparedness and response plans, hospital readiness checklists covering leadership, triage, diagnosis, surge capacity, and infection prevention and control, and continuously updated living guidelines for clinical management and therapeutics. In parallel, COVID-19 vaccines were developed with unprecedented pace, while the WHO controlled that safety and efficacy standards were not compromised.

1. SARS-CoV-2 virology

The infectious agent causing COVID-19 is the severe acute respiratory syndrome coronavirus 2 (SARS-CoV-2). SARS-CoV-2 belongs to the family Coronaviridae which comprises enveloped, positive-sense, single-stranded RNA viruses that infect a wide range of animal species as well as humans. Within this family, human coronaviruses are mainly classified into the genera *Alphacoronavirus* and *Betacoronavirus*. Alphacoronaviruses include HCoV-229E and HCoV-NL63, whereas betacoronaviruses also include HCoV-OC43, HCoV-HKU1[17,18], MERS-CoV, and the subgenus Sarbecovirus, which comprises SARS-CoV and SARS-CoV-2. HCoV-229E, HCoV-NL63, HCoV-OC43, and HCoV-HKU1 are endemic common cold coronaviruses which circulate widely in the population. Infection occurs frequently in early childhood, although multiple reinfections can occur over the course of life[19,20].

1.1. The virion

SARS-CoV-2 genome is approximately 29.9 kb in length, making it one of the largest known RNA virus genomes[21]. The RNA genome contains 14 open reading frames

(ORFs) and encodes for a total of 31 proteins: 16 non-structural proteins (NSP1–NSP16), 4 structural proteins (nucleocapsid N, membrane M, envelope E, and spike S), and 9 accessory proteins (**Figure 1A**). The first open reading frame ORF1a/b is about two-thirds of the whole genome, which encodes polyprotein1a, b (pp1a, pp1b). These polyproteins correspond to 16 NSPs required for viral replication[22,23].

SARS-CoV-2 virions have a spherical to pleomorphic shape **(Figure 1B**). The viral RNA is bound by the N proteins and enclosed within a host-derived lipid bilayer. Embedded in this lipid membrane are the M, E, and S proteins[24,25]. The four structural proteins. They are essential for the viral life cycle and represent major targets for immune recognition, diagnostic testing, and therapeutic development.

The S-protein, located on the viral surface, mediates viral attachment, membrane fusion, and subsequent viral entry into the host target cell. In addition, the S protein, when expressed on the surface of infected cells, can promote fusion with other target cells leading to the formation of syncytia which helps the virus spread directly between cells and may reduce the effect of neutralizing antibodies. The S protein has two functional subunits **(Figure 1C**): S1 which contains the receptor-binding domain (RBD) and binds to the angiotensin-converting enzyme 2 (ACE2) receptor, and S2, which mediates the fusion of the viral and host cell membranes[22,23]. Importantly, the most critical mutations associated with SARS-CoV-2 evolution occur in the spike protein, particularly in S1, where they can influence receptor binding, transmissibility, and immune evasion[23]. Because it is exposed on the viral surface and is the main target of neutralizing antibody responses, the spike protein has been the main focus of vaccines and antibody-based therapies.

The M protein is the most abundant structural protein of SARS-CoV-2 and plays a central role in viral assembly and budding[22].

The envelope (E) protein is the smallest structural protein of SARS-CoV-2 and is important for viral assembly, budding, and maturation. Its absence markedly reduces viral production and impairs virion formation[22].

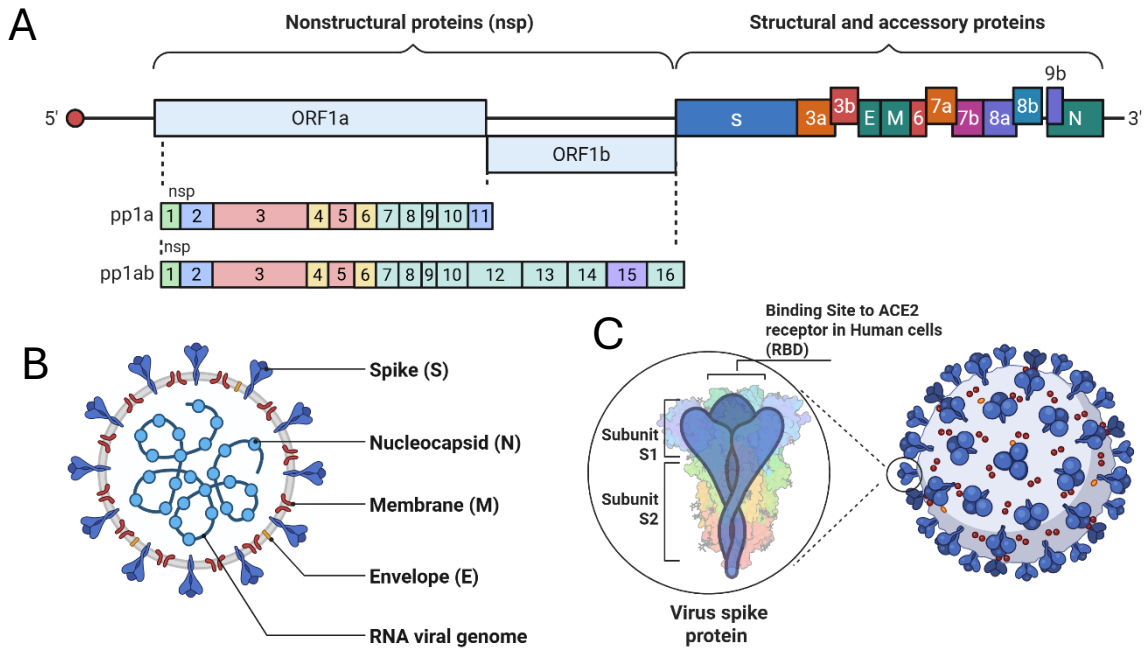


Figure 1. The genome, proteome, and structural components of SARS-CoV-2. *(A) Genomic organization of SARS-CoV-2, illustrating the viral RNA genome. (B) SARS-CoV-2 virion and localization of structural proteins with the viral RNA genome. (C) Structural organization of the spike (S) protein. Adapted from Ravi at al.[22] and Ke at al[24] .Created using BioRender.*

The N protein binds and packages the viral RNA genome and forms the nucleocapsid core[23]. It also induces a strong immune response and is widely used in diagnostic tests. Interaction between the N and M proteins stabilizes the internal core of the virion, while the M and E proteins form the viral envelope and support assembly and release of new viral particles[22].

Accessory proteins play an important role in immune evasion and pathogenesis, although they are not essential for viral RNA replication (**Figure 1A**). For example, some are involved in inhibiting cytokine secretion, and by counteracting the type I interferon response. In addition, some of them influence autophagy and apoptosis, mitochondrial function, and inflammasome activation[26,27].

1.2. Viral entry

SARS-CoV-2 is mainly transmitted through respiratory droplets and enters the body via the nasal, oral, or conjunctival mucosa. The first infection step is the binding of the virus to target cells expressing ACE2. Importantly the distribution of ACE2 expression across tissues helps explain the sites of infection and clinical manifestations. ACE2 is

found especially in nasal and airway epithelial cells, alveolar epithelial cells, intestinal enterocytes, and proximal renal tubular cells, with additional expressions reported in cardiomyocytes and vascular cells[22,25,28].

The virus initially infects cells of the upper and lower respiratory tract, where it replicates and spreads locally (**Figure 2**).

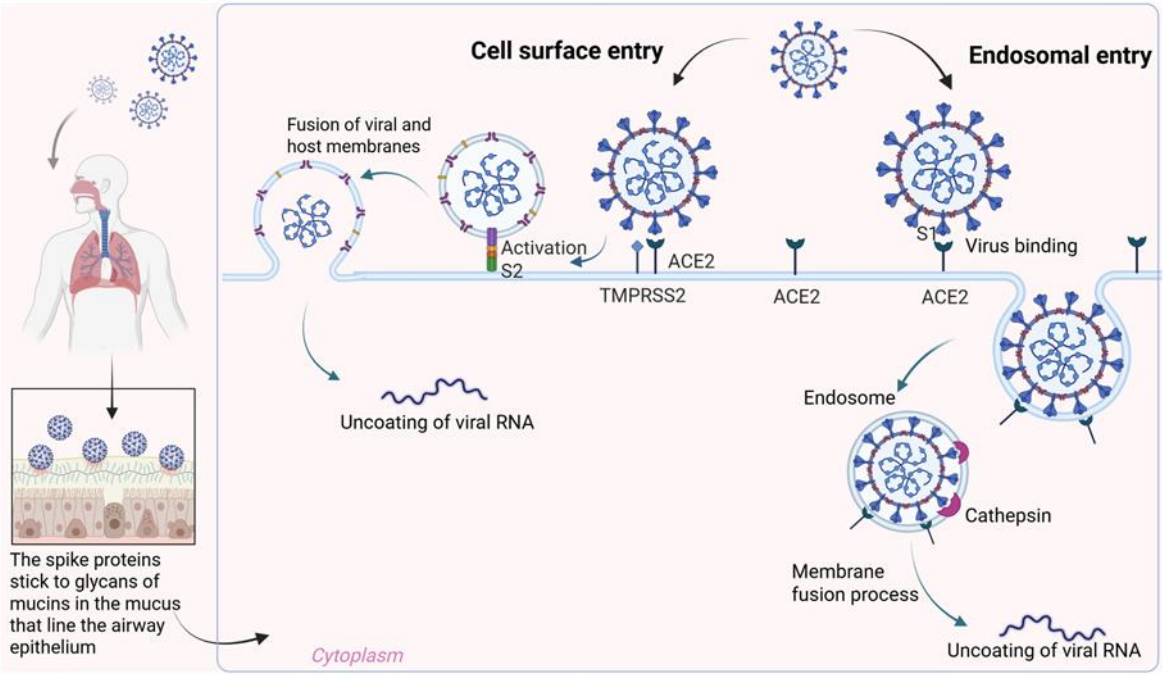


Figure 2. SARS-CoV-2 entry pathways. *Two principal routes of SARS-CoV-2 entry into host cells: cell-surface fusion and endosomal entry. Depending on the route of entry, the S2' cleavage site of the spike protein is processed by distinct host proteases. Omicron subvariants preferentially utilize the endosomal pathway. Adapted from Jackson et al[29]. Created with BioRender.com.*

SARS-CoV-2 enters host cells through interaction of RBD of the S1 subunit with the ACE2[25]. Subsequent cleavage at the S2' site by host proteases activates the fusion peptide, allowing the viral and host cell membranes to fuse.

Virus can enter cells by two main pathways (**Figure 2**). When present, the protease TMPRSS2 can mediate the cleavage/processing of the spike and subsequent fusion at the cell surface. If TMPRSS2 is absent or insufficient, the virus enters through endocytosis, and the spike processing is performed by cathepsins (**Figure 2**) present in the endosomal compartment and active at lower pH. Importantly, while early SARS-CoV-2 lineages favored the TMPRSS2 dependent pathway, Omicron variants were associated with an increased use of the endocytic pathway. This change paralleled a

shift of viral tropism for Omicron lineages, from the lower respiratory tract to the upper respiratory tract and a decreased pathogenicity.

Once inside the cytoplasm, the viral RNA uses the host cell machinery to produce viral proteins and replicate its genome. New viral particles are then assembled in intracellular compartments and released from the cell by exocytosis[22,29].

While SARS-CoV-2 primarily infects the respiratory tract, reports have indicated the presence of viral particles in the gastrointestinal tract and the cardiovascular and urinary systems. In addition, COVID-19 is often associated with neurological symptoms, and viral proteins can be found in the olfactory bulb[30].

2. Immune Response (Adults vs Children)

The immune response to SARS-CoV-2 differs between children and adults and may partly explain the generally milder acute disease observed in pediatric patients. Children may be less susceptible to severe acute SARS-CoV-2 infection partly because viral entry into airway cells is reduced. Lower airway expression of ACE2 and TMPRSS2 have been described in children, although stronger early innate antiviral responses probably also contribute to their milder disease course[31,32]. Unlike earlier variants, Omicron remains ACE2-dependent but relies less on TMPRSS2 and preferentially enters cells through the endosomal pathway in the upper respiratory tract, contributing to the more efficient spread in children[33].

2.1. Innate immune response

Innate immunity is the first line of defense against SARS-CoV-2 in both children and adults. The initial immune response begins when SARS-CoV-2 infects epithelial cells in the respiratory tract (**Figure 3A**). Intracellular viral RNA can be detected as a foreign signal by pattern-recognition receptors (PRRs) such as endosomal toll-like receptors (TLRs) 3, 7 and 8 and cytosolic RIG-I-like receptors. It was also shown that surface TLRs 2 and 4 can recognize structural components of SARS-CoV-2 [34,35]. Finally, infected cells which express S protein on their surface can fuse with neighboring cells and form syncytia. It was shown that, in this context, intracellular detection of damaged genomic DNA can activation the C-GAS STING pathway[36]. Signaling from this early viral

sensing leads to the production of type I (mainly IFN-α and IFN-β), and type III (IFN-λ) interferons, and other inflammatory mediators[37,38].

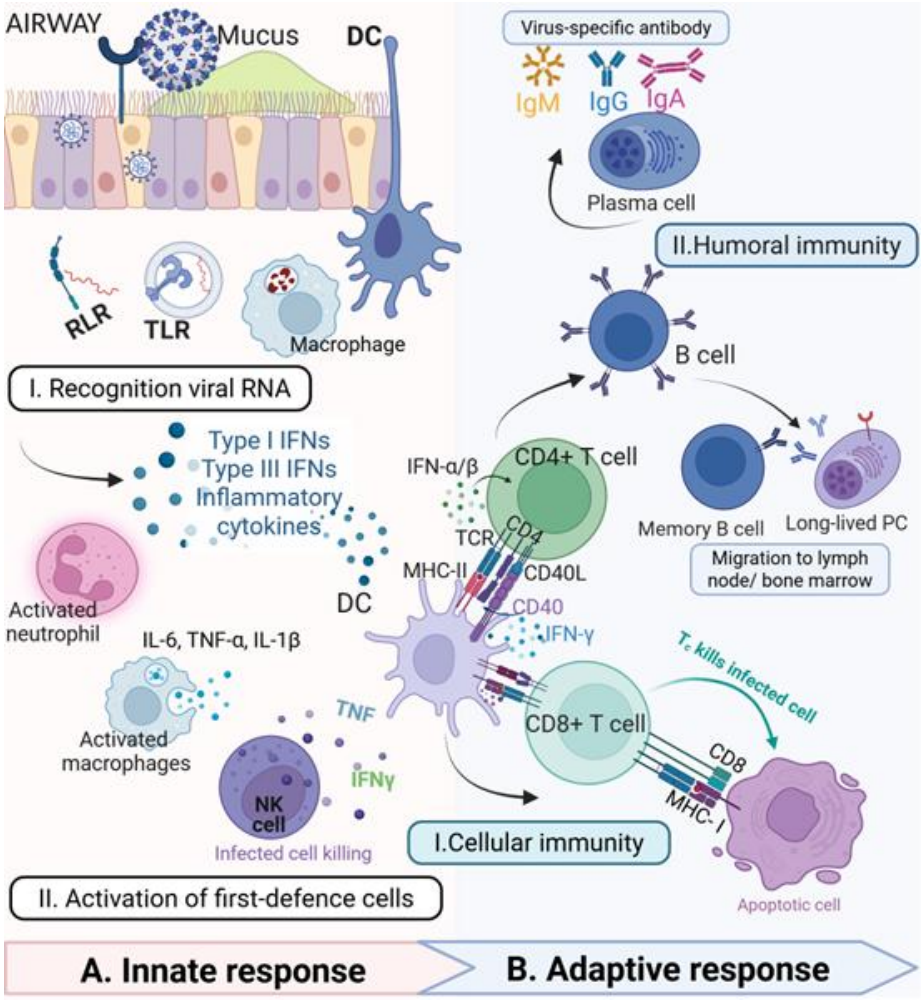


Figure 3. Innate and adaptive immune responses to SARS-CoV-2 infection. *(A) The host immune response to SARS-CoV-2 begins with recognition of viral RNA by PRRs, which induces type I and III interferons and inflammatory cytokines. This activates first-line immune cells (macrophages, neutrophils, and NK cells). Subsequently, dendritic cells initiate the adaptive immune response (B) through activation of CD4+ and CD8+ T cells, while activated B cells differentiate into plasma cells producing virus-specific antibodies (IgM, IgG, and IgA), together with memory B cells and long-lived plasma cells that contribute to immune protection. Adapted from Mohammed et al.[39] and from Kang et al[40]. Created with BioRender.com.*

The next step is the establishment of an antiviral state. Type 1 Interferons induce interferon-stimulated genes in both infected and neighboring cells, which help suppress viral replication and limit viral spread. Increased lung chemokines, including CXCL1, CXCL2, CXCL8, CCL2/ MCP-1, and CCL7/MCP-3, promote recruitment of neutrophils and monocytes which contribute to the clearance of viral particles and the release of pro-inflammatory cytokines such as IL-6, TNF-α, and IL-1β[40,41]. Finally, type

1 interferons promote the activation of natural killer (NK) cells, which contribute to early antiviral defense by killing infected cells and by producing antiviral cytokines, mainly IFN-γ and TNF-α[40]. IFN-γ, notably, plays a key role in activating resident macrophages and dendritic cells that will contribute to the development of adaptive responses. In addition, IFN-γ will induce chemokines such as CXCL9 and CXCL10 from epithelial cells which help recruit cytotoxic CD8 T cells and NK cells and will increase the expression of MHCI and II molecules at the surface of epithelial cells, therefore facilitating the elimination of infected cells by recruited lymphocytes[42].

If the response is balanced, these mechanisms help contain the infection early. However, if antiviral signaling is delayed or dysregulated, innate immune activation may be unable to control viral spread. In this setting, increased production of pro-inflammatory cytokines such as IL-6, TNF, and IL-1β, together with chemokine release, can amplify tissue inflammation and damage, leading to more severe disease[41,43]. In severe COVID-19, excessive TNF and IFN-γ signaling may also synergize to induce PANoptosis, an inflammatory cell-death pathway that amplifies cytokine release and tissue damage[37] .

Distinct Features of the Pediatric Immune Response to SARS-CoV-2.

In children, innate immunity plays a key role in controlling viral dissemination, while virus-specific lymphocytes help overcome SARS-CoV-2 strategies that suppress interferon signaling. An enhanced innate antiviral capacity in children, together with the high interferon sensitivity of SARS-CoV-2, may contribute to more effective early viral control and a lower risk of severe COVID-19 compared with adults. These age-related differences are also reflected in cytokine profiles: interferon responses are relatively low during the first two years of life, increase during childhood with higher levels of type I IFNs, IL-12, and IL-10 and lower levels of IL-6 and IL-23, and decline again with advancing age, particularly in older adults [33,44].

2.2. Adaptive immune response

Adaptive immunity develops after the initial innate response and includes both cellular immunity and humoral immunity. It usually becomes clearly detectable within about 5–10 days after symptoms onset.

2.2.1. Cellular immunity

Cellular adaptive immunity is mediated by T cells (**Figure 3B**) whose initial activation depends on professional antigen presenting cells and most notably dendritic cells (DCs). DCs directly link the innate and adaptive immunity. They scavenge antigens in peripheral tissues and upon PRR mediated pathogen detection, become activated and migrate to secondary lymphoid organs where they present antigen derived peptides on major histocompatibility complex (MHC) molecules to Naïve and central memory T cells. Cluster of differentiation (CD) 8+ T cells recognize viral peptides on MHC I molecules and after activation, become cytotoxic CD8 T cells, which can directly eliminate infected cells. CD4+ helper T cells recognize viral peptides on MHC II molecule, and in response to viral infection, preferentially differentiate into Th1 helper cells and T follicular helper cells.

Th1 CD4 T cells play a central role in organizing the antiviral response, notably by activating macrophages and supporting the CD8 T-cell response. They also play a more direct effector function at the site of infection by releasing IFN-γ in the surrounding of infected epithelial cells which contribute to maintaining the local antiviral state. Importantly, tissue resident memory CD4 T cells can rapidly reestablish the antiviral state upon new infection and antigen presentation by local macrophages. CD4 T follicular helper cells support B-cells maturation and antibody production (see humoral immunity).

SARS-CoV-2-specific T cells are essential for viral control and long-term immune memory[45–47]. SARS-CoV-2-specific T-cell responses, notably IFN-γ producing T cells, can be detected early after infection and are associated with lower viral load, faster clearance, and milder disease [39,48], especially in absence of an effective neutralizing antibody responses[49]. These responses recognize multiple viral epitopes, including S, M, N, and non-structural proteins, and generally remain more conserved across viral variants than antibody responses[46].

The high invasiveness of SARS-CoV-2 can overwhelm adaptive cellular immunity and lead to depletion of circulating NK cells and T cells, resulting in lymphopenia, which is a marker of severe disease[45,50]. These mechanisms include increased T-cells

apoptosis, inflammatory cell death driven by excessive TNF-α and IFN-γ signaling, and syncytia-mediated loss of lymphocytes, particularly CD8+ cytotoxic T cells, thereby impairing viral clearance and contributing to disease progression[45].

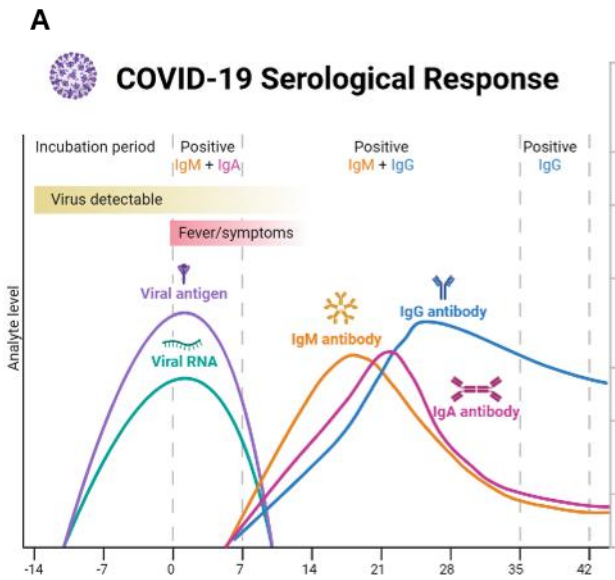
Distinct Features of the Pediatric Immune Response to SARS-CoV-2.

Although T-cell lymphopenia in blood and airway fluid is associated with severe disease in both age groups, children generally maintain higher absolute lymphocyte counts, including naïve CD4+ and CD8+ T cells. With increasing age, naïve T cells decline, memory T cells become more dominant, thymic output decreases, and T cells progressively acquire features of chronic inflammation, cytotoxicity, and exhaustion, which may impair antiviral control and increase susceptibility to severe disease[44]. Overall, the immune response in children is less pro-inflammatory and more skewed toward a Th2 profile, while severe and fatal COVID-19 in adults is more often associated with increased inflammatory mediators such as IL-1, IL-6, IL-8/ CXCL8, and CXCL10[33]. Spike-specific T-cell responses are higher in children and were also detected in many seronegative children, suggesting pre-existing cross-reactive immunity from seasonal common cold coronaviruses[51].

2.2.2. Humoral immunity

Humoral immunity to SARS-CoV-2 begins when viral antigens from the respiratory mucosa reach the draining lymph nodes and activate antigen-specific B cells with help from CD4+ T helper cells[52].

B cells initially differentiate into plasmablasts and short-lived plasma cells, producing early circulating antibody responses after SARS-CoV-2 infection (**Figure 3**)[47,53]. In acute-phase serum samples, SARS-CoV-2-specific IgM and IgA were detectable at a median of 5 days after symptom onset (IQR, 3–6 days), whereas IgG appeared later, at a median of 14 days after symptom onset (IQR, 10–18 days); IgG was detected in 77.9% of serum samples in this cohort (**Figure 4**)[54–56]. IgM levels peaked around 20 days after the first positive RT-qPCR result and then declined over the following month, while IgG responses were maintained for longer[57]. This pattern is consistent with the shorter serum half-lives of IgM and IgA compared with IgG, although IgG3 has a shorter half-life than other IgG subclasses[57].



B

IgA1	day 3–7 **after symptom onset → peak** at week 3	Early mucosal neutralization
IgA2	Mucosal protection; less consistent in blood	
IgM	day 5 → end of week 2 -3 week	First antibody; early neutralizationIg
IgG1	day 7 → week 3	Main systemic protective antibody; neutralization and Fc functions
IgG2	Minor antiviral role	
IgG3	day 7 → week 3	Strong Fc-mediated antiviral activity
IgG4	Minimal role in acute infection	

Figure 4. COVID-19 serological response. *(A). Illustration of the dynamics of viral antibody response following SARS-CoV-2 infection. Viral RNA and antigen are detectable early during the incubation period and around symptom onset. IgM and IgA antibodies appear within the first week, while IgG antibodies develop later and provide sustained systemic immunity. (B) The table summarizes the timing of antibody appearance and median seroconversion for each immunoglobulin class, together with their main functional roles in the immune response. Adapted from Sethuraman et all[54], Guo et all[55,56], and Yu et all. Created with BioRender.com.*

The humoral response generates both binding and neutralizing antibodies. Binding antibodies recognize many viral proteins (S, N, M) but do not necessarily block infection. Neutralizing antibodies, by definition, directly interferes with viral entry. SARS-CoV-2 neutralizing antibody all recognize the S protein, which mediates viral entry, and the most potent bind to the RBD[52]. On the other hand, binding antibodies that recognize viral antigens at the surface of infected cells can promote their clearance through Fc-mediated mechanisms, including antibody-dependent cellular cytotoxicity (ADCC) by NK-cells[39,45].

In parallel, some activated B lymphocytes enter germinal centers, where, with support from T follicular helper cells, they undergo clonal expansion, class switching, and somatic hypermutation. This process leads to affinity maturation and the generation of memory B lymphocytes and long-lived plasma cells, which are essential for sustained humoral immunity after viral clearance.

Class-switch recombination is a key mechanism that allows activated B lymphocytes to change the antibody isotype they produce while preserving antigen specificity[34,58].

Initially, naïve B cells express mainly IgM and IgD; after activation, antigen-specific B cells first produce IgM antibodies, including anti-RBD IgM, which can be detected as early as day 3 after symptom onset[59]. However, after activation, cytokine signals and CD40–CD40L interactions can induce switching toward other isotypes, such as IgG, IgA, or IgE[58]. Cytokines further shape antibody subclass selection. IL-4 and IL-13 are associated with type 2-related IgG4 and IgE responses, IL-21 supports IgG and IgA production, IL-10 can promote human IgG1 and IgG3 switching, TGF-β plays a central role in IgA class switching, and IFN-γ can influence Th1-associated IgG subclass responses, including IgG2-associated responses in humans[60–64]. Therefore, class switching is essential for adapting the humoral immune response to the type and location of infection. IgG includes four subclasses, IgG1, IgG2, IgG3, and IgG4, which differ in their ability to bind Fcγ receptors and activate complement. IgG1 and IgG3 are generally strong antiviral effector subclasses, whereas IgG2 and IgG4 have more restricted or less inflammatory functions[65]. Human IgA is divided into IgA1 and IgA2; IgA1 predominates in serum, while IgA2 is relatively enriched at mucosal surfaces[53,62,66].

Pre-existing antibodies against common cold coronavirus, OC43, HKU1, 229E and NL63, can cross-react with SARS-CoV-2, notably in conserved regions such as the N protein and the Spike S2 protein[67]. This is especially true for OC43 and HKU1 which belong to the same *Betacoronavirus family*. However, these antibodies generally do not neutralize the virus effectively[52]. Although it has been shown that SARS-CoV-2 infection can boost these pre-existing antibodies[68], but they do not provide protection. Worst, they may delay SARS-CoV-2 antibody responses[69] .

Distinct Features of the Pediatric Immune Response to SARS-CoV-2.

Children have been reported to show higher median IgG levels and a more spike-focused antibody response, with reduced breadth of recognition compared with adults, including lower or absent anti-nucleocapsid responses in some studies[51,70]. These age-related differences may reflect developmental changes in B-cell maturation, as the response to T-cell-independent antigens matures only after about 2 years of age; accordingly, infants produce relatively more IgG1 than IgG2, the latter preferentially recognizing polysaccharide antigens, making early childhood humoral

immunity distinct from that of adults. Similar age-related patterns are also observed for common human coronaviruses, with children producing antibodies against spike proteins and adults more frequently targeting non-structural proteins, likely reflecting cumulative immune experience[33,44]. Overall, school-age children and younger children beyond infancy appear to show the most favorable humoral response to acute SARS-CoV-2 infection, whereas infants have a relatively immature humoral compartment and older adults show the least favorable response because of immune aging and greater inflammatory dysregulation[33,44,70]. Moreover, infection is frequently restricted to the upper airways, probably due to a strong innate interferon-driven response, which may lead to lower seroconversion and milder clinical manifestations.

3. Genetic evolution and variants of SARS-CoV-2

SARS-CoV-2 evolves through the continuous accumulation of genetic changes during replication **(Figure 5A**) [49,71,72]. Early in the pandemic, viral evolution was driven mainly by selection for increased transmissibility, whereas later stages were increasingly influenced by immune evasion [72]. Consistently, most major changes have occurred in the S protein, particularly in the S1 subunit and RBD, with the acquisition of resistance to neutralizing antibodies[29,49,71,73,74]. Recurrent mutations have also been observed in the nucleocapsid (N) protein and, less commonly, in accessory proteins such as ORF8[75,76].

The naming of emerging variants of SARS-CoV-2 uses different systems: WHO Greek-letter labels (e.g., Alpha, Omicron) for major public-health variants, Pango lineage (e.g., BA.1, BA.5) for phylogenetic classification, and mutation notation (e.g., D614G) to describe individual amino acid changes.

SARS-CoV-2 sequence data were generated and shared in almost real time through the Global Initiative on Sharing All Influenza Data (GISAID). By April 2026, there were more than 22 million genetic sequences[77].

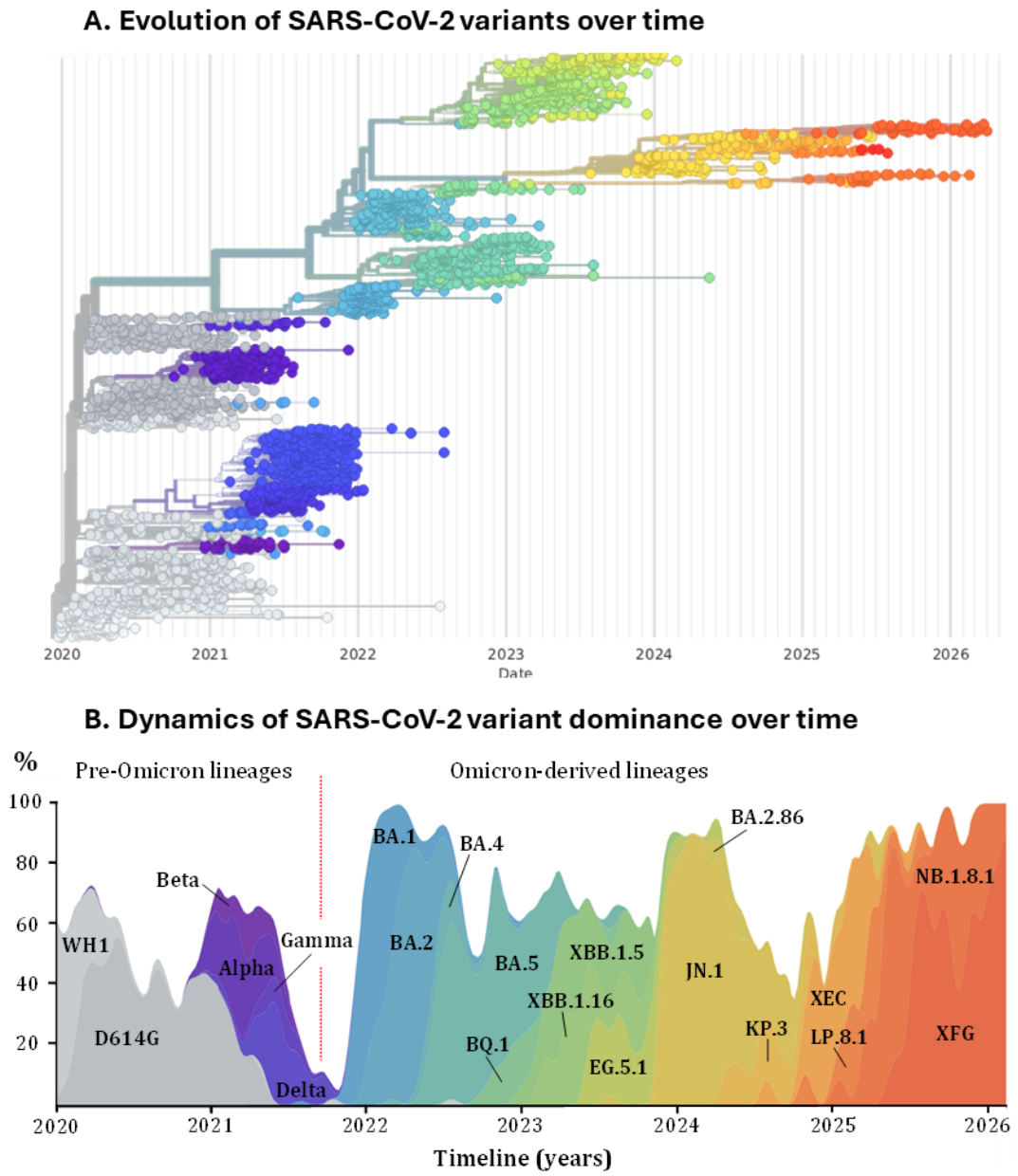


Figure 5. Evolution and temporal dynamics of SARS-CoV-2 variants. *(A) Time-resolved phylogenetic tree illustrating SARS-CoV-2 evolution, where each point represents a viral sequence and branches reflect evolutionary relationships. (B) The temporal distribution and relative prevalence of SARS-CoV-2 variants. Pre-Omicron and Omicron-derived lineages are separated by a red dashed line. Colors indicate SARS-CoV-2 variants and are consistently applied across panels A and B. Adapted from Nextstrain[78], under CC-BY-4.0 license (https://creativecommons.org/licenses/by/4.0/).*

Certain SARS-CoV-2 variants have been categorized by the World Health Organization as Variants of Concern (VOC) because their mutations may influence viral spread, clinical severity, immune escape, or vaccine performance[79,80]. Certain SARS-CoV-2 VOCs, including Alpha (B.1.1.7), Delta (B.1.617.2), and Omicron (BA.1 and BA.2), are particularly notable because of changes in transmissibility and virulence (**Figure 5B**)[73].

For example, Alpha spike mutations improved ACE2 binding and increased S1/S2 cleavage and fusogenicity, thereby promoting more efficient viral spread[74].

Delta combined high transmissibility with moderate antibody escape, as S mutations, including changes in the RBD, enhanced viral fitness while reducing sensitivity to neutralizing antibodies[74].

Omicron BA.1 represented a major antigenic shift, carrying more than 30 amino acid substitutions in the S protein, including about 15 in the RBD, which markedly reduced neutralization by antibodies induced by previous infection or the original vaccines and contributed to frequent breakthrough infections and reinfections. BA.2 remained within the Omicron lineage but was antigenically distinct from BA.1, which likely facilitated its global replacement. Subsequently, BA.4 and BA.5 showed even greater immune-evasive properties, with higher resistance to neutralization than earlier Omicron sublineages. The virus then continued to evolve within the Omicron family, and lineages such as XBB and XBB.1.5 became notable for combining strong immune escape with preserved receptor-binding fitness[74].

As well, variant tropism changed during SARS-CoV-2 evolution. D614G, Alpha, and Delta showed more efficient continued replication in lower-airway cells, whereas Omicron showed a shift toward the upper respiratory tract. Omicron replicated faster in the bronchi but less efficiently in the lung parenchyma than wild-type, D614G, Alpha, Beta, and Delta[81].

4. Immune escape

In early 2020, specific pre-existing immunity to SARS-CoV-2 was absent in the general population. Nevertheless, cross-reactive memory T cells induced by previous infections with human coronavirus may have contributed to a milder clinical course in some cases. On the other hand, antibodies from previous SARS-CoV infection demonstrated only limited protective cross-reactivity against SARS-CoV-2[74].

As strong immunity was generated by infection and vaccination, immune escape became an important component of SARS-CoV-2 evolution, whereby mutations,

particularly in the S protein, alter viral antigenicity and reduce the effectiveness of pre-existing immunity[49].

Although some mutations affected individual T-cell epitopes, overall T-cell immunity remained largely preserved across variants of concern because T cells target multiple epitopes, many of whom relatively well conserved, from several viral proteins, including S, N, M, and non-structural proteins such as ORF3a. As a result, most variants, including Omicron, had only a limited impact on total T-cell immunity, which likely contributed to the sustained efficacy of vaccines against hospitalization and death[49].

While T cells response is critical for the clearance of infected cells and protection against severe disease, neutralizing antibodies have a more direct impact on viral replication and transmission, and are, therefore, a main driver of viral evolution. Humoral immune escape refers to the ability of SARS-CoV-2 to evade antibody-mediated immunity through antigenic changes. This process affects notably antibodies directed against the S protein, thereby reducing antibody neutralizing activity. Although humoral escape often lowers protection against infection and promotes reinfections and breakthrough infections, it is usually incomplete, and protection against severe disease is better preserved than protection against infection alone[49,52]. This was especially evident with Omicron, which combined enhanced transmissibility with substantial evasion of immunity induced by prior infection or vaccination[82]. Following its emergence, immune escape became a major driver of SARS-CoV-2 evolution, resulting in successive Omicron sublineages with increasing antibody evasion and repeated updates to COVID-19 vaccine composition[83,84].

5. Immune imprinting and hybrid immunity

Immune imprinting, or “original antigenic sin” refers to the phenomenon whereby prior exposure to an earlier viral strain or vaccine antigen shapes the subsequent recall of memory B cells and antibody specificities, such that later exposures preferentially boost responses against previously encountered epitopes; in this way, pre-existing humoral immunity may contribute to convergent Omicron receptor-binding domain

evolution by favoring the repeated emergence of mutations that escape the dominant population antibody landscape[85,86].

Hybrid immunity refers to protection generated by the combination of SARS-CoV-2 infection and vaccination. It is generally associated with stronger and broader antibody responses than infection- or vaccine-induced immunity alone, partly due to repeated antigen exposure and memory B-cell recall. This improves neutralizing responses against variants such as Delta and Omicron, although Omicron neutralization remains lower than against the ancestral strain[87]. Hybrid immunity is also shaped by immune imprinting, where the first exposure influences later IgG responses: infection tends to imprint more S2/NTD-reactive antibodies, whereas vaccination more strongly induces RBD-reactive antibodies[88]. Therefore, both the sequence and number of antigen exposures may influence antibody durability, neutralization breadth, and reinfection risk, which is relevant for vaccination strategies in the endemic phase of SARS-CoV-2[88,89].

6. Epidemiology in Spain

The first confirmed case of COVID-19 in Spain was reported on 31 January 2020 in the Canary Islands, involving a patient with a travel-related infection[90]. Spain officially declared the end of the COVID-19 health crisis on 4 July 2023[91]. By 30 June 2023, a cumulative total of 13,914,811 confirmed COVID-19 cases and 121,760 deaths had been reported nationwide[92]. From them, according to the Spanish Ministry of Health and national surveillance data (RENAVE/ISCIII), approximately 1.3–1.5 million COVID-19 hospitalizations.

Spain's surveillance data, summarized in the ISCIII COVID Atlas, describe seven pandemic waves between 2020 and mid-2023 (**Figure 6**)[93].

The **first wave (March–June 2020)** was marked by one of the highest incidences in Europe[94,95].

The **second wave (June–December 2020)**, following the lifting of restrictions, the B.1.177 (20E EU1) lineage emerged in Spain and spread across Europe[96].

The **third wave (December 2020–March 2021)** was associated with a sharp increase in cases, hospitalizations, and deaths, alongside the introduction of vaccination and the co-dominance of the Alpha variant[97].

In the **fourth (March–June 2021)** and **fifth waves (June–October 2021)**, incidence and mortality declined due to increasing vaccination coverage, although the Delta variant became predominant during the fifth wave[98].

The **sixth wave (October 2021–March 2022)** represented the largest surge in case numbers, driven initially by the Delta variant and subsequently by Omicron (BA.1); this period also corresponded to the highest incidence of COVID-19 among pediatric populations, while mortality remained lower compared to earlier waves[99].

Finally, during the **seventh period (from March 2022 onwards)**, Spain transitioned to a new surveillance strategy focusing on older and hospitalized patients, coinciding with the dominance of successive Omicron subvariants and a sustained reduction in severe outcomes [97,100]

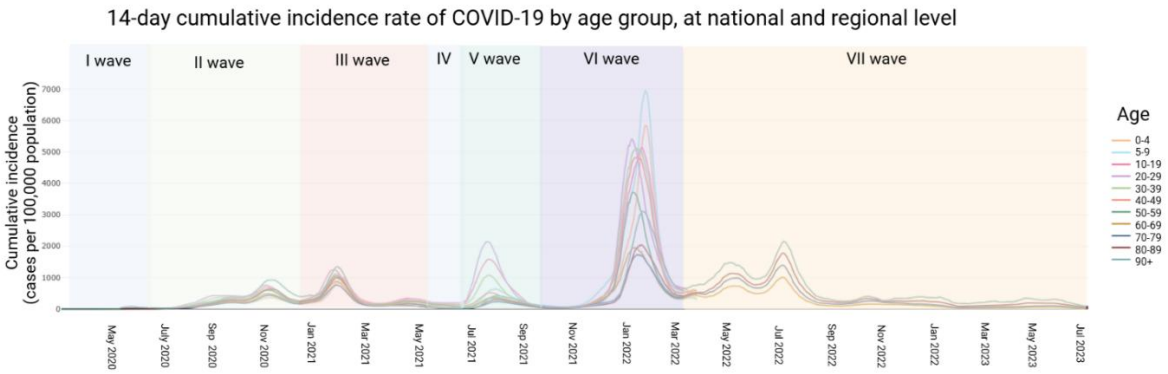


Figure 6. Evolution of 14-Day Cumulative COVID-19 Incidence in Spain by Age Group. *The evolution of 14-day cumulative COVID-19 incidence in Spain by age group, with epidemic waves and the highest peak during the sixth wave, particularly among younger populations. Adapted from ISCIII COVID-19 surveillance webpage[101].*

Overall, the pediatric population in Spain showed a lower burden of acute COVID-19 and generally milder clinical manifestations, in line with reports from other countries. In a multicenter prospective study involving 76 Spanish hospitals 1,200 children with SARS-CoV-2 infection most cases were mild, severe disease requiring admission to the PICU was primarily associated with post COVID-19 conditions, older age, and specific

underlying conditions, especially cardiac disease, asthma or recurrent wheezing, and liver disease[102].

Due to limited testing in early 2020, Spain established the Spanish National Seroepidemiological Study of SARS-CoV-2 Infection (ENE-COVID) serosurvey to better estimate SARS-CoV-2 exposure during the first wave. In June 2020, national seroprevalence was 5.2%. Values were lower in children ranging from 2.9% in those aged 5–9 years to 4.1% in those aged 10–14 years[103]. Comparable national estimates for later waves are unavailable, but regional studies showed increasing prior infection: in mid-November 2020, seroprevalence in Catalonia was 15.3% in adults and 11.5% in adolescents aged 13–15 years, while anti-nucleocapsid seroprevalence reached 58.9% in Navarre by May 2022 and 71% in the Valencian Community by October 2022[104–106].

7. Acute disease in adults and children

SARS-CoV-2 is transmitted mainly through inhalation of respiratory particles and through deposition of these particles onto the nasal, oral, or conjunctival mucosa. Transmission can occur before symptom onset.

The incubation period shortened over the course of the pandemic: pooled estimates from early 2020 were around 6.5 days, during Delta around 4.3 days, during Omicron around 3–4 days, and in one BA.5 study around 2.6 days[107,108]

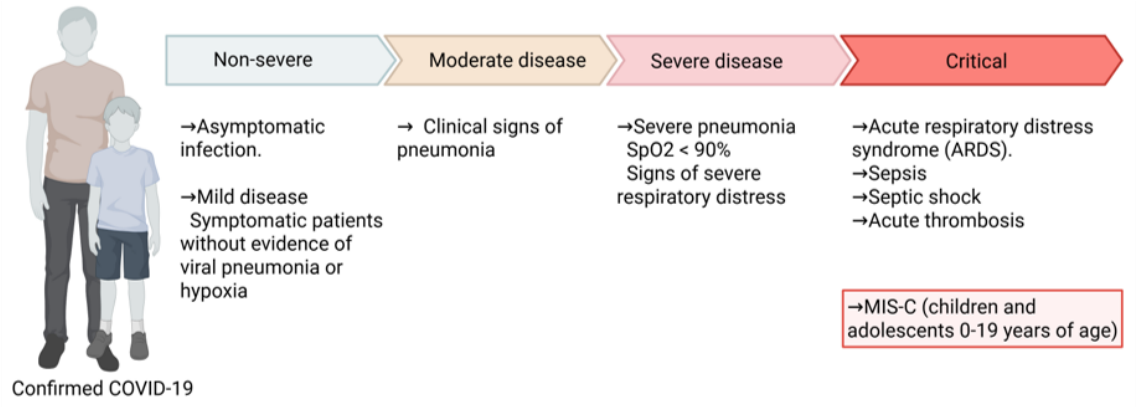


Figure 7. Clinical classification of COVID-19 severity. *The spectrum of COVID-19 severity in confirmed cases, ranging from non-severe to critical disease. Adapted from COVID-19 Clinical Management: Living Guidance (WHO)[109]. Created with BioRender.com.*

Clinical manifestation of COVID-19 can vary widely (**Figure 7**) and differs between adults and children. Children are more often asymptomatic; usually develop the same types of COVID-19 symptoms as adults, but these are generally less frequent and associated with lower rates of severe disease and death. Most often symptoms are fever and cough, although sore throat, rhinorrhea, headache, fatigue, shortness of breath, nausea, vomiting, and diarrhea are also described. Infants may present with poor feeding and unexplained fever[109].

Severe disease, in adults as in children, is more common in those with underlying conditions such as chronic lung disease, obesity, neurological disorders, cardiovascular disease, or immunosuppression[109].

Critical disease developed in about 5% of adult cases and included different complications summarized in **Figure 7**[109].

Severe to critical diseases and death were strongly associated with individual risk factors, including male sex, Asian and Black ethnic backgrounds, higher body mass index, and chronic disease[107,109].

Wave-to-wave symptom changes reflect both variant biology and changing population immunity/vaccination (**Figure 8**).

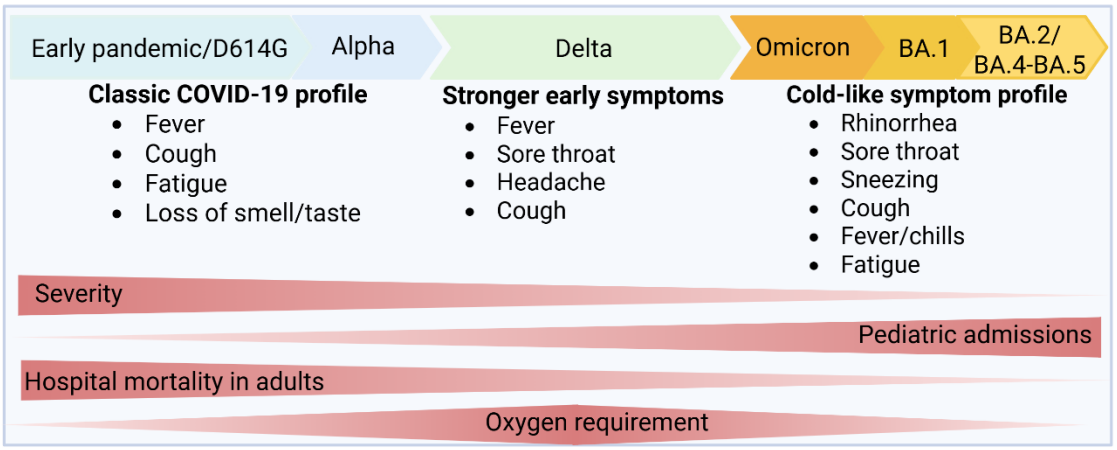


Figure 8. Changes in symptom profile and clinical outcomes across SARS-CoV-2 waves. *Over time, severity, adult hospital mortality, and oxygen requirement decreased, whereas pediatric admissions increased during the Omicron period. Created with BioRender.com.*

Early pandemic infections, including the D614G era and Alpha, were more often associated with the classic COVID-19 profile (**Figure 8**). Delta was linked to a greater

early symptom burden. The largest clinical shift occurred with Omicron, which was more presented with cold-like symptoms. Later Omicron sublineages, including BA.2 and BA.4/BA.5, generally maintained this Omicron-like symptom profile[110,111].

Studies showed that in-hospital mortality among adults hospitalized with COVID-19 declined with waves, particularly in older adults, likely owing to both increasing acquired immunity and lower average virulence of later variants. Within the Omicron period, BA.1 was also associated with higher mortality than later sublineages such as BA.2 and BA.5[112].

Regarding the pediatric population, the Omicron wave was associated with the highest number of pediatric admissions, but disease severity was lower than during the Alpha and Delta waves. The proportion of hospitalized children meeting composite severe-disease outcomes declined across waves, despite the higher number of admissions during Omicron. In addition, infants accounted for a larger proportion of hospitalizations during Omicron. The oxygen requirement was lowest during Omicron and highest during Delta for both cohorts[113–115].

The infectious period of SARS-CoV-2 is usually considered to last up to 10 days in symptomatic individuals, whereas a shorter isolation period of 5 days may be sufficient for asymptomatic infection[109].

8. Clinical management and long-term consequences of COVID-19

Viral load is a key parameter in both the diagnosis and clinical management of SARS-CoV-2 infection, as it reflects the amount of viral RNA present in a clinical specimen and provides direct information about viral replication, infectiousness, and response to antiviral treatment.

8.1. Diagnosis

Diagnosis of SARS-CoV-2 infection is based mainly on direct detection of the virus in respiratory specimens. The principal methods are transcription polymerase chain reaction (RT-qPCR) and rapid antigen tests.

RT-qPCR is the most sensitive test for the diagnostic of acute infection. The viral RNA usually becomes detectable by RT-qPCR about 2 days before symptom onset (**Figure 4A**) and, in early pandemic studies, often peaked around symptom onset or within the first few days after symptoms began. RT-qPCR positivity after the first 1–2 weeks often reflects residual viral RNA rather than ongoing infectiousness[116,117].

Diagnostic principles are largely the same in adults and children, with RT-qPCR remaining the reference standard in both groups. Age-related differences appear to affect mainly rapid antigen tests, whose sensitivity may be somewhat lower in pediatric populations[118,119]

Diagnostic principles are largely the same in adults and children, with RT-qPCR remaining the reference standard in both groups. Age-related differences appear to affect mainly rapid antigen tests, whose sensitivity may be somewhat lower in pediatric populations[120,121].

The clinical use of antibody serology tests for SARS-CoV-2 has become limited. Because most of the population has been infected and or vaccinated with S-based vaccines, many individuals already have antibodies against the S, which reduces the value of S-directed serology for identifying prior infection. Although serological tests may still be useful in selected situations, such as evaluation of previous infection through detection of anti- N antibodies or support for the diagnosis of post-infectious conditions[116,122].

8.2. Treatment

In general, the treatment of acute COVID-19 depends on disease severity and includes comprehensive supportive care aimed at relieving symptoms and preventing complications (**Figure 9**). The WHO and the Infectious Diseases Society of America (IDSA) have developed management guidelines in which treatment choice depends on several factors, including symptom duration, severity of illness, risk factors for progression, and patient age[109,123].

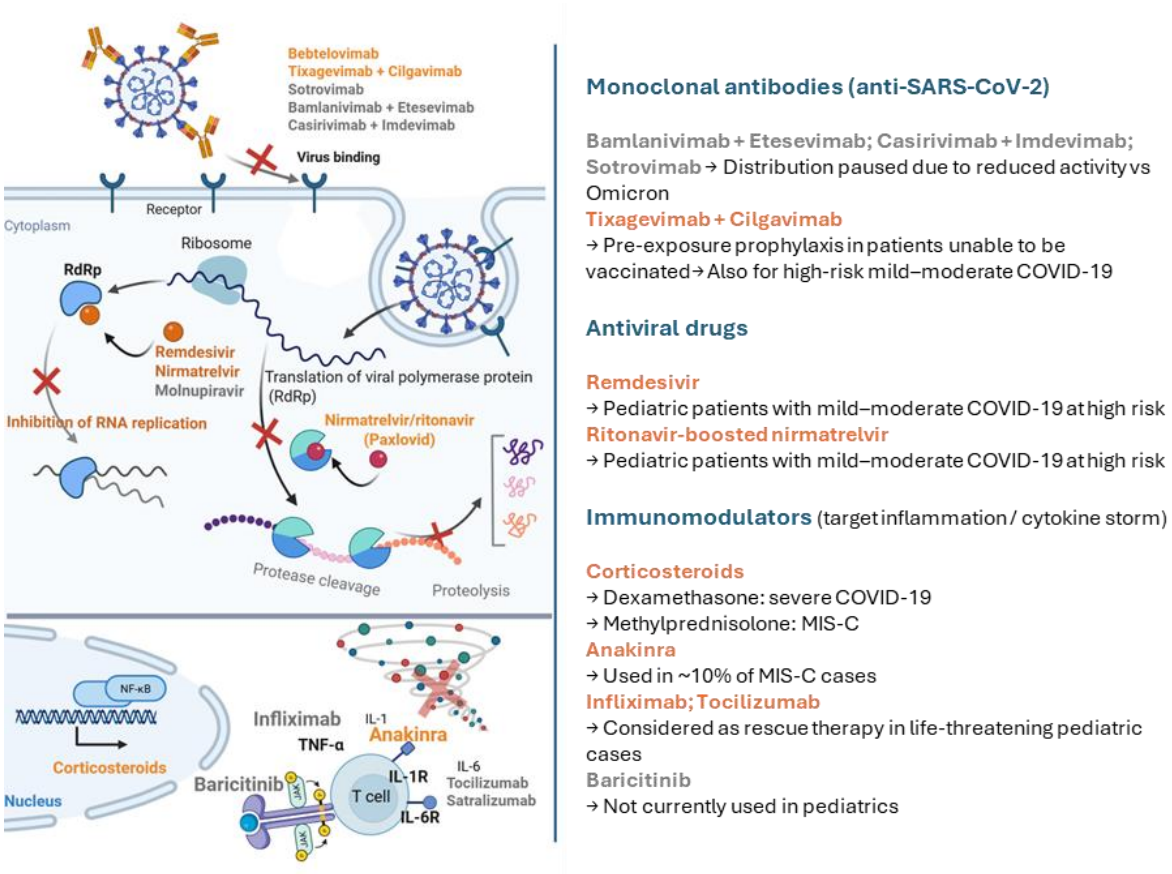


Figure 9. Therapeutic targets and treatments for SARS-CoV-2 infection. *The stages of the SARS-CoV-2 life cycle and corresponding therapeutic interventions, including viral entry, RNA replication, protein processing, and host inflammatory responses. Therapies highlighted in orange are used in pediatric patients, whereas those in grey are not routinely used. Adapted from Rotulo at all[33]. Created with BioRender.com.*

Antiviral therapy is mainly used to reduce viral replication and is most effective in the first 5–7 days after symptom onset. Recommended antiviral options include nirmatrelvir/ritonavir and remdesivir, while some patients later progress to severe disease, in which case immunomodulatory treatment such as corticosteroids, interleukin-6 inhibitors, or Janus kinase inhibitors may be indicated.

In children, acute COVID-19 management is most often supportive, although severe cases may still require targeted therapy according to clinical severity and risk profile. Nirmatrelvir/ritonavir (Paxlovid) can be used for children older than 12 years (weight ≥40 kg). Remdesivir is approved for children who are more than 28 days old with a weigh superior to 3 kg.

8.3. Vaccines

COVID-19 vaccines were developed rapidly through international collaboration, taking advantage of prior coronavirus research, and accelerated but still regulated clinical development pathways. Comirnaty, In December 2020, and Spikevax, in January 2021 were granted emergency use authorization by the European commission[124].

The first authorized vaccines platforms were mainly mRNA vaccines (Pfizer-BioNTech/Comirnaty and Moderna/Spikevax), adenoviral vector vaccines (AstraZeneca and Janssen), and later protein-based vaccines (Novavax, Bimervax).

In children, mRNA vaccines have been most widely used because they were the first to receive pediatric authorization and have remained the main products recommended in younger age groups.

In Europe, Comirnaty was first authorized for adolescents aged 12–15 years in May 2021. The vaccination of adolescents aged 12 years and older began in Spain in June 2021. Comirnaty was then authorized for children aged 5–11 years in November 2021, and Spain started vaccinating this age group on 15 December 2021. Later, the European Medicines Agency recommended extending Comirnaty to children aged 6 months to 4 years. Moderna (Spikevax) was later authorized for children; by March 2022, official Spanish documents listed Spikevax for individuals aged 6 years and older, and by October 2022 its indication had expanded to children from 6 months of age[124,125].

By 2026 there were 50 COVID-19 vaccines that have received some form of regulatory authorization (full approval, license, or emergency use) in at least one country [126].

Ongoing genetic evolution of SARS-CoV-2 and the emergence of immune-escape variants made periodic vaccine reformulation necessary, resulting in adapted EU vaccines targeting BA.1 and BA.4/5 in 2022, XBB.1.5 in 2023, JN.1 in 2024, and LP.8.1 for 2025–2026[127–129].

In Spain, COVID-19 vaccine uptake was high during the primary vaccination campaign (December 2020 – 2022), with 40.7 million people completing the full schedule, corresponding to 86.0% of the total population and 92.6% of those older than 12

years[130]. By June 2023, 57.3% of children 5-12 years old got at least one dose and 47,6% obtained full schedule[131,132].

From 2023 onwards, EU/EEA COVID-19 vaccination strategies transitioned to a targeted, risk-based approach, prioritizing older adults, individuals with chronic or immunocompromising conditions, pregnant women, healthcare workers, and residents of long-term care facilities. In the pediatric population, vaccination is currently primarily recommended for children older than 6 months with underlying medical conditions, rather than for all healthy children[133,134].

8.4. Post COVID-19 condition (long COVID)

One more condition that can occur after acute COVID-19 is post-COVID-19 condition (PCC), also known as long COVID. PCC can affect both adults and children, although it is more frequently reported in female adults[135]. Approximately 4% of children and 10–20% of patients with COVID-19 experience persistent symptoms lasting weeks to months after apparently cleared acute SARS-CoV-2 infection[136,137].

It is characterized by persistent or newly developed symptoms that usually appear within three months of the acute illness, last for at least two months, and cannot be explained by another diagnosis[138].

The pathogenesis of post-COVID-19 condition remains unclear and is likely multifactorial, involving viral persistence, immune dysregulation, autoimmunity, endothelial dysfunction, microthrombosis, and altered neuroimmune signaling[136]. Omicron infection appears to be associated with a lower risk than Delta and pre-Delta variants, while vaccination before infection and antiviral treatment during acute COVID-19 may reduce the risk. In contrast, reinfection increases the likelihood of long COVID and may either trigger new symptoms or worsen existing ones, with risk rising cumulatively after repeated infections[139].

In adults, the most reported symptoms are fatigue, dyspnea (shortness of breath), cognitive dysfunction (“brain fog”), sleep disturbance, chest pain, palpitations, and reduced exercise tolerance[135]. Adults more often report persistent cardiopulmonary and physical symptoms[140]. In children and adolescents, fatigue is also common, but

symptoms more frequently reported compared with controls include altered smell or anosmia, headache, anxiety, and other neuropsychological or functional symptoms affecting school performance, physical activity, behavior, and social interactions[141,142].

There is currently no specific curative treatment for long COVID; management is supportive, multidisciplinary, and symptom-based, focusing on rehabilitation, symptom relief, and improvement of daily functioning[143].

Multisystem inflammatory syndrome after SARS-CoV-2

As described previously, some individuals, depending on host factors such as immune response, age, and comorbidities, may develop severe or critical manifestations following SARS-CoV-2 infection[109]. However, after recovery of acute infection, in a subset of patients, an exaggerated and dysregulated immune response can lead to post-infectious complications, including multisystem inflammatory syndrome (MIS) in the short term (around one month after acute infection)[144]. In addition, still undefined mechanism(s) can lead to post COVID-19 condition, which has long term effects.

Multisystem inflammatory syndrome can affect children (MIS-C), adults (MIS-A), and, more rarely, neonates (MIS-N). Although all forms are uncommon, MIS-C is more frequently reported than MIS-A, whereas MIS-N represents the rarest presentation. MIS is characterized by a hyperinflammatory state with widespread involvement of multiple organ systems, particularly cardiovascular, gastrointestinal, and immune systems. MIS typically occurs weeks after the initial infection and is thought to result from immune dysregulation rather than direct viral injury, leading to excessive cytokine release, endothelial dysfunction, and organ damage. Treated MIS patients generally show favorable outcomes with resolution mainly cardiac dysfunction, although monitoring is advised[145]. MIS-C was first recognized in May 2020, followed by MIS-A later in October 2020, whereas the first cases of MIS-N were described in 2021[146,147].

9. Multisystem inflammatory syndrome in neonates

Multisystem inflammatory syndrome in neonates (MIS-N) is a very rare complication associated with maternal or perinatal SARS-CoV-2 exposure, currently described mainly through case reports, case series, and systematic reviews rather than population-based incident studies[148].

MIS-N is defined as an inflammatory syndrome occurring in neonates (up to 28 days of life) with confirmed maternal SARS-CoV-2 infection or exposure during pregnancy, in the absence of an alternative diagnosis[149]. The most common manifestations (**Figure 10**) are respiratory distress and cardiovascular instability, with the cardiovascular

system being the most frequently affected, including shock, cardiac dysfunction, arrhythmia, and coronary abnormalities. Respiratory involvement commonly presents distress and pulmonary complications. Neurological, gastrointestinal, hepatic, renal, and hematological systems may also be involved[148–150]. Fever and rash are observed in a proportion of cases. Mortality is estimated at approximately 9–11%[149].

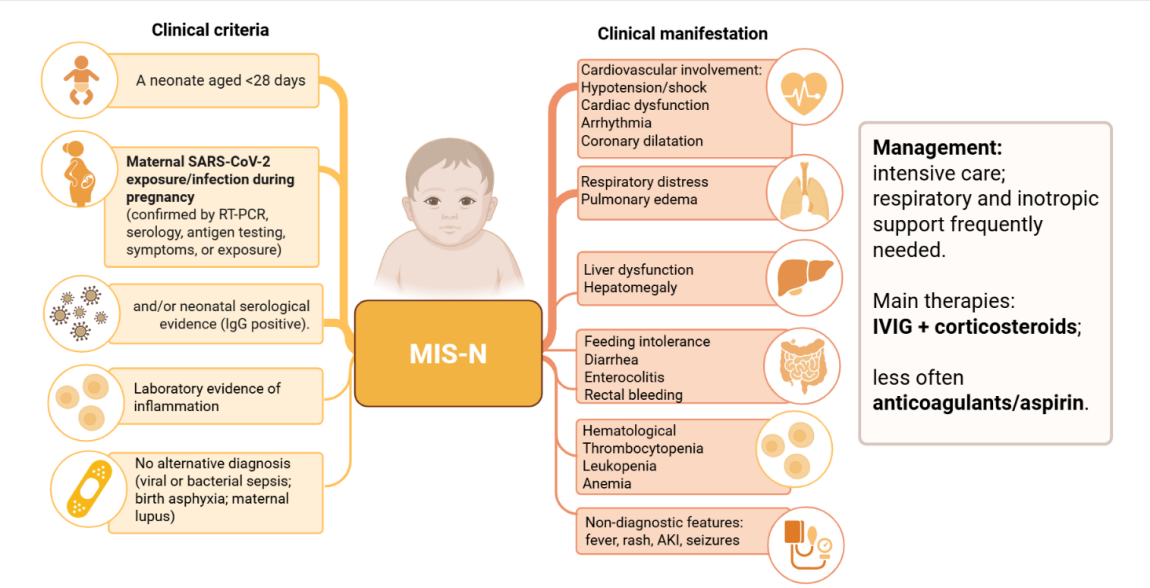


Figure 10. Overview of multisystem inflammatory syndrome in neonates (MIS-N). *Summary the clinical criteria, manifestations, and management of MIS-N. Adapted from Lakshminrusimha et al.[150], Muthiah et al[149]., and Molloy et al[148]. Created using BioRender.com.*

Laboratory findings in MIS-N commonly indicate systemic inflammation and coagulation activation, with elevated CRP, ferritin, procalcitonin, lactate dehydrogenase, D-dimer, and IL-6, as well as increased cardiac enzymes. Hematological abnormalities such as thrombocytopenia and thrombocytosis have also been described. Electrocardiographic findings may include sinus tachycardia, supraventricular tachycardia, bradycardia with prolonged QTc interval, and atrioventricular block[149].

Almost all neonates with MIS-N required admission to intensive care. Of those with available data, 40% required inotropic support and 56.1% required respiratory support, including intubation in over half of supported cases. Immunomodulatory therapy, mainly IVIG and corticosteroids, was administered in the majority of patients,

while anticoagulants and aspirin were used less frequently. No cases treated with biologic agents or convalescent serum were reported[149,150].

The underlying mechanisms are thought to involve either transplacental transfer of maternal antibodies or vertical transmission of infection leading to endogenous fetal antibody production[149]. Although maternal antibodies are generally protective, transplacentally transferred IgG may in rare cases trigger hyperinflammation and multisystem injury. The immature neonatal immune response, including limited IgM production, may further contribute to immune dysregulation and organ involvement[148].

10. Multisystem inflammatory syndrome in adults

MIS-A is a rare but severe hyperinflammatory complication of SARS-CoV-2 infection occurring in adults, typically defined in individuals ≥21 years of age, with most reported cases affecting young males to middle-aged adults[151,152]. The prevalence of MIS-A has been reported to range from 0.2% to 11.7% among studied SARS-CoV-2 infection cases[153,154]. However, the true frequency may be underestimated, as some cases can be misdiagnosed as a biphasic or recurrent course of acute COVID-19[153]

The pathophysiology of MIS-A remains incompletely understood. It is thought to occur 4-6 weeks after SARS-CoV-2 infection due to a dysregulated innate and adaptive immune response, with macrophage activation, B- and T-cell involvement, cytokine release, and antibody production leading to systemic hyperinflammation and multiorgan involvement. Proposed triggers include persistent viral antigens, autoantibodies, and viral superantigen-like activity[155].

Compared with MIS-N, MIS-A has a more clearly established case definition, developed by the CDC, largely because a greater number of adult cases have been reported and characterized[152]. The case definition and diagnostic criteria for MIS-A are summarized in **Figure 11**.

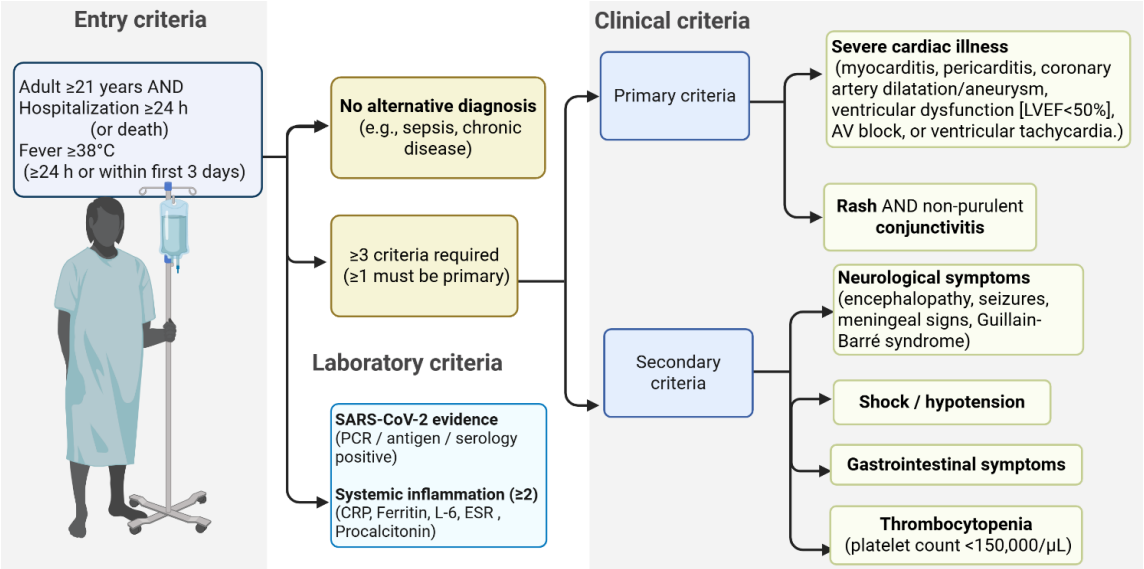


Figure 11. CDC case definition of multisystem inflammatory syndrome in adults (MIS-A). *The figure summarizes the diagnostic criteria, including entry criteria, exclusion of alternative diagnoses, ≥3 clinical criteria (≥1 primary), and laboratory evidence of SARS-CoV-2 infection and systemic inflammation. Created using BioRender.com.*

Fever and rash are among the most common presenting symptoms. The cardiovascular system is most frequently affected, followed by gastrointestinal and mucocutaneous involvement. Cardiac manifestations commonly include shock at presentation and left ventricular dysfunction, with many patients requiring intensive care admission. Compared with MIS-C, MIS-A is associated with higher mortality.[151,153,155]

Currently, there are no standardized treatment guidelines for MIS-A; management is largely extrapolated from MIS-C and severe COVID-19 and includes supportive care, immunomodulatory therapy with corticosteroids and/or IVIG, and, in severe or refractory cases, biologic agents such as IL-1 or IL-6 inhibitors. Anticoagulation is often considered because of the prothrombotic state[151,155,156].

11. Multisystem inflammatory syndrome after SARS-CoV-2 vaccination

Multisystem inflammatory syndrome after SARS-CoV-2 vaccination (MIS-V) has been rarely reported in both children and adults. It presents systemic hyperinflammation and multisystem involvement, resembling MIS-C or MIS-A. Only around 26 cases have been reported worldwide[157].

Reported MIS-V cases have mostly appeared as isolated case reports or small series during the early vaccination period. They have been described after mRNA vaccines (Pfizer-BioNTech BNT162b2 and Moderna mRNA-1273), adenoviral vector vaccines (AstraZeneca ChAdOx1 nCoV-19 and Johnson & Johnson/Janssen Ad26.COV2.S), and rarely after inactivated vaccines such as CoronaVac/Sinovac[157–159].

Overall, MIS-V appears to be extremely rare, and available evidence indicates that vaccination reduces the risk of MIS-C following SARS-CoV-2 infection[160].

12. Multisystem inflammatory syndrome in children

Despite the mild or asymptomatic nature of acute COVID-19 in children, serious post-infectious complications can develop, demonstrating that the pandemic affected the pediatric population in a distinct and clinically important way. MIS-C accounted for a substantial number of pediatric hospitalizations during the pandemic and was associated with significant disease severity, frequently requiring intensive care due to multisystem involvement and cardiovascular complications.

MIS-C was first described in spring 2020, when Riphagen et al. reported clusters of children and adolescents requiring intensive care admission for a multisystem inflammatory condition with features overlapping KD and toxic shock syndrome[12]. Following these initial reports, comparable cases were described in children from various parts of the world[161].

MIS-C is also known as pediatric multisystem inflammatory syndrome (PMIS), pediatric inflammatory multisystem syndrome temporally associated with SARS-CoV-2 (PIMS-TS), pediatric hyperinflammatory syndrome, or pediatric hyperinflammatory shock.

12.1. Case definition

MIS-C usually occurs 2–6 weeks after SARS-CoV-2 infection, with rare cases reported up to 16 weeks later[162]. By May 2020, the Royal College of Paediatrics and Child Health (RCPCH) had developed early UK guidance for PIMS-TS/MIS-C to support rapid clinical recognition and management of suspected cases during the first reports of the syndrome (**Table 1**) [163].

RCPCH PIMS-TS	Persistent fever >38.5°C **AND** systemic inflammation (neutrophilia/elevated CRP/ lymphopenia) **AND** single or multisystem organ dysfunction (shock/ cardiac/ renal/ respiratory/ gastrointestinal/ neurological involvement). **AND** exclusion of other microbial causes (bacterial sepsis, staphylococcal or streptococcal shock syndrome, enterovirus). **AND** SARS-CoV-2 RT-qPCR may be positive or negative.
WHO MIS-C	Patients 0–19 years of age + fever > 3 days **AND** 2 of the following: 1. Rash/conjunctivitis/mucocutaneous signs. 2. Hypotension/shock. 3. Cardiac involvement. 4. Evidence of coagulopathy (by PT, PTT, elevated d-Dimers). 5. Acute gastrointestinal problems. **AND** Elevated ESR, CRP, or procalcitonin. **AND** No other obvious microbial cause (including bacterial sepsis or staphylococcal/streptococcal shock syndrome). **AND** Positive RT-qPCR, antigen test, serology, or likely contact with COVID-19 case.
CDC MIS-C	<21 years of age that meets: *The clinical AND the laboratory criteria (Confirmed); OR* *The clinical criteria AND epidemiologic linkage criteria (Probable); OR* *The vital records criteria (Suspect)* **Clinical Criteria:** fever ≥38.0°C + requiring hospitalization/death + CRP ≥3.0 mg/dL (30 mg/L) **AND** ≥2 of the following: 1. Cardiac involvement. 2. Mucocutaneous involvement. 3. Shock. 4. Gastrointestinal symptoms. 5. Hematologic abnormalities (platelets <150,000/µL or ALC <1,000/µL). **AND** No more likely alternative diagnosis (including KD). **Laboratory Criteria:** evidence of SARS-CoV-2 infection: positive RT-qPCR/NAAT, antigen test, or serology up to 60 days before or during hospitalization. **Epidemiologic Linkage Criteria:** close contact with a confirmed or probable COVID-19 case within 60 days before hospitalization. **Vital records criteria:** MIS-C listed as an underlying or contributing cause of death on the death certificate.

Table 1. Comparison of MIS-C/PIMS-TS case definitions. *Summary of main diagnostic criteria proposed by the RCPCH[163], WHO[13], and CDC[164].*

Subsequently, clinical case definitions were established by the WHO and CDC to standardize diagnosis and reporting (**Table 1**)[13,164]. The WHO definition provides a broad clinical framework for identifying suspected MIS-C, whereas the CDC definition is more specific and intended for surveillance. The CDC definition was updated in 2023

to improve accuracy and reduce misclassification, particularly because respiratory involvement is more typical of acute COVID-19 than MIS-C, while renal and neurological findings may overlap between both conditions[165].

Children with MIS-C often present with severe inflammation, accompanied by persistent fever, elevated C-reactive protein (CRP) levels, and the involvement of at least 2 of 7 organ systems (**Figure 12**) [165–167].

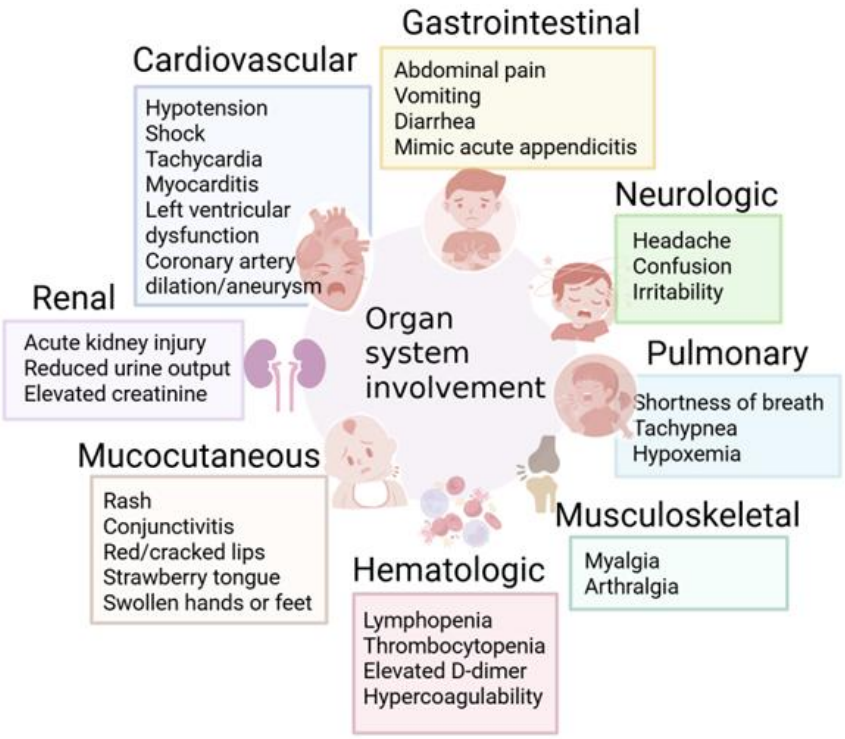


Figure 12. Organ system involvement in MIS-C. *The figure summarizes the multisystem clinical presentation of MIS-C. Adapted from El Rassi at all[168]. Created using BioRender.com.*

Multisystem involvement is a defining feature of MIS-C, with gastrointestinal and mucocutaneous manifestations among the most frequently reported (**Figure 12**). Gastrointestinal symptoms commonly include abdominal pain, vomiting, diarrhea, and elevated liver enzymes, while mucocutaneous involvement is characterized by rash, oral mucosal inflammation, conjunctival injection, and extremity changes (**Figure 13**)[166]. Cardiac involvement is a particularly concerning feature of MIS-C and represents a major determinant of disease severity and prognosis. Patients with decreased ventricular ejection fraction (≤55%), coronary artery abnormalities, or elevated troponin levels showed evidence of myocardial damage[166,169]. Hematologic abnormalities are also frequent, particularly lymphopenia, thrombocytopenia, and

anemia. Among the most typical laboratory abnormalities are elevated ESR or CRP, neutrophilia, high ferritin, hypoalbuminemia, increased D-dimer, coagulation abnormalities, and elevated fibrinogen[166,170,171].

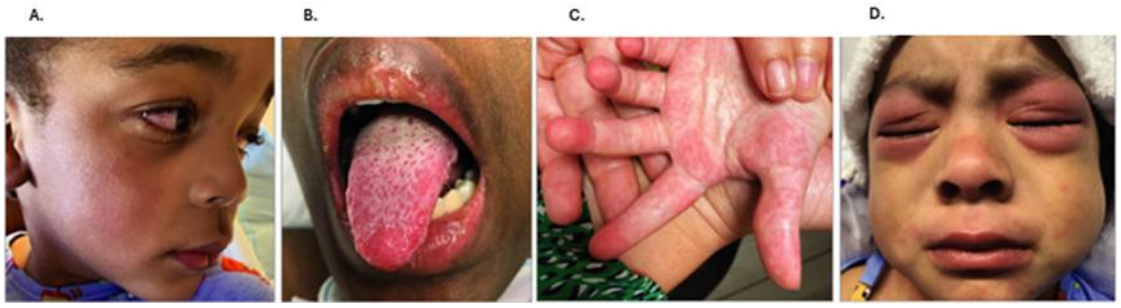


Figure 13. Peripheral mucocutaneous changes in MIS-C. *Representative mucocutaneous manifestations observed in patients with MIS-C. (A). Non-exudative conjunctival injection with malar erythema. (B). Lip hyperemia and cracking with "strawberry tongue." (C). Palmar erythema. D. Periorbital edema and erythema. Reproduced with permission from Young et al[172].*

MIS-C is a severe life threatening condition and approximately half of affected children require intensive care unit (ICU) admission because of more critical symptoms such as cardiac involvement (elevated troponin or N-terminal prohormone of brain natriuretic peptide/NT-proBNP), hemodynamic instability (shock or arrhythmia), or respiratory distress, and key parameters such as elevated inflammatory markers (D-dimer, C-reactive protein/CRP)[166,173–177]. Children in general inpatient care exhibit more stable vitals and less multi-organ involvement.

12.2. Risk factors

The exact risk factors for MIS-C are not fully established; however, several epidemiological, clinical, and immunological associations have been identified.

Proposed factors include lower pre-existing immunity to seasonal coronaviruses, school age, male sex, and certain ethnic backgrounds, particularly Black, Hispanic/Latino, and South Asian populations[164,178–180]. Children who develop MIS-C also appear more likely to have underlying conditions such as obesity, asthma, cardiac disease, and life-limiting conditions[178,181].

In addition, Lee et al. identified rare inborn errors in the OAS–RNase L antiviral pathway in a small subset of children with MIS-C, suggesting that impaired viral RNA

degradation and innate immune dysregulation may contribute to susceptibility. However, these findings explain only a minority of cases, indicating that MIS-C pathogenesis is likely heterogeneous[182]. Other genetic studies have also implicated variants in genes involved in antiviral defense and immune regulation, including DDX60, TMEM154, TLR3, TLR6, IL22RA2, and LYST, further supporting the role of innate immune dysfunction and dysregulated inflammatory responses in the development of MIS-C[183].

12.3. Epidemiology

Overall, MIS-C is an uncommon complication following SARS-CoV-2 infection and the incidence varies between populations and study periods. The incidence of MIS-C has varied substantially across countries and pandemic waves. Nationwide data from Israel showed that the incidence of MIS-C per 100,000 individuals younger than 18 years was 54.5 during the Alpha wave, 49.2 during the Delta wave, and markedly lower at 3.8 during the Omicron wave[184] Similarly, international studies have reported variable incidence rates: CDC surveillance data from the United States estimated approximately 13 MIS-C cases per 100,000 children, with a mortality rate of around 0.8%[185], while an Italian population-based study reported a cumulative incidence of 3.27 cases per 100,000 residents aged 0–18 years, and Spanish data reported approximately 8 cases per 100,000 children[186,187].

During the early stages of the pandemic, particularly in the pre-Alpha and Alpha waves, MIS-C cases were more frequent and often more severe[188–190]. However, with the rise of the Omicron variant in late 2021 and early 2022, the incidence of MIS-C cases significantly declined (**Figure 14)**. During the Omicron wave, the BA.1 subvariant became the dominant strain among patients admitted with MIS-C[190,191]. U.S. national surveillance data showed that the proportion of MIS-C cases decreased over time with successive SARS-CoV-2 variants, with 58.0% of cases occurring in the pre-Delta period compared to only 16.1% during the Omicron-dominant phase[192]. Similar trends were reported in the United Kingdom and Asian countries, including South Korea and Japan, demonstrating both reduced incidence and milder clinical presentations during the Omicron wave[193–195].

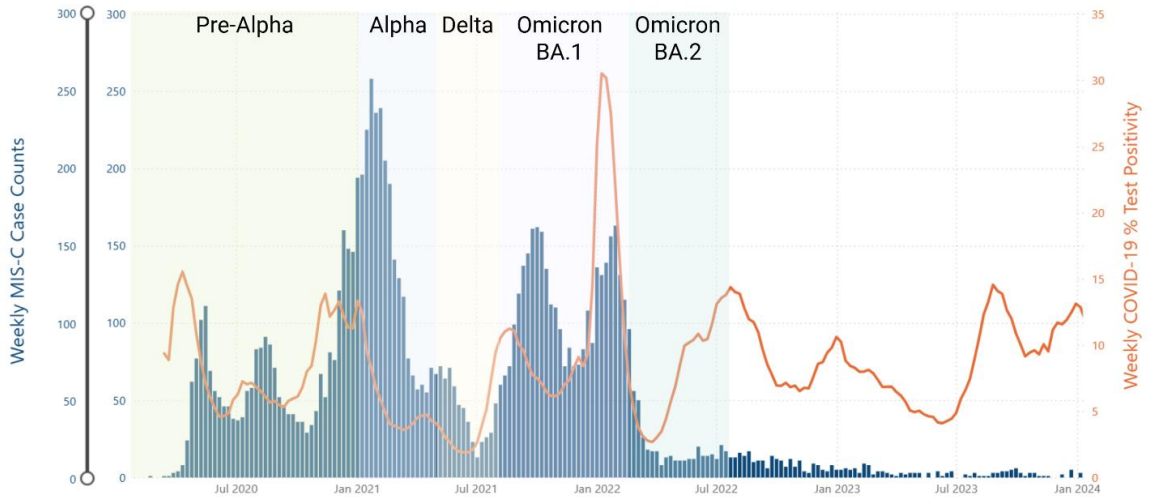


Figure 14. Epidemiology of MIS-C across SARS-CoV-2 variant waves. *Demonstration of temporal lag between peaks in SARS-CoV-2 infection and MIS-C cases. Blue columns represent weekly MIS-C case counts, while the orange line indicates weekly COVID-19 test positivity. The background shading divides the timeline into SARS-CoV-2 variant waves. Adapted from CDC data[185]; created with BioRender.*

Furthermore, Omicron-associated MIS-C cases were characterized by less severe organ involvement, with a decline in shock, cardiac, and respiratory complications, and a predominance of milder clinical phenotypes[184,194,196]. Israeli researchers, including Levy et al., reported that during the Omicron wave, MIS-C cases were associated with less severe cardiac involvement and a lower rate of intensive care unit admissions[184]. This decrease in cases is likely attributed to the lower pathogenicity of Omicron, along with increased immunity from vaccinations and prior infections, which helped to mitigate the severity and frequency of MIS-C during this period[177,181,189,197].

12.3.1. Age, sex, and ethnic distribution

MIS-C C is most often reported in school-aged children, with a median age around 8-10 years, and shows a slight male predominance[176,177,181,183]. Ethnic disparities have also been reported. MIS-C incidence was higher among Black, Hispanic/Latino, and Asian or Pacific Islander children compared with White children[176,181].

12.3.2. Epidemiology of MIS-C in Spain

In Spain, MIS-C has been reported as an uncommon but clinically important complication of pediatric SARS-CoV-2 infection. In a multicenter prospective study

including 1,200 Spanish children with SARS-CoV-2 infection, MIS-C represented 10.6% of cases and was one of the major clinical phenotypes associated with PICU admission, together with chronic cardiac disease, asthma or recurrent wheezing, and elevated inflammatory markers[102].

A Catalonia population-based study reported 152 MIS-C cases among 555,848 pediatric SARS-CoV-2 infections. The monthly MIS-C incidence was 4.1 per 1,000,000 people, and 273 per 1,000,000 SARS-CoV-2 infections, equivalent to approximately 1 MIS-C case per 3,700 infections. MIS-C incidence decreased markedly during the Omicron period[188].

13. Elements of Pathogenesis of MIS-C

MIS-C pathogenesis is multifactorial and driven by immune dysregulation, resulting in systemic hyperinflammation (**Figure 15**). Unlike acute COVID-19, MIS-C typically occurs after viral clearance, supporting a post-infectious etiology.

MIS-C typically develops several weeks after the initial SARS-CoV-2 infection, often when viral replication has already declined and patients are RT-qPCR-negative but Henderson serology-positive[198]. This timing suggests that the syndrome is not primarily caused by direct viral injury, but rather by an abnormal post-infectious immune reaction. In susceptible children, the initial immune response to SARS-CoV-2 may progress into uncontrolled activation of both innate and adaptive immunity[197].

13.1. Innate response

Innate immune dysregulation is central to MIS-C. Persistent antigen exposure leads to neutrophil overactivation, characterized by increased counts, elevated neutrophil-to-lymphocyte ratio, and upregulation of activation markers. Activated neutrophils release NETs, contributing to endothelial injury and thrombosis[199]. At the same time, innate immune cells produce high levels of cytokines (IL-1β, IL-6, TNF-α, CXCL9/10), sustaining inflammation (**Figure 15¡Error! No se encuentra el origen de la referencia.**) [200].

This occurs alongside activation of NF-κB and interferon pathways, with reduced expression of NF-κB inhibitors and increased interferon-stimulated genes in monocytes and dendritic cells[201].

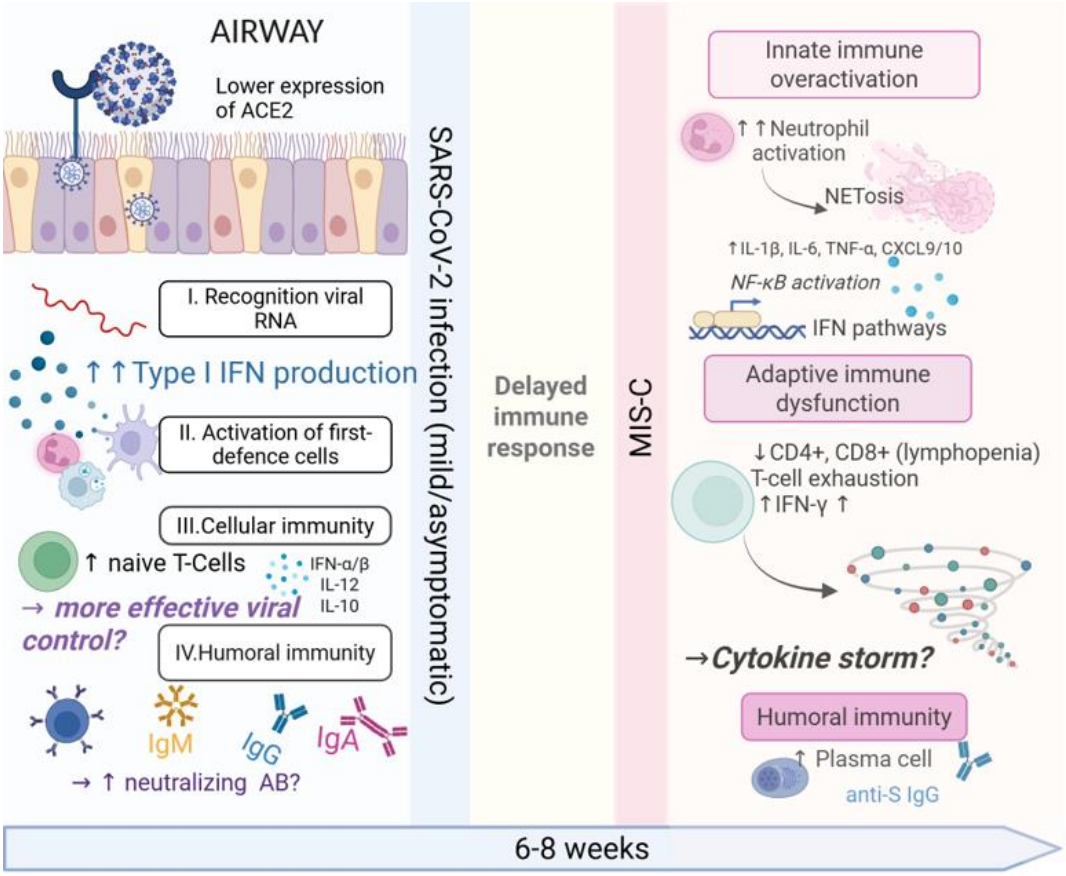


Figure 15. Immunopathogenesis of MIS-C following SARS-CoV-2 infection. *Summary of progression from acute SARS-CoV-2 infection in children to delayed immune dysregulation and MIS-C over 6–8 weeks. The hypotheses are written in italic. Adapted from Rotulo and all[33] , and Porrit and all[202]. Created by BioRender.*

13.2. Cellular response

MIS-C is characterized by lymphopenia due to apoptosis, redistribution, and impaired hematopoiesis[199].

T-cell abnormalities include reduced CD4+, CD8+, γδ T cells, and NK cells, along with CD8+ T-cell exhaustion (**Figure 15**)[203]. Despite this, abnormal activation is observed, including TRBV11-2 expansion and increased CX3CR1+ CD8+ T cells, associated with vascular inflammation[199]. A predominance of Th1 over Th2 responses further promotes inflammation[197].

Impaired cellular immunity, including reduced SARS-CoV-2–specific CD4+ and CD8+ T-cell responses, may further limit viral clearance and prolong antigen exposure[204]. This may promote IFN-γ–driven inflammation, macrophage activation, and tissue damage[197].

MIS-C is characterized by a strong cytokine storm that drives systemic inflammation and immune dysregulation. Previous reports identified elevated biomarkers associated with type II interferon (IFN) signaling (IFN-γ, CXCL9/MIG, CXCL10/IP-10), macrophage activation (IL-6, IL-10, tumor necrosis factor (TNF), CCL2/MCP1, CCL3/MIP-1-α, CCL4/MIP-1β, ferritin), and endothelial injury (vascular endothelial growth factor, VEGF)[205–207].

13.3. Humoral response

Most patients have detectable antibodies at onset despite low viral load. The response is dominated by anti-spike IgG, with lower IgM levels due to delayed timing. IgA may contribute to mucosal involvement, especially in patients with gastrointestinal manifestations[197,208].

B-cell dysregulation includes plasmablast expansion, suggesting a delayed antibody-mediated response after acute infection[208]. In severe cases, clonal B-cell expansion, somatic hypermutation, and IgG binding to activated cardiac endothelial cells have been reported, supporting a possible role for autoreactive antibodies and antibody-mediated endothelial injury[203].

13.4. The main current hypotheses for the origine of MIS-C pathogenesis

The underlying cause of MIS-C remains incompletely understood. However, current literature suggests that its development is likely multifactorial and may involve several overlapping mechanisms rather than a single cause.

Proposed triggers include persistent viral antigens, abnormal antibody responses, genetic susceptibility, and superantigen-like immune activation and are summarized in **Figure 16**.

1. Persistent viral antigen or viral reservoirs (antigenemia).

Some studies suggest that viral antigens, especially the spike protein, may persist in the body and continue to stimulate the immune system. This persistent antigenemia may act as an initial trigger for immune dysregulation in susceptible children. The presence of circulating spike protein could maintain immune activation even when viral RNA is no longer detectable in the blood[197].

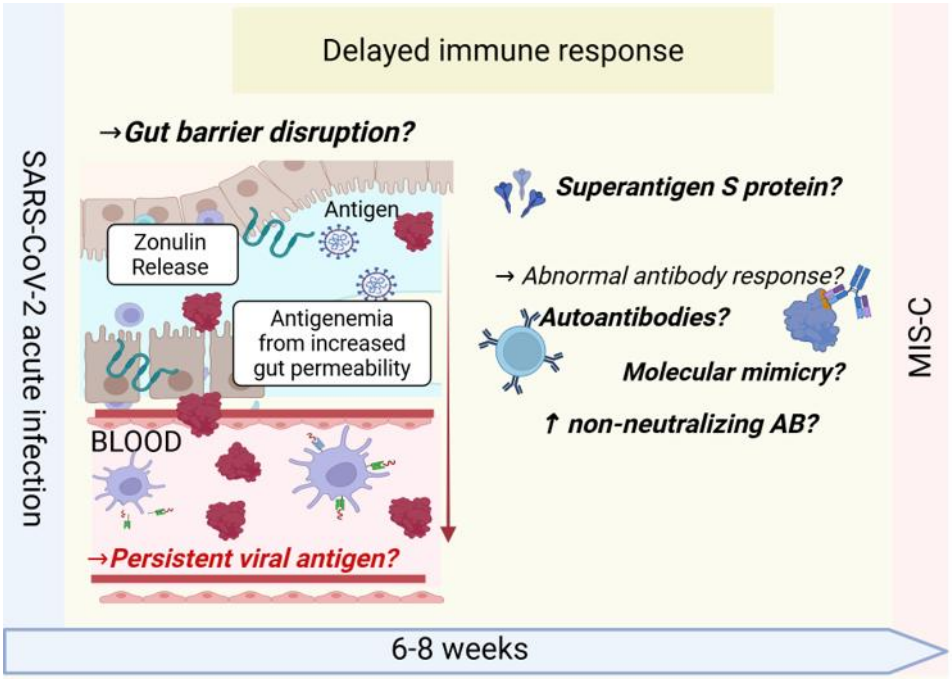


Figure 16. Proposed mechanisms involved in MIS-C pathogenesis after SARS-CoV-2 infection. *Adapted from Yonker and all[209], Boribong et all[210], and Bartsch et all[211].Created by BioRender.*

Persistent viral antigens, particularly the spike protein, may sustain immune activation despite the absence of detectable viremia. It has been proposed that the SARS-CoV-2 may persist as a reservoir in the gastrointestinal tract[209]. Circulating antigens may bind to antibodies and form immune complexes, which activate neutrophils through Fc receptors. This process can trigger NETosis, a form of neutrophil activation in which neutrophils release structures called neutrophil extracellular traps (NETs). While NETs contribute to pathogen defense, excessive formation leads to endothelial injury, thrombosis, and systemic inflammation.[210].

2. Imbalance between innate and adaptive immune responses leading to cytokine-driven hyperinflammation.

In children, the initial innate immune response, mainly mediated by type I interferons, usually limits viral replication and contributes to milder acute COVID-19[33,212].

IFN-γ typically enhances antigen presentation in various cell types, including monocytes, dendritic cells, and B cells[33,197]. Sustained IFN-γ signaling, although normally enhancing antigen presentation, may become dysregulated, contributing to impaired immune regulation[204].

Concurrently, innate immune activation results in the release of pro-inflammatory cytokines (IL-1β, IL-6, TNF-α), while Th1-driven responses further increase IFN-γ production[15]. These cytokines may amplify each other, creating a self-sustaining inflammatory loop that leads to endothelial dysfunction, increased vascular permeability, and multiorgan involvement characteristic of MIS-C[200].

3. Abnormal humoral immunity

An altered balance between protective neutralizing antibodies and Fc-mediated inflammatory antibody functions may contribute to MIS-C pathogenesis[211]. SARS-CoV-2-specific antibodies can form antigen–antibody immune complexes, which may activate Fc receptor–expressing innate immune cells and promote inflammatory pathways[213]. In support of this, MIS-C patients have been shown to maintain highly inflammatory, monocyte-activating SARS-CoV-2 IgG antibodies, while SARS-CoV-2 spike immune complexes have been reported to trigger neutrophil extracellular trap formation, suggesting a potential role for antibody-mediated innate immune activation in systemic inflammation[210,211].

4. Super-antigen-like activation

SARS-CoV-2 S has been proposed to induce superantigen-like activation, leading to broad, non-specific T-cell activation. This is supported by the expansion of TCR Vβ21.3 CD4 and CD8 T cells observed in many MIS-C cases[207,214]. Malik et al. showed that these expanded TRBV11-2+ T cells had high receptor diversity and limited SARS-CoV-2 specificity, supporting the hypothesis of broad, superantigen-like T-cell activation rather than a conventional antigen-specific response[215,216]. Such abnormal T-cell activation may contribute to cytokine release, including IFN-γ, IL-6, and TNF-α,

promoting systemic inflammation, shock, endothelial injury, and cardiac involvement[217].

Although detectable anti-spike antibody responses are commonly observed in MIS-C patients, experimental studies have not confirmed that the SARS-CoV-2 spike protein has intrinsic superantigen-like activity, and Vβ21.3-expanded T cells often show limited SARS-CoV-2 peptide specificity[218,219].

5. Autoimmunity

Molecular mimicry has been proposed as a mechanism in MIS-C, whereby immune responses against SARS-CoV-2 cross-react with host proteins after the acute infection has been resolved. For example, molecular mimicry between the SARS-CoV-2 nucleocapsid protein and the host protein Sorting nexin 8 may trigger cross-reactive antibodies and T cells, contributing to post-infectious immune activation, inflammation, and organ injury[220].

Autoantibodies may form antigen–autoantibody immune complexes that activate Fcγ receptors and complement pathways[202]. This can promote neutrophil activation, NETosis, cytokine and chemokine release. Detection of autoantibodies against cardiac, endothelial, and gastrointestinal tissues supports their role in organ injury.[180,202].

6. Gut microbiota dysbiosis

SARS-CoV-2 infection may disrupt gut microbiota and increase intestinal permeability. This allows translocation of viral antigens and microbial products into circulation, further promoting systemic inflammation[209,221]. Given the high prevalence of gastrointestinal symptoms in MIS-C, the gut–immune axis likely contributes to disease pathogenesis[183]. Permeability to bacterial antigen was proposed as an alternative explanation for the induction of TCR Vβ21.3 T cells independently of SARS-CoV-2 S protein.

13.5. The Role of the Immune System in the Change in MIS-C Epidemiology

The epidemiology of MIS-C has changed throughout the COVID-19 pandemic, with a decline in both incidence and severity over time. This reduction is likely related to increasing population immunity from previous SARS-CoV-2 exposure and vaccination, leading to more effective humoral and cellular responses (**Figure 17**) [184,197,222].

Antibody affinity maturation and immune memory may improve viral clearance, reduce persistent antigenemia, and lower the risk of dysregulated post-infectious inflammation. Cross-reactive immunity from previous SARS-CoV-2 variants or endemic coronaviruses may also support a faster and more controlled immune response. This involves memory B cells, which can rapidly produce higher-affinity antibodies, and cross-reactive CD4+ T cells, which recognize conserved coronavirus epitopes and help coordinate adaptive immunity. These responses may improve viral clearance and reduce prolonged immune activation that could contribute to MIS-C.

In addition, later variants such as Omicron have been associated with lower MIS-C rates, possibly because of differences in viral antigenicity and interactions with the immune system[184,222]. Overall, increasing immune protection and viral evolution may have raised the threshold needed to trigger the hyperinflammatory response characteristic of MIS-C (**Figure 17**).

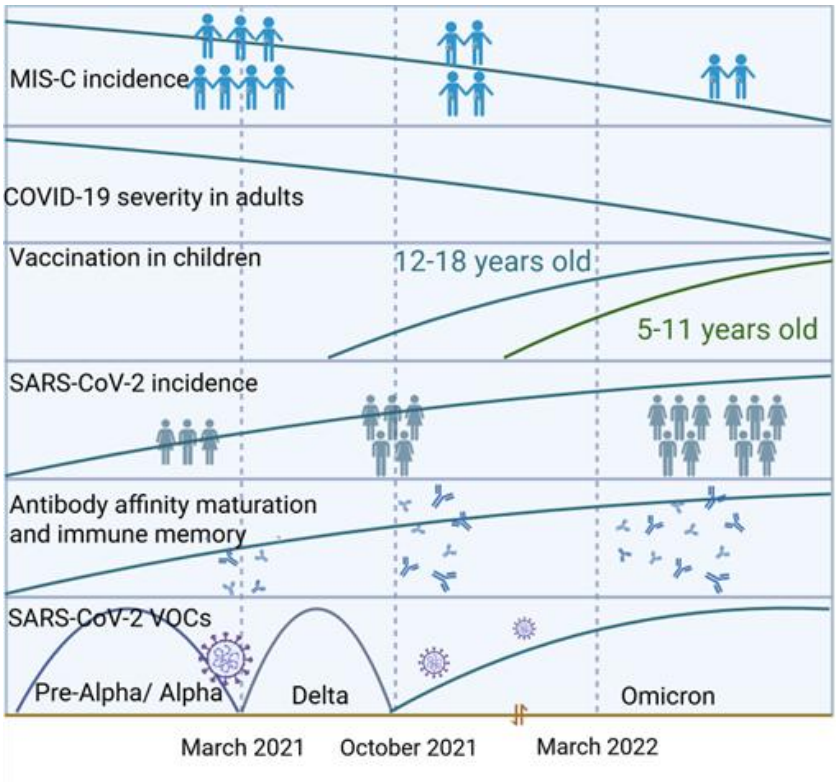


Figure 17. SARS-CoV-2 Variant Periods, Population Immunity, and MIS-C Incidence. *Schematic representation of the relationship between SARS-CoV-2 circulation, MIS-C epidemiology, and the development of immunity across the pre-Delta, Delta, and Omicron periods. Adapted from Castaldo et al. Created with BioRender.com.*

14. Diagnostic comparison with the pediatric inflammatory conditions

Hyperinflammatory syndromes in children represent a major diagnostic and therapeutic challenge because of their overlapping clinical features, heterogeneous immune mechanisms, and variable disease severity. As described above, MIS-C shares clinical and immunological overlaps with several pediatric inflammatory diseases. KD and childhood-onset Still's disease/systemic juvenile idiopathic arthritis (SD/sJIA) are among the pediatric inflammatory disorders that share several common manifestations, including persistent fever, elevated systemic inflammatory markers, mucocutaneous involvement, gastrointestinal symptoms, and potential cardiovascular complications. Despite these similarities, MIS-C, KD, and SD represent distinct inflammatory conditions with different triggers, age distributions, clinical patterns, and underlying immunopathological mechanisms[223–225]. Understanding their

similarities and differences is therefore essential for accurate differential diagnosis, appropriate treatment decisions, and identification of disease-specific biomarkers.

14.1. Other inflammatory conditions

14.1.1. Kawasaki disease.

KD is an acute systemic vasculitis of childhood that primarily affects medium-sized arteries, especially coronary arteries. It usually occurs in children under 5 years of age and is characterized by persistent fever together with mucocutaneous inflammation.

Clinically, KD presents with fever lasting at least 5 days, conjunctivitis, oral mucosal changes such as red or cracked lips and “strawberry tongue,” polymorphous rash, cervical lymphadenopathy, and changes in the hands and feet, including erythema, edema, or later desquamation. The most important complication is coronary artery involvement, including coronary artery dilation or aneurysm formation (**Figure 18**). Treatment starts early with IVIG (2g/kg) to reduce inflammation and prevent coronary artery aneurysms. High-risk or IVIG-resistant patients may need additional therapy, such as corticosteroids or infliximab. Children with coronary artery abnormalities require long-term cardiology follow-up[156].

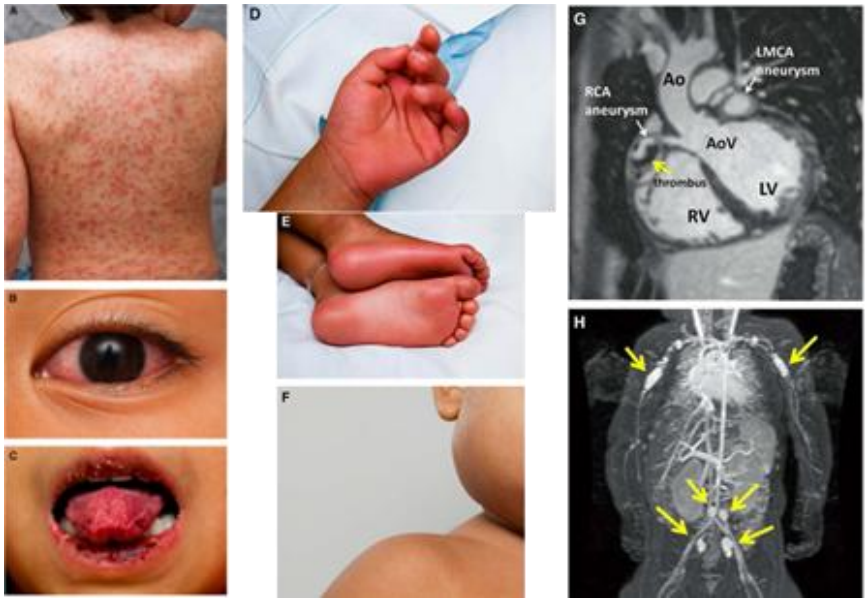


Figure 18. Clinical manifestations of classic KD. *(A). Polymorphous rash. B. Bilateral non-exudative conjunctival injection. C. Oral mucosal changes, including cracked lips and strawberry tongue. (D–E). Palmar and plantar erythema with swelling. (F). Cervical lymphadenopathy. (G). Coronary artery aneurysms. (H). Peripheral artery aneurysms. Reproduced with permission from McCrindle et al*[226].

14.1.2. Childhood-onset Still's disease, also known as Systemic Juvenile Idiopathic Arthritis.

SD is an autoinflammatory disease characterized by systemic inflammation rather than primarily joint-limited arthritis[227].

Clinically, SD typically presents with high spiking fever, evanescent salmon-colored rash, arthritis, lymphadenopathy, hepatosplenomegaly, and serositis (**Figure 19**). SD is usually a chronic or recurrent autoinflammatory disease in which arthritis is an important diagnostic feature. Laboratory findings often include markedly elevated inflammatory markers such as CRP, ESR, ferritin, leukocytosis, thrombocytosis, and anemia. A major complication is macrophage activation syndrome (MAS), a severe hyperinflammatory state with cytopenias, liver dysfunction, coagulopathy, and very high ferritin[227,228].

Treatment guidelines emphasize early control of systemic inflammation. The 2021 American College of Rheumatology guideline recommends biologic therapy for SD, especially agents targeting IL-1 or IL-6, and glucocorticoids may be used for severe systemic disease or MAS[229].

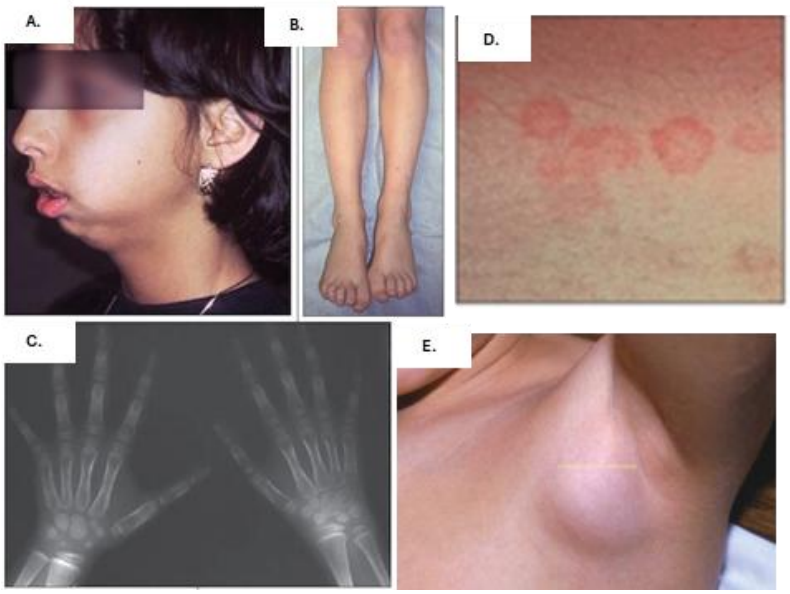


Figure 19. Clinical characteristics of juvenile idiopathic arthritis. *(A). Micrognathia. (B). Limb-length discrepancy. (C). Radiographic evidence of advanced bone maturation. (D). Salmon-pink rash. (E). Cervical lymphadenopathy. adapted from Marinescu and Ilowite[230], and from Rheum[231] with permission.*

14.2. Challenges of diagnostic criteria

An essential part of diagnosis is the exclusion of alternative causes. The main challenge is the overlap of clinical symptoms with other inflammatory, infectious, and rheumatologic conditions, such as KD, toxic shock syndrome, sepsis, macrophage activation syndrome, and SD (**Table 2**) [168].

Disease	Why it overlaps with MIS-C
KD	Fever, rash, conjunctivitis, mucosal changes, extremity changes, coronary artery involvement
Toxic shock syndrome	Fever, shock, rash, multiorgan dysfunction
Sepsis	Fever, hypotension, high inflammatory markers, organ dysfunction
Macrophage activation syndrome / HLH	Hyperferritinemia, cytopenias, liver involvement, coagulopathy, cytokine storm
SD	Fever, rash, high inflammation, arthritis, possible MAS
Acute severe COVID-19	Fever, respiratory disease, inflammation, organ involvement
Appendicitis / acute abdomen	Abdominal pain, vomiting, diarrhea, high inflammatory markers

Table 2. Diseases that overlap clinically with MIS-C. *Adapted from El Rassi and al.[168] and Henderson and al[232].*

14.2.1. MIS-C and KD phenotypes

MIS-C and KD share several clinical features, including persistent fever, mucocutaneous inflammation, rash, conjunctivitis, and possible coronary artery involvement (**Figure 20**). Because of this overlap, MIS-C was initially described in some patients as a Kawasaki-like illness. However, only a proportion of children with MIS-C meet the full diagnostic criteria for KD[168,233].

Several features help distinguish MIS-C from classic KD. MIS-C usually affects older children, most commonly school-aged children, whereas KD primarily affects children younger than 5 years. MIS-C is also more frequently associated with gastrointestinal symptoms, neurologic manifestations, shock, and left ventricular dysfunction. In contrast, KD is more classically associated with coronary artery aneurysms, although coronary abnormalities can also occur in MIS-C[234,235].

Laboratory findings also differ. Compared with KD, MIS-C is more often associated with lymphopenia, thrombocytopenia or lower platelet counts, and markedly elevated inflammatory markers such as CRP[234].

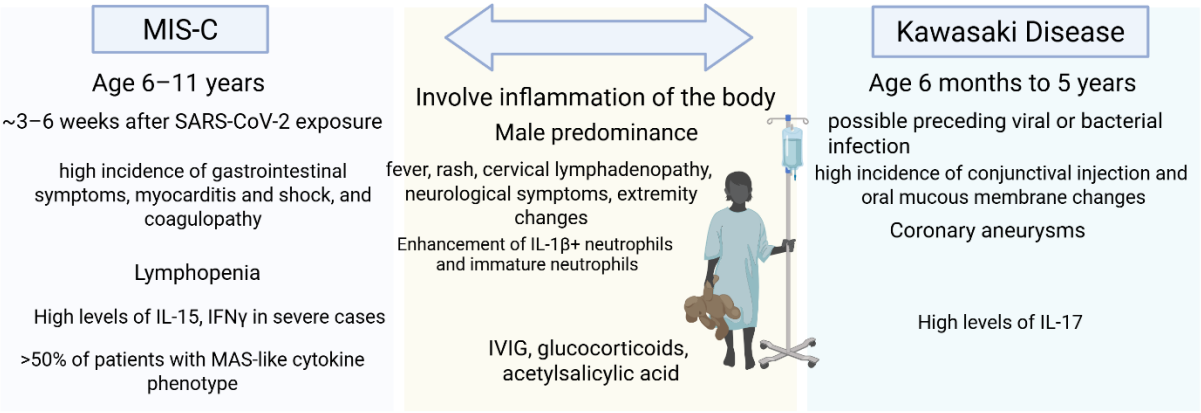


Figure 20. Comparison of MIS-C and KD. *The figure highlights key clinical and immunological similarities and differences between MIS-C and KD. Adapted from Sharma et al[223].; created with BioRender.*

14.2.2. Systemic juvenile idiopathic arthritis and MIS-C overlap.

It overlaps with MIS-C because both can show fever, rash, high CRP/ferritin, elevated cytokines, lymphocyte abnormalities, and multiorgan inflammation. Both conditions can also be complicated by macrophage activation syndrome, which may present with cytopenias, liver dysfunction, coagulopathy, hyperferritinemia, and shock[224,236].

The main distinction is that SD is usually a chronic or recurrent inflammatory disease, often with arthritis. MIS-C more often includes gastrointestinal symptoms, cardiac dysfunction, and evidence of recent SARS-CoV-2 infection[224].

15. Clinical management

The management of MIS-C is well established and based on current clinical Henderson guidelines[156,237]. The main goals of MIS-C treatment are to stabilize patients with life-threatening manifestations and to prevent long-term complications, including coronary artery aneurysms, myocardial fibrosis or scarring, and persistent cardiac conduction abnormalities. Long-term management includes cardiac follow-up as well as consideration of COVID-19 vaccination to provide ongoing protection (**Figure 21**).

15.1. Initial therapy

Initial management focuses on immunomodulatory therapy, antithrombotic treatment, and supportive care (**Figure 21**).

First-line therapy for most hospitalized patients consists of a combination of intravenous immunoglobulin (IVIG) and glucocorticoids. IVIG is administered at a dose of 2 g/kg, while glucocorticoids are used at low to moderate doses (1–2 mg/kg/day) as adjunctive therapy **(Figure 9**). IVIG monotherapy may be considered in patients with mild disease or contraindications to steroids, but close monitoring is required[156].

Intravenous immunoglobulin (IVIG) is a pooled preparation of IgG antibodies from many healthy donors. At high doses, it has broad immunomodulatory effects and can reduce excessive inflammation by affecting Fc receptors, complement activation, cytokine production, autoantibodies, and the activity of innate and adaptive immune cells[238,239].

In MIS-C and KD, one proposed effect is the reduction of innate immune activation. Zhu et al. showed that IVIG treatment in patients with KD and MIS-C was also associated with reduced numbers of activated IL-1β-producing neutrophils, suggesting that suppression of innate immune activation may represent an important component of its anti-inflammatory effect[240].

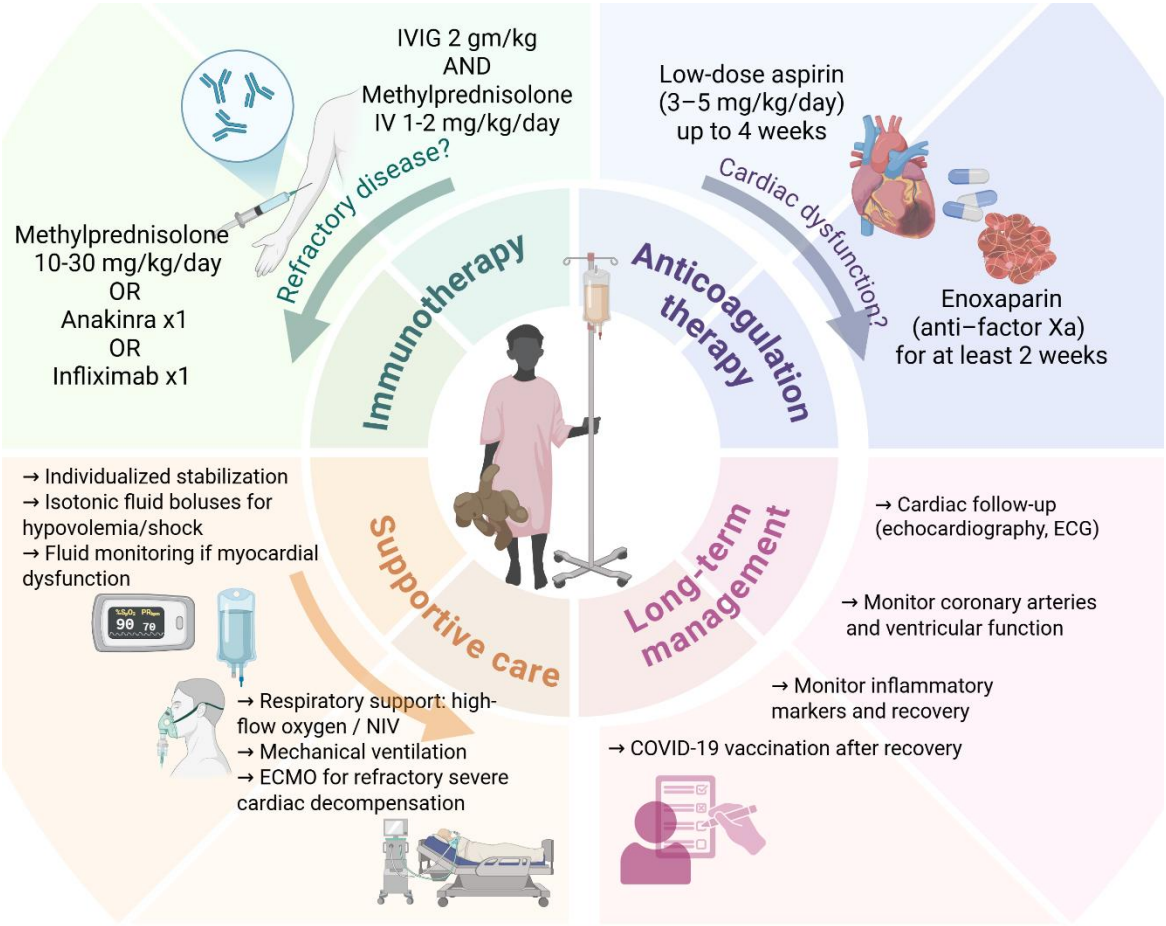


Figure 21. Overview of management strategies in MIS-C. *Immunomodulatory therapy, anticoagulation, supportive care, and long-term follow-up, included as management strategies. Arrows represent the escalation of treatment from first-line therapy to more advanced interventions. Adapted from El-Rassi et al.*[168] *and Henderson et al*[241]*. Created with BioRender.*

Antiplatelet and anticoagulation therapy in MIS-C is largely based on experience from KD and myocarditis, as well as emerging evidence from adult COVID-19. Low-dose aspirin (3–5 mg/kg/day, up to 81 mg daily) is recommended in most patients due to the risk of platelet activation, endothelial injury, and thrombosis. Treatment continues until normalization of platelet count and confirmation of normal coronary arteries at least 4 weeks after diagnosis.

Supportive care focuses on patient stabilization and prevention of end-organ damage. It includes cautious fluid resuscitation, hemodynamic support with vasoactive or inotropic agents, and respiratory support when needed[168].

15.2. Advanced therapy

Children with MIS-C may require PICU monitoring in cases of persistent shock, hemodynamic instability, significant cardiac involvement, respiratory failure, or multiorgan dysfunction.

Anticoagulation is indicated in high-risk MIS-C patients, particularly those with large coronary artery aneurysms (z-score ≥10) or moderate to severe left ventricular dysfunction, due to the increased risk of coronary or intracardiac thrombosis. Therapeutic anticoagulation is typically initiated with enoxaparin (**Figure 21**)[232].

Supportive care should also be individualized: small isotonic fluid boluses may be used for hypovolemia or shock, but careful monitoring as fluid overload can worsen pulmonary edema in patients with myocardial dysfunction. Respiratory support may range from high-flow oxygen or non-invasive ventilation to mechanical ventilation, while ECMO may be considered in refractory cases with severe cardiac decompensation[168].

Refractory MIS-C is defined by persistent fever and/or significant end-organ involvement despite initial immunomodulatory treatment. Clinical improvement is usually assessed within 24 hours after IVIG administration, and in the absence of improvement, should be considered escalation to alternative therapies such as high-dose glucocorticoids, Anakinra, or Infliximab (**Figure 9** and **Figure 21**). Repeating IVIG is generally not recommended[156].

Several cohort studies have shown that initial treatment with IVIG and glucocorticoids is associated with faster cardiac recovery, reduced risk of treatment failure, shorter intensive care unit stay, and decreased need for treatment escalation compared to IVIG alone[241,242].

HYPOTHESES AND OBJECTIVES

Hypotheses

Considering that MIS-C occurs after recovery from acute SARS-CoV-2 infection, and that it appears during the post-infectious phase rather than during active viral replication, we hypothesized that:

- An unbalanced humoral response may contribute to the development of MIS-C, and the magnitude and quality of antibody responses against SARS-CoV-2 may be associated with the disease.

Considering the described role of seasonal human coronaviruses and EBV infection/reactivation in multisystem pediatric diseases, we hypothesized that:

- Previous exposure or altered immune responses to other viruses may contribute to the immune profile of MIS-C and other COVID-19 unrelated inflammatory pediatric syndromes (namely, KD).

Specific clinical parameters have been associated with severe MIS-C and may help predict clinical outcomes, including ICU admission. Therefore, we hypothesized that:

- A full inflammatory profiling of MIS-C could help to predict disease severity.

Limited information is available about possible long-term evolution of inflammatory markers and potential sequelae after MIS-C; therefore, we hypothesize that:

- The longitudinal analysis of inflammatory markers may be relevant for improving knowledge of the disease and its long-term consequences.

MIS-C shares clinical features with KD and SD, however, these conditions might have distinct inflammatory signatures that can be identified using inflammatory biomarker analysis; therefore, we hypothesized that:

- Pediatric inflammatory diseases could be differentiated by their inflammatory biomarker profile.

Objectives

General objective: Characterize patients with MIS-C and carry out a comprehensive analysis of the immunological and inflammatory response 3-6 weeks after COVID-19, with follow-up over 2- and 18-month period in a subgroup of MIS-C patients to determine persistence of immunological alterations or resolution over time.

Specific objectives:

1. **Characterize the humoral response against SARS-CoV-2 and in MIS-C and identify potential markers:**
    a. Determine the level of total and neutralizing anti-SARS-CoV-2 antibodies.
    b. Determine the anti-SARS-CoV-2 antibody subtype usage.
    c. Characterize the antibody reactivity against common cold coronaviruses and EBV in MIS-C and KD.

2. **Characterize the inflammatory response in MIS-C, identify specific markers, and compare with other inflammatory conditions:**
    a. Compare the Inflammatory profile of MIS-C and Convalescent COVID group.
    b. Identify of inflammatory biomarkers associated with MIS-C severity, defined by ICU admission.
    c. Evaluate of the inflammatory profile of MIS-C patients at 2-month and 18-month follow-up.
    d. Compare MIS-C with Kawasaki and Still disease to identify shared and distinct inflammatory signatures.

METHODS

1. Study cohort

1.1. Study Approval

This study was approved by the local Ethical Review Board and conducted according to the Declaration of Helsinki. The protocol was approved by the Ethics Committee of Hospital Sant Joan de Déu (PIC-58-60). Pediatric blood samples were taken in Hospital Sant Joan de Déu, Universitat de Barcelona (Spain). Written informed consent was obtained from parents or legal guardians of all participants, and assent was obtained from children when appropriate.

1.2. Sample processing and storage

Serum samples were stored at −80°C. A fraction of serum was kept non-inactivated for the detection of inflammatory biomarkers using the Olink platform. The remaining serum was heat-inactivated at 56°C for 30 minutes and used for the characterization of humoral immune responses by Luminex and neutralization assays.

1.3. Cohort description

The study included five pediatric groups (**Figure 22**): healthy children (HC), CC, MIS-C, KD, and SD.

All samples included in this study were collected at Hospital Sant Joan de Déu, Barcelona, Spain. Samples from the MIS-C and CC groups were collected between March 2020 and February 2022. The KD and HC cohorts were collected before the SARS-CoV-2 pandemic to avoid potential overlap with SARS-CoV-2-related inflammatory conditions. The SD cohort included samples collected between 2015 and 2024.

The MIS-C group included 22 pediatric patients. Samples were obtained at diagnosis, before the initiation of specific treatment, including intravenous immunoglobulin or corticosteroids, to capture the acute inflammatory phase of the disease.

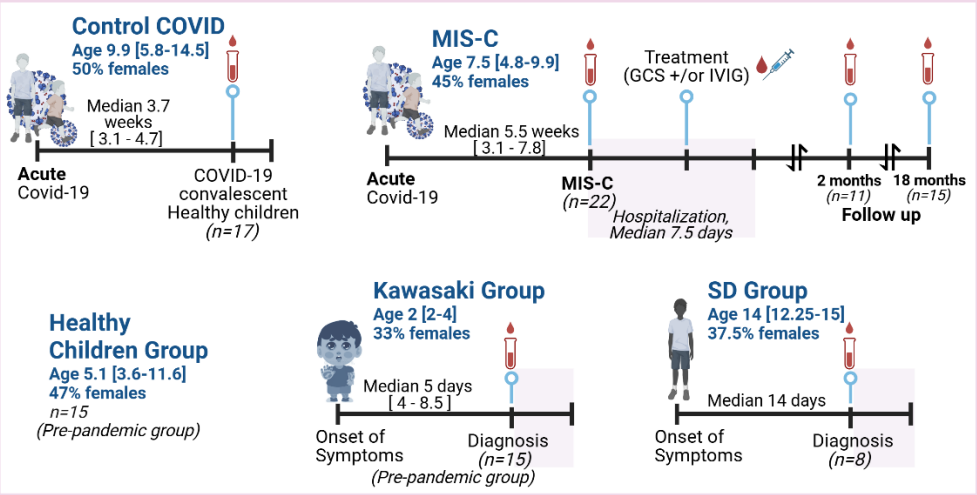


Figure 22. Study cohort and sampling timeline. *Representation of the study groups included in the analysis and their corresponding sampling time points, including acute and longitudinal MIS-C samples, CC, HC, KD, and SD. Created with BioRender.*

MIS-C diagnosis occurred at a median of 5.5 weeks [IQR 3.1–7.8] after SARS-CoV-2 infection. However, this timeframe should be interpreted with caution, as many MIS-C patients were asymptomatic or had mild symptoms during acute COVID-19, making the exact infection date difficult to determine. Nevertheless, the estimated interval was consistent with previously published studies. MIS-C diagnosis was established according to the clinical criteria proposed by the WHO, CDC, and the Royal College of Paediatrics and Child Health. Since patients were diagnosed and sampled early in the pandemic, neurological, respiratory, and renal organ system involvement were retained in the case definition, in accordance with the original MIS-C definitions used at that time.

The MIS-C cohort also included a longitudinal component. Follow-up samples were collected from a subset of patients at 2 months (n = 11) and 18 months (n = 15) after MIS-C diagnosis, allowing evaluation of the evolution and persistence of inflammatory and humoral immune signatures over time. Importantly, longitudinal follow-up data included information on SARS-CoV-2 reinfection and vaccination status, allowing immune responses over time to be interpreted in the context of possible additional antigen exposure.

The CC group included 17 pediatric individuals who had recovered from SARS-CoV-2 infection. Serum samples were collected during the convalescent phase, at a median

of 3.7 weeks [IQR 3.1–4.7] after infection, to evaluate the inflammatory profile during recovery from COVID-19. This group served as the main control group for MIS-C.

The KD group included 15 pediatric patients. Samples were collected before treatment initiation and before the SARS-CoV-2 pandemic. This allowed the KD cohort to be used as a non-SARS-CoV-2-related inflammatory comparator and reduced the possibility of diagnostic overlap with MIS-C. KD diagnosis was confirmed according to the American Heart Association classification criteria in effect at the time of patient enrollment[156].

The SD group included 8 patients sampled between 2015 and 2024. Samples were obtained at first disease onset, before the initiation of biological therapy. All patients fulfilled the International League of Associations for Rheumatology classification criteria for systemic juvenile idiopathic arthritis[156].

The HC group included 15 children between 2 and 13 years of age. Samples were collected before the SARS-CoV-2 pandemic to exclude potential post-infectious or MIS-C-related immune alterations. This group served as the control population for comparison with KD and SD.

Overall, the inclusion of pre-treatment samples across disease cohorts minimized the potential confounding effect of immunomodulatory therapies and supported the comparative analysis of disease-specific inflammatory signatures. The longitudinal MIS-C samples further allowed assessment of the durability and potential long-term consequences of the inflammatory response after MIS-C.

2. Total antibody quantification

Total antibody isotype and subclass levels were measured in serum samples using the ProcartaPlex™ Human Antibody Isotyping Panel 7-Plex (Thermo Fisher Scientific), a Luminex/xMAP-based multiplex assay. We quantified seven circulating antibody isotypes and subclasses: IgG1, IgG2, IgG3, IgG4, IgA, IgE, and IgM.

A total of 79 serum samples were included in this analysis: 17 CC samples, 21 acute MIS-C samples, 15 healthy controls, and 15 KD samples.

Serum samples were thawed on ice, mixed thoroughly, and centrifuged to remove particulates. Samples were then diluted in Universal Assay Buffer according to the manufacturer's instructions. Diluted serum samples were incubated with magnetic capture beads specific to each antibody isotype or subclass. After washing, the detection antibody mix was added, followed by streptavidin-phycoerythrin (PE). The beads were then resuspended in reading buffer, and fluorescence was acquired using a Luminex 100/200 xMAP-compatible instrument.

Data was analyzed using xPONENT software 3.1. Antibody concentrations were calculated from standard curves generated with the supplied isotyping standard mix. Median fluorescence intensity values were interpolated using a 5-parameter logistic regression curve, and the concentration of each immunoglobulin isotype or subclass was reported as µg/mL.

Values below the lower limit of quantification were reported as below the LLOQ, and values above the upper limit of quantification were reported as above the ULOQ. The assay-specific LLOQ and ULOQ values were defined separately for each immunoglobulin isotype or subclass. When values could not be accurately quantified at the primary dilution, the second dilution was used when available.

3. Neutralization activity

The neutralizing activity of serum samples from MIS-C patients and COVID-19 controls was determined using a human immunodeficiency virus type 1 (HIV-1)-based luciferase reporter pseudoviruses expressing the SARS-CoV-2 spike protein, as previously described by Trinité et al[243] and Pradenas et al[244].

Pseudoviruses were produced by co-transfecting Expi293F cells with the pNL4-3 LucR-E- HIV-1-based luciferase reporter plasmid and SARS-CoV-2 SctΔ19 spike expression plasmids corresponding to the ancestral D614G and the Alpha, Beta, Delta, Omicron BA.1. Control pseudoviruses were generated by replacing the SARS-CoV-2 spike expression plasmid with a VSV-G expression plasmid. Transfections were performed using ExpiFectamine 293 Reagent. Supernatants were harvested 72 hours after

transfection, filtered through a 0.45 µm filter, aliquoted, and stored at −80°C until use. Pseudoviruses were titrated on HEK293T cells overexpressing human ACE2.

Neutralization assay was performed in duplicate in 96-well cell culture plates. Three-fold serial dilutions of heat-inactivated serum samples, ranging from 1:60 to 1:14,580, were incubated with 200 TCID50 of pseudovirus for 1 hour at 37°C. Then, 1×10^4 hACE2 expressing HEK293T cells, treated with Diethylaminoethyl-Dextran, were added to each well.

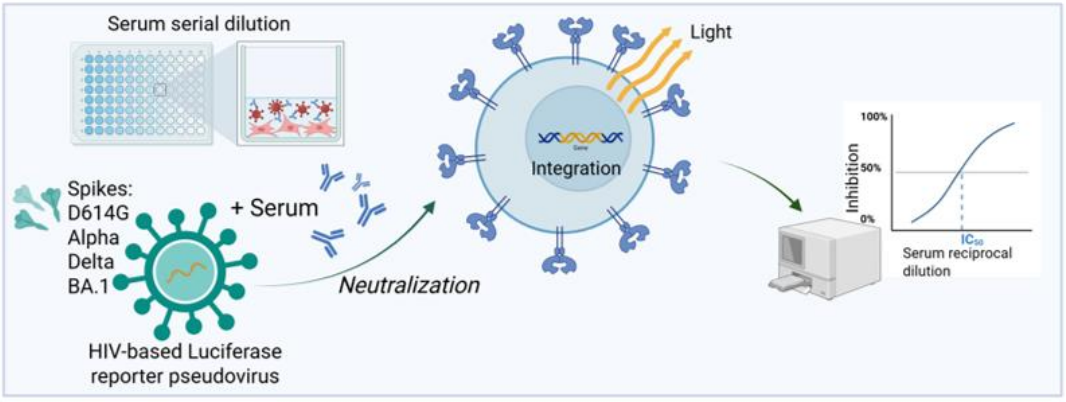


Figure 23. Schematic overview of the neutralization assay. *Serially diluted serum samples were incubated with SARS-CoV-2 spike-pseudotyped viruses representing different variants. Neutralizing antibodies block pseudovirus entry into target cells, reducing luciferase signal. Neutralization activity was expressed as the reciprocal serum dilution inhibiting 50% of infection (ID50). Created with BioRender.*

After 48 hours of incubation, luciferase activity was measured using BriteLite Plus Luciferase reagent and an EnSight Multimode Plate Reader. Neutralization values were normalized, and the ID50, defined as the reciprocal serum dilution inhibiting 50% of infection, were calculated by fitting the log-transformed serum dilution versus response curve using a four-parameter logistic equation in Prism 8.4.3. The lower and upper limits of detection were 60 and 14,580 (corresponding to first and last serum dilution), respectively.

Neutralizing activity against D614G and the three variants of concern were assessed in the initial cohort, including 22 MIS-C patients sampled at two time points (11 samples from 2-month follow up and 15 samples from 18-month follow-up) and 18 COVID-19 controls, corresponding to 66 serum samples.

4. Measurement of antigen-specific antibodies

Antigen-specific humoral responses were measured using a multiplex bead-based Luminex assay following previous work by Dobaño and colleagues[245]. IgG, IgG subclasses, IgM, IgA, and IgA subclasses were quantified using antigen-coated magnetic microspheres and FlexMap 3D technology (**Figure 24**).

SARS-CoV-2 target antigens included: SARS-CoV-2 [245] RBD proteins obtained from the Krammer laboratory; full S and N proteins produced in-house [245]; SARS-CoV-2 S1 (GenScript Biotech) and S2 proteins (Sino Biologicals)[245], SARS-CoV-2 S1+S2 (SinoBiologicals)[246]. HCoV target antigens included: N proteins of HCoV-229E, NL63, OC43, and HKU1 produced and purified in house[246]; HCoV-NL63 S1+S2 (40604-V08B), HCoV-229E S1+S2 (40605-V08B), HCoV-OC43 S1+S2 (40607-V08B), and HCoV-HKU1 S1+S2 (40606-V08B) were purchased from Sino Biological. EBV target antigens included: VCAp18 and ZEBRA produced in house as previously described by Aguilar at al[247].

Two experiments were performed. The first assay included SARS-CoV-2 antigens and seasonal human coronavirus antigens. For SARS-CoV-2, antibody responses were measured against S, S1, S2, RBD against ancestral strain. RBD variants correspond to WUH1, Alpha, Delta, and Omicron BA.1. In addition, N antigen was included for the measurement of IgG, IgA, and IgM responses. For seasonal human coronaviruses, total IgG responses were measured against 229E, NL63, OC43, and HKU1. A total of 70 serum samples were analyzed: 18 CC controls, 22 acute MIS-C samples, 15 MIS-C samples collected at 18-month follow-up, and 4 HC.

A second experiment assessed antigen-specific antibody responses against SARS-CoV-2, seasonal coronaviruses 229E, NL63, OC43, and HKU1. Responses to S1+S2 and N antigens were measured for IgG, IgA, IgM, IgG1–4, and IgA1–2. EBV-specific responses were also assessed against ZEBRA and VCAp18 antigens. It included a total of 80 serum samples: 18 CC controls, 21 acute MIS-C samples, 11 MIS-C samples collected at 2-month follow-up, 15 HC, and 15 KD samples.

Each assay plate included positive controls consisting of an 8-point, three-fold serial dilution prepared from a pool of positive samples. In addition, controls from the

National Institute for Biological Standards and Control (NIBSC, UK) were included on each plate. Both the positive control and NIBSC control curves were used to monitor assay quality and inter-plate performance.

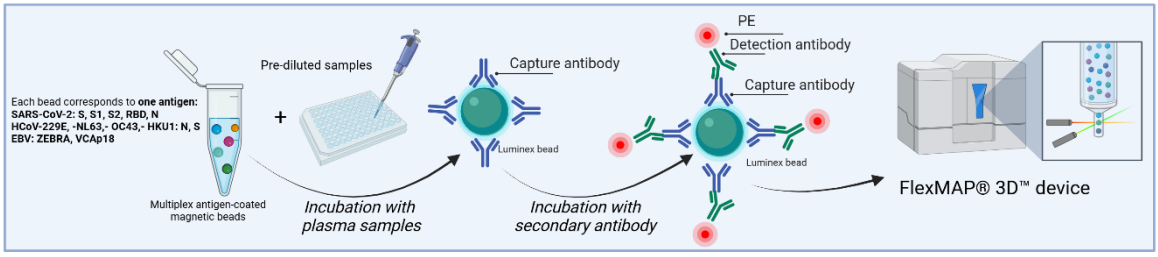


Figure 24. Multiplex Luminex assay for measurement of antigen-specific antibodies. *Pre-diluted serum samples were incubated with multiplex antigen-coated magnetic beads, with each bead region corresponding to a specific viral antigen. After binding of antigen-specific antibodies, PE-conjugated secondary antibodies were added to detect the corresponding antibody class or subclass. Beads were then acquired on a FlexMAP 3D instrument, and antibody reactivity was reported as MFI. Created with BioRender.*

Serum samples were pre-diluted according to the antibody class or subclass to be measured. For IgG and IgG subclasses, test samples were pre-diluted at 1:50 and 1:10, respectively, and then further diluted 10-fold in the assay plate, resulting in final dilutions of 1:500 for IgG and 1:100 for IgG subclasses. For IgM, IgA, and IgA subclasses, samples were pre-diluted at 1:10 in anti-human IgG depletion reagent to remove IgG and reduce potential interference. The final dilution was 1:500 for IgM and IgA, and 1:25 for IgA1 and IgA2 subclasses.

Pre-diluted serum samples and controls were incubated with the multiplex bead solution for 1 hour at room temperature with shaking at 600 rpm, allowing antigen-specific antibodies present in the samples to bind to their corresponding antigens (**Figure 24**). After incubation, the plates were washed three times with PBS containing 0.05% Tween-20 using a magnetic plate washer to remove unbound antibodies and serum components.

Bound antibodies were then detected using phycoerythrin-conjugated secondary antibodies specific for human IgG, IgA, IgM, IgG subclasses, or IgA subclasses. Plates were incubated with the secondary antibody solution for 30 minutes at room temperature with shaking at 600 rpm, followed by three additional washing steps.

Finally, beads were resuspended in 100 µL of Luminex buffer per well and shaken for 2 minutes at 600 rpm before acquisition on a FlexMap/Luminex instrument.

The instrument identified each bead region and quantified the phycoerythrin fluorescence signal associated with each antigen-antibody interaction. Antibody reactivity was reported as median fluorescence intensity (MFI) and used to compare antigen-specific humoral immune profiles between study groups.

5. Proteomic analysis of inflammatory biomarkers

The circulating inflammatory protein profile was analyzed in non-inactivated serum samples using the Olink multiplex platform (Olink Proteomics AB, Uppsala, Sweden). Five study groups were included: MIS-C, CC, HC, KD, and SD.

Inflammatory biomarkers were measured using the Olink Target 96 Inflammation panel, which includes 92 inflammation-related proteins and four internal controls. The assay is based on proximity extension assay (PEA) technology. During the incubation step, pairs of oligonucleotide-labelled antibodies bind to their respective target proteins in the samples. When both antibodies bind the same specific target protein in close proximity, the attached oligonucleotides hybridize and are extended by DNA polymerase, generating a unique DNA reporter sequence. This DNA barcode is then pre-amplified and quantified by high-throughput qPCR. The resulting signal reflects the relative abundance of each target protein.

Two Olink experiments were performed. The first experiment focused on MIS-C and CC samples, including longitudinal MIS-C samples, to characterize the inflammatory profile of MIS-C and evaluate its evolution over time. The second experiment included acute MIS-C, CC, HC, KD, and SD samples, allowing comparison of MIS-C with other pediatric inflammatory and hyperinflammatory conditions. Samples were prepared according to the manufacturer's standard protocol (**Figure 25**)[248]. Serum samples were incubated with antibody probe pairs targeting inflammation-associated proteins. After oligonucleotide hybridization, DNA extension, pre-amplification, and qPCR detection, the generated signals were normalized using Olink's built-in quality control system. Internal controls were used to monitor technical performance across the main

assay steps, including incubation, extension, and amplification/detection. External controls, including external sample controls, negative controls, and inter-plate controls, were used to assess background signal, plate-to-plate variability, and overall assay performance.

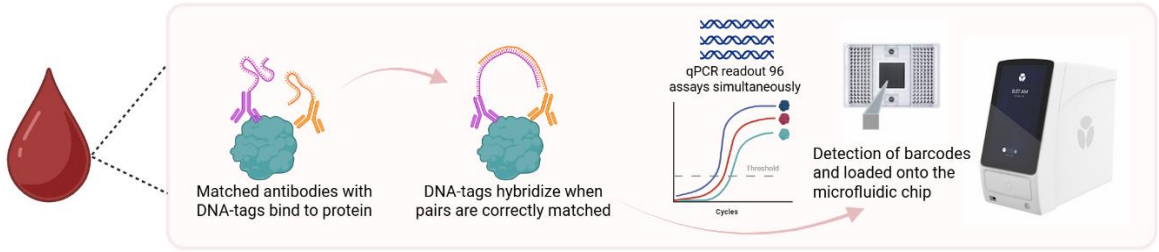


Figure 25. Principle of the Olink proximity extension assay (PEA). *Antibody pairs labelled with DNA tags bind the target protein, allowing oligonucleotide hybridization and extension when in proximity. The generated DNA reporter sequence is subsequently amplified and detected by microfluidic qPCR. Adapted from Olink Proteomics*[248,249] *and created with BioRender.com.*

Protein expression values were reported as Normalized Protein eXpression (NPX) values on a log2 scale, where higher NPX values correspond to higher relative protein abundance. NPX is a relative quantification unit derived from qPCR Ct values after normalization and is specific to each protein assay. Therefore, NPX values allow comparison of relative protein abundance across samples for the same protein but do not represent absolute protein concentrations.

In total, 103 non-inactivated serum samples were tested. The Olink assay was performed at the Immune Response and Biomarkers Core Facility at ISGlobal, Barcelona, Spain.

6. Statistical analysis

Analysis was performed with GraphPad Prism (Version 10.4, Graphpad Software, La Jolla, CA) and R (version 4.3.2).

Random Forest analysis was used to identify variables with the strongest discriminatory capacity between groups. This approach was applied to humoral response data to distinguish MIS-C patients from CC, as well as KD patients from HC.

Random Forest analysis was also used to identify inflammatory biomarkers that best differentiated MIS-C from CC and biomarkers associated with severe disease. Feature selection was based on the Mean Decrease Gini importance scores. Variables were ranked according to their importance, and biomarkers were retained up to the first major inflection point (elbow) in the ranked importance curve, thereby preserving the variables contributing most strongly to model discrimination. Model performance was evaluated using out-of-bag (OOB) predictions generated from bootstrap samples. OOB accuracy and the OOB confusion matrix, including class-specific error rates, were extracted to assess the discriminative performance. Additionally, stratified analysis by sex was performed to assess potential differences in biomarker behavior across male and female patients.

For humoral response analyses, differences between MIS-C and CC were assessed using the Mann–Whitney test for each antibody subtype. For antibody responses against common cold coronaviruses and Epstein–Barr virus, multiple-group comparisons were performed using the Kruskal–Wallis test followed by Dunn's multiple comparison test. All tests were unpaired and non-parametric.

Group differences based on the selected variables by RF were visualized through heatmaps and hierarchical clustering was applied to both variables and patients to reveal patterns of similarity. Using GraphPad Prism, the levels of MIS-C patients were compared according to their severity, alongside the CC group, and non-parametric comparison tests (Kruskal-Wallis with Dunn's multiple comparison test) were performed.

To reveal associations between cytokines and clinical markers, a discovery process was performed using linear regression models for each cytokine and each clinical marker, and p-values were adjusted for multiple comparisons using the Benjamini-Hochberg false discovery rate (FDR). Significant associations were then re-evaluated by adjusting for sex and age to account for potential confounding effects.

Protein-protein interaction network analysis was performed using the STRING database. Only high-confidence interactions, defined as an interaction score of 0.9, were included in the network analysis.

Comparisons of demographic characteristics, clinical symptoms, and other clinical parameters between groups were performed using non-parametric tests. Continuous variables were compared using the Mann–Whitney U test and are presented as median and interquartile range. Categorical variables, including symptom frequency and percentages, were compared using the chi-square or Fisher's exact test, as appropriate, and are presented as number and percentage. A p-value < 0.05 was considered statistically significant.

RESULTS

1. Cohort description

The initial study cohort included 22 patients diagnosed with MIS-C and a control group of 17 CC. Importantly, both groups were sampled at a comparable time after acute SARS-CoV-2 infection, with a median of 5.5 weeks [IQR: 3.1–7.8] in the MIS-C group and 3.7 weeks [IQR: 3.1–4.7] in the CC group. This indicates that both groups represented a similar post-infectious timepoint. However, while children in the CC group recovered without developing inflammatory complications, patients in the MIS-C group developed a delayed multisystem inflammatory syndrome.

For the comparative inflammatory biomarker analysis, MIS-C patients were compared with two pediatric hyperinflammatory disease cohorts: pre-pandemic 15 patients with KD and 8 patients with SD. The use of a pre-pandemic KD cohort allowed KD to serve as a non-SARS-CoV-2-related inflammatory comparator, minimizing potential diagnostic overlap with MIS-C. Pre-pandemic HC (n=15) served as the control group for KD and SD groups. This comparison allowed us to evaluate whether MIS-C shares inflammatory features with other pediatric hyperinflammatory diseases or presents a distinct biomarker signature.

1.1. Convalescent COVID-19

CC participants were diagnosed with SARS-CoV-2 infection by RT-qPCR during acute infection and samples were obtained 3.7 [3.1-4.7] (median [IQR]) weeks after COVID-19 diagnosis **(Figure 22).** Clinically, at the time of acute SARS-CoV2 infection, 22% reported respiratory symptoms, 17% gastrointestinal symptoms, and 28% neurological symptoms (headache), all of them were mild. At the time of sample collection and analysis, all CC tested negative by RT-qPCR. Infection was subsequently confirmed by anti-nucleocapsid protein serology. Blood analyses showed no significant abnormalities.

CC had a median age of 9.9 years, and females represented 50% of the group. Anti-SARS-CoV-2 IgG positivity was observed in 82% CC, which was significantly lower than in MIS-C patients. RT-pPCR positivity at sampling and anti-SARS-CoV-2 IgM positivity were not significantly different between groups. Overall, demographic characteristics, including age and sex distribution, were comparable between MIS-C patients and CC

(**Table 3**). Laboratory parameters showed clear differences between MIS-C patients and CC (**Table 3**).

1.2. Participants COVID-19 onset distribution

First, we evaluated the distribution of the SARS-CoV-2 infections in study participants across the different pandemic waves from March 2020 to March 2022. For CC patients, we analyzed the actual reported acute COVID-19 disease onset dates. For MIS-C patients we estimated the theoretical date of acute COVID-19 onset by subtracting 5 weeks from the MIS-C onset date, reflecting the typical delay between SARS-CoV-2 infection and MIS-C presentation. MIS-C participants were infected during several different waves including Pre-Alpha, Alpha, Delta, and early Omicron circulation. On the other hand, CC participants were almost all exclusively infected during the early pre-Alpha period at the beginning of the pandemic, except for one child infected during the Delta wave (**Figure 26**). Probably because, early in the pandemic, during the most uncertain times, parents were more willing to let their children participate in clinical studies. Later, it became much more difficult to enroll healthy children.

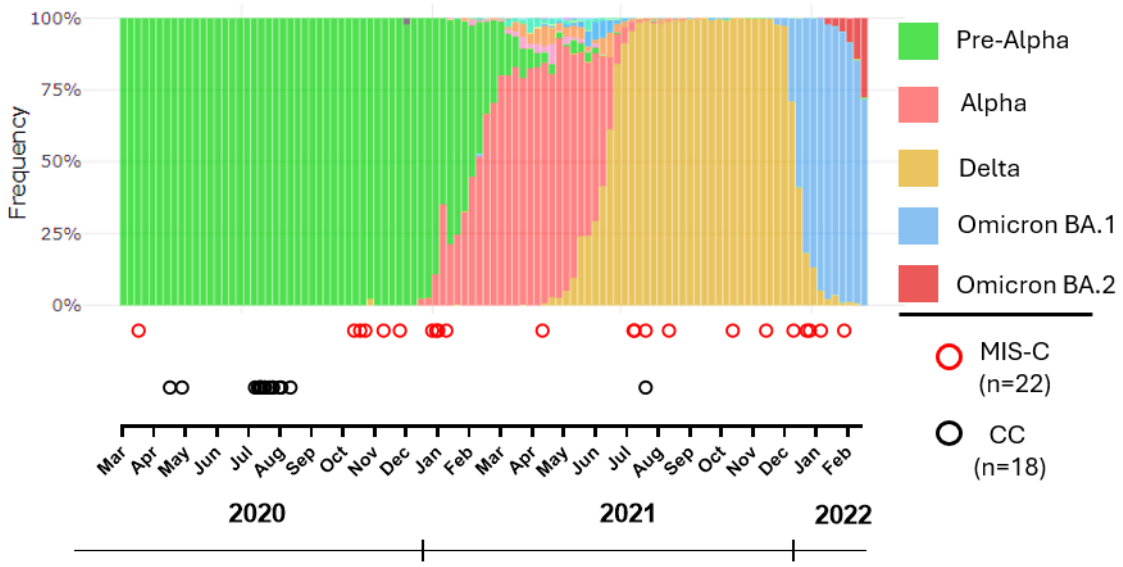


Figure 26. Distribution of CC and MIS-C sample infection timing in relation to SARS-CoV-2 variant circulation. *Colored bars show the circulation of SARS-CoV-2 variants from March 2020 to February 2022. Black dots indicate acute onset dates of CC. Red dots indicate estimated SARS-CoV-2 infection dates for MIS-C patients, calculated by subtracting 5 weeks from MIS-C onset. The figure shows that samples were distributed across different pandemic waves and variant periods.*

1.3. Healthy children participants

The healthy control group consisted of 15 children, aged between 2 and 13 years, with females representing 47% of the group (**Figure 22** and **Table 5**). Because samples were collected before the SARS-CoV-2 pandemic, this group provided a baseline control population without potential SARS-CoV-2-related immune alterations. HC were also used as the reference group for comparisons with KD and SD.

1.4. MIS-C participants

The study included a total of 22 MIS-C patients, with a median age of 7.5 years, and females represented 45% of the group. MIS-C cases were identified 5.5 [3.1–7.8] weeks after COVID-19 diagnosis, which was slightly later than in CC children, although this difference was not statistically significant (**Table 3** and **Figure 22**). All MIS-C patients were positive for anti-SARS-CoV-2 IgG, and two patients (9%) had a positive RT-qPCR test at the time of MIS-C onset. Anti-SARS-CoV-2 IgM positivity was not significantly different compared with CC.

Clinical inflammatory markers were markedly elevated in MIS-C patients. All patients showed increased C-reactive protein (CRP) and D-dimer levels, while 86% had elevated procalcitonin levels, 91% had elevated ferritin levels, and 59% had low platelet counts. MIS-C patients also showed signs of liver and tissue injury, with elevated lactate dehydrogenase (LDH) levels observed in 81% of cases. Increased alanine aminotransferase (ALT) was present in 45% of patients, whereas aspartate aminotransferase (AST) elevation was less frequent, occurring in 23% of cases.

Most MIS-C patients experienced involvement of at least three organ systems. The most affected systems were gastrointestinal (95%), hematological (86%), and mucocutaneous (83%). Gastrointestinal involvement was observed in 95% of MIS-C patients and was mainly characterized by abdominal pain, diarrhea, and/or vomiting. Hematological involvement characterized mainly by thrombocytopenia and lymphopenia, with median platelet counts of 115 $\times 10^3$/µL [IQR: 103–212] and lymphocyte counts of 800/µL [IQR: 500–1225]. Mucocutaneous involvement included bilateral conjunctivitis, oral mucosal changes, peripheral extremity changes, polymorphous rash, and lymphadenopathy. Bilateral conjunctivitis was the most

common feature, present in 77% of MIS-C patients, followed by polymorphous rash (59%), oral mucosal changes (27%), peripheral extremity changes (18%), and lymphadenopathy (14%).

	MIS-C (n=22)	Convalescent-COVID-19 (n=17)	*p*-value[A]
Demographics			
Age (years), Median [IQR]	7.5 [4.8-9.9]	9.9 [5.8-14.5]	0.0907
Female sex at birth, n (%)	10 (45%)	9 (50%)	0.6428
Ethnicity, n (%)			
Caucasian Spanish	10 (45%)	9 (50%)	
Latin American	6 (27%)	8 (44%)	
Romani	3 (14%)	1 (6%)	
North African	2 (9%)		
Eastern Europe	1 (5%)		
COVID-19			
Period from COVID-19 diagnosis to sampling (weeks), Median [IQR]	5.5 [3.1-7.8]	3.8 [3.1-4.7]	0.0875
Positive SARS-CoV-2 RT-pCR at sampling, n (%)	2 (9%)	0	0.2018
Positive anti-SARS-CoV-2 IgG, n (%)	22 (100%)	14 (82%)	0.0403
Positive anti-SARS-CoV-2 IgM, n (%)	8 (36%)	5 (28%)	0.6479
COVID-19 vaccination, n (%)	3 (14%)	0	0.0728
MIS-C symptoms & diagnosis			
Fever duration (days), Median [IQR]	5.0 [4.0-6.0]	n.a.	
Respiratory symptoms, n (%)	7 (32%)	n.a.	
Gastrointestinal symptoms, n (%)	21 (95%)	n.a.	
Neurologic symptoms, n (%)	13 (59%)	n.a.	
Bilateral conjunctivitis, n (%)	17 (77%)	n.a.	
Oral/pharynx erythema), n (%)	6 (27%)	n.a.	
Peripheral extremity changes, n (%)	4 (18%)	n.a.	
Polymorphous rash, n (%)	13 (59%)	n.a.	
Lymphadenopathy, n (%)	3 (14%)	n.a.	
Cardiological complications, n (%)	10 (45%)	n.a.	
Hb (g/dL), Median [IQR]	12 [11-13]	13 [13-14]	0.0003
Platelets (x10^3/µL), Median [IQR]	115 [103-212]	294 [274-368]	<0.0001
Leukocytes (x10^3/ µL), Median [IQR]	7.85 [5.5-11.8]	8.1 [6.0-10.2]	0.9088
Lymphocytes (/µL), Median [IQR]	800 [500-1225]	3200 [2100-4200]	<0.0001
Neutrophils (/µL), Median [IQR]	4850 [3850-6875]	3500 [2700-3900]	0.0083
CRP (mg/dL), Median [IQR]	193 [127-241]	0.45 [0.2-1.3]	<0.0001
Procalcitonin (ng/mL), Median [IQR]	3.7 [1.6-11]	0.01 [0.002-0.02]	<0.0001
ALT (U/L), Median [IQR]	33 [17-75]	15 [11-19]	0.0003
AST (U/L), Median [IQR]	39 [31-54]	26 [17-29]	<0.0001
LDG (U/L), Median [IQR]	662 [530-727]	537 [452-635]	0.0156

[A] Mann-Whitney test for continuous variables and Chi square test for percentages.
IQR, interquartile range**;** Hb, hemoglobin; CRP, C-reactive protein; ALT, alanine aminotransferase; AST, aspartate aminotransferase; LDG, lactate dehydrogenase.

Table 3. Demographic, clinical, and laboratory characteristics of MIS-C patients and CC participants.

Cardiovascular involvement was observed in 10 patients (45%, **Table 3**): 7 of them developed myocarditis, 2 had pericarditis, and 3 were diagnosed with valve dysfunction. Importantly, no cases of coronary artery aneurysms were identified.

Most patients (21 out of 22, 95%) received a single dose of IVIG (**Table 3**). All patients were treated with intravenous corticosteroids and anticoagulation therapy. All MIS-C patients received intravenous antibiotic therapy during hospitalization. The most administered antibiotic was ceftriaxone, used in 82% of patients, followed by cefotaxime in 14% and piperacillin-tazobactam in 9%. Patient M12 received combined treatment with piperacillin-tazobactam and ceftriaxone due to appendicitis. The median [IQR] hospital stay was 7.5 [5.0 - 10.0] days.

The MIS-C cohort was divided into two subgroups: the ICU-admitted group (n=12, 55%), who required intensive care due to severe symptoms, and the non-ICU-admitted group (n=10), who were managed in the general inpatient department.

ICU-admitted patients showed a more severe clinical phenotype than non-ICU patients (**Table 4**). They had a significantly higher number of organ system involvements, with a median of 4.5 [IQR: 4–5] compared with 3 [IQR: 3–4] in the non-ICU group. Shock was observed in 92% of ICU-admitted patients and in none of the non-ICU patients. Cardiac involvement was also more frequent in the ICU group (67% vs. 20%) and was reflected by significantly higher NT-proBNP levels (6556 [IQR: 3583–12317] ng/L vs. 263 [IQR: 203–3011] ng/L).

ICU-admitted patients showed more pronounced hematological, inflammatory, and tissue injury alterations than non-ICU patients (**Table 4**). Hematological involvement was more frequent in the ICU group, affecting 100% of ICU-admitted patients compared with 70% of non-ICU patients. This was supported by significantly lower platelet counts in ICU patients ($p < 0.05$). Inflammatory markers were also increased in ICU-admitted patients, including higher procalcitonin ($p < 0.05$, Table 4Table 4). Finally, ICU patients showed higher markers of tissue and liver injury, with significantly increased AST (44 U/L [IQR: 39–93] vs. 34 U/L [IQR: 26–39]) and LDH (700 U/L [IQR: 628–758] vs. 566 U/L [IQR: 475–680]). ICU admission was also associated with a longer

hospital stay. ICU-admitted patients stayed in hospital for a median of 9.5 days [IQR: 6.3–10.0], compared with 5.5 days [IQR: 4.0–8.3] in non-ICU patients.

	ICU-admitted (n=12)	Non-ICU-admitted (n=10)	*p*-value[A]
Demographics			
Age (years), Median [IQR]	7.8 [6.9-12.05]	6.1 [3.5-9.8]	0.1970
Female sex at birth, n (%)	3 (25%)	7 (70%)	0.0348
MIS-C symptoms & diagnosis[B]			
OSI hematological, n (%)	12 (100%)	7 (70%)	0.0412
OSI mucocutaneous, n (%)	9 (75%)	9(90%)	0.1052
OSI musculoeskeletal, n (%)	0	0	
OSI cardiac, n (%)	8 (67%)	2 (20%)	0.0286
OSI neurological, n (%)	8 (67%)	5 (50%)	0.4285
OSI respiratory, n (%)	4 (33%)	3 (30%)	>0.9999
OSI renal, n (%)	0	0	
OSI gastrointestinal, n (%)	12 (100%)	9 (90%)	0.2622
Number of OSIs (total), Median [IQR]	4.5 [4-5]	3 [3-4]	0.0167
Shock, n (%)	11 (92%)	0	<0.0001
Treatment and outcomes			
IVIG treatment	12	9 (90%)	0.2622
IVIG repeated course	0	0	
Corticosteroids	12 (100%)	10 (100%)	
Anticoagulation therapy	12 (100%)	10 (100%)	
Stay in hospital, days	9.5 [6.3 - 10.0]	5.5 [4.0 - 8.3]	0.0272
Laboratory data			
Hb(g/dL), Median [IQR]	11.8 [10.2-12.9]	12 [11.3-12.7]	0.8085
Platelets (x10^3/ µL), Median [IQR]	108 [96-138]	207 [108-262]	0.0358
Leukocytes (x10^3/µL), Median [IQR]	7.15 [4.825-13.65]	8.15 [6.35-9.475]	0.7846
Lymphocytes (/µL), Median [IQR]	800 [325-1150]	1050 [500-2175]	0.2076
Neutrophils (/µL), Median [IQR]	4100 [3100-9100]	5350 [4250-6800]	0.5711
CRP (mg/dL), Median [IQR]	223 [148-251]	151 [107-229]	0.1072
D-Dimer (ng/ml), Median [IQR]	5850 [2393-18633]	3520 [2310-4405]	0.1932
Procalcitonin (ng/mL), Median [IQR]	7.5 [2.9-41.5]	2.3 [0.24-4.5]	0.0249
Ferritin (microg/L), Median [IQR]	941 [379-1204]	376 [232-590]	0.0345
NT-proBNP (ng/L), Median [IQR]	6556 [3583-12317]	263 [203-3011]	0.0023
Troponin I (ng/ml), Median [IQR]	0.018 [0.01-0.84]	0.008 [0.001-0.023]	0.0736
ALT (U/L), Median [IQR]	39 [23-95]	21 [14-43]	0.0716
AST (U/L), Median [IQR]	44 [39-93]	34 [26-39]	0.0237
LDG (U/L), Median [IQR]	700 [628-758]	566 [475-680]	0.0358
Albumin (g/dL), Median [IQR]	4.5 [4-5]	3.8 [3-4]	0.0517

[A] Mann-Whitney test for continuous variables and Chi square test for percentages.

[B] Organ System Involvement (OSI) was defined from the following specific symptoms: Hematological (platelets <150,000/µL or ALC <1,000/µL), Mucocutaneous (rash, conjunctivitis, oral changes, or hand erythema/edema), Musculoskeletal (myalgia, arthralgia, or myositis), Cardiac (LVEF <55%, coronary changes, or elevated troponin), Neurologic (altered mental status, headache, weakness, or paresthesia), Respiratory (need for oxygen, lower respiratory infection, chest x-ray infiltrates, effusion, bronchospasm, or hemorrhage), Renal (acute kidney injury or renal replacement therapy), Gastrointestinal (abdominal pain, vomiting, or diarrhea). IQR, interquartile range; Hb, hemoglobin; CRP, C-reactive protein; ALT, alanine aminotransferase; AST, aspartate aminotransferase; LDG, lactate dehydrogenase.

Table 4. Comparison of clinical features and inflammatory biomarkers between ICU- and non-ICU-admitted MIS-C patients.

Longitudinal follow-up samples were available for a subgroup of MIS-C patients. Eleven patients had samples collected at the 2-month follow-up, while 15 patients had samples available at the 18-month follow-up (**Figure 22**). All cardiological complications developed during the acute phase of MIS-C resolved over time, and by the 18-month follow-up, no alterations of cardiac function were observed. Most patients with 2-month samples also had paired 18-month samples, although several patients had only 18-month follow-up samples available. During follow-up, three patients (M02, M04, and M14) received COVID-19 vaccination. Additionally, evidence of subsequent SARS-CoV-2 infection or household exposure before the 18-month follow-up was documented in three patients (M02, M05, and M12).

1.5. Kawasaki disease participants

The KD cohort included 15 pre-pandemic pediatric patients, allowing KD to serve as a non-SARS-CoV-2 inflammatory comparator and reducing the possibility of diagnostic overlap with MIS-C. Diagnosis of KD was confirmed based on the American Heart Association classification criteria in effect at the time of patient enrollment[156]. KD patients were younger than MIS-C patients, with a median age of 2 years [IQR: 2–4], compared with 7.5 years [IQR: 4.8–9.9] in the MIS-C group (**Figure 22** and **Table 5**).

Clinically, KD patients showed prominent mucocutaneous and cardiac involvement. Mucocutaneous involvement was observed in 100% of KD patients, while cardiac involvement was present in 67%. Despite frequent cardiac involvement in the KD cohort, no patients developed coronary artery aneurysms. Gastrointestinal involvement was less frequent in KD than in MIS-C, affecting 40% of KD patients compared with 95% of MIS-C patients. Neurological involvement was also less common in KD, occurring in 7% of patients compared with 59% in MIS-C.

All KD patients fulfilled diagnostic criteria for KD[233]. Among them, 46% (n = 7) had complete KD, 27% (n = 4) had incomplete KD, and 27% (n = 4) presented with KD shock syndrome.

Laboratory findings showed that KD patients had higher platelet counts than MIS-C patients, with a median of 386 $\times 10^3$/µL [IQR: 294–457], while MIS-C patients showed thrombocytopenia. Inflammatory markers were elevated in KD, including CRP with a

median of 152 mg/dL [IQR: 67.7–221.9], but procalcitonin levels were lower than in MIS-C. NT-proBNP was also increased in KD, although levels were lower than in MIS-C.

Regarding treatment, all KD patients received IVIG and anticoagulation therapy, while 47% received corticosteroids. Only one KD patient received anti-IL-1 therapy. ICU admission was less frequent in KD than in MIS-C, occurring in 20% of KD patients compared with 55% of MIS-C patients.

1.6. Still disease participants

The SD cohort included 8 pediatric patients. These patients were older than both MIS-C and KD patients, with a median age of 14 years [IQR: 12.5–15]. Females represented 37.5% of the SD group (**Table 5**).

Clinically, SD patients showed a different pattern of organ involvement compared with MIS-C and KD. Fever duration was longer in SD, with a median of 14 days [IQR: 14–14], compared with 5 days in MIS-C and 6 days in KD. Musculoskeletal involvement was one of the main features of SD, present in 75% of patients, while it was absent in MIS-C and rare in KD. Mucocutaneous involvement was also frequent in SD, affecting 75% of patients. Cardiac involvement was less frequent in SD (25%) than in KD (67%) and MIS-C (45%). SD is presented with prolonged fever and less severe organ dysfunction.

Laboratory findings showed that SD patients had strong systemic inflammation, with elevated CRP and particularly high ferritin levels. Ferritin was highest in the SD group, with a median of 2051 µg/L [IQR: 697–8982], compared with 574.5 µg/L in MIS-C and 221 µg/L in KD (Table 5). Platelet counts were also higher in SD than in MIS-C, contrasting with the thrombocytopenia observed in MIS-C.

Using the 2016 EULAR/ACR/PRINTO classification criteria for MAS in SD, MAS was assessed based on ferritin elevation together with cytopenia, increased AST, hypertriglyceridemia, and/or hypofibrinogenemia[250]. In our cohort, only one Still disease patient, SD8, fulfilled criteria for confirmed MAS. No additional MAS cases were identified in the remaining cohorts.

	HC (n=15)	CC (n=17)	MIS-C (n=22)	KD (n=15)	SD (n=8)	p-value[A]
Demographics						
Age (years), Median [IQR]	5.1 [3.6-11.6]	9.9 [5.8-14.5]	7.5 [4.8-9.9]	2 [2-4]	14 [12.25-15]	0,0126
Female sex at birth, n (%)	7 (47%)	9 (50%)	10 (45%)	5 (33%)	3 (37.5 %)	0,9276
Ethnicity, n (%)						0,0291
Caucasian Spanish		9 (50%)	10 (45%)	10 (67%)	4 (50%)	
Latin American		8 (44%)	6 (27%)	2 (13%)		
Romani		1 (6%)	3 (14%)			
North African			2 (9%)	2 (13%)		
Eastern Europe			1 (5%)		1 (12,5 %)	
Asian				1 (7%)		
Indian					3 (37.5%)	
Symptoms						
Fever duration (days), Median [IQR]		n.a.	5.0 [4.0-6.0]	6.0 [4.0-8.0]	14 [14-14]	<0,0001
Laboratory data						
Hb (g/dL), Median [IQR]		13 [13-14]	12 [11-13]	10.9 [10-11.6]	11 [9.5-12]	0,0268
Platelets (x103/µL), Median [IQR]		294 [274-368]	115 [103-212]	386 [294-457]	388.5 [249-437]	<0,0001
Leukocytes (x103/ µL), Median [IQR]		8.1 [6.0-10.2]	7.85 [5.5-11.8]	n.a.	n.a.	
Lymphocytes (/µL), Median [IQR]		3200 [2100-4200]	800 [500-1225]	3300 [1800-6400]	2000 [1000-2100]	<0,0001
Neutrophils (/µL), Median [IQR]		3500 [2700-3900]	4850 [3850-6875]	10528 [5100-13600]	10700 [6300-19500]	0,0116
CRP (mg/dL), Median [IQR]		0.45 [0.2-1.3]	193 [127-241]	152 [67.7-221.9]	148 [51.7-313.7]	0,5043
Procalcitonin (ng/mL), Median [IQR]		0.01 [0.002-0.02]	3.7 [1.6-11]	1.25 [0.5-3.09]	n.a.	<0,0001
ALT (U/L), Median [IQR]		15 [11-19]	33 [17-75]	38 [14-109]	28 [16.7-44.5]	0,9266
AST (U/L), Median [IQR]		26 [17-29]	39 [31-54]	30 [18-43]	39.5 [22-57]	0,1507
LDG (U/L), Median [IQR]		537 [452-635]	662 [530-727]	554 [487-845]	477.5 [368-1015]	0,6811
Ferritin (microg/L), Median [IQR]		n.a.	574.5 [286-1096]	221 [173.4-435.8]	2051 [697-8982]	0,0022
Albumin (g/dL), Median [IQR]		n.a.	3.5 [2.5-3.9]	3.5 [2.9-3.9]	3.3 [3.1-3.8]	0,8343
NT-proBNP (ng/L), Median [IQR]		n.a.	3442 [310-8449]	1326 [552-4126]	n.a.	0,0384
Organ system involvement[B]						
OSI hematological, n (%)			19 (86%)	5 (33%)	1 (12.5%)	<0,0001
OSI mucocutaneous, n (%)			18 (82%)	15 (100%)	6 (75%)	0,1101
OSI musculoeskeletal, n (%)			0	1 (7%)	6 (75%)	<0,0001
OSI cardiac, n (%)			10 (45%)	10 (67%)	2 (25%)	0,1538
OSI neurological, n (%)			13 (59%)	1 (7%)	0	0,0002
OSI respiratory, n (%)			7 (32%)	3 (20%)	2 (25%)	0,8239

OSI renal, n (%)	0	0	0	
OSI gastrointestinal, n (%)	21 (95%)	6 (40%)	2 (25%)	<0,0001
Number of OSIs (total), Median [IQR]	4 [3-5]	3 [2-3]	2 [2-3]	
Shock, n (%)	11 (50%)	4 (27%)	n.a.	0,0276
ICU, n (%)	12 (55%)	3 (20%)	n.a.	0,0063
Treatment and outcomes				
IVIG treatment	21 (95%)	15 (100%)	n.a.	<0,0001
IVIG repeated course	0	1 (7%)	n.a.	0,5111
Corticosteroids	22 (100%)	7 (47%)	5 (63%)	0,0001
Anticoagulation therapy	22 (100%)	15 (100%)	n.a.	
IL-1	n.a	n.a.	3 (38%)	

[A] Fisher´s exact test for percentages and Kruskal-Wallis test for continuous variables.

[B] Organ System Involvement (OSI) was defined from the following specific symptoms: Hematological (platelets <150,000/μL or ALC <1,000/μL), Mucocutaneous (rash, conjunctivitis, oral changes, or hand erythema/edema), Musculoskeletal (myalgia, arthralgia, or myositis), Cardiac (LVEF <55%, coronary changes, or elevated troponin), Neurologic (altered mental status, headache, weakness, or paresthesia), Respiratory (need for oxygen, lower respiratory infection, chest x-ray infiltrates, effusion, bronchospasm, or hemorrhage), Renal (acute kidney injury or renal replacement therapy), Gastrointestinal (abdominal pain, vomiting, or diarrhea). IQR, interquartile range; Hb, hemoglobin; CRP, C-reactive protein; ALT, alanine aminotransferase; AST, aspartate aminotransferase; LDG, lactate dehydrogenase.

Table 5. Demographic, clinical, and laboratory characteristics.

1.7. Total immunoglobulin levels

As an exploratory analysis, we evaluated total immunoglobulin levels across the study groups to assess whether major differences were present (**Table 6**). Overall, IgG subtypes, IgE, IgA, and IgM showed comparable values between CC, MIS-C, HC, and KD groups, with no clear group-specific differentiation. This suggests that the different diseases were not associated with any non-specific skewing of antibody isotype and IgG subtype usage.

	HC	CC	MIS-C	KD	p-values
IgE, MFI Median, [IQR]	0.440 [0.310- 0.640]	0.5400 [0.4050- 0.6950]	0.500 [0.335- 0.805]	0.3600 [0.3100- 0.5200]	0.1137
IgA, MFI Median, [IQR]	669.4 [473.4- 1052]	571.0 [426.5- 1021]	701.1 [430.8-2317]	539.2 [361.8- 1207]	0.3981
IgM, MFI Median, [IQR]	10139 [6037- 12592]	6037 [5092- 9708]	7816 [4991- 23022]	5884 [3923- 8350]	0.1092
IgG1, MFI Median, [IQR]	17077 [8141-107074]	13333 [11338- 19534]	11448 [7112- 31949]	7928 [6356- 19360]	0.1294
IgG2, MFI Median, [IQR]	6992 [6651-9292]	7733 [5136-8937]	12401 [5697- 12401]	6878 [5697-7340]	0.6519
IgG3, MFI Median, [IQR]	704.2 [427.8- 950.8]	670.5 [515.7- 998.3]	587.7 [456.5- 1112]	547.7 [496.8- 708.1]	0.465
IgG4, MFI Median, [IQR]	142.7 [109.2-313.4]	173.6 [122.4-333.1]	284.9 [131.8-494.3]	172.0 [99.32-352.2]	0.4022

Table 6. Total immunoglobulin levels across four groups: CC, MIS-C, HC, and KD.

2. Humoral response in MIS-C and CC

Here, we characterized the anti-SARS-CoV-2 humoral response in MIS-C patients at the time of diagnostic and before treatment, in comparison with CC serum samples collected at the theoretical time of MIS-C onset (4 to 6 weeks after acute COVID-19). Although, this analysis focuses primarily on MIS-C and Control-COVID-19 individuals, we also explored KD and HC groups in specific comparisons notably regarding the humoral response against other common cold coronaviruses and EBV.

2.1. SARS-CoV-2-specific humoral immune responses

To evaluate SARS-CoV-2-specific humoral responses we measured IgA, IgM, and IgG responses against the following SARS-CoV-2 antigens: RBD variants corresponding to WH1, Alpha, Delta, and Omicron BA.1, trimeric S, recombinant S1 and S2 from the ancestral strain, and N protein (**Figure 27**) in both MIS-C and convalescent-COVID-19 individuals.

In general, IgM responses against the different antigens analyzed tended to be lower in MIS-C patients compared with CC, however none of these differences reached statistical significance (**Figure 27A**). IgA levels showed similar values in both groups for most antigens (**Figure 27B**) except for S2-specific IgAs, which were higher in MIS-C compared with CC (p=0.0319). Of note, in both groups, IgA cross-reactivity against the highly mutated Omicron BA.1 RBD was extremely low, in line with what was observed in adults[87].

IgG responses were generally high in both groups and showed strong overlap for most antigens. The main difference was observed for RBD BA.1-specific IgGs, which were strongly reduced in both groups but significantly higher in MIS-C compared with CC (**Figure 27C**). Importantly, 3 MIS-C participants infected during the Delta wave were vaccinated prior to MIS-C. Interestingly, their IgG levels were always among the strongest against all antigens except N. This is especially relevant in the case of BA.1 where hybrid immunity was shown to significantly boost weak pre-acquired humoral response. When the analysis was restricted to pre-Alpha infected patients, this difference was no longer significant. Of note, 2 CC did not seroconvert despite RT-qPCR positive results.

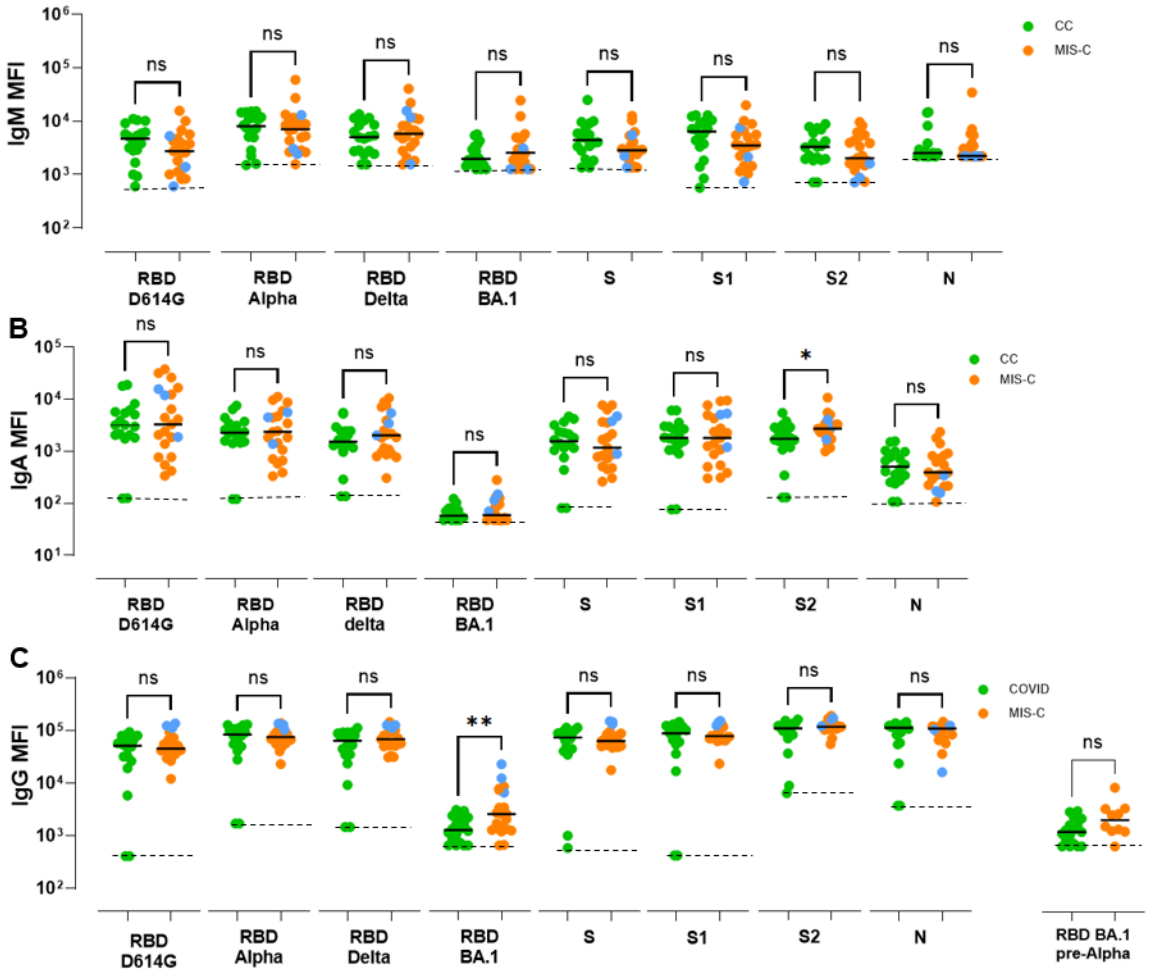


Figure 27. SARS-CoV-2 antigen-specific IgM, IgA, and IgG responses in MIS-C and CC. *(A) IgM, (B) IgA and (C) IgG responses against SARS-CoV-2 antigens, including RBD variants corresponding to WH1, Alpha, Delta, and Omicron BA.1, as well as S, S1, S2, and N antigens. An additional comparison of RBD BA.1-specific IgG responses in pre-Alpha only patients was included. Each dot represents an individual sample, and horizontal lines indicate the median antibody signal. Blue dots represent MIS-C patients who were vaccinated before developing MIS-C. Responses are presented as mean fluorescence intensity (MFI). The lower detection threshold was defined as the mean MFI value of HC, and values below this threshold were adjusted to the threshold value.*

Therefore, MIS-C was not associated with broad differences in SARS-CoV-2-specific antibody responses, but rather with limited antigen-specific changes.

2.2. Neutralizing anti-SARS-CoV-2 humoral immune responses

Next, we evaluated the neutralizing antibody response in MIS-C patients and CC. Since neutralization capacity has been associated with the infecting SARS-CoV-2 variant [251,252], we analyzed neutralization against dominant variants during the study period: D614G, Alpha, Delta, and Omicron BA.1. In the absence of viral sequencing data, the

infecting variant of each participant was estimated based on their theoretical time of SARS-CoV-2 infection and their profile of cross-neutralization among the variants described above (**Figure 28**). MIS-C were estimated to include 10 pre-Alpha, 2 Alpha, 9 Delta, and 1 Omicron BA.1 infections (**Figure 28A**), which demonstrated clearly distinctive neutralization profiles. Vaccinated individuals present among MIS-C, were mainly represented during the Delta period showed the highest neutralizing responses. In contrast, CC participants were all infected during the pre-alpha period, except for 1 putative Delta infection (**Figure 28B**). As expected, the non-seroconverts CC participants did not develop detectable neutralizing antibodies.

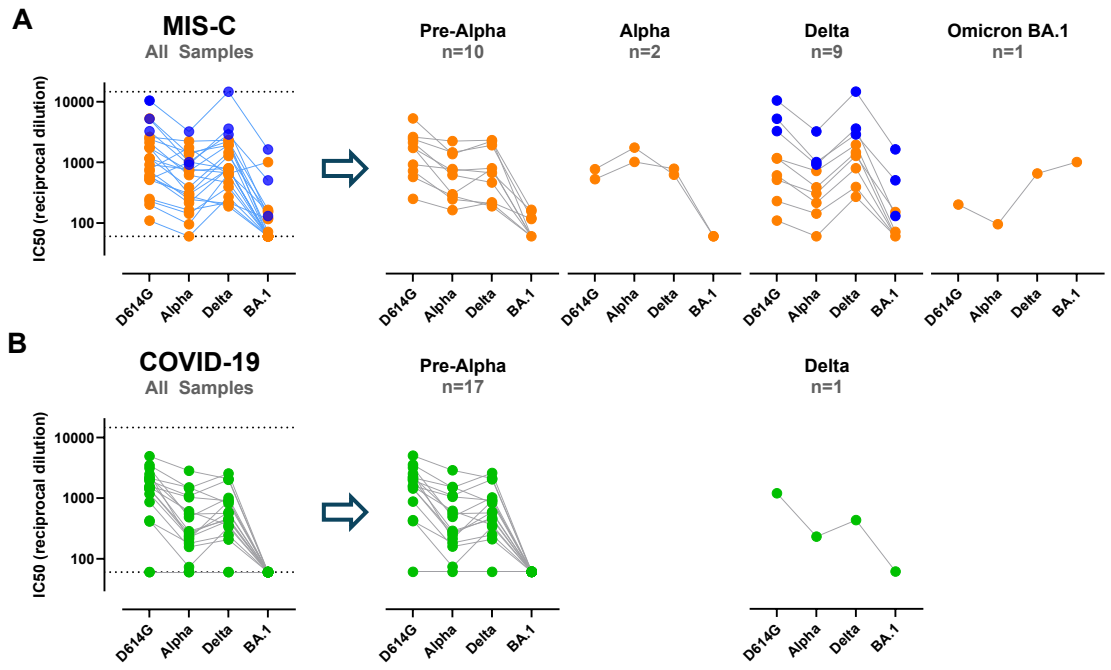


Figure 28. Predicted infecting variant based on infection timing and cross-neutralization profile. *Neutralization profiles showing individual neutralizing antibody titers against D614G, Alpha, Delta, and Omicron BA.1 variants. Neutralization profiles of (A) MIS-C participants, (B) CC. Vaccinated individuals are highlighted in blue. Each dot represents an individual sample, horizontal lines indicate the median titer, and dotted lines show the minimum and maximum IC50 thresholds.*

When we compared the neutralizing antibody responses in MIS-C patients and CC (**Figure 29A)**, no significant differences were observed for most variants. The only difference was a modest increase in cross-neutralizing reactivity against Omicron BA.1 in MIS-C patients. As predicted from the Luminex results, neutralizing response were strongly impaired against BA.1 in both MIS-C and CC; however, in this context several MIS-C participants, including both vaccinated and non-vaccinated, still showed

superior titers. When restricting the analysis to patients infected during the pre-Alpha period (**Figure 29B**), we could still observe 4 MIS-C patients with superior increased neutralizing titers against BA.1.

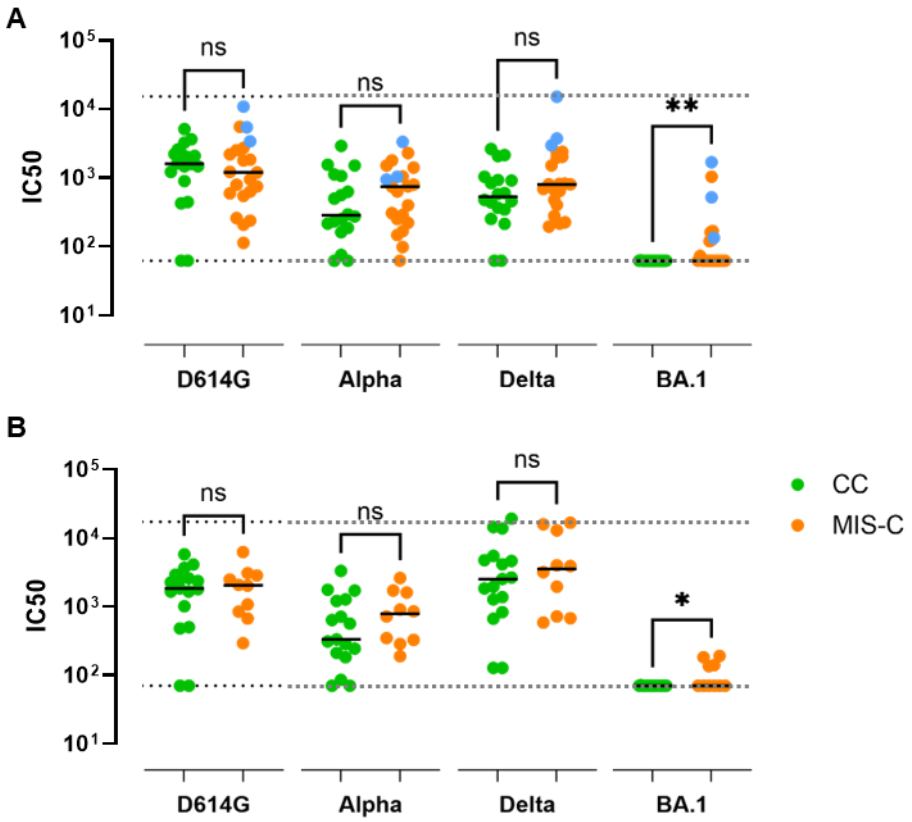


Figure 29. Neutralizing antibody responses against SARS-CoV-2 variants in MIS-C and CC. *Neutralizing antibody titers were measured against D614G, Alpha, Delta, and Omicron BA.1 variants. (A) Neutralizing antibody titers in the total cohort. Blue dots indicate vaccinated MIS-C patients. (B) Neutralizing antibody titers in patients infected during the pre-Alpha period. Each dot represents an individual sample, horizontal lines indicate the median titer, and dotted lines show the minimum and maximum IC50 thresholds.*

Overall, MIS-C patients did not show a major difference in SARS-CoV-2 neutralizing antibody responses compared with CC. Although MIS-C patients showed a tendency toward broader cross-neutralizing activity, particularly against BA.1, this difference was limited and should be interpreted cautiously due to the small cohort size. Therefore, these results suggest that MIS-C is not associated with a major alteration of the neutralizing antibody responses against SARS-CoV-2.

2.3. SARS-CoV-2-specific IgA and IgG subclasses

We further assessed differences in IgA and IgG subclasses. Regarding IgA (**Figure 30**), an increased S2-specific response in MIS-C was consistent across both IgA1 and IgA2, with significantly higher levels compared with CC (p=0.0046 and p=0.0090, respectively). Furthermore, these differences were maintained when only pre-Alpha individuals were analyzed.

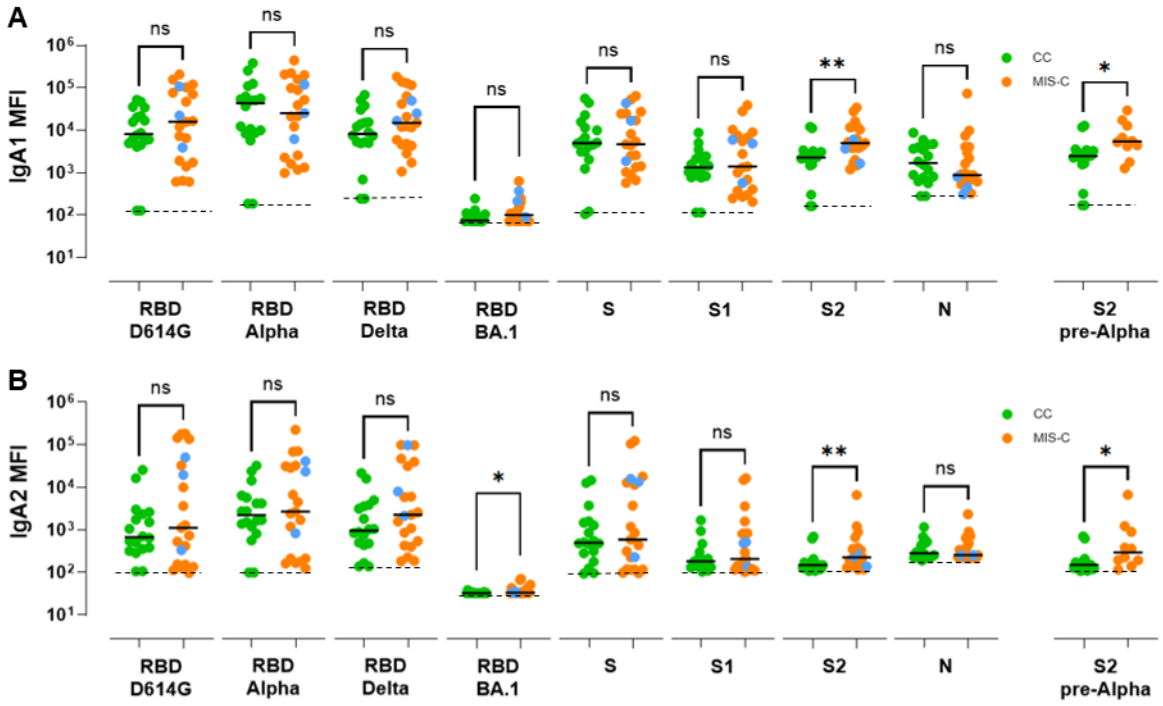


Figure 30. SARS-CoV-2 antigen-specific IgA1 and IgA2 responses in MIS-C and CC. *IgA subclass responses were measured against SARS-CoV-2 antigens, including RBD variants, S, S1, S2, and N with separate graph with patients from pre-Alpha period. (A) IgA1, (B) IgA2 responses against SARS-CoV-2 antigens. Each dot represents an individual sample, and horizontal lines indicate the median antibody signal. Blue dots represent MIS-C patients who were vaccinated before developing MIS-C. Responses are presented as MFI. The lower detection threshold was defined as the mean MFI value of HC, and values below this threshold were adjusted to the threshold value.*

We also assessed SARS-CoV-2 antigen-specific IgG subclasses. IgG1, IgG2, IgG3, and IgG4 responses were measured against RBD variants, S, S1, S2, and N antigens (**Figure 31**). We did not identify major differences in IgG1 responses between MIS-C and CC patients, except for the expected response against RBD BA.1 (**Figure 31A**). This increase appeared to be mainly driven by vaccinated individuals and patients infected during the post-Alpha period. However, IgG2 against RBD variants and spike-related proteins, including trimeric S, and recombinant S1, and S2, were elevated in MIS-C

patients compared with CC **(Figure 31B**). The IgG2 response against the N protein was also seemingly elevated, but this difference did not reach statistical significance (p=0.0653). Importantly, this increase did not appear to be driven by vaccinated individuals, as they were not among the highest responders (except for BA.1 RBD).

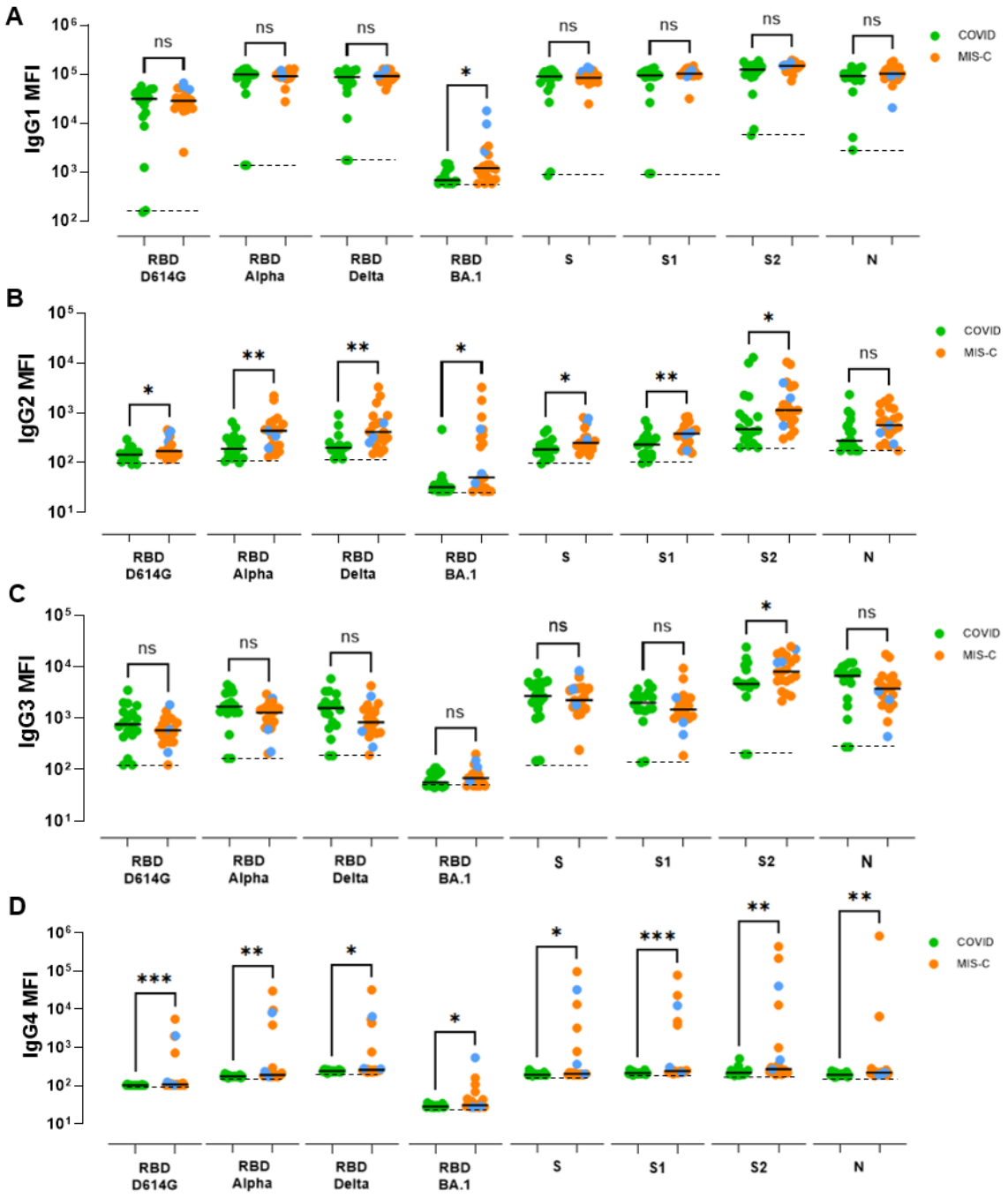


Figure 31. SARS-CoV-2 antigen-specific IgG subclass responses in MIS-C and CC. *(A) IgG1, (B) IgG2, (C) IgG3, and (D) IgG4 responses were measured against SARS-CoV-2 antigens, including RBD variants, S, S1, S2, and N. Each dot represents an individual sample, and horizontal lines indicate the median antibody signal. Blue dots represent MIS-C patients who were vaccinated before developing MIS-C. Responses are presented as MFI.*

IgG3 responses demonstrated a different pattern compared with the other IgG subclasses. Overall, most SARS-CoV-2 antigen-specific IgG3 showed a non significant trend towards a reduced response in MIS-C patients compared with CC, against most antigens (**Figure 31**Figure 31**C**). One exception was S2-specific IgG3 which showed significantly increased values in MIS-C patients (p= 0.0296), suggesting a selective enhancement of the S2-specific IgG3 response in MIS-C similarly to IgG2 and IgA responses.

IgG4 responses were mostly undetected across SARS-CoV-2 antigens in both MIS-C and CC patients (**Figure 31D**). However, MIS-C group revealed significantly higher titers, driven by a minority of individuals that showed consistent detectable IgG4 signal against most SARS-CoV-2 antigens, with an unclear relationship with vaccination status.

2.4. Antibody isotype/Subclass ratios

To further assess the relative balance of antibody isotypes, we calculated antibody subclass ratios to normalize the responses and evaluate the contribution of each subclass to the total antibody signal. Specifically, we analyzed IgG2/IgG1, IgG3/IgG1, and IgA/IgG ratios (**Figure 32**).

We previously observed a general significant increase of IgG2 responses in MIS-C against most SARS-CoV2 targets. When calculating IgG2/IgG1 ratios, significance was lost, although a trend for an increase response was still visible against most SARS-CoV-2 antigens (**Figure 32A**). This may reflect a small relative enrichment of the IgG2 response in MIS-C. This pattern was observed across multiple RBD and spike-related antigens, while vaccinated individuals were not consistently among the highest responders.

We previously observed a trend for decreased IgG3 response in MIS-C. IgG3/IgG1 ratios exacerbated this observation in MIS-C here showing significant reduction in MIS-C for RBDs, S1 and N (**Figure 32B**). The discrepancy with the S2-specific IgG3 response was still visible, albeit not significant, supporting a possible selective S2-associated IgG3 response in MIS-C.

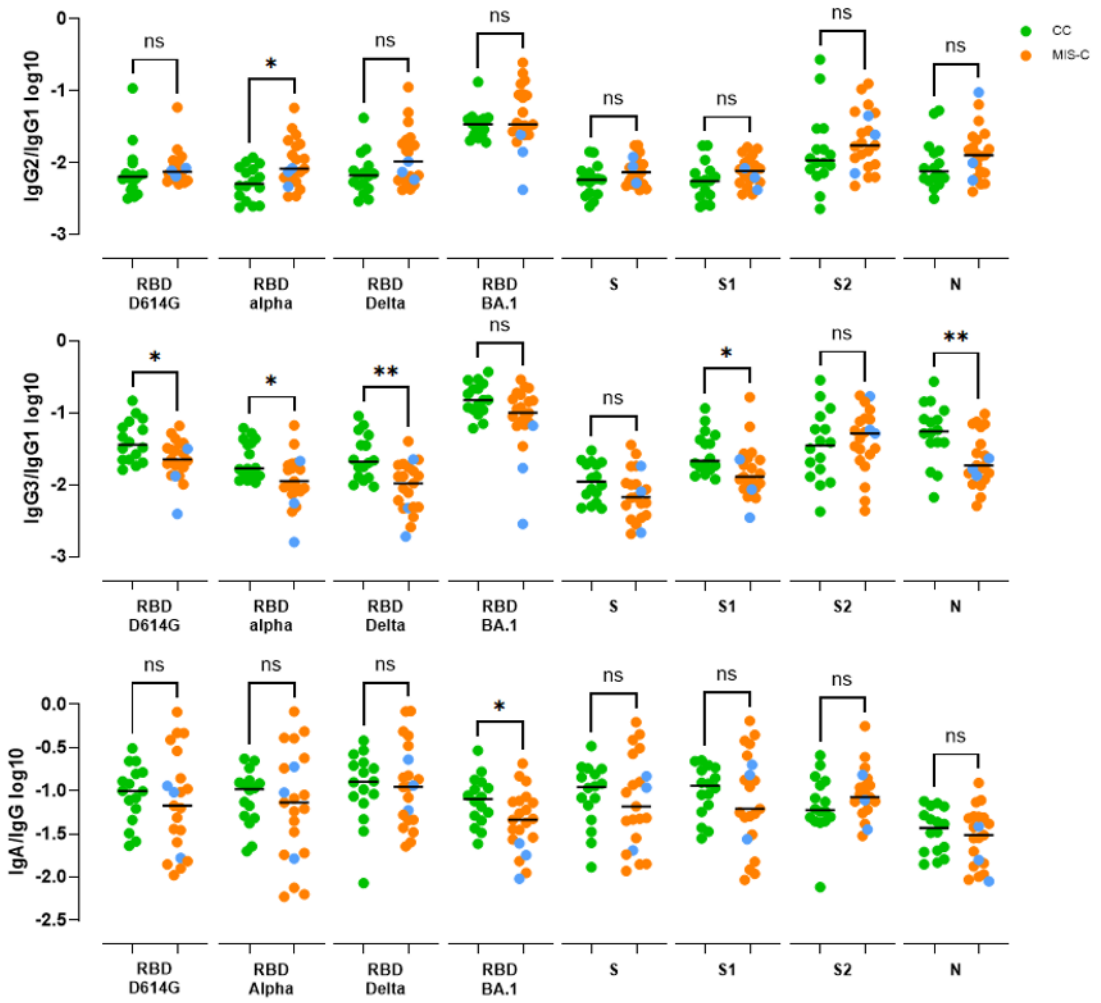


Figure 32. SARS-CoV-2 antigen-specific antibody isotype ratios in MIS-C and CC. *(A) IgG2/IgG1, (B) IgG3/IgG1, and (C) IgA/IgG ratios were calculated to normalize subclass responses relative to the dominant antibody signal. Each dot represents an individual sample, and horizontal lines indicate the median ratio. Blue dots represent MIS-C patients who were vaccinated before developing MIS-C.*

IgA/IgG ratios tended to be reduced in MIS-C patients across most SARS-CoV-2 antigens (**Figure 32C**). However, the S2-specific IgA/IgG ratio was relatively higher in MIS-C, consistent with the significantly increased total IgA and subtypes response observed against the S2 protein.

Overall, although MIS-C patients did not show any major humoral response alteration, we noticed some significant variations in the magnitude of IgG2, IgG3 and IgA responses and their relative ratio to the main IgG1 response. In addition, we observed a specific increase in S2 specific IgG2s, IgG3s and IgA1 and IgA2 responses.

2.5. Correlation analysis of SARS-CoV-2-specific markers

Next, we performed a correlation analysis between spike-derived antigen-specific antibody responses and neutralizing activity (**Figure 33**). For this we intentionally excluded IgG4 responses which tend to overshadow some results.

The CC group humoral response showed mainly correlations between IgG1, IgG3 and Neutralizing responses (**Figure 33A**). This pattern may reflect a more pro-inflammatory antibody profile. In contrast, MIS-C patients demonstrated a different correlation pattern, with neutralizing activity less correlated with IgG3 responses, but better associated with IgG2 and IgA responses (**Figure 33B**).

Altogether, these results suggest that a different tuning of the humoral and neutralizing response is operating in MIS-C patients. Importantly this analysis is based on a relatively small number of participants and should be taken with the necessary caution.

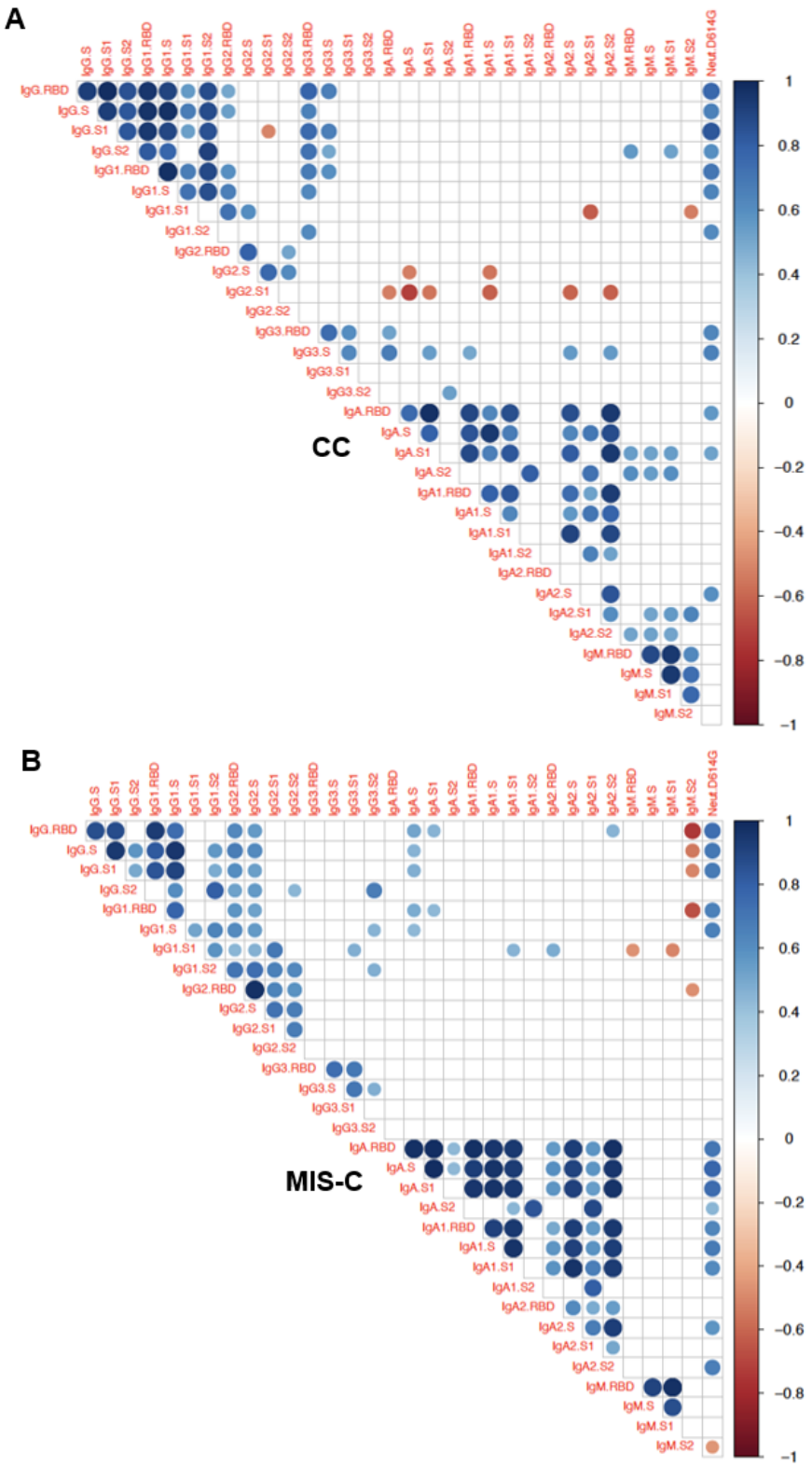


Figure 33. Correlation analysis among SARS-CoV-2-specific antibody responses and neutralizing activity in MIS-C and CC. *Spearman correlation analysis was performed to assess associations between antigen-specific antibody responses and neutralizing antibody titers. (A) Correlation matrix for CC, (B) MIS-C patients. Correlation values were adjusted for multiple comparisons. Blue circles indicate positive correlations, while red circles indicate negative correlations. The size and intensity of the circles represent the strength of the correlation. Only significant correlations are shown.*

2.6. Biomarker selection and participants classification

Finally, we performed a Random Forest analysis to identify antibody features that could distinguish MIS-C patients from CC (**Figure 34**). The out-of-bag (OOB) estimated error rate was 28.21%, indicating a moderate classification performance based on the selected antibody markers. According to the confusion matrix, 13 out of 18 CC samples were correctly classified, while 5 were misclassified as MIS-C. In the MIS-C group, 15 out of 21 patients were correctly classified as MIS-C, while 6 were misclassified as CC. Using an arbitrary threshold, we selected 7 most informative antibodies, including RBD-specific antibodies (IgG4 against ancestral variant and IgG2 against Delta), S1-specific antibodies (IgG2 against ancestral variant), and S2-specific antibodies (IgA1 and IgG4 against ancestral variant), and then performed unsupervised hierarchical clustering based on these features. Notably, increased antibodies against Delta RBD could be explained by the presence of individuals infected during Delta period in MIS-C.

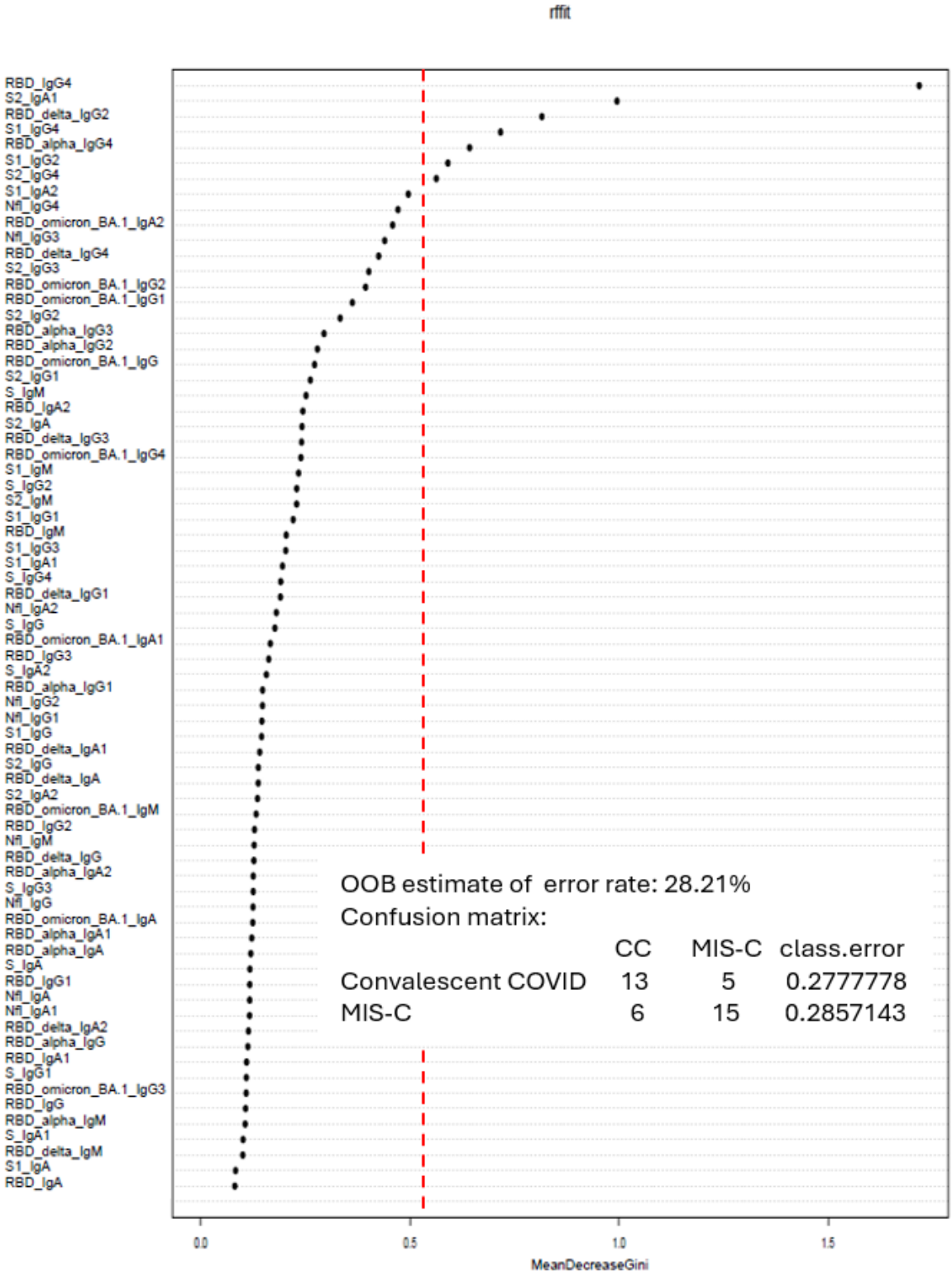


Figure 34. SARS-CoV-2-specific humoral response profiling in MIS-C and CC. *Random Forest analysis of antibody features distinguishing CC from acute MIS-C patients. Ranking of SARS-CoV-2-specific antibody markers differentiating CC and acute MIS-C patients according to Random Forest analysis.*

Using unsupervised hierarchical clustering of the participants using the top 7 antibody features selected by Random Forest analysis, we observed partial separation between MIS-C patients and CC (**Figure 35**). We observed the first cluster (upper part) of five patients with high levels of IgG4 responses against ancestral RBD, RBD Alpha, S1, and S2. In the second cluster (lower part), more than half of the MIS-C participants showed upregulation of RBD Delta-specific IgG2, S1-specific IgG2, and S2-specific IgA1 responses. These findings suggest that the selected antibody markers may partially distinguish MIS-C from CC.

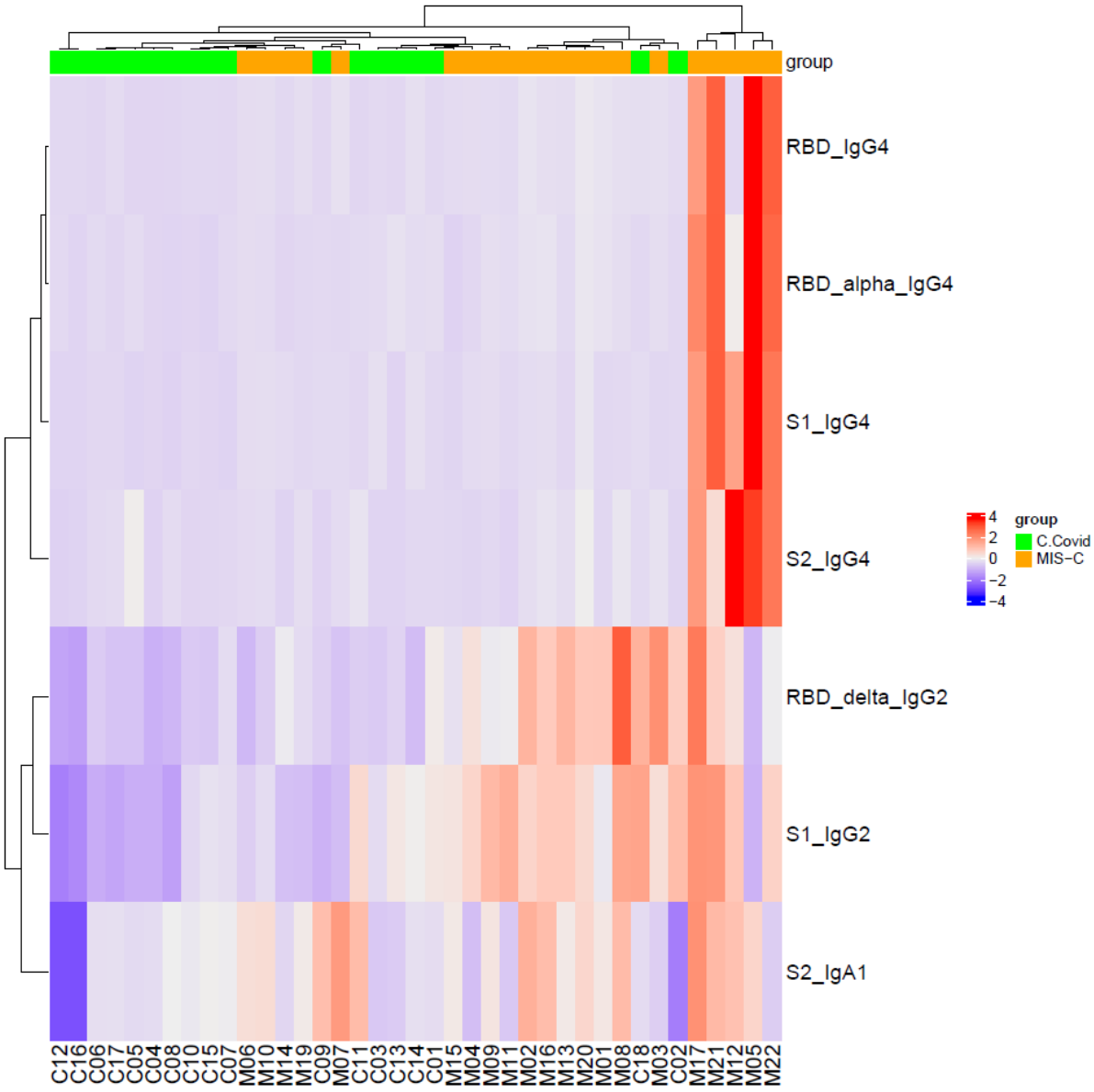


Figure 35. Selected antibody features distinguishing MIS-C and CC. *The top 7 antibody features identified by Random Forest analysis as the most informative for distinguishing MIS-C from CC were visualized using unsupervised hierarchical clustering. Blue indicates low expression levels, while red represents high expression levels.*

3. Characterization of the antibody reactivity against common cold coronaviruses and EBV in MIS-C, KD, and control groups.

A recent study has implicated EBV reactivation as a trigger for MIS-C associated hyperinflammation[253]. EBV was also proposed to play a role in KD[254,255], and common cold coronavirus are suggested as possible triggers of KD[256,257]. Here, our goal was to determine whether MIS-C patients showed a distinct antibody profile against common cold coronaviruses and EBV compared with CC. In this analysis, we also included a KD patient group and HC.

3.1. Humoral responses against common cold coronaviruses

First, we assessed antibody reactivity against common cold coronaviruses, including HCoV-229E, HCoV-NL63, HCoV-OC43, and HCoV-HKU1 as well as SARS-CoV-2. For each virus, responses against the spike (S1+S2) and nucleocapsid (N) proteins were analyzed including IgM, IgA, IgG, and IgG subtypes IgG1, IgG2, IgG3, and IgG4. These responses were compared between MIS-C, KD, CC, and pre-pandemic HC groups.

Overall, IgM levels we low and showed broad overlap between MIS-C, CC, HC, and KD groups, with no clear group-specific differences for most antigens (**Figure 36**). The main exception was the IgM response against the S protein of HCoV-NL63, where both MIS-C and CC patients showed higher titers compared with HC and KD groups (**Figure 36B**). As expected, both MIS-C and CC demonstrated elevated response against SARS-CoV-2, especially the spike. Finally, Kawasaki samples did not show any significant differences with the Healthy control group.

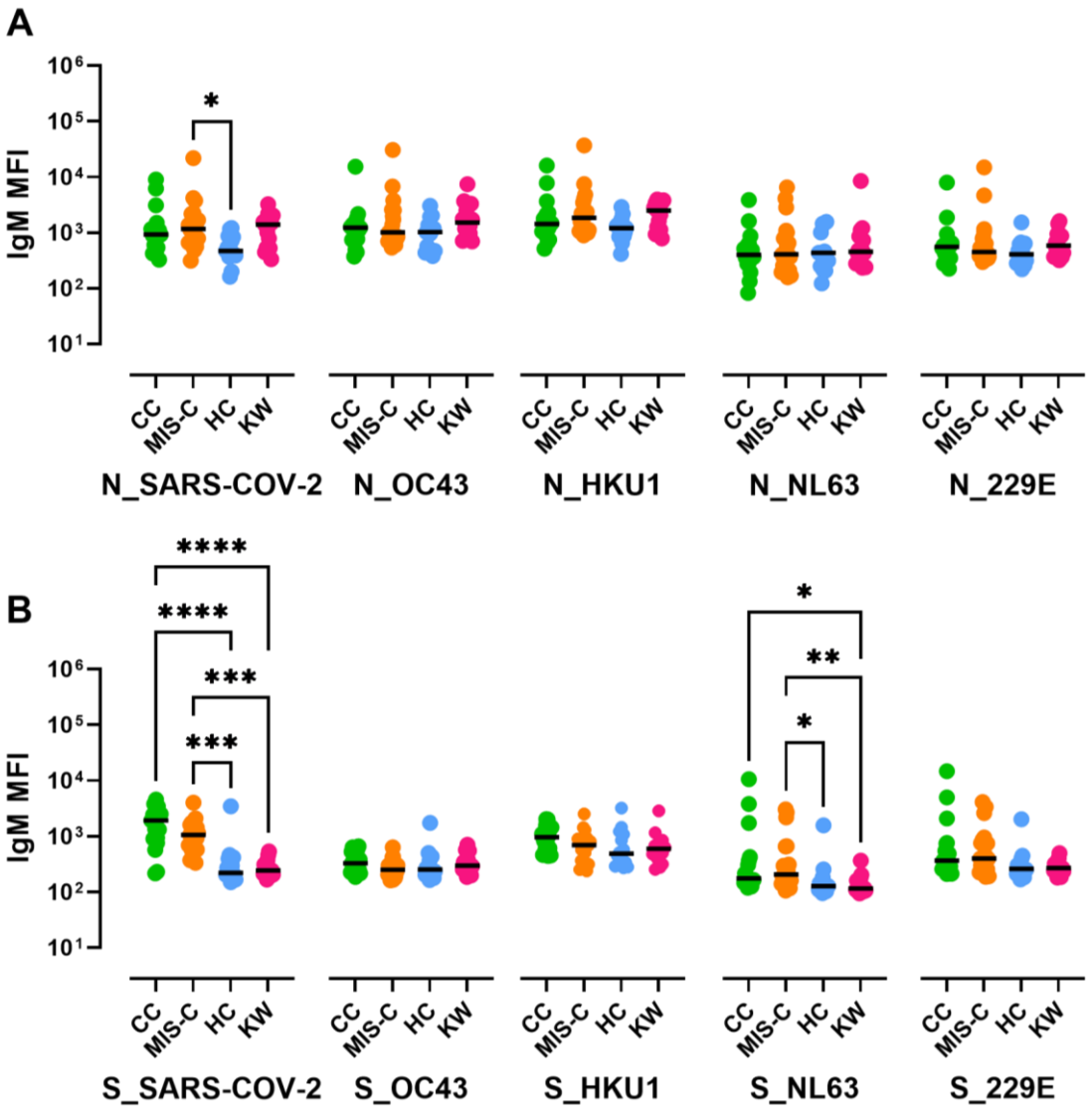


Figure 36. IgM responses against common cold coronaviruses and SARS-CoV-2. IgM antibody responses were measured against HCoV-229E, HCoV-NL63, HCoV-OC43, and HCoV-HKU1, as well as SARS-CoV-2. *(A) IgM responses against N proteins; (B) S proteins. Each dot represents an individual sample, and horizontal lines indicate the median antibody signal.*

Similarly, IgA responses against common cold coronaviruses did not differ significantly between groups, with broadly overlapping antibody levels across MIS-C, CC, HC, and KD patients (**Figure 37**). However, we observed a tendency toward higher IgA responses against the S proteins of HCoV-HKU1 and HCoV-229E in MIS-C and CC groups.

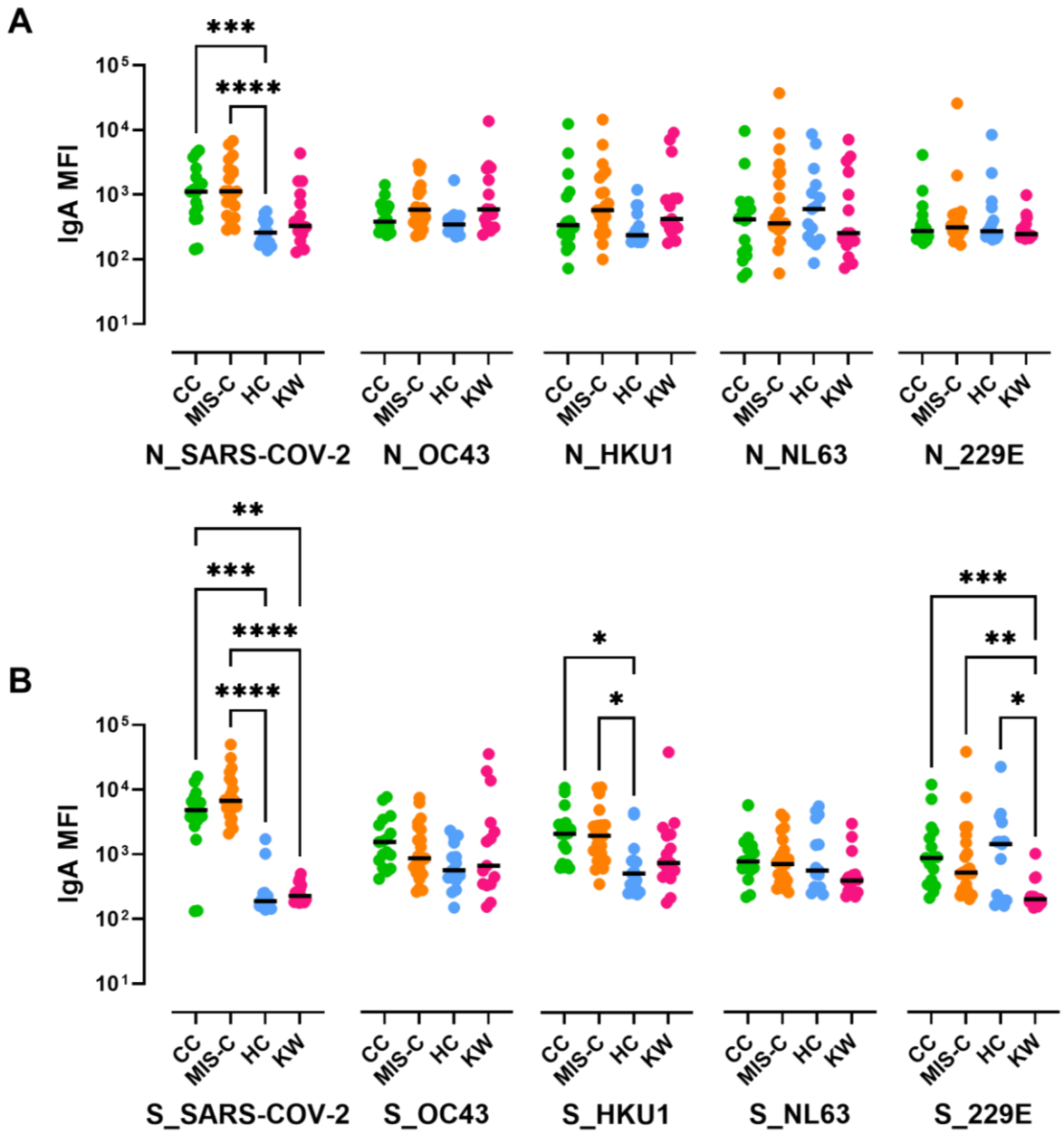


Figure 37. IgA responses against common cold coronaviruses and SARS-CoV-2. IgA antibody responses were measured against HCoV-229E, HCoV-NL63, HCoV-OC43, and HCoV-HKU1, as well as SARS-CoV-2. *(A) IgA responses against N proteins, S proteins. Each dot represents an individual sample, and horizontal lines indicate the median antibody signal.*

When comparing IgG responses against common cold coronaviruses, we first observed a significant increase of IgG against OC43 and HKU1 in both MIS-C and CC possibly corresponding to a boost of preexisting IgG against these 2 viruses. We observed that KD patients showed higher titers against the N protein of HCoV-OC43 and HCoV-HKU1 (**Figure 38A**). In contrast, IgG responses against the S proteins of the same coronaviruses were slightly lower in KD patients compared with MIS-C and CC groups (**Figure 38B**).

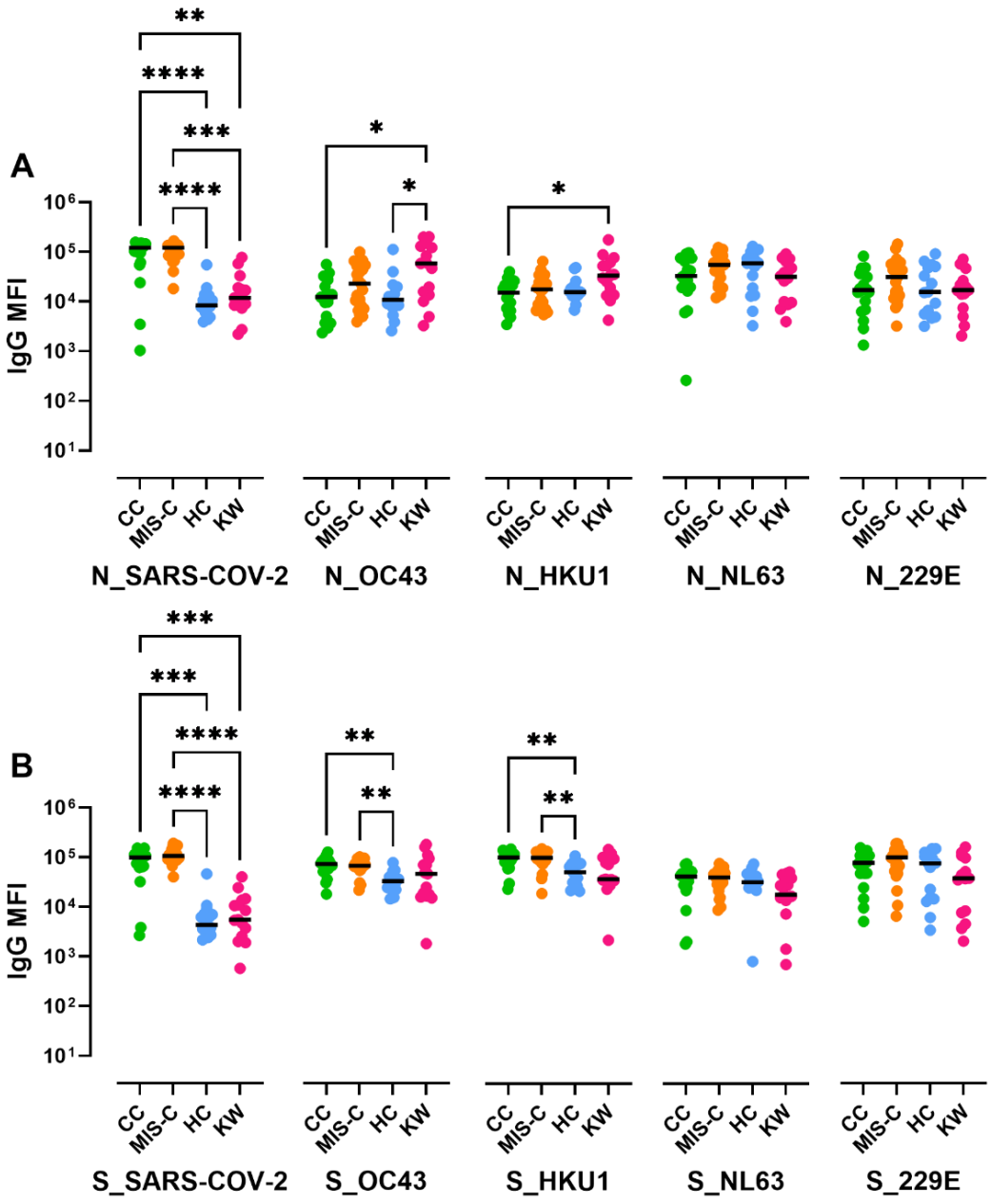


Figure 38. IgG responses against common cold coronaviruses and SARS-CoV-2. IgG antibody responses were measured against HCoV-229E, -NL63, -OC43, and -HKU1, as well as SARS-CoV-2. *(A) IgG responses against N proteins, (B) S proteins. Each dot represents an individual sample, and horizontal lines indicate the median antibody signal.*

IgG1, IgG2, and IgG3 antibody responses against other common cold coronaviruses were also evaluated, but no significant differences were observed between groups (data not shown). IgG4 responses showed a small subgroup of MIS-C patients with higher antibody levels against common cold coronaviruses, including elevated responses against the NL63 N protein (**Figure 39A**). However, when individual patients were examined, the patients with increased IgG4 responses were not always the same for N and S proteins (**Figure 39B**). The main exception was patient M17, who showed increased IgG4 responses across almost all tested antigens. In addition, each study group contained at least one patient with antibody titers that were higher than those of the other individuals within the same group.

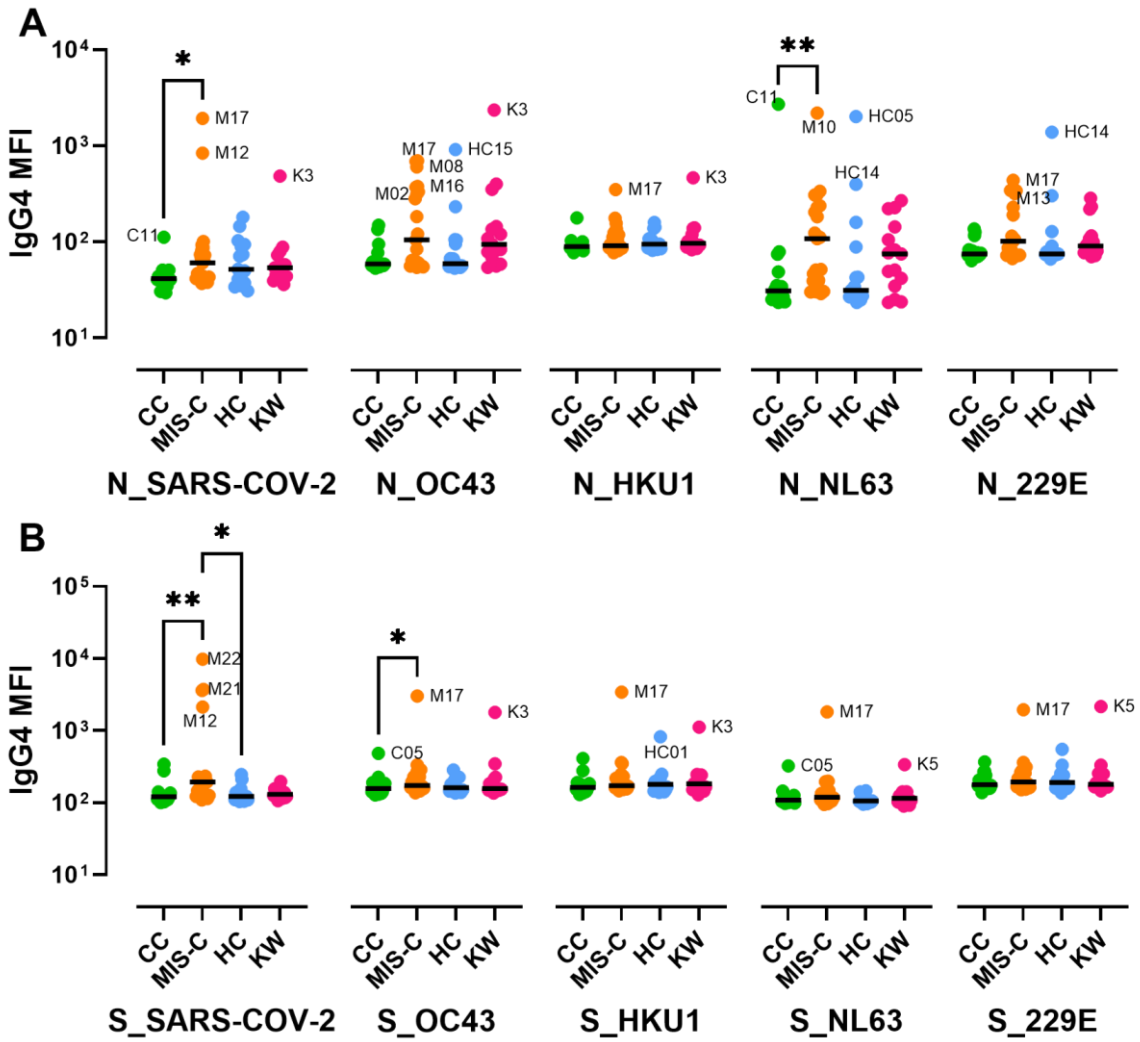


Figure 39. IgG4 responses against common cold coronaviruses and SARS-CoV-2. IgG4 antibody responses were measured against HCoV-229E, HCoV-NL63, HCoV-OC43, and HCoV-HKU1, as well as SARS-CoV-2. IgG4 responses against*. (A) N proteins, (B) S proteins. Each dot represents an individual sample, and horizontal lines indicate the median antibody signal.*

3.2. Humoral responses against Epstein–Barr virus

Finally, we assessed antibody responses against Epstein–Barr virus. We measured reactivity against VCA p18, which is used to identify previous EBV exposure during the patient's lifetime, and ZEBRA, which is associated with viral reactivation. This allowed us to evaluate whether MIS-C patients showed evidence of altered EBV-specific antibody responses or possible EBV reactivation compared with the other study groups.

Overall, no significant differences between groups were identified for EBV-specific IgM, IgA, or total IgG responses (**Figure 40**). However, when IgG subclasses were analyzed, MIS-C patients revealed increased responses against the EBV Zebra protein for IgG3 and IgG4 compared with CC, reaching statistical significance for both IgG3 (p=0.0352) and IgG4 (p=0.0020). Besides, IgG2 levels against Zebra tended to be higher in MIS-C patients than in CC, although this difference was not statistically significant (p=0,0814). In contrast, a significant increase was observed when MIS-C patients were compared with healthy controls (p=0,0428).

The increased antibody response against EBV ZEBRA may suggest enhanced recognition of EBV lytic/reactivation-associated antigens in MIS-C patients, although this finding alone does not confirm active EBV reactivation.

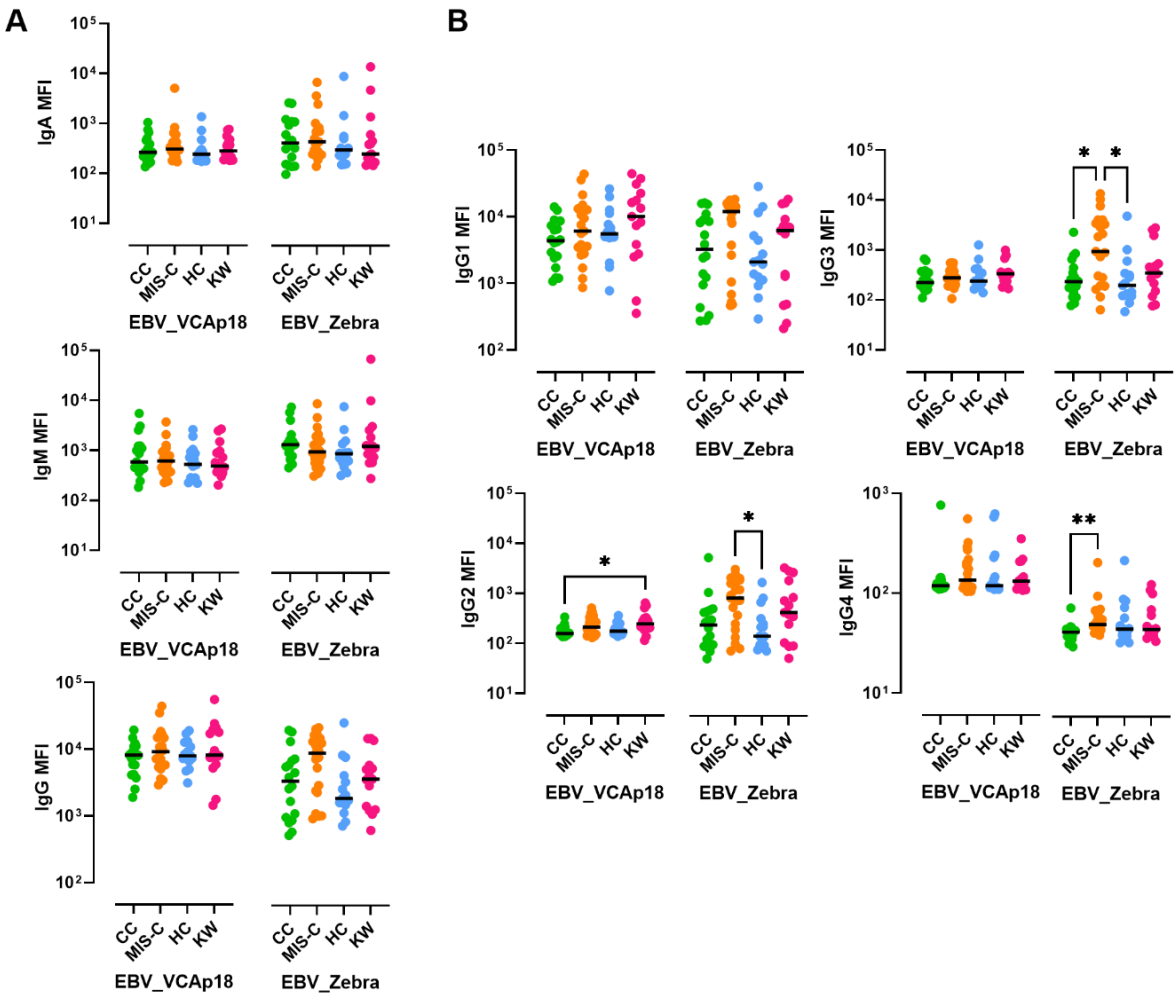


Figure 40. Antibody responses against Epstein–Barr virus in CC, MIS-C, HC, and KD. *(A) IgA, IgM, and IgG; (B) IgG antibody subclasses against Epstein–Barr virus were measured using VCA p18 and ZEBRA antigens. Each dot represents an individual sample, and horizontal lines indicate the median antibody signal.*

3.3. Biomarker selection and participants classification

To further evaluate whether MIS-C and KD showed distinct antibody profiles compared with their respective control groups, we performed Random Forest analyses. These analyses focused on humoral responses against common cold coronaviruses and Epstein–Barr virus. We first compared MIS-C patients with CC (**Figure 41**). The Random Forest model revealed an out-of-bag (OOB) error rate of 28.21%, corresponding to an overall classification accuracy of approximately 71.79%. It correctly classified 15 out of 18 CC controls and 13 out of 21 MIS-C patients. Overall, the selected antibody markers have some discriminatory capacity, but the separation between MIS-C and CC is limited. We identified 9 antibody markers that contributed most to distinguishing the two groups.

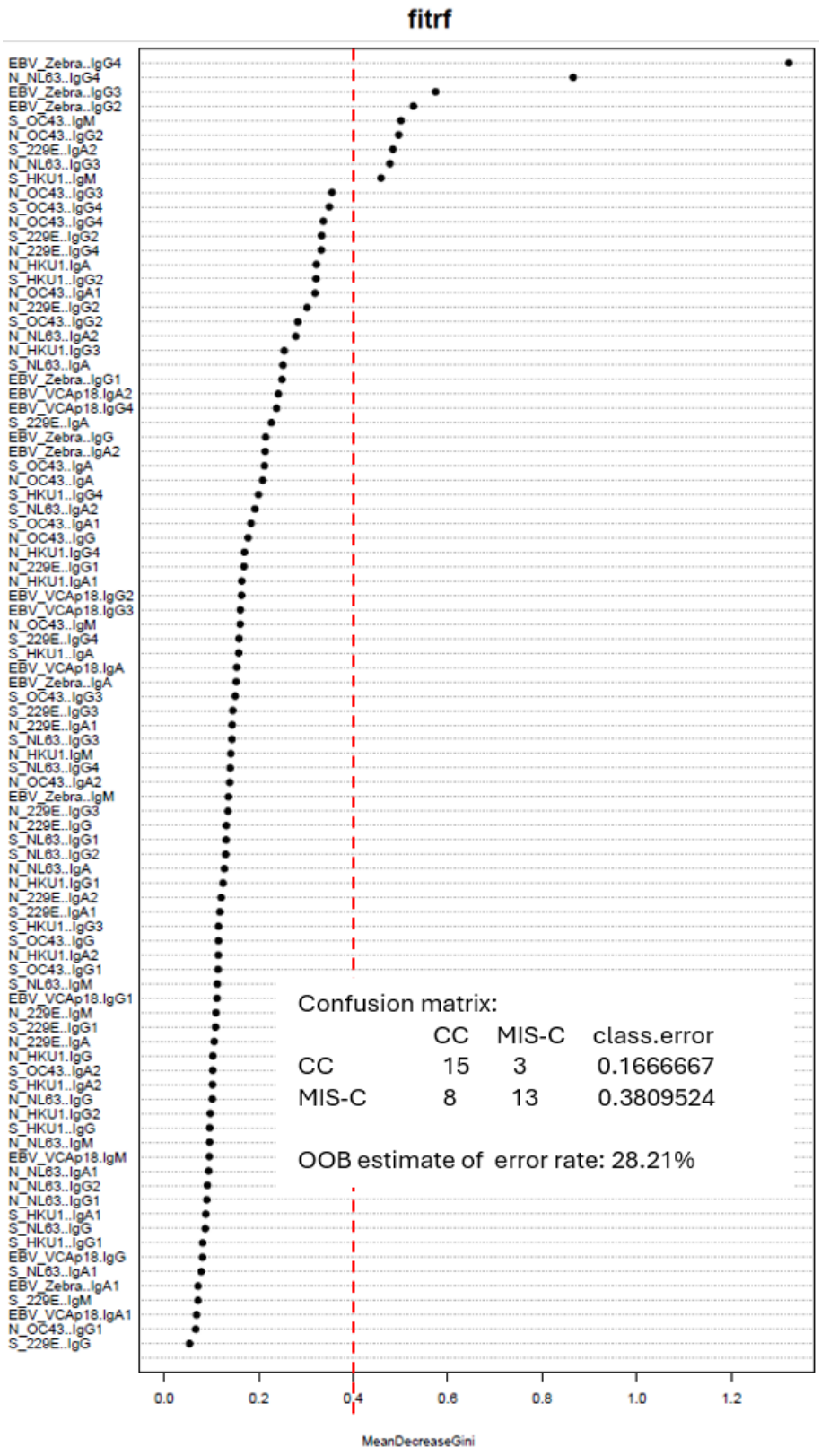


Figure 41. Random Forest analysis of antibody responses against common cold coronaviruses and Epstein–Barr virus distinguishing MIS-C and CC. *Antibody features are ranked according to their MeanDecreaseGini importance score. The red dashed line indicates the threshold used to select the most informative markers. The confusion matrix shows the classification performance of the model, with an OOB error rate of 28.21%.*

Unsupervised hierarchical clustering of the 9 antibody markers selected by Random Forest analysis did not clearly separate MIS-C patients from CC (**Figure 42**). However, a subgroup of MIS-C patients showed higher antibody signals for several selected markers, particularly EBV ZEBRA-specific IgG subclasses, including IgG2, IgG3, and IgG4, as well as selected antibody responses against common cold coronaviruses. These findings suggest that the selected markers may contribute to the differentiation of MIS-C from CC, although the separation between the groups was incomplete. Importantly, EBV ZEBRA-specific IgG4 was the top marker selected by Random Forest analysis for distinguishing MIS-C patients from CC. This supports the relevance of EBV ZEBRA-specific IgG4 responses in the differential antibody profile observed in MIS-C.

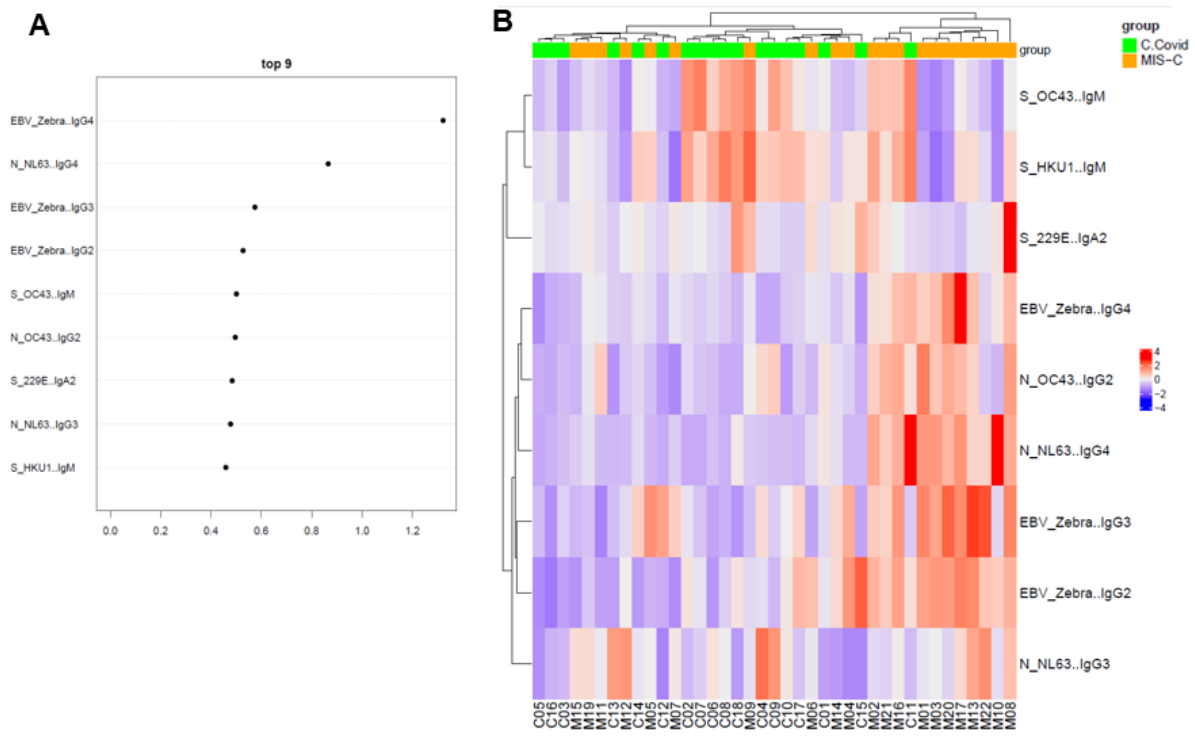


Figure 42. Selected antibody markers distinguishing MIS-C and CC based on common cold coronavirus and EBV responses. *(A) The 9 antibody markers selected by Random Forest analysis as the most informative for distinguishing MIS-C patients from CC. (B) Unsupervised hierarchical clustering based on these 9 selected antibody markers. The top annotation indicates the clinical group, including MIS-C and CC samples. Blue indicates lower antibody levels, while red indicates higher antibody levels.*

Using the same strategy, we performed Random Forest analysis to distinguish KD patients from HC based on antibody responses against common cold coronaviruses and Epstein–Barr virus (**Figure 43**). The model showed an OOB error rate of 30%, indicating limited classification performance. According to the confusion matrix, 10

out of 15 KD patients and 11 out of HC were correctly classified. These results suggest that the selected antibody markers only partially distinguish KD from HC.

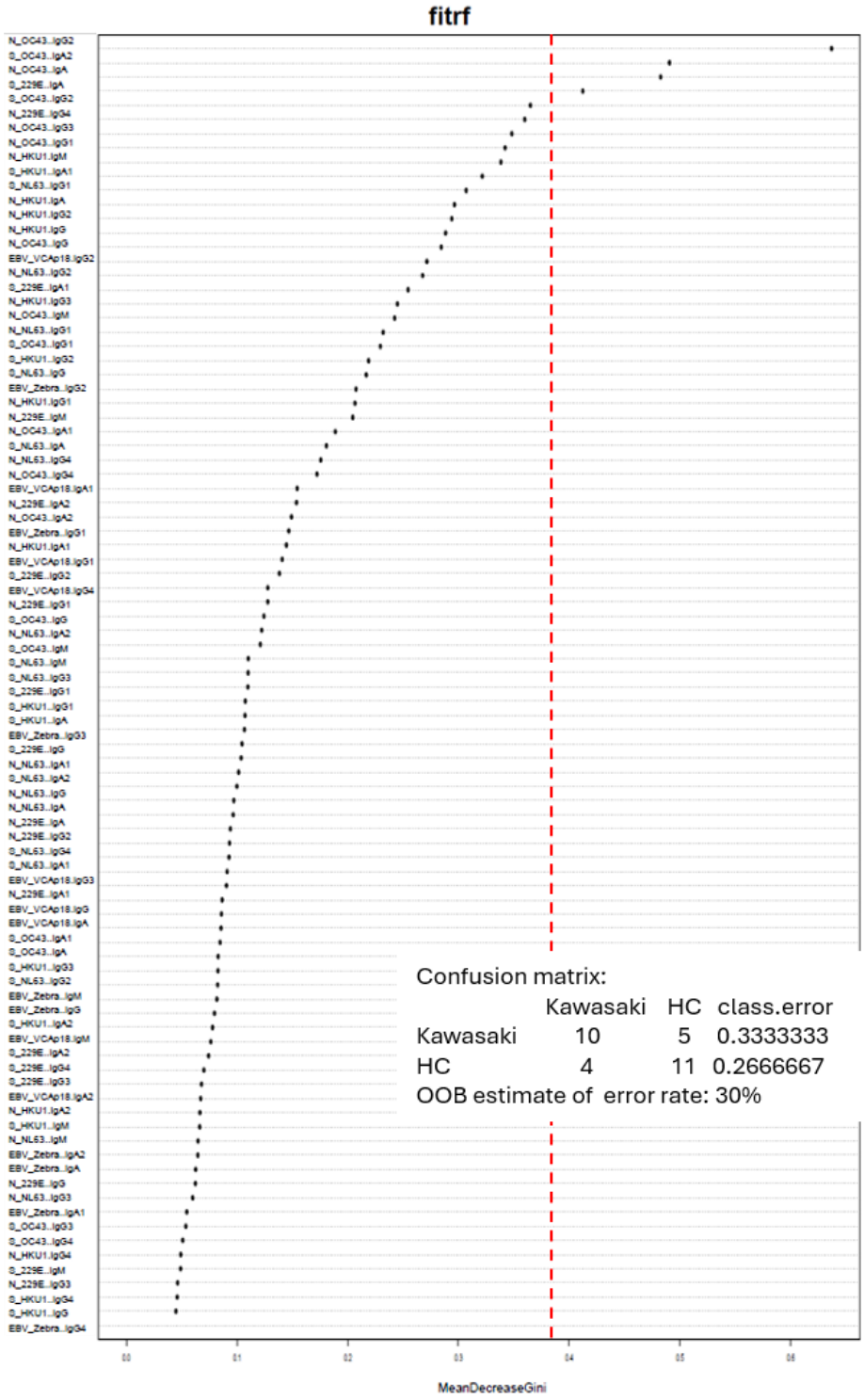


Figure 43. Random Forest analysis of antibody responses against common cold coronaviruses and Epstein–Barr virus distinguishing KD and HC. *Antibody features are ranked according to their MeanDecreaseGini importance score. The red dashed line indicates the threshold used to select the most informative markers. The confusion matrix shows the classification performance of the model, with an OOB error rate of 30%.*

Random Forest analysis selected 4 antibody markers as the most informative for distinguishing KD patients from HC (Figure 44A). These markers were N-OC43-specific IgG2, N-OC43-specific IgA, S-OC43-specific IgG2, and S-229E-specific IgA.

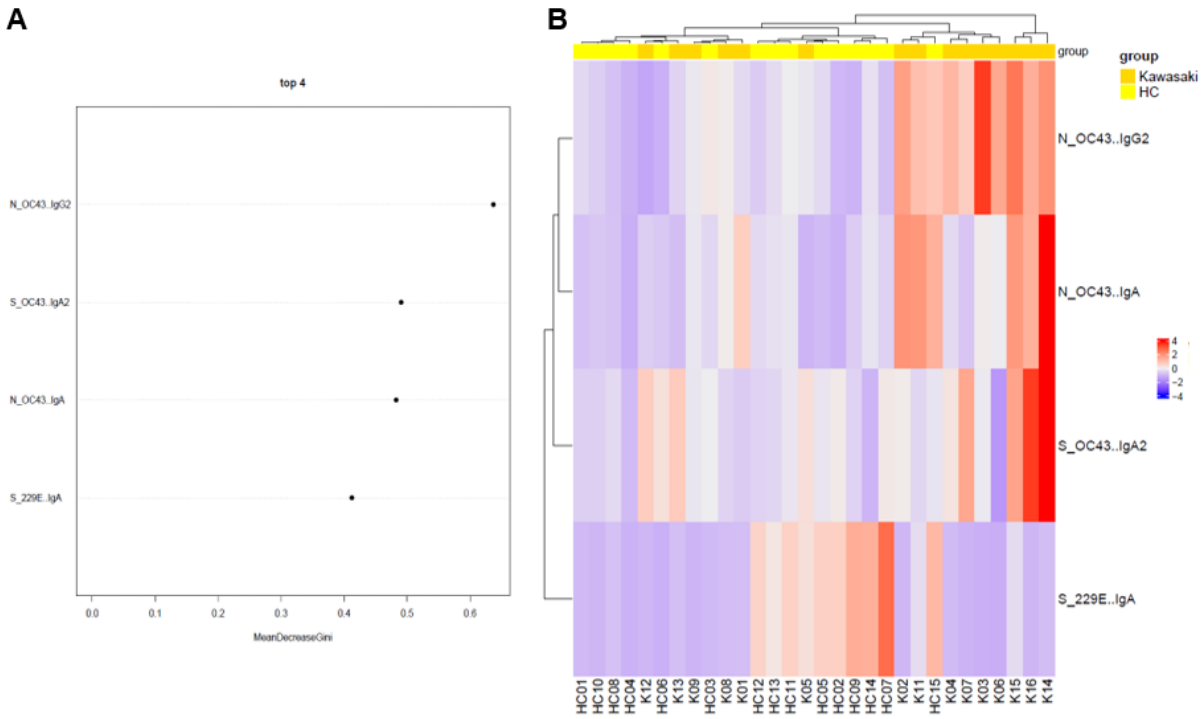


Figure 44. Unsupervised hierarchical clustering of antibody markers selected by Random Forest analysis. *(A) 4 antibody markers selected by Random Forest analysis as the most informative for distinguishing KD patients from HC were visualized using unsupervised hierarchical clustering. The top annotation indicates the clinical group, including KD and HC samples. (B) The heatmap shows relative antibody levels, with blue indicating lower responses and red indicating higher responses.*

Unsupervised hierarchical clustering of the selected antibody markers revealed only limited separation between KD patients and HC **(Figure 44**). A subgroup of KD patients clustered together and demonstrated higher antibody responses for several HCoV-OC43-related markers, especially N-OC43-specific IgG2, N-OC43-specific IgA, and S-OC43-specific IgG2. However, the groups were not completely separated, as part of KD and HC participants were still mixed across the heatmap. S-229E-specific IgA showed a different pattern, with higher signals in only a subset of samples from HC and one from KD (KD5). Overall, these findings suggest that the selected markers may contribute to distinguishing KD from HC, but the separation remains incomplete.

4. Inflammatory response associated with MIS-C

As MIS-C is characterized by systemic inflammation and immune dysregulation, we aimed to define its inflammatory profile, identify biomarkers associated with disease severity, and evaluate their relationship with clinical parameters. We also explored the longitudinal evolution of inflammatory markers after the acute phase to better understand potential long-term immune alterations.

4.1. Inflammatory biomarkers associated with acute MIS-C

We first compared the inflammatory response between acute pre-treatment MIS-C and CC participants. Serum samples were analyzed using the T96 Olink technology for 92 inflammatory biomarkers. A direct fold-change analysis identified 29 biomarkers with significant differences between the two groups (**Figure 45**), including 24 showing higher levels in MIS-C and 5 showing higher levels in CC. The most overexpressed biomarkers in MIS-C were IL-6, IL-10 and IFN-γ and the most downmodulated were stem cell factor (SCF) and TNF-related activation-induced cytokine (TRANCE).

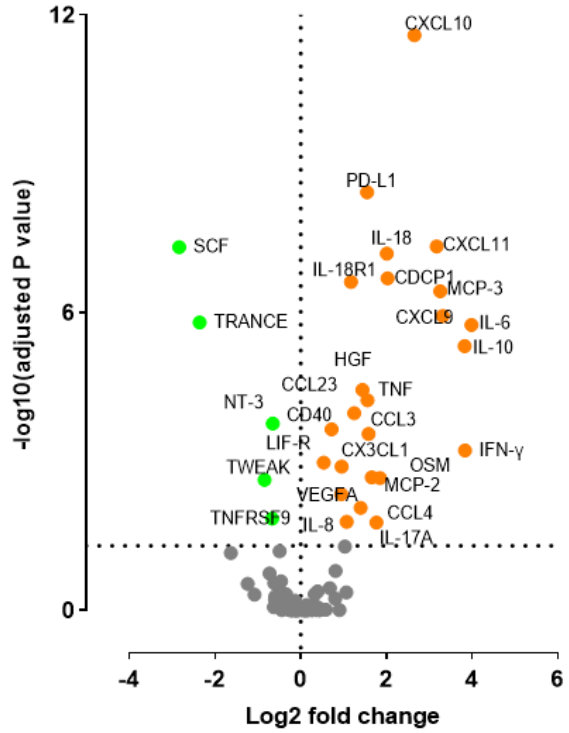


Figure 45. Comparative analysis of inflammatory biomarkers between MIS-C and CC: Volcano plot. *Volcano Plot representation of the relative levels (Log2-fold change) of biomarkers in MIS-C compared to CC. Horizontal dashed line indicates the threshold to 95% certainty. Protein highlighted in green were significantly upregulated in MIS-C while protein highlighted in orange were significantly downregulated.*

We next performed a Random Forest analysis to narrow down the best differentiating parameters (**Figure 46**). The out of the box (OOB) estimated error rate was 5.13% (**Figure 46**). Specifically, all 17 CC samples were properly classified, but 2 out of 22 MIS-C cohort patients were misclassified as part of the CC group.

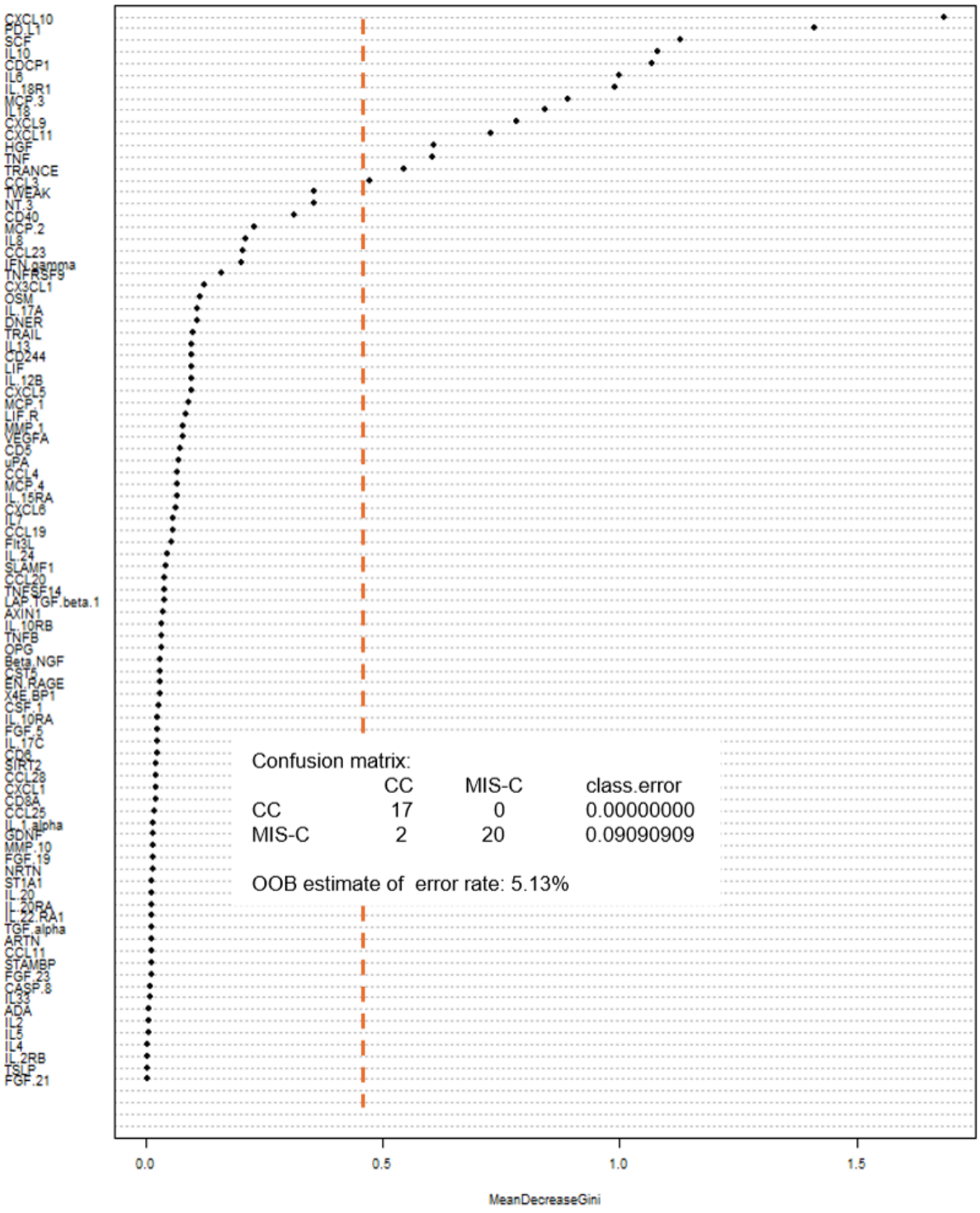


Figure 46. Analysis of inflammatory biomarkers between MIS-C and CC: Random Forest analysis. *Random Forest analysis comparing CC and acute MIS-C patients. Biomarkers are ranked according to their importance in differentiating the two groups.*

From this analysis, we identified 18 markers considered to have the most influence on the classification of MIS-C and CC (**Figure 47A**). All these markers were among the 29 identified by the 2 fold-change analysis and included pro-inflammatory cytokines IL-6, TNFα, IL-18 and its receptor IL-18R1, the anti-inflammatory cytokine IL-10, the chemokines CXCL9, CXCL10, CXCL11/I-TAC, CCL3 and MCP3/CCL7, several regulatory molecule such as CD40, CUB domain-containing protein 1 (CDCP1)/CD318, programmed death-ligand 1 (PDL1), TRANCE and TNF-related weak inducer of apoptosis (TWEAK), and the growth factors hepatocyte growth factor (HGF), SCF and neurotrophin-3 (NT3).

Using this set of 18 biomarkers, we performed an unsupervised clustering of acute MIS-C and CC samples in which two main groups were identified (**Figure 47**). One group included the majority of the MIS-C individuals (20 out of 22). Most differentiating biomarkers were upregulated in the MIS-C cluster, while TRANCE, TWEAK, SCF, and NT-3 were downregulated. The second group included all CC individuals as well as 2 MIS-C diagnosed individuals who showed a biomarker profile indistinguishable from the CC group.

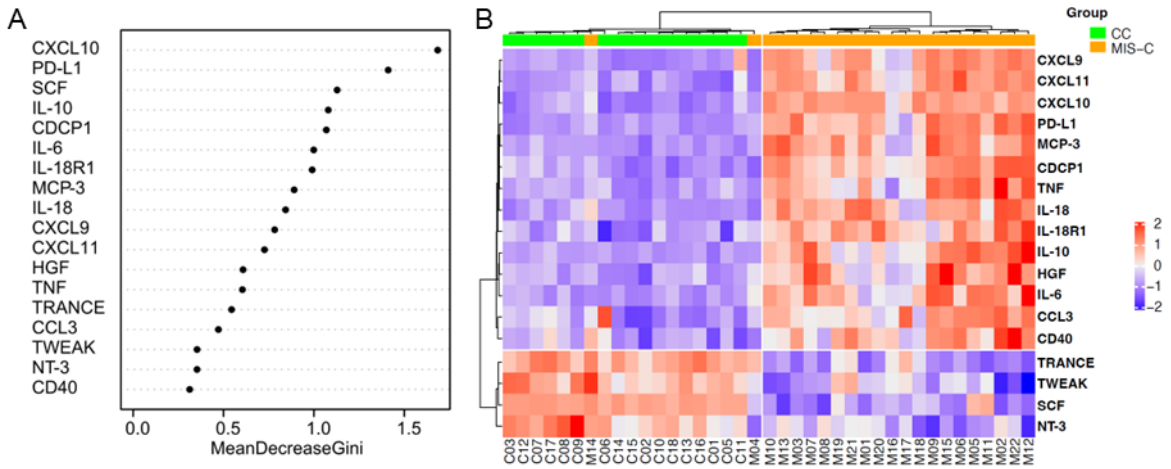


Figure 47. Key inflammatory biomarkers distinguishing acute MIS-C from CC. *(A). Top 18 cytokines distinguishing MIS-C from convalescent group extracted from random forest analysis (Fig 25B). (B). Clustered heatmap showing the levels pattern of key inflammatory markers selected from Random Forest analysis. Blue indicates low expression levels, while red represents high expression levels.*

To further investigate the functional relationships among the 29 selected biomarkers from the volcano plot, we conducted a functional protein–protein interaction analysis using the STRING database (**Figure 48**), which revealed the involvement of TNF, IL-10 and INF-γ pathways in the pathophysiology of MIS-C.

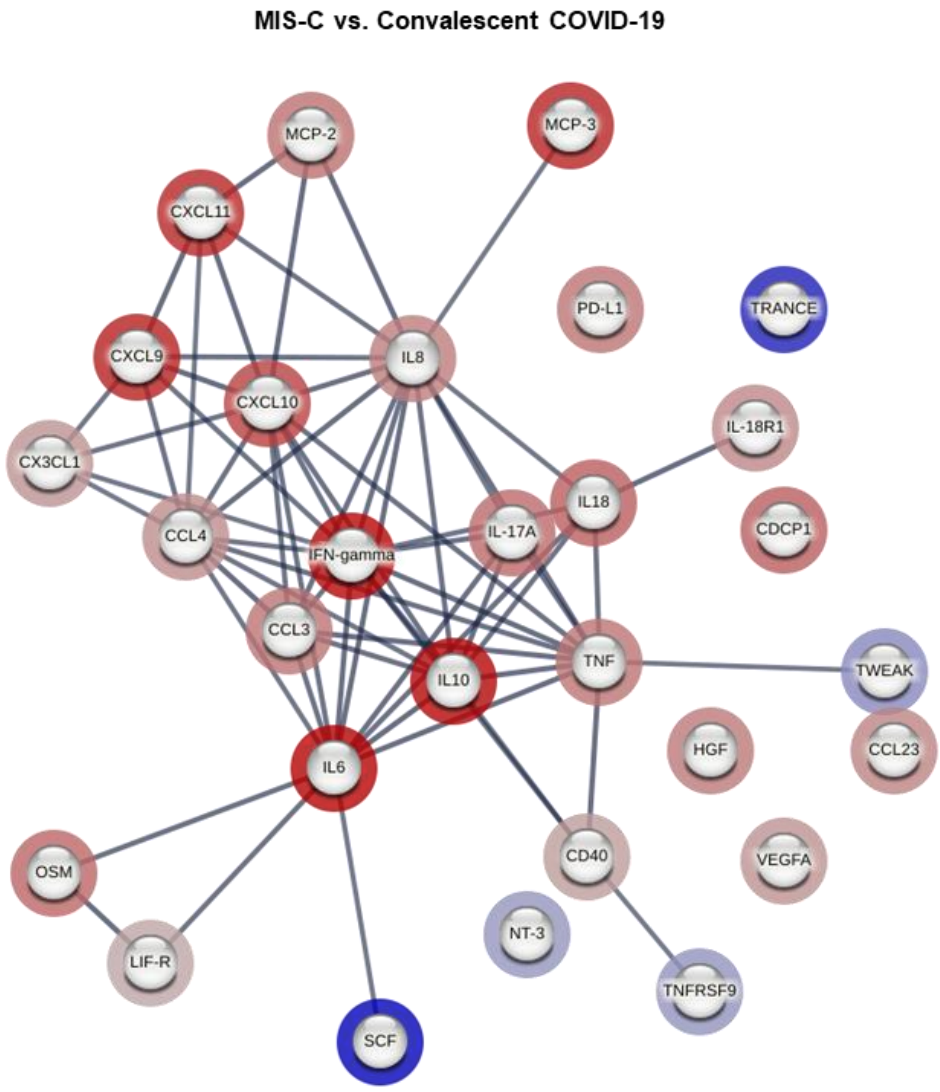


Figure 48. Protein-protein Interaction Network Based on STRING Analysis. STRING network analysis visualizing the protein-protein interactions among differentially expressed biomarkers. *The classification is based on volcano test (Fig.2A). Proteins shown in red are upregulated in MIS-C group, while blue nodes represent downregulated proteins. The highest positive values for MIS-C were IL-6 (3.988), IFN-γ (3.834), IL-10 (3.829), with lowest values of SCF (-2.831) and TRANCE (-2.355).*

Sex stratified random forest analyses identified separate sets of biomarkers differentiating MIS-C vs. CC within male and female participants with only 9 markers common to both analyses: IL-10, CDCP1, CXCL10, CXCL11, IL-18, PD-L1, MCP-3/ CCL7, SCF and IL-6 **(Figure 49 A** and **B**). Notably, the classification of female participants between CC and MIS-C was less effective (**Figure 49C**) and included the two MIS-C samples misclassified as CC in random forest and clustering analyses.

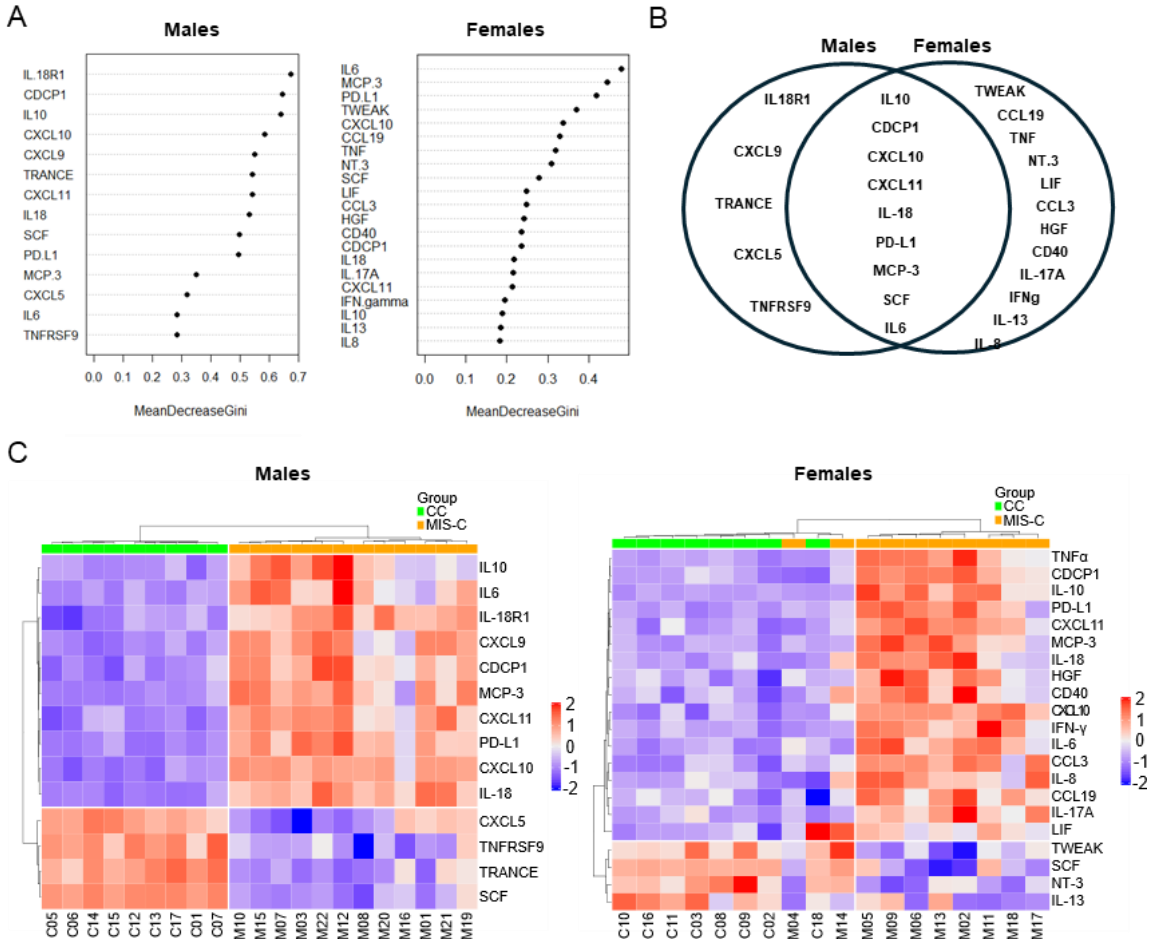


Figure 49. Sex stratified random forest analysis between CC and acute MISC. *(A). Top cytokines identified by random forest analysis in each sex group. The random forest analysis highlights the most important cytokines distinguishing CC and acute MIS-C for males (left panel) and females (right panel). (B). Venn Diagram of sex-specific and shared cytokines. The Venn diagram compares cytokines identified by random forest analysis in males and females. Shared cytokines (center) are involved in both groups, while sex-specific cytokines (left for males, right for females) indicate potential sex-based immune response differences. (C). Heatmaps of cytokine levels. Heatmaps illustrate the levels patterns of cytokines selected by random forest analysis in males (left) and females (right). Red indicates higher levels, while blue represents lower levels, showing distinct profiles.*

4.2. Severity-associated inflammatory biomarkers in MIS-C

Next, we analyzed inflammatory responses between the more severe MIS-C cases requiring ICU care and the less severe cases managed in the general inpatient unit. This grouping strategy was expected to identify biomarkers that could predict the requirement for ICU admission. Main characteristics of these subgroups are shown in Table 4, identifying a high percentage of males in the ICU group.

Following the same strategy described above, we identified by random forest analysis the inflammatory markers best capable of discriminating ICU-admitted from non-ICU-admitted MIS-C cases (**Figure 50** and **Figure 51A**).

Among the 6 best biomarkers, two markers upregulated in severe cases (IL-2 and IL-33), and four markers downregulated in severe cases (soluble CD8α, TNF-receptor superfamily 9 (TNFRSF9), CD244 and SCF, **Figure 51A**). Applying these 6 parameters in an unsupervised clustering of the MIS-C participants allowed for the separation of all patients except for one non-ICU MIS-C whose biomarker profile resembled the one of ICU participants (**Figure 51B**). When comparing individually these markers in CC, MIS-C non-ICU and MIS-C ICU, we observed three main situations (**Figure 51C**). TNFRSF9 and SCF both showed a trend for downregulation within MIS-C non-ICU vs. convalescents and lower levels in MIS-C ICU vs. non-ICU. CD244 was significantly decreased in MIS-C ICU ($p=0.0005$) but was similar in convalescent and MIS-C non-ICU groups. IL-33 and soluble CD8α both showed differential levels between MIS-C non-ICU and MIS-C ICU ($p=0.0087$, $p=0.0034$, respectively) but no significant difference between MIS-C groups and CC. Notably, IL-2 showed the most surprising pattern with a strong downregulation in MIS-C non-ICU compared to both CC ($p=0.0404$) and MIS-C ICU ($p=0.0113$), but no difference between CC and MIS-C ICU.

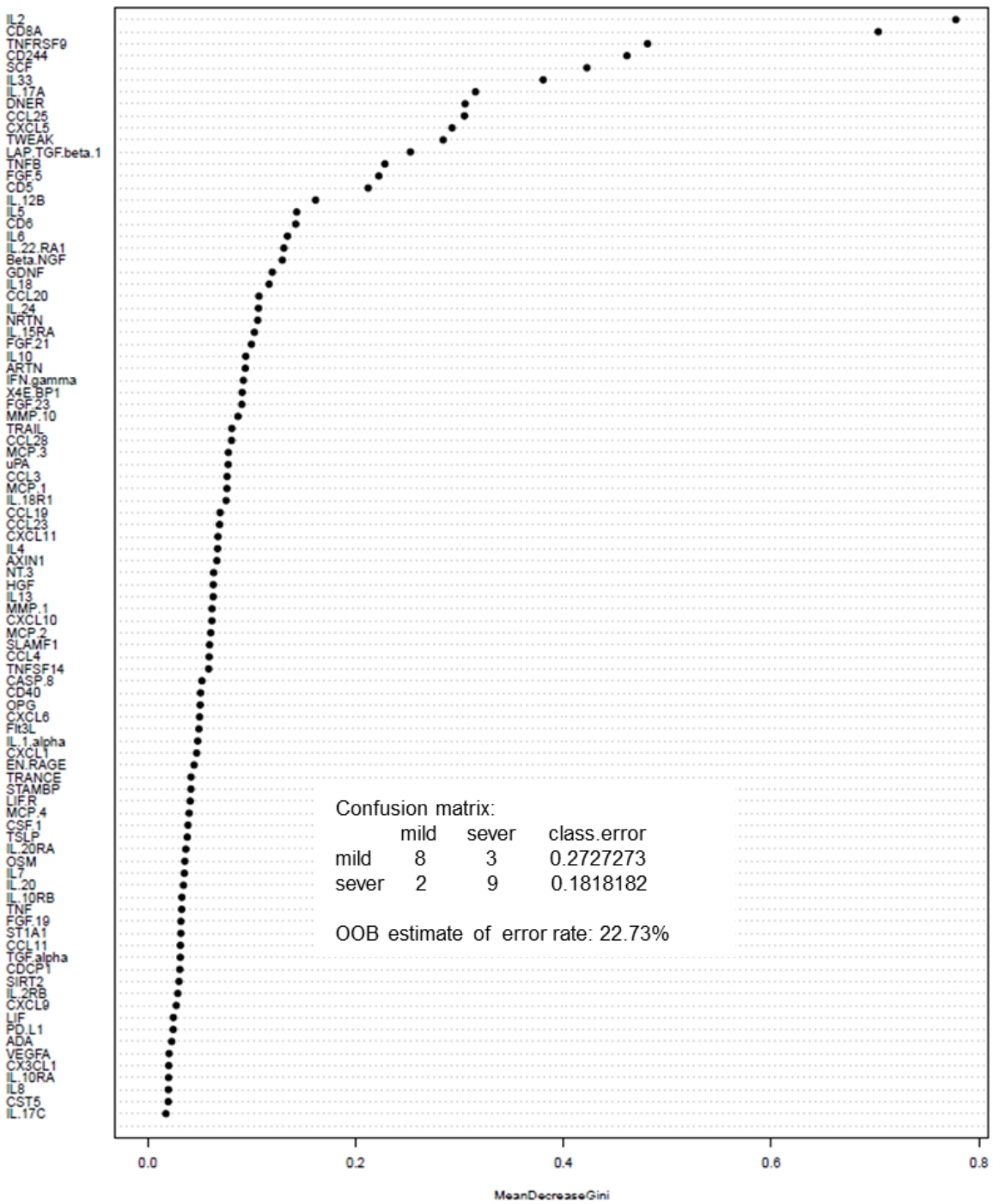


Figure 50. Random forest analysis between ICU-admitted and non-ICU-admitted MIS-C patients. *A random forest-based ranking was conducted to identify the key soluble inflammatory markers measured by Olink that best distinguish between severe MIS-C cases requiring ICU care and milder cases treated in the general inpatient unit.*

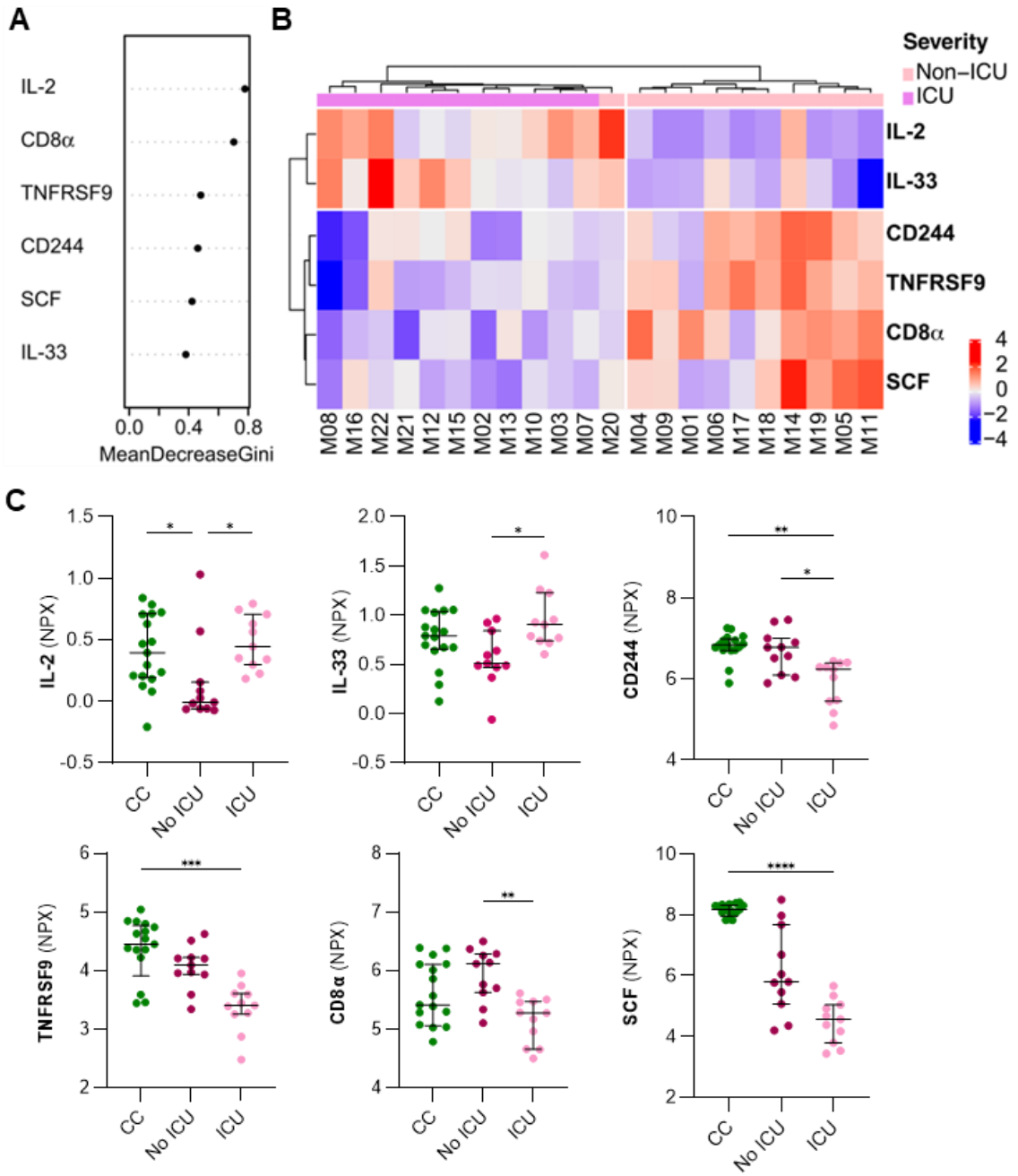


Figure 51. Inflammatory Biomarkers signature of MIS-C ICU-admission. *(A). Top 6 biomarkers Identified by Random Forest Analysis discriminating MIS-C cases with ICU admission vs. non-ICU. (B). Clustering - Heatmap of Cytokine levels differentiating ICU- and non-ICU admitted MIS-C cases based on the most significant inflammatory markers. (C). Top 6 biomarkers individual levels comparing CC group, ICU, and non-ICU MIS-C cases. P values were analyzed using Kruskal-Wallis test, with significance levels indicated as follows: * P ≤ 0.05, ** P ≤ 0.01, *** P ≤ 0.001, **** P ≤ 0.0001. Horizontal bars indicate median values, and error bars show interquartile ranges.*

4.3. Co-associations between inflammatory biomarkers and clinical parameters in MIS-C

We used linear regression models to evaluate the association between the key biomarkers identified above and routine clinical parameters assessed for diagnosis within the MIS-C group. **Figure 52A** shows the standardized obtained coefficients and their p-values corrected for multiple testing using False discovery rate method. Significant associations discovered were re-evaluated, adjusting for age and sex, to verify that the effect was not confounded by these variables **(Figure 52B**). We observed an association between lower CD244 levels and both elevated procalcitonin levels (p=0.0003) and longer hospitalization duration (p=0.0001). Shock was associated with the downregulation of CD8α (p=0.0023) and TNFRSF9 (p=0.0199), with TNFRSF9 also associated with prolonged hospitalization (p=0.0018). In addition, increased CXCL11 levels were associated with high AST (p=0.0008) and LDH levels (p=0.0010). Finally, we also identified a relationship between platelet loss and increased IL-18 (p=0.003) and a positive link between IL-18R1 and ALT levels (p=0.0184), further highlighting the complex interplay between inflammation, organ function, and disease severity in MIS-C.

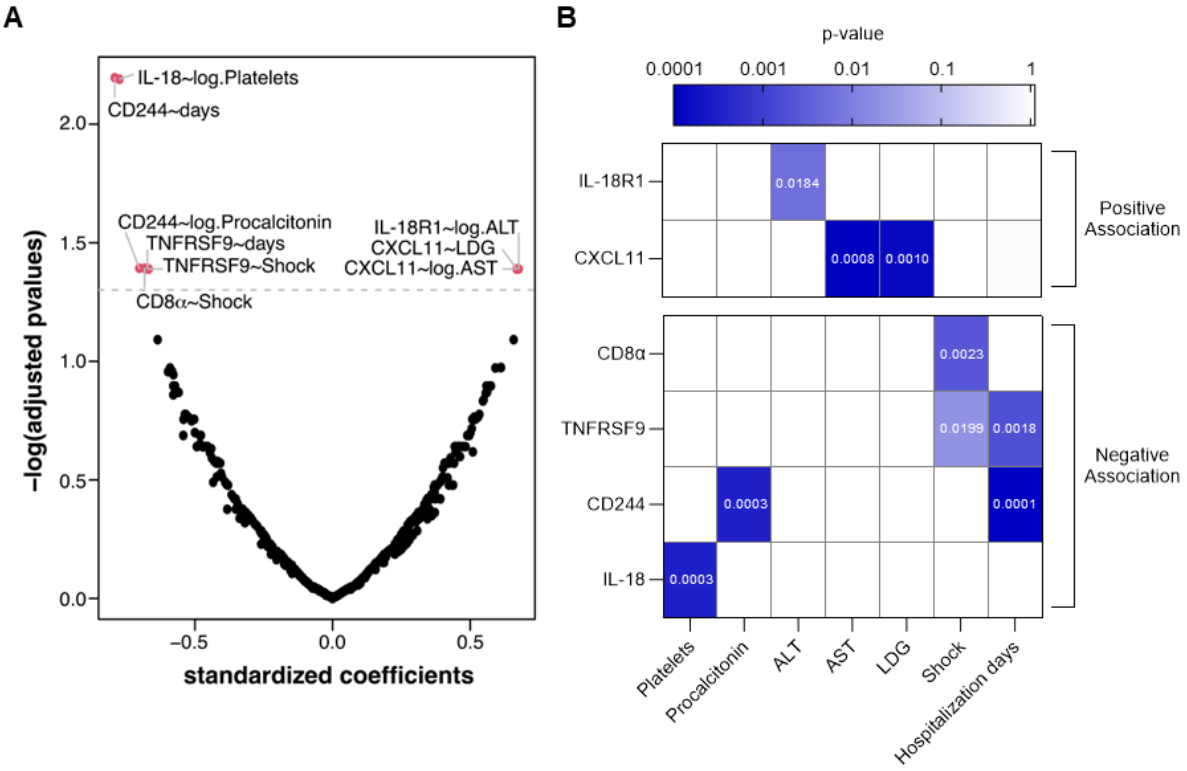


Figure 52. Co-associations between biomarkers and clinical parameters. *(A). The plot shows the standardized coefficients from regression analyses, allowing for comparison across different biomarkers and clinical parameters. The y-axis represents the negative log-transformed adjusted p-values (-log10), indicating the significance of associations. Higher values suggest stronger statistical significance, with key biomarkers indicated. Positive coefficients indicating a positive association and negative coefficients indicating a negative association. The horizontal dashed line marks the significance threshold corresponding to an adjusted p-value of 0.05. (B). A table representing the significant associations between biomarkers and clinical parameters, using linear regression models, adjusting by age and sex. The color gradient represents the p-values, with darker blue indicating stronger significance in the association. P-values are only indicated for significant associations. The upper section of the heatmap includes biomarkers positively associated with clinical parameters (IL-18R1 and CXCL11), while the lower section includes negatively associated biomarkers (CD8A, TNFRSF9, CD244, and IL-18).*

4.4. Longitudinal Stabilization of Biomarker Profiles Post-MIS-C Treatment

Some of the MIS-C participants provided blood samples 2 and/or 18 months after acute disease (**Figure 22**). Our longitudinal analysis of biomarker levels post-treatment for MIS-C revealed a normalization of the 18 biomarkers previously identified by 2 months after the disease onset that was sustained until 18 months (**Figure 53A**). Principal Component Analysis (PCA) shown in **Figure 53B**, using the same set of biomarkers, suggested that the inflammatory marker landscape in the 2-month and 18-month follow-up timepoints were undistinguishable from that of the CC group, in stark contrast to the distinct profile observed during acute MIS-C. This convergence suggests a rapid and full immunological recovery over the extended follow-up period.

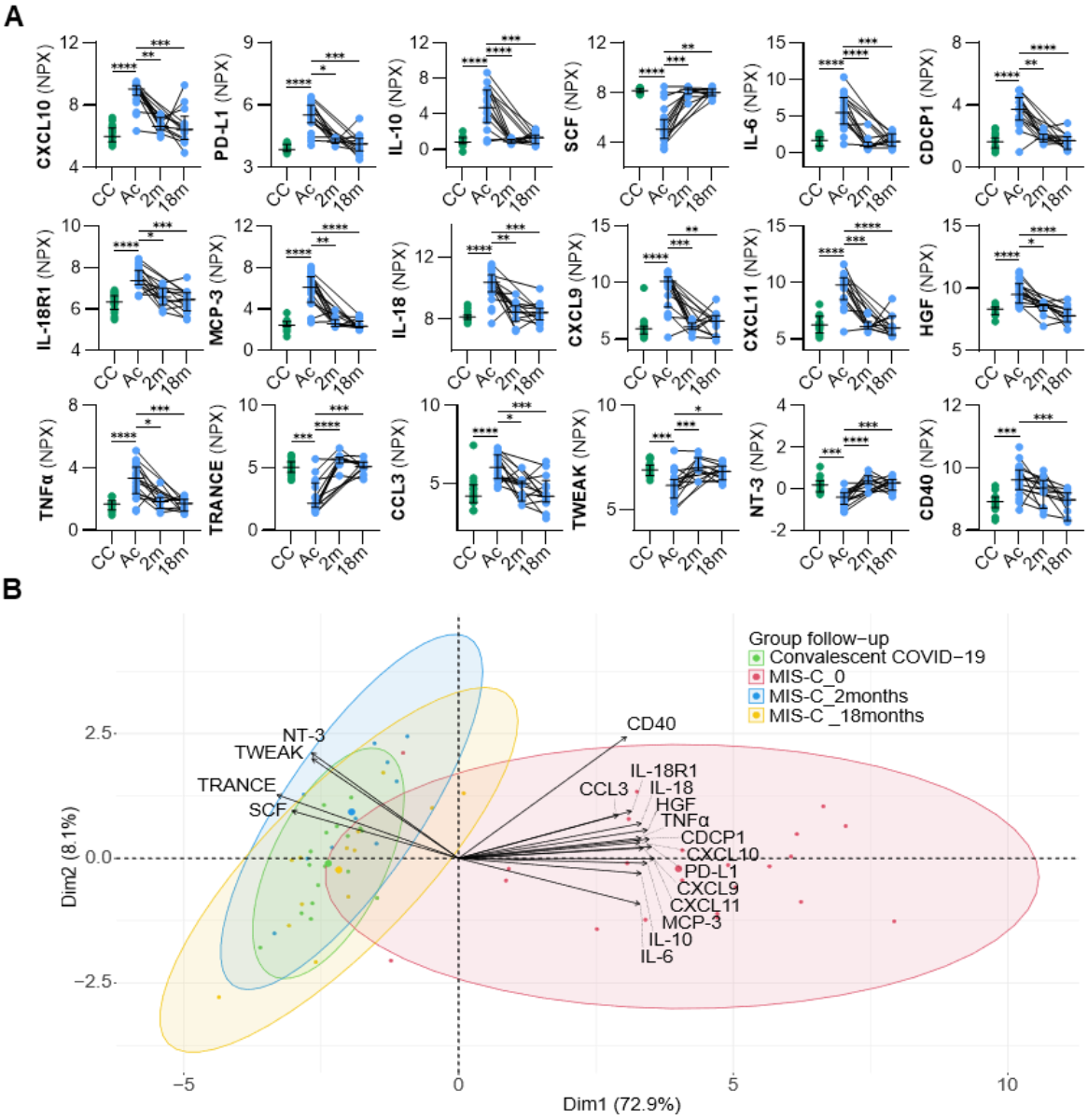


Figure 53. Biomarkers stabilization post-MIS-C treatment. *(A). Biomarker stabilization over time: Individual biomarkers dot plots showing their levels in CC and across MIS-C follow-up, at acute disease, 2-month later, and 18-month later. Differences between groups and timepoints were analyzed using Kruskal-Wallis test, with significance values indicated as follows: * P ≤ 0.05, ** P ≤ 0.01, *** P ≤ 0.001, **** P ≤ 0.0001. Horizontal bars indicate median values and error bars show Interquartile ranges. (B). Principal Component Analysis (PCA): Representation of acute MIS-C, 2-month and 18- month MIS-C follow-ups, and CC using the first two components of the PCA analysis on soluble biomarkers.*

5. Comparative inflammatory profiling of MIS-C, Kawasaki disease, and childhood-onset Still's disease

Because MIS-C shares clinical and inflammatory features with other pediatric inflammatory diseases, such as KD and SD, we compared their biomarker profiles to determine whether these conditions could be distinguished by specific inflammatory signatures.

5.1. Inflammatory biomarkers of the acute phase of MIS-C, SD, and KD.

To characterize the systemic inflammatory landscape of untreated MIS-C, KD, and SD, we utilized the Olink Target 96 Inflammation panel to screen 92 biomarkers. We first analyzed differentially expressed soluble biomarkers comparing each disease group with its respective control group (**Figure 54** and **Figure 55**).

When comparing MIS-C and CC groups, we observed the significant upregulation of 28 markers and downregulation of 6 **(Figure 54A**). Among these, we observed a strong IFN-γ driven response (CXCL9, CXCL10, CXCL11, IFN-γ), and a broad upregulation of inflammatory cytokines (IL-6, IL-18, TNF-α, IL-17A), regulatory proteins (IL-10, PD-L1) chemokines (CX3CL1, MCP-1/2/3, CCL3/4), and repair and growth factors HGF and VEGFA. In addition, several molecules, including SCF, TRANCE, TWEAK, TNFRSF9, NT-3, and DNER, were downregulated in MIS-C.

The KD group was compared to pre-pandemic HC and was characterized by the upregulation of a smaller set of 16 biomarkers (Figure 54**Figure 54B**). These included the pro-inflammatory molecules EN-RAGE, IL-17A, CDCP1, chemokines MCP-3/4 and CCL-4/19/23, and repair and growth factors HGF, and VEGFA. Importantly, IL-6 and SCF were also highly dysregulated albeit not reaching significance because of the heterogeneity across KD participants. The SD and HC group comparison showed the narrowest set of dysregulated proteins with the significant upregulation of 10 biomarkers and downmodulation of 4 (**Figure 54C**). These included the pro-inflammatory proteins IL-6, OSM, IL-18, and EN-RAGE, repair and growth factors TGF-α, HGF and VEGFA, chemokine CCL23, and regulatory protein IL-18R1. SCF and TRANCE were strongly downregulated.

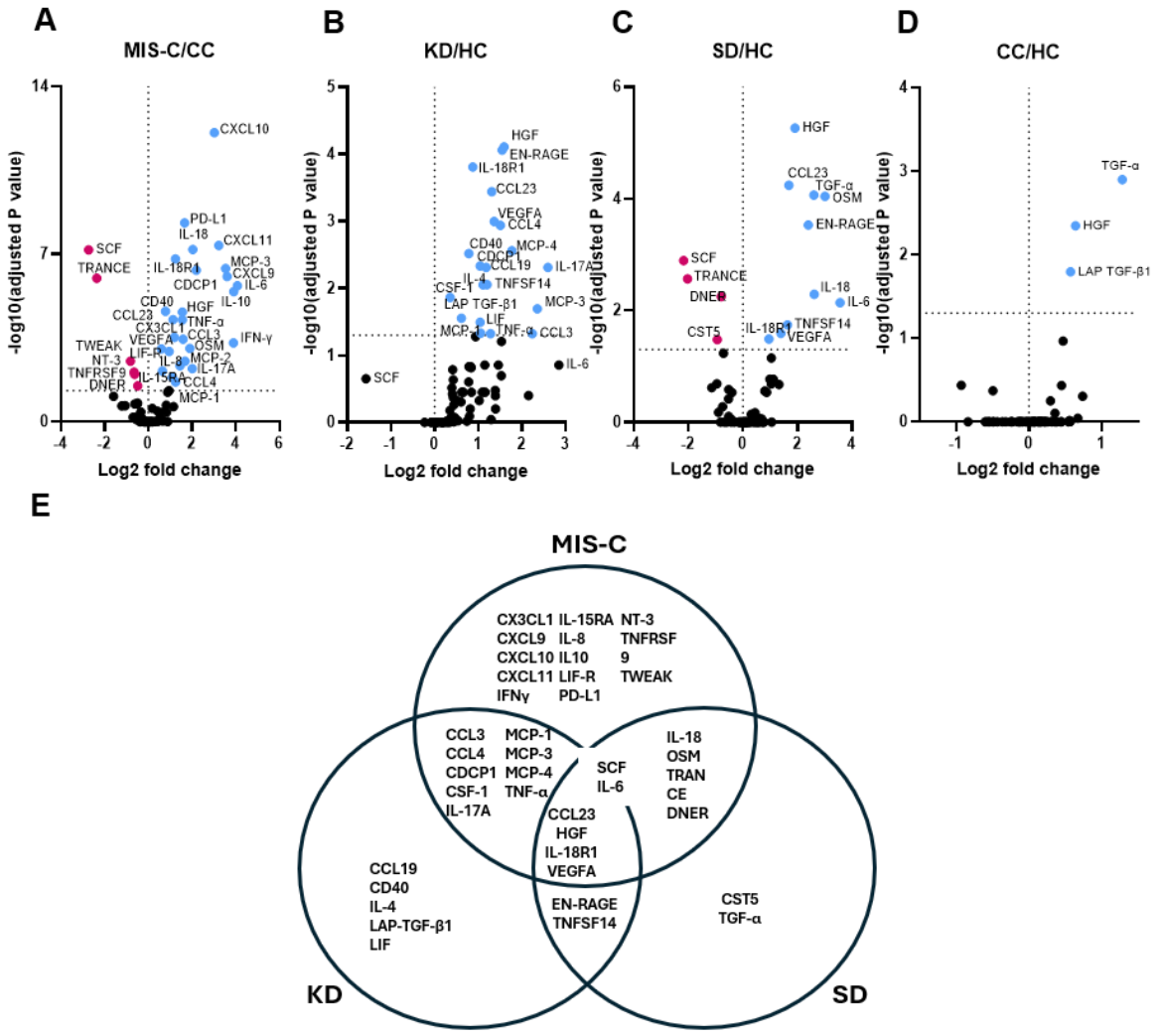


Figure 54. Differential inflammatory protein signatures across pediatric hyperinflammatory conditions - MIS-C, KD, and SD. *Targeted proteomic profiling using the Olink platform was performed to assess circulating inflammatory biomarkers. Results are presented as volcano plots (VP), displaying Log_2 fold changes versus $-log_{10}$ adjusted P values to visualize significant differential protein expression. The horizontal dashed line indicates the statistical significance threshold corresponding to 95% confidence. Proteins highlighted in blue represent significantly upregulated biomarkers, whereas proteins highlighted in pink represent significantly downregulated biomarkers. Comparisons include as follows, from left to right: (A). Comparison of biomarker expression in MIS-C versus CC; (B) Comparison of biomarker expression in KD versus HC; (C) Comparison of biomarker expression in SD versus HC; (D) Comparison of biomarker expression in CC versus HC. (E). Venn diagram displaying significantly dysregulated soluble biomarkers in each disease group. SCF and IL-6 showed high but not significant fold change in KD are represented as borderline common to all groups.*

Finally, as an additional control, we compared CC and HC groups. As expected, minimal changes were observed and only 3 growth and repair proteins HGF, TGF-α and LAP TGF-β1 (a surrogate of TFG-β1 activation) were significantly upregulated, suggesting that 3 to 4 weeks after mild COVID-19, children were still in active immunological reset (**Figure 54D**).

Importantly, 6 biomarkers were shared among all the inflammatory conditions: HGF, CCL23, VEGFA and IL-18R1 IL-6 and SCF (**Figure 54E**), although the two latter did not reach significance in the KD group, despite being strongly dysregulated. While IFN-γ and its downstream cytokines were strongly upregulated in the majority of MIS-C individuals, only a mild shift was observed in KD and SD. Interestingly, while HGF and TGF-α were also dysregulated in all 3 disease groups, LAP TGF-β1 was only upregulated in MIS-C and KD but not in SD.

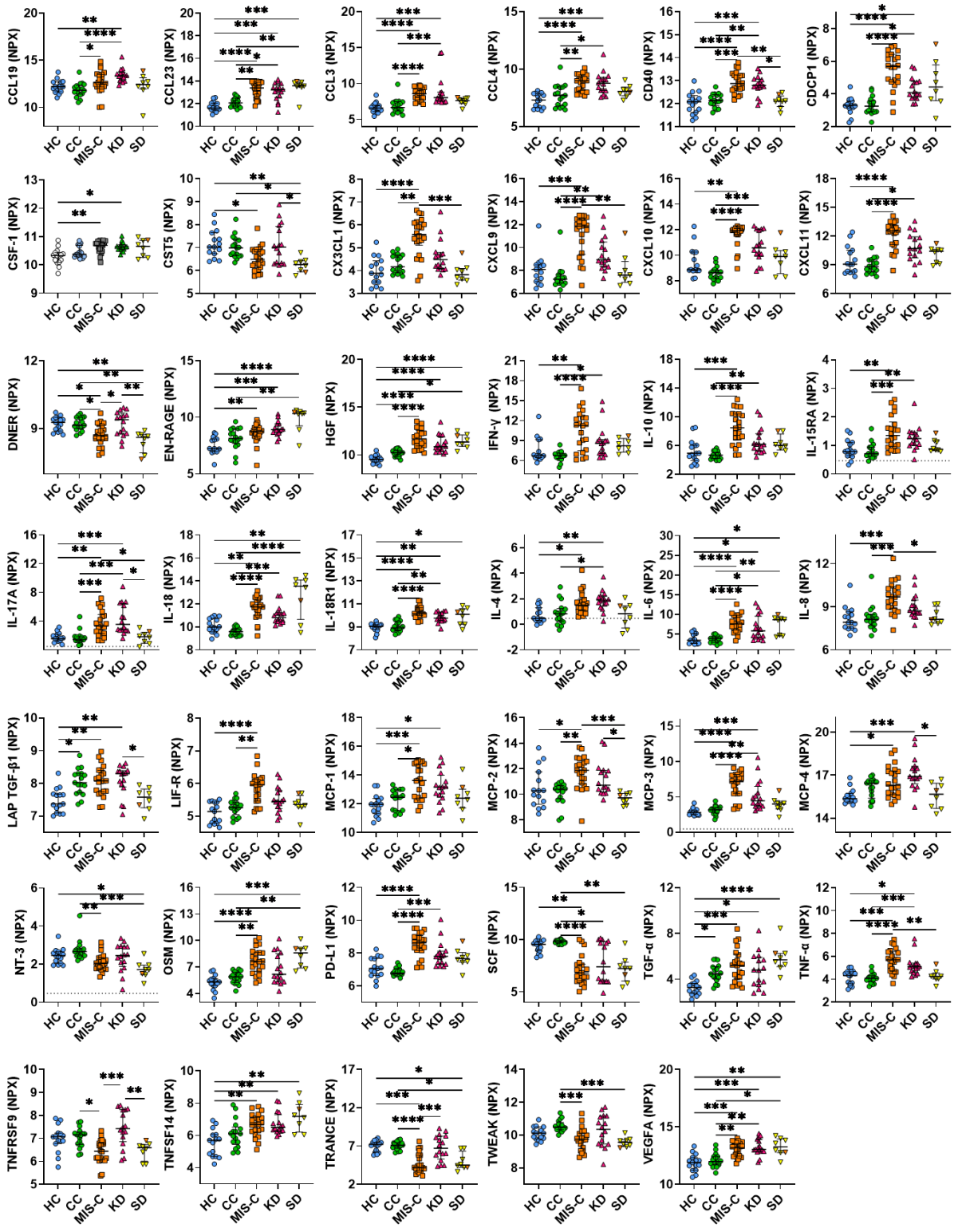


Figure 55. Soluble biomarkers showing significant dysregulation in each disease group. *Detection levels of all soluble biomarkers showing significant dysregulation in volcano plot analysis (Figure 54). Data includes healthy controls (HC), convalescent pediatric COVID-19 (CC), MIS-C, KD, and children onset still disease (SD). P values were analyzed using Kruskal-Wallis test, with significance levels indicated as follows: *P ≤ 0.05, **P ≤ 0.01, ***P ≤ 0.001, ****P ≤ 0.0001. Horizontal bars indicate median values, error bars show interquartile ranges.*

5.2. Inflammatory biomarkers differentiating MIS-C, SD, and KD

Next, to identify biomarkers capable of differentiating the three disease groups (MIS-C, KD, and SD), we applied a Random Forest model to classify the patients into their respective disease groups based on the expression of all 92 biomarkers, alongside age and sex **(Figure 56**). The model achieved an out-of-bag (OOB) error rate of 22.22%, indicating that approximately 78% of patients were correctly categorized (**Figure 56**). According to the confusion matrix, 16 out of 22 (73%) MIS-C, 12 out of 15 (80%) KD patients, and 7 out of 8 (87.5%) SD patients were accurately classified. However, given the limited sample size and high dimensionality, these findings should be interpreted as exploratory.

An arbitrary threshold was used to select 12 high-impact biomarkers (TNFRSF9, MMP10, MCP-2, CX3CL1, CD8α, CD40, PD-L1, EN-RAGE, CXCL5, CCL25, IL-18, and CXCL9) discriminating between MIS-C, KD, and SD (**Figure 57A**). To visualize overall group separation and covariance structure of these biomarkers we performed a principal component analysis (PCA) analysis (**Figure 57B**). In addition, we checked the expression levels of each biomarker in all the disease and control groups (**Figure 57C**). A first set of markers, composed of CXCL9, CX3CL1, PD-L1, MCP-2, and CD40, were markedly upregulated in MIS-C while showing the lowest levels in SD. Notably, the levels of CX3CL1, CD40, MCP-2, and CXCL9 in SD were comparable to HC except for one SD patient, SD8, which was diagnosed with MAS and showed upregulation of CXCL9 and CX3CL1. A second set of biomarkers composed of TNFRSF9, MMP-10, CXCL5, CCL25, and CD8a demonstrated upregulation and/or lack of downmodulation in KD patients in comparison to the other 2 groups. Finally, two markers, IL-18 and EN-RAGE showed strong upregulation in 6 out of 8 SD patients. IL-18 level was the highest in SD, followed by MIS-C and KD in that order. EN-RAGE level was the highest in SD while KD and MIS-C showed mild up-regulation.

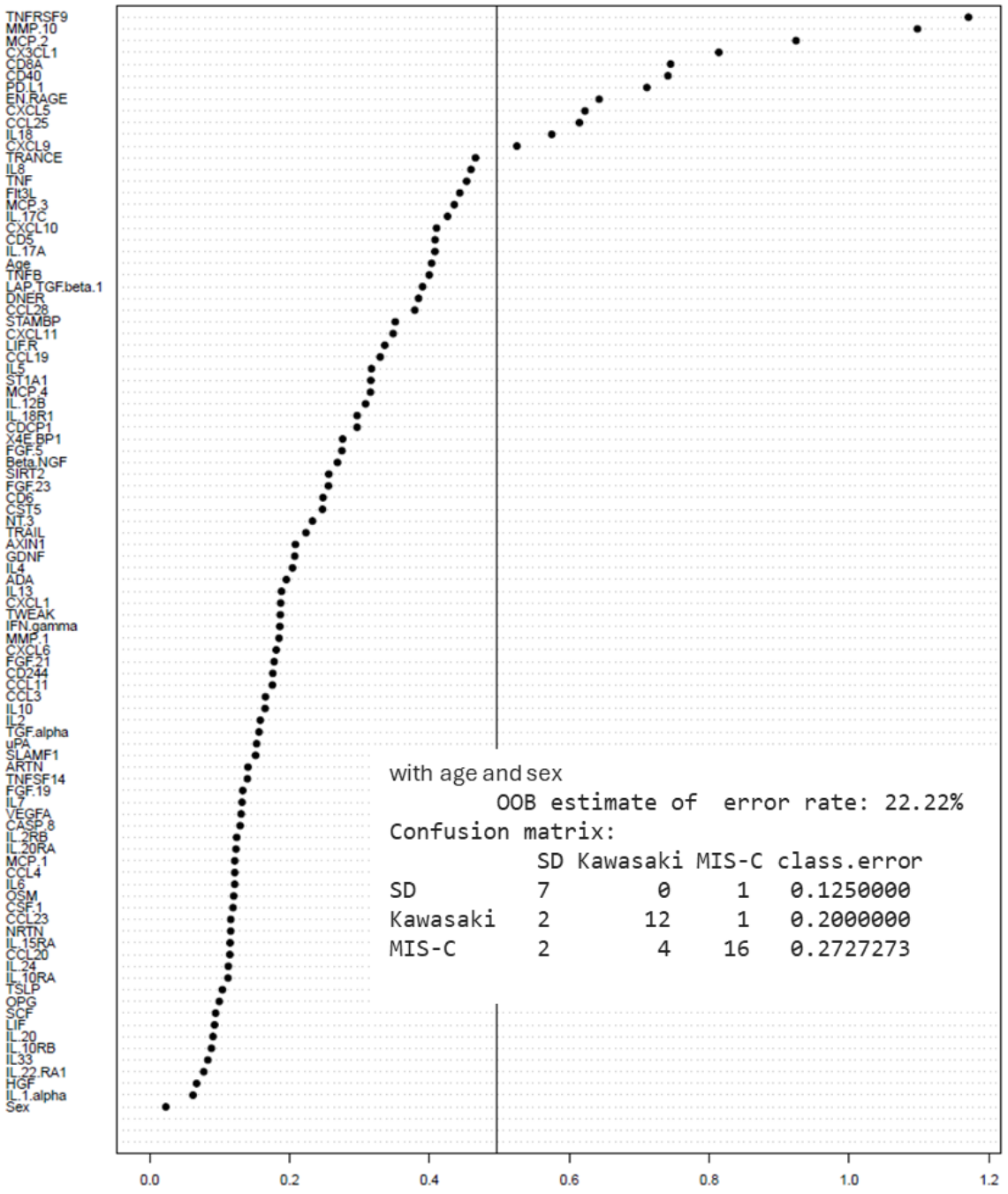


Figure 56. Random forest analysis distinguishing acute MIS-C, KD, and SD. Random Forest modeling was performed to identify soluble biomarkers differentiating MIS-C, KD, and SD, adjusted for age and sex. *Variable importance ranking showing soluble biomarkers contributing to group classification based on the random forest model. An arbitrary importance threshold was applied to define the subset of top biomarkers used for analyses. Insert: Model performance including out-of-bag (OOB) error estimate and confusion matrix demonstrating classification accuracy across disease groups.*

Finally, we performed unsupervised hierarchical clustering of the MIS-C, SD and KD participants using the 12 key soluble biomarkers identified by Random Forest analysis (**Figure 57D**). The analysis identified two main cytokine clusters, the top cluster included CXCL3, PDL1, CXCL9, MCP2, CD40 and IL-18, and bottom cluster was defined by TNFRSF9, MMP-10, CXCL5, CCL25, CD8α, and EN-RAGE. In addition, three patient clusters, each one associated with one inflammatory condition were identified. Cluster 1 showed intermediate levels of top cluster cytokines and the highest levels of bottom cluster cytokines and included 14 (out of 16) KD individuals, Cluster 2 with the lowest values of both cytokine clusters (except for IL-18 and EN-RAGE) included 7 (out of 8) SD individuals and Cluster 3, showing highest values of top and lowest values of bottom cytokines, included 15 (out of 22) MIS-C individuals. Two KD individuals (K12 and K13) were found within the MIS-C group due to a strong signal for CXCL3, PD-L1, CXCL9, MCP-2, CD40 and IL-18. Interestingly, one SD individual (SD08) which was diagnosed with MAS, was clustered within the KD group. Finally, a total of 7 MIS-C individuals were clustered separately from the main MIS-C group, mostly due to lower activation of top clustered cytokines; 3 of them (M14, 17 and 18) were clustered deep within the KD group, while M04, 08, 20 and 16 showed a low levels of inflammation with an undefined pattern and were clustered within the SD group.

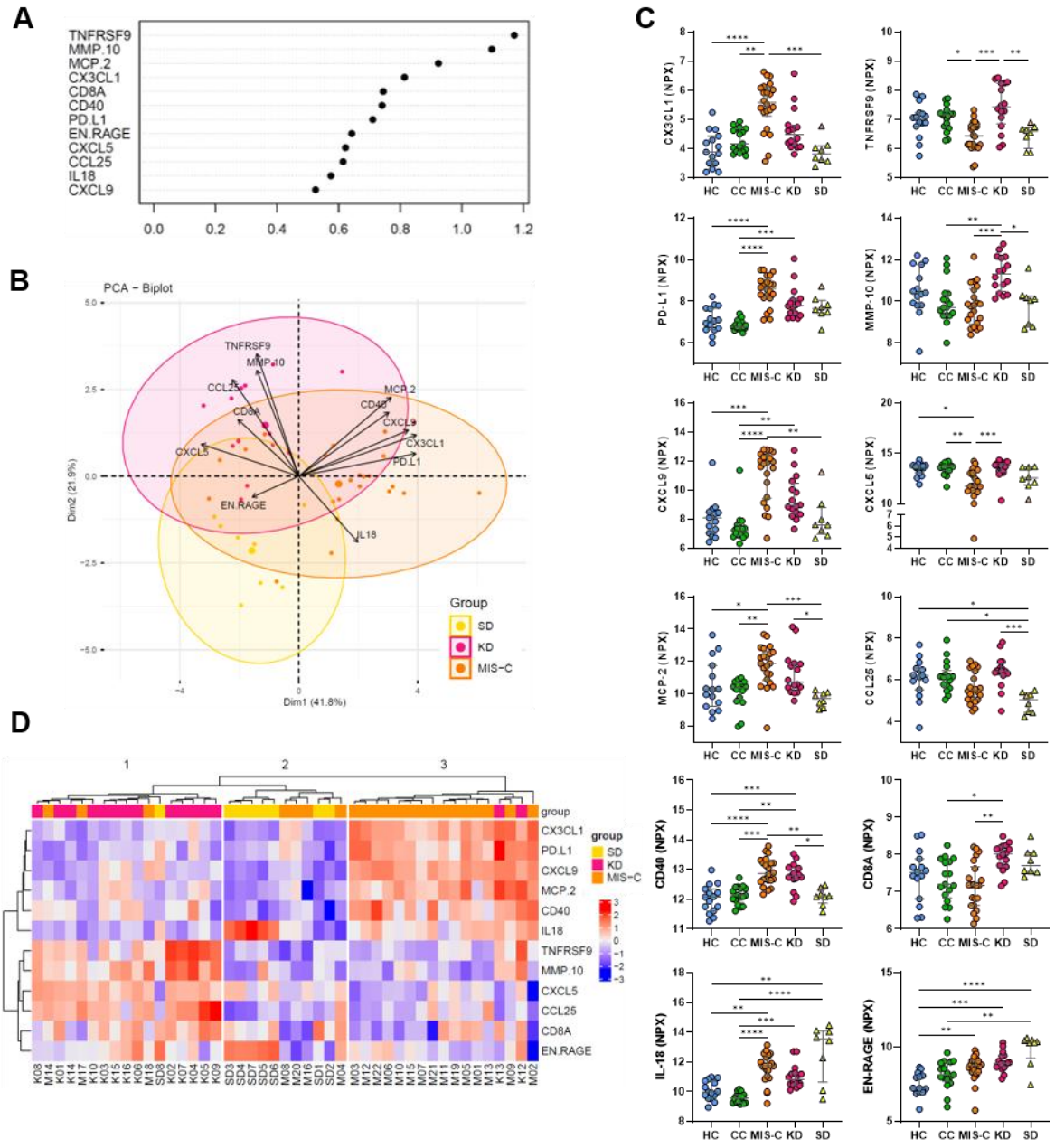


Figure 57. Identification of the biomarkers distinguishing pediatric hyperinflammatory conditions. *A. Top 12 soluble biomarkers distinguishing acute MIS-C, KD, and SD patients extracted from random forest analysis (Fig. S3) B. PCA conducted using selected soluble biomarker to visualize relationships among acute MIS-C, KD, and SD patients. The biplot displays the first two principal components (Dim1: 41.8%; Dim2: 21.9%), showing distinct clustering of the three conditions. Points represent individual samples colored by disease group, and ellipses indicate group clustering. Vector arrows represent biomarker, where direction indicates disease association and length reflects contribution strength. In the biplot, vector direction reflected association with specific disease groups, while vector length indicated the strength of biomarker contribution; biomarkers oriented in similar directions were positively correlated, and those positioned closer to an axis were more strongly associated with the corresponding principal component. C. Clustered Heatmap of the 3 patient groups and top 12 soluble biomarkers. Color intensity reflects relative expression levels, with blue indicating lower expression and red indicating higher expression.*

5.3. Pairwise associations within top inflammatory biomarkers and clinical parameters.

To evaluate the relationships between the selected inflammatory biomarkers and clinical parameters across MIS-C, SD, and KD patients, we performed a co-association analysis across all diseases correcting by age and sex (**Figure 58**). First, platelet loss revealed an association with CX3CL1, CXCL9, MCP-2 and PD-L1, suggesting a correlation between platelet loss and the IFN-γ pathway. Looking specifically at CX3CL1, a correlation was confirmed within MIS-C but not KD nor SD where platelet levels were mostly unchanged (**Figure 59**), except for 2 KD patients, K4 and K13, who also showed both elevated CX3CL1 and strong platelet loss. Similar negative associations were observed between lymphocyte count and both CX3CL1 and PD-L1 (**Figure 58** and **Figure 59**). In fact, CXCL1 and PD-L1 showed correlation with each other (**Figure 59**). In addition, CX3CL1 demonstrated significant correlation with CXCL9 in MIS-C and with TNF-α for all diseases.

Of note, in a previous study we observed co-association between IL-18 and platelet loss in the MIS-C cohort. Although we confirm here this association for MIS-C, no clear platelet loss was observed in SD despite strong IL-18 expression. PCA results suggested a unique behavior of IL-18 (**Figure 59**). Indeed, applying Spearman correlation, we observed a significant association between IL-18 and CXCL9 in MIS-C but not in SD despite superior IL-18 levels in the latter (**Figure 58**). One exception was SD8 which was diagnosed with MAS and did show elevated levels of both CXCL9 and IL-18. In KD, although IL-18 level was the least elevated, 2 patients, K12 and K13, showed both strong IL-18 and CXCL9 expressions, paralleling MIS-C behavior. On the other hand, we observed that in SD but not in MIS-C nor KD, all IL-18 high samples demonstrated positive levels of EN-RAGE. Because of the limited number of samples in SD, we did not see any significant correlation applying Spearman although we could approximate a significant correlation by Pearson ($R2=0.7$, $p=0.01$). Altogether these results suggest that IL-18 follows a different regulatory path in SD compared to MIS-C and KD.

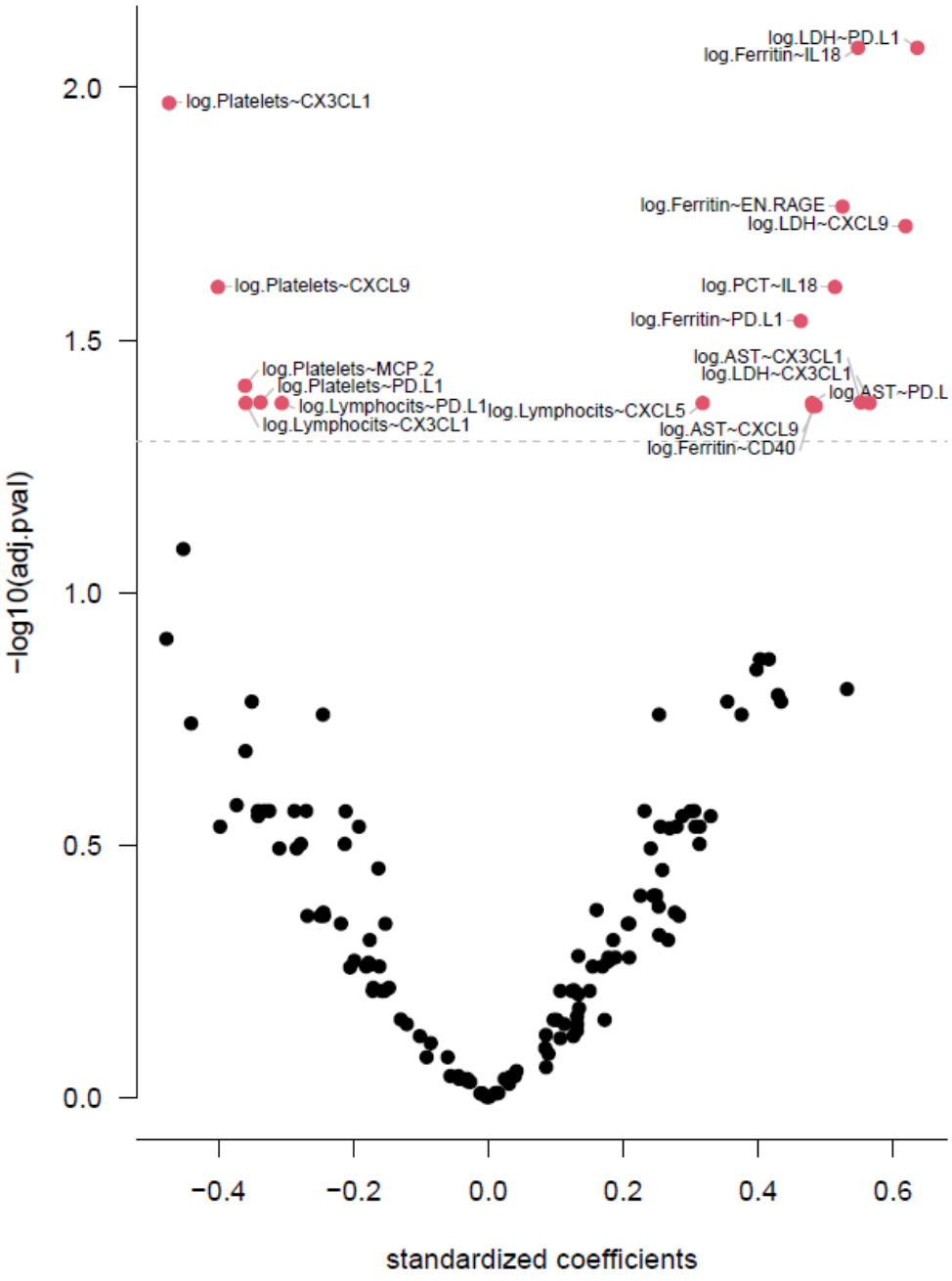


Figure 58. Co-associations among biomarkers and clinical parameters. *Relationships between inflammatory biomarkers and clinical parameters across MIS-C, SD, and KD patients were analyzed using the 12 biomarkers identified by Random Forest analysis. The plot shows standardized regression coefficients on the x-axis and statistical significance as −log10(adjusted p-value) on the y-axis. The dashed horizontal line indicates the significance threshold after multiple-testing correction, with points above the line representing significant associations.*

Specifically in KD, we observed good correlations between MMP-10 and TNFRSF9 and between IL-17A and IL-6. Other notable global co-associations were observed between Ferritin and IL-18 and between LDH and PD-L1, CXCL9, and CX3CL1, while AST demonstrated similar associations with CX3CL1, PD-L1, and CXCL9. Procalcitonin (PCT) was significantly associated with IL-18 levels.

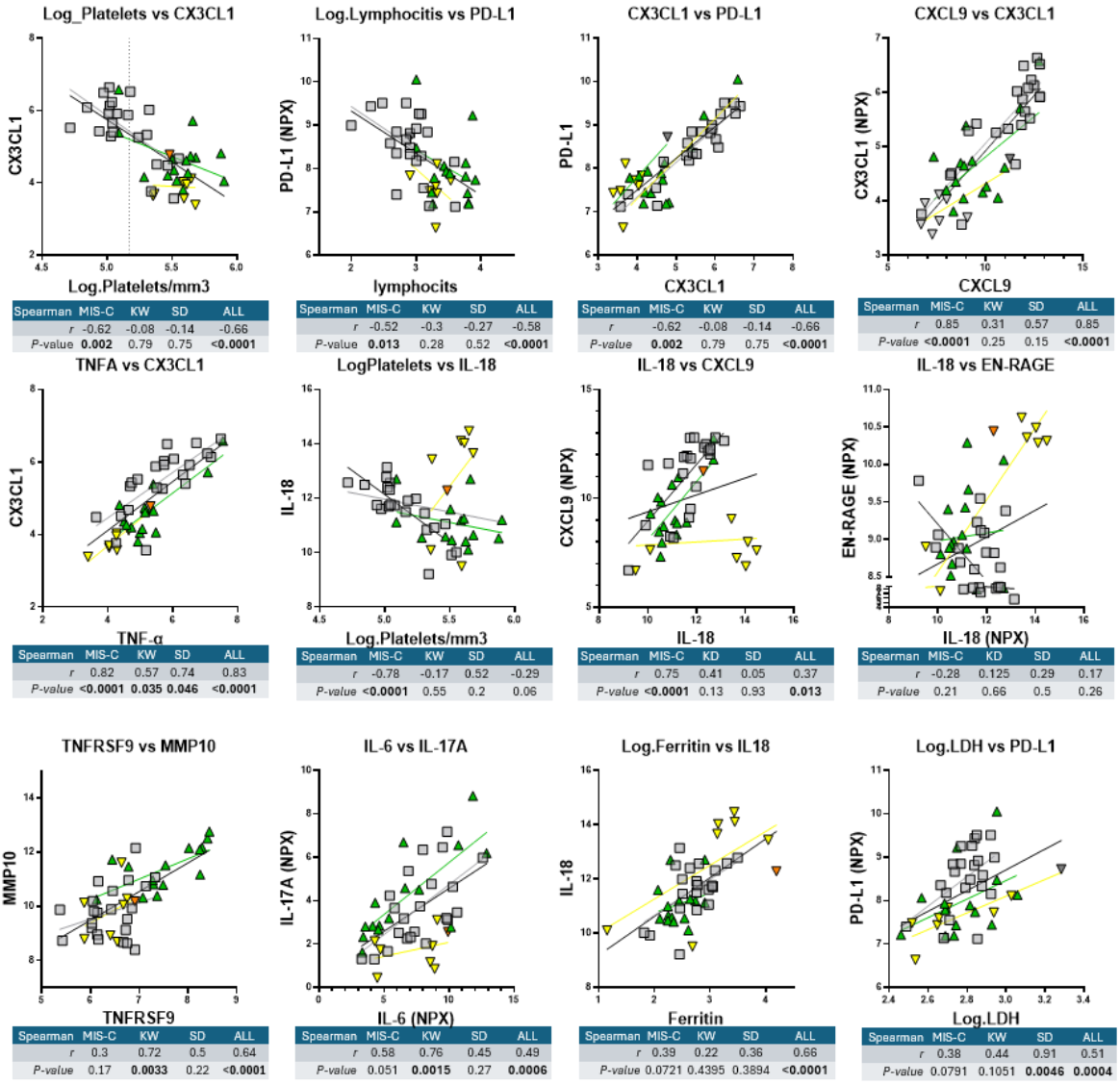


Figure 59. Selected correlations among soluble biomarkers and clinical parameters. *Select comparisons among soluble biomarkers and clinical parameters for each disease group (MIS-C, KD, and SD) or combining all participants (ALL). Correlations were calculated using Spearman. r- and p-values are indicated for each group. Simple linear regressions are also indicated.*

DISCUSSION

The impact of SARS-CoV-2 infection on the immune system is still not fully understood, and the immune mechanisms involved in MIS-C development remain complex and unclear. MIS-C develops several weeks after acute SARS-CoV-2 infection, suggesting that it is not directly related to viral replication, but rather to a delayed and dysregulated immune response[198]. Both innate and adaptive immunity are likely to contribute to this process, including inflammatory cytokine responses, and cellular and humoral immunity[208]. In this thesis, two main aspects of MIS-C immunopathology were investigated: the humoral immune response and the inflammatory biomarker profile.

A major strength of our study is the use of a well-matched convalescent pediatric COVID-19 control group. Therefore, both groups had a comparable timing after SARS-CoV-2 infection: one group recovered without developing MIS-C, while the other developed the hyperinflammatory syndrome. This design was particularly relevant for the analysis of the antibody response which is very dynamic during the first few weeks after infection. Many published studies compared MIS-C patients with children during acute COVID-19 or with adult COVID-19 cohorts, which makes direct comparison difficult [258,259]. To our knowledge only a few studies used convalescent pediatric COVID-19 for the comparison[260,261]. In contrast, as a general limitation, the unavailability of PBMC samples from study participants prevented the full characterization of immune responses.

Humoral response associated with MIS-C

Antibodies are one of the key components of the adaptive immune response to viral infections, including SARS-CoV-2. They can contribute to protection through viral neutralization and Fc-mediated effector functions, but they may also reflect previous antigen exposure, immune activation, or altered immune regulation[262,263]. Importantly, the biological effect of antibodies depends not only on their levels, but also on their antigen specificity, isotype, subclass distribution, and functional capacity[263]. In this context, our study aimed to determine whether MIS-C patients showed a distinct SARS-CoV-2 specific humoral immune profile compared with CC. We focused on SARS-CoV-2-specific antibody responses and their neutralizing activity against SARS-CoV-2 variants. However, we expanded this analysis to antibody responses against

common cold coronaviruses and Epstein–Barr virus. For this latter analysis, KD patients and HC were also included.

In general, we did not observe any clear differences among total SARS-CoV-2 specific IgM, IgA, and IgG responses against RBD, S1 and total S protein comparing MIS-C patients and CC. However, we observed a significant increase in IgA1, IgA2, IgG2 and IgG3 against the S2 subunit in MIS-C patients.

To our knowledge, 2 studies from Gruber et al. and Thiriard et al. report a global increase in S, S1, and or S2 specific IgA responses in MIS-C compared to CC. Although both studies mention comparisons with CC participants, the timing of the sampling is not clearly disclosed. Moreover, in Gruber et al. control convalescent COVID-19 included mostly adults and Thiriard et al. used a control convalescent COVID-19 group from a different institution and country[205,260]. Although an increase in IgA in MIS-C could make sense in the context of gut inflammation, the comparison with convalescent controls needs to be handled with care. In our study, we only observed, in MIS-C, an increase of IgA, including IgA1 and IgA2 subclasses, against S2[262]. Since IgAs are closely linked to mucosal immunity, this may reflect differences in mucosal immune activation, potentially involving gastrointestinal sites[264,265]. This interpretation is supported by studies showing gut barrier disruption and persistent SARS-CoV-2 antigen exposure in MIS-C[209]. Interestingly, our correlation analysis showed that neutralizing activity in MIS-C was associated with IgA responses against several Spike antigens, an association that was mostly absent in CC, suggesting that IgA better contributes to the neutralizing antibody profile in MIS-C group[266].

Total SARS-CoV-2-specific IgG responses were high in both groups, MIS-C and CC. The main differences were observed at the subclass level. MIS-C patients showed increased IgG2 responses against RBD and spike S1 and S2. This finding is interesting because IgG2 usually has weaker Fc-mediated effector functions, compared with IgG1 and IgG3, and is therefore considered as anti-inflammatory[267,268] . Therefore, the increased IgG2 response may reflect early differences in antibody class-switching, antigen recognition, or immune regulation after SARS-CoV-2 infection, or late cytokines mediated class switching, consecutive to MIS-C inflammatory environment[200,269]. IgG3 responses showed a distinct pattern in MIS-C. Overall, they

tended to be lower compared with CC; further analysis of the IgG3/IgG1 ratios revealed significant differences, suggesting reduced IgG3 class switch in MIS-C. However, S2-specific IgG3 showed the opposite behavior and was increased in MIS-C, suggesting that the IgG3 response was not globally reduced but rather antigen-specific. This difference was also reflected in the correlation analysis. In CC patients, IgG1 and IgG3 responses correlated with each other, suggesting a coordinated IgG1/IgG3-driven response, which has also been described in convalescent COVID-19 adults, supporting the idea that this may represent a typical antibody subclass organization after SARS-CoV-2 infection[270]. In contrast, MIS-C showed a less coordinated IgG3 profile. Since increased RBD- and S-specific IgG3 responses have been associated with severe adult COVID-19, the selective S2-specific IgG3 increase in MIS-C may point to an antigen-specific inflammatory antibody feature rather than a broad IgG3-dominated response[270]. In contrast, in MIS-C patients, IgG3 correlations appeared less dominant and were more often linked with IgG2 responses, indicating a different subclass organization.

Together, these findings suggest that MIS-C is not characterized by a general increase in SARS-CoV-2-specific antibody levels, but rather by a qualitative change in the humoral response. In line with Weisberg et al., who showed that pediatric SARS-CoV-2 antibody responses are mainly focused on anti-spike IgG, our data suggest that the reactivity against S2 region contributes to different overall humoral profile in MIS-C, while inflammatory environment may modulate antibody subclass distribution[70,271].

In a few MIS-C patients, we observed increased IgG4 responses against SARS-CoV-2 RBD, S, and N proteins. IgG4 is an anti-inflammatory subclass and is not usually dominant in early antiviral responses. Increased IgG4 has been reported after repeated antigen exposure to SARS-CoV-2 infection or mRNA vaccination[272,273]; however, in our setting, it may reflect individual differences in antibody class-switching, possibly related to differences in the cytokine environment[271,272].

Despite the differences observed and the large collection of parameters defining the humoral responses to SARS-CoV-2, random forest and clustering approaches failed to classify MIS-C and CC individuals. Overall, the data generated suggests that humoral

responses are not good biomarker candidates for MIS-C, but further research is needed to define the causes of unbalanced antibody class switch.

An alternative strategy, still focused on humoral responses, was exploring the impact of other viruses on the onset of inflammatory conditions. Therefore, we next compared antibody reactivity against the N and S proteins of four common cold human coronaviruses: HCoV-OC43, HCoV-HKU1, HCoV-NL63, and HCoV-229E. As human coronaviruses have been associated with KD, this analysis included MIS.C, KD, and their respective control groups, and aimed to determine whether MIS-C or KD shared similar humoral profiles against common cold coronaviruses or showed distinct patterns of reactivity. It also allowed us to explore whether previous exposure to seasonal coronaviruses could be associated with susceptibility to MIS-C after SARS-CoV-2 infection.

In our cohort, MIS-C and CC patients showed increased IgM responses against S-NL63, as well as higher IgA responses against S-HKU1 and S-229E. IgG responses against OC43 and HKU1 were also higher in MIS-C and CC compared with the other study groups. Previous studies support the idea that SARS-CoV-2 infection can boost pre-existing antibody responses against seasonal human coronaviruses[51,68]. This effect has been observed for both beta-coronaviruses, such as HCoV-OC43 and HCoV-HKU1, and alphacoronaviruses, including HCoV-NL63 and HCoV-229E[51]. However, cross-reactive responses appear to be stronger for OC43 and HKU1, particularly through the more conserved S2 region. Therefore, the increased responses against selected seasonal coronavirus antigens in both MIS-C and CC groups may reflect SARS-CoV-2-associated boosting of pre-existing coronavirus immunity. Importantly, previous seasonal coronavirus exposure did not appear to prevent MIS-C, as similar antibody increases were observed in both MIS-C and CC patients[274].

Interestingly, KD patients showed higher IgG responses against the N protein of OC43. Moreover, Random Forest analysis selected several HCoV-OC43-related antibody responses, including N-OC43-specific IgG2, N-OC43-specific IgA, and S-OC43-specific IgG2, as markers contributing to the differentiation of KD patients from HC. Although previous studies on human coronaviruses and KD have reported conflicting

results, our data may support a possible involvement of HCoV-OC43 in KD-related immune activation[68,257,275,276].

Epstein–Barr virus has been implicated in several inflammatory and immune-mediated diseases, where viral persistence or reactivation may contribute to immune dysregulation[277]. Several studies have linked EBV reactivation with SARS-CoV-2 infection, particularly in severe COVID-19 and long COVID[278–280]. We therefore assessed EBV-specific antibody responses in MIS-C, CC, and KD patients. In our cohort, MIS-C patients showed increased IgG3 and IgG4 responses against the EBV ZEBRA protein, while ZEBRA-specific IgG2 was also elevated but showed a weaker, non-significant trend. Since ZEBRA is associated with the lytic phase of EBV infection, this finding may suggest a stronger EBV reactivation-associated antibody response in children who developed MIS-C. This interpretation is supported by recent findings from Goetzke et al., who reported evidence of EBV reactivation in MIS-C and proposed that impaired T-cell control of EBV may contribute to hyperinflammation[253]. Moreover, EBV reactivation may activate B cells, promote class switching, and immunoglobulin production[281,282]. Together with the increased EBV ZEBRA-specific IgG2, IgG3, and IgG4 responses, these findings suggest broader dysregulation of class-switched antibody responses in MIS-C, potentially involving both SARS-CoV-2-specific and EBV reactivation-associated humoral immunity.

Overall, MIS-C patients showed an altered humoral profile rather than a uniform increase in antibody responses. SARS-CoV-2-specific responses showed increased IgG2, generally lower IgG3 (except S2-specific IgG3), and elevated S2-specific IgA1 and IgA2. Some MIS-C patients also exhibited increased SARS-CoV-2 specific IgG4 responses. Together with increased EBV ZEBRA-specific IgG2, IgG3, and IgG4, these findings suggest dysregulated class-switched antibody responses in MIS-C. However, their potential as biomarkers is limited as assessed by classification analyses.

Inflammatory response associated with MIS-C

In the next step, we characterized the inflammatory profile of MIS-C in comparison with CC and other pediatric hyperinflammatory conditions, including KD and SD using Olink-based soluble biomarker profiling.

First, we aimed to identify inflammatory biomarkers specifically associated with MIS-C by comparing acute MIS-C patients with CC. This comparison was particularly relevant because both groups had evidence of previous SARS-CoV-2 infection and were sampled at a comparable post-infectious timepoint. Therefore, differences between the groups were more likely to reflect MIS-C-specific immune alterations rather than immune changes related only to SARS-CoV-2 exposure or recovery.

Using Olink technology, we analyzed 92 inflammation-related soluble biomarkers and identified 24 biomarkers significantly upregulated and 5 biomarkers downmodulated in MIS-C compared with CC. The upregulated biomarkers included CXCL10, CXCL9, CXCL11, MCP3, IL-6, IL-10, TNF, CCL3, PD-L1, CD40, HGF, IL-18, and CDCP1. This inflammatory profile is generally consistent with previous studies comparing acute MIS-C with healthy controls using different technologies, including Olink, Meso Scale Discovery, Proximity Extension Assay, and cytometric bead-based multiplex panels[180,200,205,207,283–285]. Importantly, our comparison with CC suggests that these changes are not simply a consequence of previous SARS-CoV-2 infection, but are more specifically linked to the development of MIS-C.

Random Forest analysis further narrowed this profile to a set of 18 biomarkers capable of differentiating MIS-C from CC. Among the selected biomarkers, CXCL11 showed a significant association with liver damage markers. Previous studies have described CXCL10 and CXCL11 as potential biomarkers of acute liver injury [286,287]. In addition, the combined elevation of CXCL9, CXCL10, and CXCL11 together with increased NT-proBNP has been associated with cardiac injury[288,289]. CXCL10 is also well established as a key chemokine in the immunopathology of SARS-CoV-2 infection in adults[290] , and our findings suggest a similar pathogenesis may be present in children with MIS-C.

IL-18 was another relevant biomarker increased in MIS-C, in line with previous reports[283,285]. In our cohort, increased IL-18 was strongly associated with lower platelet counts. Since platelets are an important source of IL-18 in blood and release this cytokine upon activation[291], and IL-18 levels have been correlated with thrombocytopenia in sepsis[292], our data suggest that IL-18 may act as a surrogate marker of platelet activation or consumption in MIS-C.

Consistent with previous studies, we also identified increased IFN-γ expression in MIS-C patients[200,205,207,234]. However, IFN-γ itself was only ranked highly in the female-specific Random Forest analysis and was more variable in males. In contrast, CXCL9, a downstream chemokine of IFN-γ, was retained as a key biomarker when all participants were considered. This suggests that downstream IFN-γ-induced chemokines may represent more stable markers of the MIS-C inflammatory profile than IFN-γ alone.

Finally, we observed downregulation of SCF, TRANCE, TWEAK, and TNFRSF9 in MIS-C. TRANCE and TNFRSF9 downmodulation have previously been reported by Reiter et al.[283], and Sacco et al. also identified SCF downmodulation as a classifying marker of MIS-C compared with acute COVID-19[207].

Sex-stratified Random Forest analysis also identified different biomarker sets in male and female MIS-C patients, with only partial overlap between them. This suggests that sex-related differences may influence the immunopathogenesis of MIS-C. Two female MIS-C patients, M04 and M14, showed divergent biomarker profiles and were misclassified as CC. While the definition of MIS-C has evolved since 2020 and was revised in 2023[169], overlap remains between MIS-C and other inflammatory diseases, particularly KD[165]. M14 met laboratory criteria for MIS-C and presented with hematological, neurological, gastrointestinal, and mucocutaneous involvement. In contrast, M04 was the least severe MIS-C case in our cohort, with only gastrointestinal and hematological involvement.

After defining the general inflammatory profile of MIS-C, we next aimed to identify biomarkers associated with disease severity, particularly ICU admission. This analysis was important because not all MIS-C patients develop the same clinical course, and biomarkers associated with ICU admission could help identify patients at higher risk of severe disease. Using Random Forest analysis, we identified six biomarkers with the capacity to classify MIS-C patients according to ICU admission: IL-2, IL-33, CD244, soluble TNFRSF9, soluble CD8α, and SCF. These markers suggest that severe MIS-C is not defined only by stronger global inflammation but may also involve specific immune regulatory pathways.

Soluble TNFRSF9 (also called CD137 or 4-1BB) was significantly reduced in MIS-C compared with CC and was identified as a key marker differentiating ICU-admitted from non-ICU MIS-C patients. It also showed a significant negative association with shock and length of hospital stay. Altogether, these findings suggest that circulating soluble TNFRSF9 may be a valuable biomarker for early prediction of MIS-C outcomes. Reiter et al. also reported soluble TNFRSF9 downmodulation in MIS-C and proposed a potential link with myocarditis[283]. In our cohort, soluble TNFRSF9 downmodulation was associated with myocardial dysfunction in univariate analyses, but this association was lost after adjustment for age and sex. In contrast, its association with shock and ICU admission appeared more robust.

Soluble CD8α downmodulation also showed an association with shock. Low levels of both soluble TNFRSF9[293,294] and soluble CD8α[294] have been associated with reduced CD8+ T-cell activation. On the other hand, soluble TNFRSF9 and soluble CD8α can also have immunosuppressive activity[295,296], and their downmodulation could therefore be related to the stronger inflammatory response observed in severe MIS-C. In either case, these findings support a potential role of CD8+ T-cell dysregulation in the pathophysiology of ICU-admitted MIS-C. Interestingly, soluble TNFRSF9 has been shown to increase in ICU-admitted severe COVID-19 cases, suggesting a different role in MIS-C compared with acute severe COVID-19[297].

IL-33 was significantly upregulated in ICU-admitted patients, and previous studies have linked IL-33 levels to disease severity and cytotoxic storm responses[298,299]. We noticed a strong association between IL-33 levels and male sex in both MIS-C ($p= 0.005645$) and CC ($p=0.0464$), a pattern that has been reported in prior research[300]. As male sex was overrepresented in our cohort of ICU-admitted participants, it could be a confounding factor for IL-33 association to ICU admission, however, we lack the statistical power to either validate or invalidate this hypothesis. Therefore, additional studies will be necessary to evaluate IL-33 as a marker associated with MIS-C ICU admission[297].

IL-2 showed an unexpected pattern. While IL-2 levels were similar in CC and ICU-admitted MIS-C patients, they were clearly decreased in non-ICU MIS-C patients. Although a recent study reported elevated IL-2 levels in ICU-associated MIS-C[301], additional work is needed to confirm and clarify this observation.

CD244 downregulation in ICU-admitted patients was associated with prolonged hospital stay and elevated procalcitonin levels, suggesting that CD244 may also be linked to more severe MIS-C. Procalcitonin is a well-established inflammatory biomarker, particularly elevated in bacterial infections and commonly used to differentiate bacterial from viral inflammation. Previous studies have reported reduced CD244 levels in bacterial infections and MIS-C, similar to what was observed in our study[302]. This parallel between CD244 downregulation and elevated procalcitonin may indicate a shared immune dysregulation pathway between MIS-C and severe infectious inflammatory states.

Importantly, one male participant, M20, was misclassified as ICU-admitted MIS-C but did not develop severe complications. The only distinguishing parameters were Eastern European ethnicity and complete COVID-19 vaccination one month before MIS-C diagnosis. However, two additional children in our cohort were vaccinated before MIS-C onset, including a 13-year-old child fully vaccinated five months before MIS-C who required ICU admission. Although vaccination has been associated with a reduction in MIS-C cases and possibly less severe presentations[303], the limited number of vaccinated patients in our cohort does not allow firm conclusions.

Another relevant objective of this study was to evaluate whether the inflammatory alterations observed during acute MIS-C persist over time or normalize after recovery. Although several studies have described clinical follow-up of MIS-C patients, limited information is available on the long-term behavior of soluble inflammatory biomarkers[304–306]. Our longitudinal analysis showed complete normalization of all upregulated and downregulated biomarkers to levels comparable to CC as early as two months after diagnosis. This normalization was further confirmed at the long-term follow-up, 18 months after diagnosis. These findings suggest that the soluble inflammatory signature of MIS-C is largely transient and resolves after the acute phase.

After characterizing MIS-C in comparison with CC and evaluating severity and follow-up, we aimed to determine whether MIS-C could be distinguished from other pediatric hyperinflammatory conditions. The clinical presentation of MIS-C, KD, and SD often involves overlapping features of hyperinflammation, making differential diagnosis a clinical challenge. Here, our primary objective was twofold: first, to identify conserved

biomarkers that act as universal indicators of a cytokine storm across these pediatric cohorts, and second, to isolate specific biomarkers that can accurately separate each disease.

The shared elevation of HGF, CCL23, and VEGFA across MIS-C, KD, and Still disease suggests that these clinically distinct syndromes converge on a common immunovascular inflammatory program. HGF, CCL23 and VEGFA are all consistent with endothelial activation, vascular injury, and tissue repair signaling[307,308], while CCL23 may also drive the recruitment of monocytes and neutrophils into the inflamed vascular environment[309]. Supporting this interpretation, a recent model placed HGF and VEGFA within a shared endothelial signaling network, showing that both promote endothelial proliferation but differ in vascular permeability, with HGF supporting barrier stability and VEGFA promoting leakiness[307]. Together, this supports a broader axis of endothelial dysfunction and angiogenic activation. The increased HGF levels still visible in COVID-19 convalescent children are also consistent with reports of persistent HGF elevation after recovery from COVID-19 in adults, particularly after more severe disease, supporting the idea of ongoing endothelial repair and tissue regeneration following SARS-CoV-2 infection[310]. In KD, it is more consistent with vascular inflammation and coronary artery involvement[309,311]; and in SD, it may represent systemic autoinflammation accompanied by endothelial and myeloid activation[309,312]. Thus, although HGF, CCL23, and VEGFA are not disease-specific markers, their concurrent elevation across all three conditions suggests overlapping vascular-inflammatory biology that may contribute to shared features of tissue injury. The shared downregulation of SCF, TRANCE, and DNER in MIS-C and Still disease is also notable because a similar pattern has also been reported in pediatric inflammatory bowel disease[313] and sepsis[314], suggesting that these changes may reflect a broader state of severe systemic inflammation and disrupted immune homeostasis rather than a disease-specific process.

Random Forest analysis selected CXCL9 as a good classifying parameter for the differentiation of the 3 diseases and SD clearly demonstrated an absence of CXCL9 upregulation compared to HC except for a patient diagnosed with MAS. On the other hand, most KD showed an intermediate upregulation of CXCL9, although some

showed a strong upregulation. In line with our results, most previous studies report a stronger IFN-γ signature in MIS-C compared to KD, however at least 1 report, from Consiglio *et al.,* indicated superior CXCL9 and 10 upregulation in KD[180]. This suggests that both MIS-C and KD conditions exist on a spectrum of the type 2 interferon response. Important hallmarks of MIS-C are thrombocytopenia and lymphopenia, which are not commonly observed in KD. Here, we observed a strong negative correlation between platelet counts and CX3CL1 in MIS-C. CX3CL1 was highly correlated with both CXCL9 and TNF-α and indeed, it is well documented that both IFN-γ and TNF-α contribute to CX3CL1 upregulation consistent with endothelial inflammatory activation [315,316]. Interestingly, the CX3CL1-CX3CR1 axis has been implicated in platelets recruitment, activation, and thrombocytopenia[317–320] suggesting a direct functional connection. PD-L1 was highly correlated with CX3CL1 in MIS-C and both showed good negative correlation with lymphocyte counts. Taking together, these results suggest strong endothelial inflammation associated with T cell recruitment and overactivation.

Our KD classification was more complex and relied in part on biomarkers, CXCL5 and CCL25, that were not actually dysregulated in KD when compared to healthy control groups and contrary to MIS-C and or SD. Biomarkers that showed a more pronounced, albeit not significant, upregulation in KD compared to the control groups were soluble CD8a, TNFRSF9 and MMP-10. Increased soluble CD8a could be indicative of an increased activation of CD8 T cells which play a central role in KD pathogenesis and the associated vasculitis. Level of metalloproteinases such as MMP-3 and MMP-9 have been previously associated with KD and are believed to play a role in KD associated vascular remodeling and arterial injury[321,322]. Here we show that MMP-10 is also a good biomarker specifically upregulated in KD. Interestingly, Consiglio *et al.* also identified MMP-10 as good differentiator between KD and MIS-C despite their relatively divergent cohorts (see above). Regarding soluble TNFRSF9, our findings indicate its downmodulation in MIS-C, as previously described, particularly in patients with more severe clinical presentations and shock. Soluble TNFRSF9 was rather upregulated in KD and, interestingly, we noticed a good correlation between soluble TNFRSF9 and MMP10 levels, specifically in KD. Finally, IL-17 upregulation has been a key cytokine

signature associated with KD. However, in line in with other studies, we show that IL-17A was also elevated in MIS-C and does not permit a good separation of MIS-C and KD[283]. One study suggested that IL-17F could be a better biomarker more specifically upregulated in KD[323]. We saw a good correlation between IL-17A and IL-6 in both MIS-C and KD but not SD where IL-17A remained low despite elevated IL-6 levels. This was consistent the low level of LAP TGF-β1 observed specifically in SD and an absence of T cells involvement.

In our cohort, differentiation of SD from MIS-C and KD was primarily associated with the absence of an IFN-γ signature and very high level of EN-RAGE and IL-18. IL-18 and EN-RAGE were also upregulated in MIS-C and KD; however, levels were more extreme in the majority of SD patients. Interestingly, IL-18 was correlated with CXCL9 in MIS-C and to some extent in KD, but not in SD. One exception was a SD patient that presented with MAS and showed elevated CXCL9. While SD patients showed the lowest overall IFN-gamma signature, they demonstrated extreme hyperferritinemia associated with high IL-18 and EN-RAGE expression, which is consistent with previous studies[324]. The association between ferritin and EN-RAGE likely reflects a shared myeloid-driven hyperinflammatory state, rather than a single linear pathway, where ferritin reflecting macrophage activation and systemic inflammation[325]. CCL25 downmodulation in SD was the best differentiator between SD and KD. We did not identify any clear interpretation for CCL25 behavior, but our results are consistent with recent reports of lower baseline CCL25 in systemic JIA/Still disease subsets. However, increased CCL25 has been linked with the SD associated lung disease phenotype, suggesting that the role of this chemokine may differ across clinical subgroups and may reflect distinct tissue-associated immune programs[326,327].

Our study has several limitations. Firstly, the size of the SD cohort may impact statistical power and hamper the identification of other potential biomarkers. In addition, the absence of peripheral blood cell phenotyping and functional analyses, related to limitations in sample availability, limits the functional implications of this analysis.

Despite these limitations, in our cohort, MIS-C was clearly defined by a strong IFN-γ dependent response and elevated blood CX3CL1 and PD-L1, which were correlated

with thrombocytopenia and lymphopenia. IL-17A could not differentiate MIS-C from KD and classification of the latter was primarily enabled by markers of vascular inflammation and remodeling such as MMP-10. Finally, SD was primarily associated with a strong IL-18/IL-6 axis but no IFN-γ response, except in the patient presenting with MAS, in line with its autoinflammatory nature. The inflammatory patterns identified in this study are flawed by the inherent heterogeneity in clinical and inflammatory parameters. The identification of KD individuals with a stronger IFN-γ signature, conversely, some MIS-C patients showing more modest IFN-γ imprint, and finally, heterogeneity in SD patients suggest that rather than clear-cut conditions, these pediatric inflammatory diseases may present as a heterogeneous and mixed pattern spectrum of inflammatory responses.

Taken together, these findings suggest that MIS-C is a clinically heterogeneous post-SARS-CoV-2 inflammatory reaction characterized by selective humoral dysregulation and IFN-γ-driven endothelial inflammation. The altered antibody profile observed in MIS-C, including shifts in SARS-CoV-2-specific isotype and subclass responses, supports the concept that qualitative features of the humoral immune response may contribute to disease pathogenesis. In addition, the increase in EBV ZEBRA-specific IgG3 and IgG4 responses, together with the weaker increase in IgG2, may suggest an EBV reactivation-associated humoral response in MIS-C. This indicates that the dysregulated antibody profile in MIS-C may involve not only SARS-CoV-2-specific responses, but also broader class-switched responses against latent or reactivated viral antigens.

Whether these antibody alterations act as direct triggers of inflammation or arise as a consequence of the underlying immune dysregulation remains unresolved. Previous studies have proposed that aberrant antibody responses and Fc-mediated immune activation may contribute to tissue inflammation in MIS-C, while others suggest that the observed humoral changes reflect ongoing immune activation rather than a primary pathogenic mechanism[205,211,260,271]. In parallel, several cytokines and soluble immune mediators associated with disease severity, including IL-33, soluble TNFRSF9, soluble CD8α, IL-2, CD244, and SCF, point to the involvement of T-cell activation,

immune regulation, and endothelial dysfunction in the progression to severe disease. Further mechanistic and longitudinal studies will be required to determine the causal relationship between antibody responses and hyperinflammation and to clarify how humoral and cytokine-mediated pathways interact in the development and severity of MIS-C.

Although MIS-C often presents with severe acute inflammation and may require ICU, most treated patients recover well after the acute phase[328]. In contrast to KD, where coronary abnormalities can persist, cardiac involvement in MIS-C is usually transient, with ventricular dysfunction and coronary changes generally improving over time[257,328,329]. These observations are consistent with our longitudinal study and suggest that, despite the intensity of the acute inflammatory response, clinical recovery after MIS-C is generally favorable with appropriate treatment and monitoring.

CONCLUSIONS

General objective: MIS-C is associated with distinct humoral and inflammatory immune alterations that cannot be explained only by previous SARS-CoV-2 infection. Overall, MIS-C appears to represent a specific post-infectious immune syndrome involving both altered humoral immunity and a transient but intense inflammatory response.

Individual conclusions for each specific objective are described as follows:

Specific objective 1. Characterization of the humoral response against SARS-CoV-2 and identification of potential markers.

a. Determine the level of total and neutralizing anti-SARS-CoV-2 antibodies.

MIS-C patients showed similar total and neutralizing SARS-CoV-2 antibody responses to CC.

b. Determine the anti-SARS-CoV-2 antibody subtype usage.

MIS-C is associated with selective dysregulation of class-switched humoral responses and increased S2-specific IgA, IgA1, and IgA2. IgA responses may contribute to neutralizing activity in MIS-C.

c. Compare the antibody reactivity against common cold coronaviruses and EBV in MIS-C and KD.

MIS-C patients showed increased EBV ZEBRA-specific IgG3 and IgG4 responses, with a weaker increase in IgG2. These findings may indicate an EBV reactivation-associated humoral response in MIS-C.

Specific objective 2. Characterization of the inflammatory response in MIS-C, identification of specific markers, and comparison with other inflammatory conditions.

a. Compare the Inflammatory profile of MIS-C and CC group.

MIS-C patients showed a distinct inflammatory profile compared with CC children defined by strong upregulation of IFN-γ-related chemokines, including CXCL9, CXCL10, and CXCL11.

b. Identify the inflammatory biomarkers associated with MIS-C severity, including ICU admission.

Several biomarkers were associated with clinical severity, including soluble TNFRSF9, soluble CD8α, IL-33, IL-2, CD244, and SCF.

c. Evaluate the inflammatory profile of MIS-C patients at 2-month and 18-month follow-up.

Soluble inflammatory signature of MIS-C normalized after recovery, indicating that the inflammatory biomarker profile is largely transient.

d. Compare MIS-C with KD and Still disease to identify shared and distinct inflammatory signatures.

Comparison with KD and SD showed that these pediatric hyperinflammatory conditions share some vascular and inflammatory pathways, but also retain distinct immune signatures.

BIBLIOGRAPHY

1 Pneumonia of unknown cause – China. https://www.who.int/emergencies/disease-outbreak-news/item/2020-DON229?utm_source=chatgpt.com (accessed 8 Apr2026).

2 Wang D, Hu B, Hu C, Zhu F, Liu X, Zhang J *et al.* Clinical Characteristics of 138 Hospitalized Patients With 2019 Novel Coronavirus–Infected Pneumonia in Wuhan, China. *JAMA* 2020; **323**: 1061–1069.

3 WHO Director-General's opening remarks at the media briefing on COVID-19 - 11 March 2020. https://www.who.int/news-room/speeches/item/who-director-general-s-opening-remarks-at-the-media-briefing-on-covid-19---11-march-2020?utm_source=chatgpt.com (accessed 8 Apr2026).

4 Statement on the fifteenth meeting of the IHR (2005) Emergency Committee on the COVID-19 pandemic. https://www.who.int/news/item/05-05-2023-statement-on-the-fifteenth-meeting-of-the-international-health-regulations-%282005%29-emergency-committee-regarding-the-coronavirus-disease-%28covid-19%29-pandemic?utm_source=chatgpt.com (accessed 8 Apr2026).

5 SARS-CoV-2 variants of concern as of 27 March 2026. https://www.ecdc.europa.eu/en/covid-19/variants-concern (accessed 8 Apr2026).

6 COVID-19 cases | WHO COVID-19 dashboard. https://data.who.int/dashboards/covid19/cases?n=c (accessed 8 Apr2026).

7 20241224_covid-19_epi_update_special-edition. .

8 COVID-19 disease in children. https://iris.who.int/server/api/core/bitstreams/64da099a-02e0-44d0-971e-3c878289a60d/content (accessed 20 Apr2026).

9 COVID-19 disease in children and adolescents. https://iris.who.int/server/api/core/bitstreams/64da099a-02e0-44d0-971e-3c878289a60d/content (accessed 31 May2026).

10 Viner RM, Ward JL, Hudson LD, Ashe M, Patel SV, Hargreaves D *et al.* Systematic review of reviews of symptoms and signs of COVID-19 in children and adolescents. Arch. Dis. Child. 2021; **106**: 802–807.

11 Parri N, Maria Magistà A, Marchetti F, Cantoni B, Arrighini A, Romanengo M *et al.* Characteristic of COVID-19 infection in pediatric patients: early findings from two Italian Pediatric Research Networks. doi:10.1007/s00431-020-03683-8.

12 Riphagen S, Gomez X, Gonzalez-Martinez C, Wilkinson N, Theocharis P. Hyperinflammatory shock in children during COVID-19 pandemic. *The Lancet* 2020; **395**: 1607–1608.

13 Multisystem inflammatory syndrome in children and adolescents temporally related to COVID-19. https://www.who.int/news-room/commentaries/detail/multisystem-inflammatory-syndrome-in-children-and-adolescents-with-covid-19 (accessed 26 Apr2026).

14 Brodsky NN, Ramaswamy A, Lucas CL. The Mystery of MIS-C Post-SARS-CoV-2 Infection. *Trends Microbiol* 2020; **28**: 956.

15 Diorio C, Henrickson SE, Vella LA, McNerney KO, Chase J, Burudpakdee C *et al.* Multisystem inflammatory syndrome in children and COVID-19 are distinct presentations of SARS–CoV-2. *J Clin Invest* 2020; **130**: 5967.

16 Overall global risk and confidence Overall risk statement. 2026.

17 Jacob Machado D, Scott R, Guirales S, Janies DA. Fundamental evolution of all Orthocoronavirinae including three deadly lineages descendent from Chiroptera-hosted coronaviruses: SARS-CoV, MERS-CoV and SARS-CoV-2. *Cladistics* 2021; **37**: 461–488.

18 Gorbalenya AE, Baker SC, Baric RS, de Groot RJ, Drosten C, Gulyaeva AA *et al.* The species Severe acute respiratory syndrome-related coronavirus: classifying 2019-nCoV and naming it SARS-CoV-2. *Nature Microbiology 2020 5:4* 2020; **5**: 536–544.

19 Paules CI, Marston HD, Fauci AS. Coronavirus Infections—More Than Just the Common Cold. *JAMA* 2020; **323**: 707–708.

20 Zimmermann P, Curtis N. Coronavirus Infections in Children Including COVID-19: An Overview of the Epidemiology, Clinical Features, Diagnosis, Treatment and Prevention Options in Children. *Pediatr Infect Dis J* 2020; **39**: 355.

21 Yao H, Song Y, Chen Y, Wu N, Xu J, Sun C *et al.* Molecular Architecture of the SARS-CoV-2 Virus. *Cell* 2020; **183**: 730-738.e13.

22 Ravi V, Saxena S, Panda PS. Basic virology of SARS-CoV 2. *Indian J Med Microbiol* 2022; **40**: 182–186.

23 Gorkhali R, Koirala P, Rijal S, Mainali A, Baral A, Bhattarai HK. Structure and Function of Major SARS-CoV-2 and SARS-CoV Proteins. *Bioinform Biol Insights* 2021; **15**: 11779322211025876.

24 Ke Z, Oton J, Qu K, Cortese M, Zila V, McKeane L *et al.* Structures and distributions of SARS-CoV-2 spike proteins on intact virions. *Nature 2020 588:7838* 2020; **588**: 498–502.

25 Cevik M, Kuppalli K, Kindrachuk J, Peiris M. Virology, transmission, and pathogenesis of SARS-CoV-2. *BMJ* 2020; **371**. doi:10.1136/BMJ.M3862.

26 Zandi M, Shafaati M, Kalantar-Neyestanaki D, Pourghadamyari H, Fani M, Soltani S *et al.* The role of SARS-CoV-2 accessory proteins in immune evasion. *Biomedicine & Pharmacotherapy* 2022; **156**: 113889.

27 Ito H, Tamura T, Wang L, Mori K, Tsuda M, Suzuki R *et al.* Involvement of SARS-CoV-2 accessory proteins in immunopathogenesis. *Microbiol Immunol* 2024; **68**: 237–247.

28 Hikmet F, Méar L, Edvinsson Å, Micke P, Uhlén M, Lindskog C. The protein expression profile of ACE2 in human tissues. *Mol Syst Biol* 2020; **16**: e9610.

29 Jackson CB, Farzan M, Chen B, Choe H. Mechanisms of SARS-CoV-2 entry into cells. *Nature Reviews Molecular Cell Biology 2021 23:1* 2021; **23**: 3–20.

30 Jin X, Ren L, Ren X, Wang J. A survey of SARS-CoV-2 tropism. *Infectious Diseases and Immunity* 2025; **5**: 289–302.

31 Saheb Sharif-Askari N, Saheb Sharif-Askari F, Alabed M, Temsah MH, Al Heialy S, Hamid Q *et al.* Airways Expression of SARS-CoV-2 Receptor, ACE2, and TMPRSS2 Is Lower in Children Than Adults and Increases with Smoking and COPD. *Mol Ther Methods Clin Dev* 2020; **18**: 1–6.

32 Loske J, Röhmel J, Lukassen S, Stricker S, Magalhães VG, Liebig J *et al.* Pre-activated antiviral innate immunity in the upper airways controls early SARS-CoV-2 infection in children. *Nature Biotechnology 2021 40:3* 2021; **40**: 319–324.

33 Rotulo GA, Palma P. Understanding COVID-19 in children: immune determinants and post-infection conditions. *Pediatric Research 2023 94:2* 2023; **94**: 434–442.

34 Choudhury A, Mukherjee S. In silico studies on the comparative characterization of the interactions of SARS-CoV-2 spike glycoprotein with ACE-2 receptor homologs and human TLRs. *J Med Virol* 2020; **92**: 2105.

35 Khan S, Shafiei MS, Longoria C, Schoggins J, Savani RC, Zaki H. SARS-CoV-2 spike protein induces inflammation via TLR2-dependent activation of the NF-κB pathway. *bioRxiv* 2021; : 2021.03.16.435700.

36 Zhou Z, Zhang X, Lei X, Xiao X, Jiao T, Ma R *et al.* Sensing of cytoplasmic chromatin by cGAS activates innate immune response in SARS-CoV-2 infection. *Signal Transduction and Targeted Therapy 2021 6:1* 2021; **6**: 382-.

37 Diamond MS, Kanneganti TD. Innate immunity: the first line of defense against SARS-CoV-2. *Nature Immunology 2022 23:2* 2022; **23**: 165–176.

38 Kim YM, Shin EC. Type I and III interferon responses in SARS-CoV-2 infection. *Experimental & Molecular Medicine 2021 53:5* 2021; **53**: 750–760.

39 Mohammed RN, Tamjidifar R, Rahman HS, Adili A, Ghoreishizadeh S, Saeedi H *et al.* A comprehensive review about immune responses and exhaustion during coronavirus disease (COVID-19). *Cell Communication and Signaling 2022 20:1* 2022; **20**: 79-.

40 Kang YW, Park S, Lee KJ, Moon D, Kim YM, Lee SW. Understanding the Host Innate Immune Responses against SARS-CoV-2 Infection and COVID-19 Pathogenesis. *Immune Netw* 2021; **21**: e1.

41 Lamers MM, Haagmans BL. SARS-CoV-2 pathogenesis. *Nature Reviews Microbiology 2022 20:5* 2022; **20**: 270–284.

42 Metzemaekers M, Vanheule V, Janssens R, Struyf S, Proost P. Overview of the mechanisms that may contribute to the non-redundant activities of interferon-inducible CXC chemokine receptor 3 ligands. *Front Immunol* 2018; **8**: 303731.

43 Buszko M, Park JH, Verthelyi D, Sen R, Young HA, Rosenberg AS. The dynamic changes in cytokine responses in COVID-19: a snapshot of the current state of knowledge. *Nature Immunology 2020 21:10* 2020; **21**: 1146–1151.

44 Chou J, Thomas PG, Randolph AG. Immunology of SARS-CoV-2 infection in children. *Nature Immunology 2022 23:2* 2022; **23**: 177–185.

45 Li Q, Wang Y, Sun Q, Knopf J, Herrmann M, Lin L *et al.* Immune response in COVID-19: what is next? *Cell Death & Differentiation 2022 29:6* 2022; **29**: 1107–1122.

46 Grifoni A, Weiskopf D, Ramirez SI, Mateus J, Dan JM, Moderbacher CR *et al.* Targets of T Cell Responses to SARS-CoV-2 Coronavirus in Humans with COVID-19 Disease and Unexposed Individuals. *Cell* 2020; **181**: 1489-1501.e15.

47 Sette A, Crotty S. Adaptive immunity to SARS-CoV-2 and COVID-19. *Cell* 2021; **184**: 861–880.

48 Tan AT, Linster M, Tan CW, Le Bert N, Chia WN, Kunasegaran K *et al.* Early induction of functional SARS-CoV-2-specific T cells associates with rapid viral clearance and mild disease in COVID-19 patients. *Cell Rep* 2021; **34**: 108728.

49 Carabelli AM, Peacock TP, Thorne LG, Harvey WT, Hughes J, de Silva TI *et al.* SARS-CoV-2 variant biology: immune escape, transmission and fitness. *Nature Reviews Microbiology 2023 21:3* 2023; **21**: 162–177.

50 Zhang S, Asquith B, Szydlo R, Tregoning JS, Pollock KM. Peripheral T cell lymphopenia in COVID-19: potential mechanisms and impact. *Immunotherapy Advances* 2021; **1**: ltab015.

51 Dowell AC, Butler MS, Jinks E, Tut G, Lancaster T, Sylla P *et al.* Children develop robust and sustained cross-reactive spike-specific immune responses to SARS-CoV-2 infection. *Nature Immunology 2021 23:1* 2021; **23**: 40–49.

52 Qi H, Liu B, Wang X, Zhang L. The humoral response and antibodies against SARS-CoV-2 infection. *Nature Immunology 2022 23:7* 2022; **23**: 1008–1020.

53 Laidlaw BJ, Ellebedy AH. The germinal centre B cell response to SARS-CoV-2. *Nat Rev Immunol* 2021; **22**: 7.

54 Sethuraman N, Jeremiah SS, Ryo A. Interpreting Diagnostic Tests for SARS-CoV-2. *JAMA* 2020; **323**: 2249–2251.

55 Yu S, An J, Liao X, Wang H, Ma F, Li D *et al.* Distinct kinetics of immunoglobulin isotypes reveal early diagnosis and disease severity of COVID-19: A 6-month follow-up. *Clin Transl Med* 2021; **11**: e342.

56 Guo L, Ren L, Yang S, Xiao M, Chang D, Yang F *et al.* Profiling Early Humoral Response to Diagnose Novel Coronavirus Disease (COVID-19). *Clinical Infectious Diseases* 2020; **71**: 778–785.

57 Moncunill G, Mayor A, Santano R, Jiménez A, Vidal M, Tortajada M *et al.* SARS-CoV-2 Seroprevalence and Antibody Kinetics Among Health Care Workers in a Spanish Hospital After 3 Months of Follow-up. *J Infect Dis* 2020; **223**: 62.

58 Stavnezer J, Guikema JEJ, Schrader CE. Mechanism and Regulation of Class Switch Recombination. *Annu Rev Immunol* 2008; **26**: 261.

59 Chao YX, Rötzschke O, Tan EK. The role of IgA in COVID-19. *Brain Behav Immun* 2020; **87**: 182.

60 Avery DT, Bryant VL, Ma CS, De R, Malefyt W, Tangye SG. IL-21-Induced Isotype Switching to IgG and IgA by Human Naive B Cells Is Differentially Regulated by IL-4. *The Journal of Immunology* 2008; **181**: 1767–1779.

61 Punnonen J, Aversa G, Cocks BG, McKenzie ANJ, Menon S, Zurawski G *et al.* Interleukin 13 induces interleukin 4-independent IgG4 and IgE synthesis and CD23 expression by human B cells. *Proc Natl Acad Sci U S A* 1993; **90**: 3730–3734.

62 Cerutti A. The regulation of IgA class switching. *Nat Rev Immunol* 2008; **8**: 421.

63 Pollard KM, Cauvi DM, Toomey CB, Morris K V., Kono DH. Interferon-γ and Systemic Autoimmunity. *Discov Med* 2013; **16**: 123.

64 Malisan F, Brière F, Bridon JM, Harindranath N, Mills FC, Max EE *et al.* Interleukin-10 induces immunoglobulin G isotype switch recombination in human CD40-activated naive B lymphocytes. *J Exp Med* 1996; **183**: 937.

65 Vidarsson G, Dekkers G, Rispens T. IgG Subclasses and Allotypes: From Structure to Effector Functions. *Front Immunol* 2014; **5**: 520.

66 Lin M, Du L, Brandtzaeg P, Pan-Hammarstrom A. IgA subclass switch recombination in human mucosal and systemic immune compartments. *Mucosal Immunol* 2014; **7**: 511–520.

67 Sealy RE, Hurwitz JL. Cross-Reactive Immune Responses toward the Common Cold Human Coronaviruses and Severe Acute Respiratory Syndrome Coronavirus 2 (SARS-CoV-2): Mini-Review and a Murine Study. *Microorganisms 2021, Vol 9,* 2021; **9**. doi:10.3390/MICROORGANISMS9081643.

68 Anderson EM, Goodwin EC, Verma A, Arevalo CP, Bolton MJ, Weirick ME *et al.* Seasonal human coronavirus antibodies are boosted upon SARS-CoV-2 infection but not associated with protection. *Cell* 2021; **184**: 1858-1864.e10.

69 Lin CY, Wolf J, Brice DC, Sun Y, Locke M, Cherry S *et al.* Pre-existing humoral immunity to human common cold coronaviruses negatively impacts the protective SARS-CoV-2 antibody response. *Cell Host Microbe* 2022; **30**: 83-96.e4.

70 Weisberg SP, Connors TJ, Zhu Y, Baldwin MR, Lin WH, Wontakal S *et al.* Distinct antibody responses to SARS-CoV-2 in children and adults across the COVID-19 clinical spectrum. *Nature Immunology 2020 22:1* 2020; **22**: 25–31.

71 Yao Z, Zhang L, Duan Y, Tang X, Lu J. Molecular insights into the adaptive evolution of SARS-CoV-2 spike protein. *Journal of Infection* 2024; **88**: 106121.

72 Markov P V., Ghafari M, Beer M, Lythgoe K, Simmonds P, Stilianakis NI *et al.* The evolution of SARS-CoV-2. *Nature Reviews Microbiology 2023 21:6* 2023; **21**: 361–379.

73 Khateeb J, Li Y, Zhang H. Emerging SARS-CoV-2 variants of concern and potential intervention approaches. *Critical Care 2021 25:1* 2021; **25**: 244-.

74 Uraki R, Korber B, Diamond MS, Kawaoka Y. SARS-CoV-2 variants: biology, pathogenicity, immunity and control. *Nature Reviews Microbiology 2025 24:1* 2025; **24**: 8–28.

75 Arduini A, Laprise F, Liang C. SARS-CoV-2 ORF8: A Rapidly Evolving Immune and Viral Modulator in COVID-19. *Viruses 2023, Vol 15,* 2023; **15**. doi:10.3390/V15040871.

76 Abbasian MH, Mahmanzar M, Rahimian K, Mahdavi B, Tokhanbigli S, Moradi B *et al.* Global landscape of SARS-CoV-2 mutations and conserved regions. *Journal of Translational Medicine 2023 21:1* 2023; **21**: 152-.

77 GISAID - gisaid.org. https://gisaid.org/ (accessed 22 Apr2026).

78 Hadfield J, Megill C, Bell SM, Huddleston J, Potter B, Callender C *et al.* NextStrain: Real-time tracking of pathogen evolution. *Bioinformatics* 2018; **34**: 4121–4123.

79 Choi JY, Smith DM. SARS-CoV-2 Variants of Concern. *Yonsei Med J* 2021; **62**: 961.

80 Tracking SARS-CoV-2 variants. https://www.who.int/activities/tracking-SARS-CoV-2-variants (accessed 13 Apr2026).

81 Hirotsu Y, Kakizaki Y, Saito A, Tsutsui T, Hanawa S, Yamaki H *et al.* Lung tropism in hospitalized patients following infection with SARS-CoV-2 variants from D614G to Omicron BA.2. *Communications Medicine 2023 3:1* 2023; **3**: 32-.

82 Wasim R, Sumaiya, Ahmad A. Across-the-board review on Omicron SARS-CoV-2 variant. *Inflammopharmacology 2024 33:1* 2024; **33**: 1–10.

83 Chemaitelly H, Ayoub HH, Coyle P, Tang P, Hasan MR, Yassine HM *et al.* Differential protection against SARS-CoV-2 reinfection pre- and post-Omicron. *Nature 2025 639:8056* 2025; **639**: 1024–1031.

84 Statement on the antigen composition of COVID-19 vaccines. https://www.who.int/news/item/15-05-2025-statement-on-the-antigen-composition-of-covid-19-vaccines (accessed 13 Apr2026).

85 Cao Y, Jian F, Wang J, Yu Y, Song W, Yisimayi A *et al.* Imprinted SARS-CoV-2 humoral immunity induces convergent Omicron RBD evolution. *Nature 2022 614:7948* 2022; **614**: 521–529.

86 Urschel R, Bronder S, Klemis V, Marx S, Hielscher F, Abu-Omar A *et al.* SARS-CoV-2-specific cellular and humoral immunity after bivalent BA.4/5 COVID-19-vaccination in previously infected and non-infected individuals. *Nature Communications 2024 15:1* 2024; **15**: 3077-.

87 Pradenas E, Marfil S, Urrea V, Trigueros M, Pidkova T, Pons-Grífols A *et al.* Impact of hybrid immunity booster vaccination and Omicron breakthrough infection on SARS-CoV-2 VOCs cross-neutralization. *iScience* 2023; **26**: 106457.

88 Voss WN, Mallory MA, Byrne PO, Marchioni JM, Knudson SA, Powers JM *et al.* Hybrid immunity to SARS-CoV-2 arises from serological recall of IgG antibodies distinctly imprinted by infection or vaccination. *Cell Rep Med* 2024; **5**: 101668.

89 Altarawneh HN, Chemaitelly H, Ayoub HH, Tang P, Hasan MR, Yassine HM *et al.* Effects of Previous Infection and Vaccination on Symptomatic Omicron Infections. *New England Journal of Medicine* 2022; **387**: 21–34.

90 Oliver N, Barber X, Roomp K, Roomp K. Assessing the Impact of the COVID-19 Pandemic in Spain: Large-Scale, Online, Self-Reported Population Survey. *J Med Internet Res* 2020; **22**: e21319.

91 COVID-19 - CNE - ISCIII Portal Web. https://cne.isciii.es/covid-19-pandemia (accessed 20 Apr2026).

92 SITUACIÓN EN ESPAÑA. .

93 Atlas COVID-19. https://atlascovid.isciii.es/P7TIA (accessed 20 Apr2026).

94 Pollán M, Pérez-Gómez B, Pastor-Barriuso R, Oteo J, Hernán MA, Pérez-Olmeda M *et al.* Prevalence of SARS-CoV-2 in Spain (ENE-COVID): a nationwide, population-based seroepidemiological study. *The Lancet* 2020; **396**: 535–544.

95 Redondo-Bravo L, Moros MJS, Sanchez EVM, Lorusso N, Ubago AC, Garcia VG *et al.* The first wave of the COVID-19 pandemic in Spain: Characterisation of cases and risk factors for severe outcomes, as at 27 April 2020. *Eurosurveillance* 2020; **25**: 2001431.

96 Hodcroft EB, Zuber M, Nadeau S, Vaughan TG, Crawford KHD, Althaus CL *et al.* Spread of a SARS-CoV-2 variant through Europe in the summer of 2020. *Nature 2021 595:7869* 2021; **595**: 707–712.

97 Peláez A, Ruiz del Árbol N, Vázquez Sellán A, Castellano JM, Soriano JB, Ancochea J *et al.* Clinical characteristics and outcomes among hospitalised COVID-19 patients across epidemic waves in Spain: An unCoVer analysis. *Med Clin (Barc)* 2024; **162**: 523–531.

98 Martín-Sánchez V, Ruiz-Garcia A, Vitelli-Storelli F, Serrano-Cumplido A, Barquilla-Garcia A, Micó-Pérez RM *et al.* Case-fatality rate of SARS-CoV-2 infection during the third and fifth epidemic waves in Spain: Impact of vaccination. *Semergen* 2023; **49**: 102026.

99 COVID-19. https://cnecovid.isciii.es/covid19/?utm_source=chatgpt.com (accessed 20 Apr2026).

100 San Martín-López JV, Mesa N, Bernal-Bello D, Morales-Ortega A, Rivilla M, Guerrero M *et al.* Seven Epidemic Waves of COVID-19 in a Hospital in Madrid: Analysis of Severity and Associated Factors. *Viruses* 2023; **15**: 1839.

101 COVID-19. https://cnecovid.isciii.es/covid19/?utm_source (accessed 23 Apr2026).

102 Tagarro A, Cobos-Carrascosa E, Villaverde S, Sanz-Santaeufemia FJ, Grasa C, Soriano-Arandes A *et al.* Clinical spectrum of COVID-19 and risk factors associated with severity in Spanish children. *European Journal of Pediatrics 2021 181:3* 2021; **181**: 1105–1115.

103 Julio D DE. ESTUDIO ENE-COVID: INFORME FINAL ESTUDIO NACIONAL DE SERO-EPIDEMIOLOGÍA DE LA INFECCIÓN POR SARS-COV-2 EN ESPAÑA. http://www.thelancet.com/journals/lancet/article/PIIS0140-6736 (accessed 20 Apr2026).

104 Castilla J, Lecea Ó, Martín Salas C, Quílez D, Miqueleiz A, Trobajo-Sanmartín C *et al.* Rapid communication Seroprevalence of antibodies against SARS-CoV-2 and risk of COVID. ; : 1.

105 García-Sempere A, Giménez E, Vanaclocha H, Limón R, Peiró S, Navarro D *et al.* Seroprevalencia de anticuerpos frente al SARS-CoV-2 en la Comunidad Valenciana (España) en octubre de 2022. *Gac Sanit* 2023; **37**: 102312.

106 Karachaliou M, Moncunill G, Espinosa A, Castaño-Vinyals G, Jiménez A, Vidal M *et al.* Infection induced SARS-CoV-2 seroprevalence and heterogeneity of antibody responses in a general population cohort study in Catalonia Spain. *Scientific Reports 2021 11:1* 2021; **11**: 21571-.

107 Clinical Presentation | Covid | CDC. https://www.cdc.gov/covid/hcp/clinical-care/covid19-presentation.html (accessed 15 Apr2026).

108 Ogata T, Tanaka H. SARS-CoV-2 Incubation Period during the Omicron BA.5–Dominant Period in Japan - Volume 29, Number 3—March 2023 - Emerging Infectious Diseases journal - CDC. *Emerg Infect Dis* 2023; **29**: 595–598.

109 *Clinical management of COVID-19*. World Health Organization, 2025 doi:10.2471/B09467.

110 Whitaker M, Elliott J, Bodinier B, Barclay W, Ward H, Cooke G *et al.* Variant-specific symptoms of COVID-19 in a study of 1,542,510 adults in England. *Nature Communications 2022 13:1* 2022; **13**: 6856-.

111 Townsley H, Gahir J, Russell TW, Greenwood D, Carr EJ, Dyke M *et al.* COVID-19 in non-hospitalised adults caused by either SARS-CoV-2 sub-variants Omicron BA.1, BA.2, BA.4/5 or Delta associates with similar illness duration, symptom severity and viral kinetics, irrespective of vaccination history. *PLoS One* 2024; **19**: e0294897.

112 Hedberg P, Parczewski M, Serwin K, Marchetti G, Bai F, Ole Jensen BE *et al.* In-hospital mortality during the wild-type, alpha, delta, and omicron SARS-CoV-2 waves: a multinational cohort study in the EuCARE project. *The Lancet Regional Health - Europe* 2024; **38**: 100855.

113 Bahl A, Mielke N, Johnson S, Desai A, Qu L. Severe COVID-19 outcomes in pediatrics: an observational cohort analysis comparing Alpha, Delta, and Omicron variants. *The Lancet Regional Health - Americas* 2023; **18**: 100405.

114 Kenney PO, Chang AJ, Krabill L, Hicar MD. Decreased Clinical Severity of Pediatric Acute COVID-19 and MIS-C and Increase of Incidental Cases during the Omicron Wave in Comparison to the Delta Wave. *Viruses* 2023; **15**: 180.

115 Zhu Y, Almeida FJ, Baillie JK, Bowen AC, Britton PN, Brizuela ME *et al.* International Pediatric COVID-19 Severity Over the Course of the Pandemic. *JAMA Pediatr* 2023; **177**: 1073.

116 Diagnostic testing. https://iris.who.int/server/api/core/bitstreams/7caa3b48-f99b-4cc2-b0f3-a954da4060d7/content (accessed 20 Apr2026).

117 Hanson KE, Caliendo AM, Arias CA, Hayden MK, Englund JA, Lee MJ *et al.* The Infectious Diseases Society of America Guidelines on the Diagnosis of COVID-19: Molecular Diagnostic Testing (January 2021). *Clinical Infectious Diseases* 2024; **78**: e170–e207.

118 Drain PK. Rapid Diagnostic Testing for SARS-CoV-2. *New England Journal of Medicine* 2022; **386**: 264–272.

119 Antigen-detection. https://iris.who.int/server/api/core/bitstreams/a0c8a267-2706-4d5a-b2ba-b82729377488/content (accessed 20 Apr2026).

120 Fujita-Rohwerder N, Beckmann L, Zens Y, Verma A. Diagnostic accuracy of rapid point-of-care tests for diagnosis of current SARS-CoV-2 infections in children: a systematic review and meta-analysis. *BMJ Evid Based Med* 2022; **27**: 274–287.

121 Ford L, Whaley MJ, Shah MM, Salvatore PP, Segaloff HE, Delaney A *et al.* Antigen Test Performance Among Children and Adults at a SARS-CoV-2 Community Testing Site. *J Pediatric Infect Dis Soc* 2021; **10**: 1052–1061.

122 Hayden MK, El Mikati IK, Hanson KE, Englund JA, Humphries RM, Lee F *et al.* Infectious Diseases Society of America Guidelines on the Diagnosis of Coronavirus Disease 2019: Serologic Testing. *Clinical Infectious Diseases* 2024. doi:10.1093/CID/CIAE121.

123 Bhimraj A, Falck-Ytter Y, Baden LR, Bedimo R, Cawcutt K, Cheng VCC *et al.* 2025 Clinical Practice Guideline Update by the Infectious Diseases Society of America on the Treatment and Management of COVID-19: Pemivibart for Pre-exposure Prophylaxis, Vilobelimab for Critical Illness, and Abatacept or Infliximab for Severe or Critic…. *Clin Infect Dis* 2026; **81**. doi:10.1093/CID/CIAF424.

124 EMA . https://www.ema.europa.eu/en/documents/other/one-year-first-covid-19-vaccine-approval-eu_en.pdf (accessed 22 Apr2026).

125 First COVID-19 vaccine approved for children aged 12 to 15 in EU | European Medicines Agency (EMA). https://www.ema.europa.eu/en/news/first-covid-19-vaccine-approved-children-aged-12-15-eu?utm_source=chatgpt.com (accessed 22 Apr2026).

126 Vaccines – COVID19 Vaccine Tracker. https://covid19.trackvaccines.org/vaccines/approved/#vaccine-list (accessed 22 Apr2026).

127 COVID-19 medicines | European Medicines Agency (EMA). https://www.ema.europa.eu/en/human-regulatory-overview/public-health-threats/coronavirus-disease-covid-19/covid-19-medicines (accessed 22 Apr2026).

128 Spikevax (previously COVID-19 Vaccine Moderna) | European Medicines Agency (EMA). https://www.ema.europa.eu/en/medicines/human/EPAR/spikevax (accessed 22 Apr2026).

129 Comirnaty | European Medicines Agency (EMA). https://www.ema.europa.eu/en/medicines/human/EPAR/comirnaty (accessed 22 Apr2026).

130 Ministerio de Sanidad - Áreas - Estrategia de vacunación COVID-19 en España. https://www.sanidad.gob.es/areas/alertasEmergenciasSanitarias/alertasActuales/nCov/vacunaCovid19.htm?utm_source=chatgpt.com (accessed 22 Apr2026).

131 Ministerio de Sanidad - Áreas - Cuadro de mando resumen de datos de vacunación. https://www.sanidad.gob.es/areas/alertasEmergenciasSanitarias/alertasActuales/nCov/pbiVacunacion.htm?utm (accessed 22 Apr2026).

132 Vacunación. https://www.sanidad.gob.es/areas/alertasEmergenciasSanitarias/alertasActuales/nCov/documentos/Informe_GIV_comunicacion_20230630.pdf?utm_source=chatgpt.com (accessed 22 Apr2026).

133 Questions and answers on COVID-19: Vaccines. https://www.ecdc.europa.eu/en/covid-19/questions-answers/questions-and-answers-vaccines (accessed 22 Apr2026).

134 Vaccine Scheduler | ECDC. https://vaccine-schedule.ecdc.europa.eu/Scheduler/ByDisease?SelectedCountryIdByDisease=-1&SelectedDiseaseId=52& (accessed 22 Apr2026).

135 Geng LN, Erlandson KM, Hornig M, Letts R, Selvaggi C, Ashktorab H *et al.* 2024 Update of the RECOVER-Adult Long COVID Research Index. *JAMA* 2025; **333**: 694–700.

136 Davis HE, McCorkell L, Vogel JM, Topol EJ. Long COVID: major findings, mechanisms and recommendations. *Nature Reviews Microbiology 2023 21:3* 2023; **21**: 133–146.

137 Mandel H, Yoo YJ, Allen AJ, Abedian S, Verzani Z, Karlson EW *et al.* Long COVID Incidence Proportion in Adults and Children Between 2020 and 2024: An Electronic Health Record-Based Study From the RECOVER Initiative. *Clin Infect Dis* 2025; **80**: 1247–1261.

138 A clinical case definition of post COVID-19 condition by a Delphi consensus. https://iris.who.int/server/api/core/bitstreams/53c01712-a322-446e-ad9f-4e078b757267/content (accessed 24 Apr2026).

139 Al-Aly Z, Davis H, McCorkell L, Soares L, Wulf-Hanson S, Iwasaki A *et al.* Long COVID science, research and policy. *Nat Med* 2024; **30**: 2148–2164.

140 Tsampasian V, Bäck M, Bernardi M, Cavarretta E, Dębski M, Gati S *et al.* Cardiovascular disease as part of Long COVID: a systematic review. *Eur J Prev Cardiol* 2025; **32**: 485–498.

141 Lopez-Leon S, Wegman-Ostrosky T, Ayuzo del Valle NC, Perelman C, Sepulveda R, Rebolledo PA *et al.* Long-COVID in children and adolescents: a systematic review and meta-analyses. *Scientific Reports 2022 12:1* 2022; **12**: 9950-.

142 A CLINICAL CASE DEFINITION FOR POST COVID-19 CONDITION IN CHILDREN AND ADOLESCENTS BY EXPERT CONSENSUS. https://iris.who.int/server/api/core/bitstreams/269e1f3a-5fa9-475b-a22d-ac4df32d9628/content (accessed 24 Apr2026).

143 Long COVID Clinical Guidance | Long COVID | CDC. https://www.cdc.gov/long-covid/hcp/clinical-guidance/index.html (accessed 24 Apr2026).

144 About MIS | MIS | CDC. https://www.cdc.gov/mis/about/index.html (accessed 1 Jun2026).

145 La Vecchia G, Del Buono MG, Bonaventura A, Vecchiè A, Moroni F, Sanna T *et al.* Inflammatory Heart Disease in Multisystem Inflammatory Syndrome. *Curr Cardiol Rep* 2025; **27**: 10.

146 Sapna Bamrah Morris M, Noah G. Schwartz M, Pragna Patel M, Lilian Abbo M, Laura Beauchamps M, Shuba Balan M *et al.* Case Series of Multisystem Inflammatory Syndrome in Adults Associated with SARS-CoV-2 Infection — United Kingdom and United States, March–August 2020. *MMWR Morb Mortal Wkly Rep* 2025; **69**: 1450–1456.

147 Kappanayil M, Balan S, Alawani S, Mohanty S, Leeladharan SP, Gangadharan S *et al.* Multisystem inflammatory syndrome in a neonate, temporally associated with prenatal exposure to SARS-CoV-2: a case report. *Lancet Child Adolesc Health* 2021; **5**: 304–308.

148 Molloy EJ, Nakra N, Gale C, Dimitriades VR, Lakshminrusimha S. Multisystem inflammatory syndrome in children (MIS-C) and neonates (MIS-N) associated with COVID-19: optimizing definition and management. *Pediatric Research 2022 93:6* 2022; **93**: 1499–1508.

149 Muthiah D, Chan M, Low YW, Ramasamy SN, Amin Z, Chan-Ng PPL *et al.* Multisystem inflammatory syndrome in neonates (MIS-N): an updated systematic review. *Front Pediatr* 2024; **12**: 1382133.

150 Lakshminrusimha S, More K, Shah PS, Wynn JL, Sánchez PJ. Multisystem inflammatory syndrome in neonates (MIS-N) associated with perinatal SARS CoV-2 infection: Does it exist? *Semin Fetal Neonatal Med* 2023; **28**: 101433.

151 Patel P, Decuir J, Abrams J, Campbell AP, Godfred-Cato S, Belay ED. Clinical Characteristics of Multisystem Inflammatory Syndrome in Adults: A Systematic Review. *JAMA Netw Open* 2021; **4**: e2126456–e2126456.

152 Case Definitions and Reporting | MIS | CDC. https://www.cdc.gov/mis/hcp/case-definition-reporting/index.html?utm (accessed 24 Apr2026).

153 Worku D. Multisystem Inflammatory Syndrome in Adults (MIS-A) and SARS-CoV2: An Evolving Relationship. *BioMed 2023, Vol 3, Pages 195-201* 2023; **3**: 195–201.

154 Serin I, Sari ND, Gunaltili M, Karakilic A, Gulesir B, Kal Kolik B *et al.* Enigma of COVID-19: is “multisystem inflammatory syndrome in adults” (MIS-A) predictable? *BMC Infect Dis* 2022; **22**: 300.

155 Kunal S, Ish P, Sakthivel P, Malhotra N, Gupta K. The emerging threat of multisystem inflammatory syndrome in adults (MIS-A) in COVID-19: A systematic review. *Heart & Lung* 2022; **54**: 7–18.

156 Henderson LA, Canna SW, Friedman KG, Gorelik M, Lapidus SK, Bassiri H *et al.* American College of Rheumatology Clinical Guidance for Multisystem Inflammatory Syndrome in Children Associated With SARS–CoV-2 and Hyperinflammation in Pediatric COVID-19: Version 3. *Arthritis and Rheumatology* 2022; **74**: e1–e20.

157 Elsaid M, Nune A, Hesham D, Fouad FM, Hassan H, Hamouda H *et al.* Multisystem Inflammatory Syndrome (MIS) following SARS-CoV-2 vaccinations; a systematic review. *Trop Dis Travel Med Vaccines* 2023; **9**: 19.

158 Bova C, Vigna E, Gentile M. Multisystem Inflammatory Syndrome after Ad26.COV2.S vaccination. *IDCases* 2022; **27**: e01411.

159 Nune A, Iyengar KP, Goddard C, Ahmed AE. Multisystem inflammatory syndrome in an adult following the SARS-CoV-2 vaccine (MIS-V). *BMJ Case Reports CP* 2021; **14**: e243888.

160 Zambrano LD, Newhams MM, Olson SM, Halasa NB, Price AM, Orzel AO *et al.* BNT162b2 mRNA Vaccination Against Coronavirus Disease 2019 is Associated With a Decreased Likelihood of Multisystem Inflammatory Syndrome in Children Aged 5–18 Years—United States, July 2021 – April 2022. *Clinical Infectious Diseases* 2023; **76**: e90–e100.

161 Ecdc. Suggested citation: European Centre for Disease Prevention and Control. Paediatric inflammatory multisystem syndrome and SARS-CoV-2 infection in children Paediatric inflammatory multisystem syndrome and SARS-CoV-2 infection in children. 2020.

162 Cirks BT, Rowe SJ, Jiang SY, Brooks RM, Mulreany MP, Hoffner W *et al.* Sixteen Weeks Later: Expanding the Risk Period for Multisystem Inflammatory Syndrome in Children. *J Pediatric Infect Dis Soc* 2021; **10**: 686–690.

163 Guidance: Paediatric multisystem inflammatory syndrome temporally associated with COVID-19. .

164 Case Definitions and Reporting | MIS | CDC. https://www.cdc.gov/mis/hcp/case-definition-reporting/index.html (accessed 26 Apr2026).

165 Day-Lewis M, Berbert L, Baker A, Dionne A, Newburger JW, Son MBF. Updated Case Definition of MIS-C and Implications for Clinical Care. *Pediatrics* 2024. doi:10.1542/peds.2023-063259.

166 Feldstein LR, Rose EB, Horwitz SM, Collins JP, Newhams MM, Son MBF *et al.* Multisystem Inflammatory Syndrome in U.S. Children and Adolescents. *New England Journal of Medicine* 2020; **383**: 334–346.

167 Whittaker E, Bamford A, Kenny J, Kaforou M, Jones CE, Shah P *et al.* Clinical Characteristics of 58 Children With a Pediatric Inflammatory Multisystem Syndrome Temporally Associated With SARS-CoV-2. *JAMA* 2020; **324**: 259–269.

168 El Rassi C, El Darzi R, Abou Mansour M, Arabi M. MIS-C: Diagnosis, Management, and Outcomes. *Open Forum Infect Dis* 2025; **13**. doi:10.1093/OFID/OFAF762.

169 Beth M, Son F, Burns JC, Newburger JW. A New Definition for Multisystem Inflammatory Syndrome in Children. 2023. doi:10.1542/peds.2022-060302.

170 Lee PI, Hsueh PR. Multisystem inflammatory syndrome in children: A dysregulated autoimmune disorder following COVID-19. Journal of Microbiology, Immunology and Infection. 2023; **56**: 236–245.

171 Tiwari V, Daniel AA. Literature Review Multisystem Inflammatory Syndrome in Children: A Year in Review. doi:10.5152/eurjrheum.2022.21114.

172 Young TK, Shaw KS, Shah JK, Noor A, Alperin RA, Ratner AJ *et al.* Mucocutaneous Manifestations of Multisystem Inflammatory Syndrome in Children During the COVID-19 Pandemic. *JAMA Dermatol* 2021; **157**: 207–212.

173 Abrams JY, Oster ME, Godfred-Cato SE, Bryant B, Datta SD, Campbell AP *et al.* Factors linked to severe outcomes in multisystem inflammatory syndrome in children (MIS-C) in the USA: a retrospective surveillance study. *Lancet Child Adolesc Health* 2021; **5**: 323–331.

174 COVID-19: Multisystem inflammatory syndrome in children (MIS-C) management and outcome - UpToDate. https://www.uptodate.com/contents/covid-19-multisystem-inflammatory-syndrome-in-children-mis-c-management-and-outcome?search=diagnostic%20criteria%20for%20MIS-C%20to%20ICU%20admissions&source=search_result&selectedTitle=2~150&usage_type=default&display_rank=2 (accessed 9 Oct2024).

175 Belhadjer Z, Méot M, Bajolle F, Khraiche D, Legendre A, Abakka S *et al.* Acute Heart Failure in Multisystem Inflammatory Syndrome in Children in the Context of Global SARS-CoV-2 Pandemic. *Circulation* 2020; **142**: 429–436.

176 Santos MO, Gonçalves LC, Silva PAN, Moreira ALE, Ito CRM, Peixoto FAO *et al.* Multisystem inflammatory syndrome (MIS-C): a systematic review and meta-analysis of clinical characteristics, treatment, and outcomes. *J Pediatr (Rio J)* 2021; **98**: 338.

177 Molloy MJ, Auger KA, Hall M, Shah SS, Schondelmeyer AC, Parikh K *et al.* Epidemiology and Severity of Illness of MIS-C and Kawasaki Disease During the COVID-19 Pandemic. *Pediatrics* 2023; **152**: e2023062101.

178 Rhedin S, Lundholm C, Horne AC, Smew AI, Osvald EC, Haddadi A *et al.* Risk factors for multisystem inflammatory syndrome in children – A population-based cohort study of over 2 million children. *The Lancet Regional Health - Europe* 2022; **19**: 100443.

179 Yousaf AR, Miller AD, Lindsey K, Shah AB, Wu MJ, Melgar M *et al.* Multisystem Inflammatory Syndrome in Children (MIS-C) Among Persons who Completed a Two-Dose COVID-19 Vaccine Primary Series Compared with those Reporting No COVID-19 Vaccination, U.S. National MIS-C Surveillance. *Pediatr Infect Dis J* 2023; **42**: e476.

180 Consiglio CR, Cotugno N, Sardh F, Pou C, Amodio D, Rodriguez L *et al.* The Immunology of Multisystem Inflammatory Syndrome in Children with COVID-19. *Cell* 2020; **183**: 968-981.e7.

181 Carzaniga T, Calcaterra V, Casiraghi L, Inzani T, Carelli S, Del Castillo G *et al.* Dynamics of Multisystem Inflammatory Syndrome in Children (MIS-C) associated to COVID-19: steady severity despite declining cases and new SARS-CoV-2 variants—a single-center cohort study. *Eur J Pediatr* 2025; **184**: 327.

182 Lee D, Le Pen J, Yatim A, Dong B, Aquino Y, Ogishi M *et al.* Inborn errors of OAS-RNase L in SARS-CoV-2-related multisystem inflammatory syndrome in children. *Science (1979)* 2023; **379**. doi:10.1126/SCIENCE.ABO3627;PAGE:STRING:ARTICLE/CHAPTER.

183 Scaltrito F, Grimaldi MT, Tolfa G, De Benedetto R, Adduce D, Pastore M *et al.* Multisystem Inflammatory Syndrome in Children (MIS-C): A clinical and research overview in the framework of a personalized medicine approach. *Global Pediatrics* 2026; **15**: 100313.

184 Levy N, Koppel JH, Kaplan O, Yechiam H, Shahar-Nissan K, Cohen NK *et al.* Severity and Incidence of Multisystem Inflammatory Syndrome in Children During 3 SARS-CoV-2 Pandemic Waves in Israel. *JAMA* 2022; **327**: 2452–2454.

185 About MIS | MIS | CDC. https://www.cdc.gov/mis/about/ (accessed 27 Apr2026).

186 Kreisel U. Joint ECDC-ESPID Webinar on Multisystem Inflammatory Syndrome in Children (MIS-C) Executive summary. 2022.

187 La Torre F, Elicio MP, Monno VA, Chironna M, Moramarco F, Campanozzi A *et al.* Incidence and Prevalence of Multisystem Inflammatory Syndrome in Children (MIS-C) in Southern Italy. *Children* 2023; **10**: 766.

188 Pino R, Antoñanzas JM, Paredes-Carmona F, Perramon A, Rivière JG, Coma M *et al.* Multisystem inflammatory syndrome in children and SARS-CoV-2 variants: a two-year ambispective multicentric cohort study in Catalonia, Spain. *Eur J Pediatr* 2023; **182**: 1897.

189 Shingleton J, Burton L, Williams HE, Finnie TJR, Bennett E, Birrell P *et al.* Risk of paediatric multisystem inflammatory syndrome (PIMS-TS) during the SARS-CoV-2 alpha and delta variant waves: National observational and modelling study, 2020–21, England. *Front Pediatr* 2022; **10**. doi:10.3389/FPED.2022.1034280/FULL.

190 Laird-Gion J, Dionne A, Gauvreau K, Baker A, Day-Lewis M, de Ferranti S *et al.* MIS-C across three SARS-CoV-2 variants: Changes in COVID-19 testing and clinical characteristics in a cohort of U.S. children. *Eur J Pediatr* 2023; **182**: 2865–2872.

191 Shingleton J, Williams H, Oligbu G, Powell A, Cohen J, Arditi M *et al.* The changing epidemiology of PIMS-TS across COVID-19 waves: prospective national surveillance, January 2021 to July 2022, England. *J Infect* 2022; **85**: 702.

192 Yousaf AR, Lindsey KN, Wu MJ, Shah AB, Free RJ, Simeone RM *et al.* Morbidity and Mortality Weekly Report Notes from the Field Surveillance for Multisystem Inflammatory Syndrome in Children-United States, 2023. *Centers for Disease Control and Prevention | MMWR* 2024; **73**.https://www.cdc. (accessed 27 Apr2026).

193 Matsubara D, Matsubara Y, Ayusawa M, Hamada H, Seki M, Yamagishi H *et al.* Nationwide Survey of Multisystem Inflammatory Syndrome in Children Associated with Coronavirus Disease 2019 in Japan. *Journal of Clinical Immunology 2024 45:1* 2024; **45**: 51-.

194 Ward JL, Harwood R, Kenny S, Cruz J, Clark M, Davis PJ *et al.* Pediatric Hospitalizations and ICU Admissions Due to COVID-19 and Pediatric Inflammatory Multisystem Syndrome Temporally Associated With SARS-CoV-2 in England. *JAMA Pediatr* 2023; **177**: 947.

195 Choe YJ, Choi EH, Choi JW, Eun BW, Eun LY, Kim YJ *et al.* Change in Severity and Clinical Manifestation of MIS-C Over SARS-CoV-2 Variant Outbreaks in Korea. *J Korean Med Sci* 2023; **38**. doi:10.3346/JKMS.2023.38.E225.

196 Ma KC, Yousaf AR, Miller A, Lindsey KN, Wu MJ, Melgar M *et al.* Phenotypic Classification of Multisystem Inflammatory Syndrome in Children Using Latent Class Analysis. *JAMA Netw Open* 2025; **8**: e2456272.

197 Castaldo P, d'Alanno G, Biserni GB, Moratti M, Conti F, Fabi M *et al.* Exploring Factors Influencing Changes in Incidence and Severity of Multisystem Inflammatory Syndrome in Children. *Pathogens 2023, Vol 12,* 2023; **12**. doi:10.3390/PATHOGENS12080997.

198 Henderson LA, Yeung RSM. MIS-C: early lessons from immune profiling. *Nature Reviews Rheumatology 2020 17:2* 2020; **17**: 75–76.

199 Filippatos F, Tatsi EB, Michos A. Immunology of Multisystem Inflammatory Syndrome after COVID-19 in Children: A Review of the Current Evidence. *International Journal of Molecular Sciences 2023, Vol 24,* 2023; **24**. doi:10.3390/IJMS24065711.

200 Diorio C, Shraim R, Vella LA, Giles JR, Baxter AE, Oldridge DA *et al.* Proteomic profiling of MIS-C patients indicates heterogeneity relating to interferon gamma dysregulation and vascular endothelial dysfunction. *Nature Communications 2021 12:1* 2021; **12**: 1–14.

201 Isaza-Correa J, Ryan L, Kelly L, Allen J, Melo A, Jones J *et al.* Innate immune dysregulation in multisystem inflammatory syndrome in children (MIS-C). *Scientific Reports 2023 13:1* 2023; **13**: 16463-.

202 Porritt RA, Binek A, Paschold L, Rivas MN, McArdle A, Yonker LM *et al.* The autoimmune signature of hyperinflammatory multisystem inflammatory syndrome in children. *J Clin Invest* 2021; **131**: e151520.

203 Ramaswamy A, Brodsky NN, Sumida TS, Comi M, Asashima H, Hoehn KB *et al.* Immune dysregulation and autoreactivity correlate with disease severity in SARS-CoV-2-associated multisystem inflammatory syndrome in children. *Immunity* 2021; **54**: 1083-1095.e7.

204 Singh V, Obregon-Perko V, Lapp SA, Horner AM, Brooks A, Macoy L *et al.* Limited induction of SARS-CoV-2–specific T cell responses in children with multisystem inflammatory syndrome compared with COVID-19. *JCI Insight* 2022; **7**. doi:10.1172/JCI.INSIGHT.155145.

205 Gruber CN, Patel RS, Trachtman R, Lepow L, Amanat F, Krammer F *et al.* Mapping Systemic Inflammation and Antibody Responses in Multisystem Inflammatory Syndrome in Children (MIS-C). *Cell* 2020; **183**: 982-995.e14.

206 Yeoh S, Estrada-Rivadeneyra D, Jackson H, Keren I, Galassini R, Cooray S *et al.* Plasma Protein Biomarkers Distinguish Multisystem Inflammatory Syndrome in Children From Other Pediatric Infectious and Inflammatory Diseases. *Pediatric Infectious Disease Journal* 2024; **43**: 444–453.

207 Sacco K, Castagnoli R, Vakkilainen S, Liu C, Delmonte OM, Oguz C *et al.* Immunopathological signatures in multisystem inflammatory syndrome in children and pediatric COVID-19. *Nat Med* 2022; **28**: 1050–1062.

208 Vella LA, Rowley AH. Current Insights Into the Pathophysiology of Multisystem Inflammatory Syndrome in Children. *Curr Pediatr Rep* 2021; **9**: 83.

209 Yonker LM, Gilboa T, Ogata AF, Senussi Y, Lazarovits R, Boribong BP *et al.* Multisystem inflammatory syndrome in children is driven by zonulin-dependent loss of gut mucosal barrier. *J Clin Invest* 2021; **131**. doi:10.1172/JCI149633.

210 Boribong BP, LaSalle TJ, Bartsch YC, Ellett F, Loiselle ME, Davis JP *et al.* Neutrophil profiles of pediatric COVID-19 and multisystem inflammatory syndrome in children. *Cell Rep Med* 2022; **3**: 100848.

211 Bartsch YC, Wang C, Zohar T, Fischinger S, Atyeo C, Burke JS *et al.* Humoral signatures of protective and pathological SARS-CoV-2 infection in children. *Nature Medicine 2021 27:3* 2021; **27**: 454–462.

212 Pierangeli A, Gentile M, Oliveto G, Frasca F, Sorrentino L, Matera L *et al.* Comparison by Age of the Local Interferon Response to SARS-CoV-2 Suggests a Role for IFN-ε and -ω. *Front Immunol* 2022; **13**: 873232.

213 Junqueira C, Crespo Â, Ranjbar S, de Lacerda LB, Lewandrowski M, Ingber J *et al.* FcγR-mediated SARS-CoV-2 infection of monocytes activates inflammation. *Nature 2022 606:7914* 2022; **606**: 576–584.

214 Moreews M, Le Gouge K, Khaldi-Plassart S, Pescarmona R, Mathieu AL, Malcus C *et al.* Polyclonal expansion of TCR Vbeta 21.3+ CD4+ and CD8+ T cells is a hallmark of Multisystem Inflammatory Syndrome in Children. *Sci Immunol* 2021; **6**: eabh1516.

215 Malik A, Tóth EN, Teng MS, Hurst J, Watt E, Wise L *et al.* Distorted TCR repertoires define multisystem inflammatory syndrome in children. *PLoS One* 2022; **17**: e0274289.

216 Porritt RA, Paschold L, Rivas MN, Cheng MH, Yonker LM, Chandnani H *et al.* HLA class I–associated expansion of TRBV11-2 T cells in multisystem inflammatory syndrome in children. *J Clin Invest* 2021; **131**. doi:10.1172/JCI146614.

217 Kouo T, Chaisawangwong W. SARS-CoV-2 as a superantigen in multisystem inflammatory syndrome in children. *J Clin Invest* 2021; **131**. doi:10.1172/JCI149327.

218 Burns JC. MIS-C: myths have been debunked, but mysteries remain. *Nature Reviews Rheumatology 2023 19:2* 2023; **19**: 70–71.

219 Anderson EM, Diorio C, Goodwin EC, McNerney KO, Weirick ME, Gouma S *et al.* SARS-CoV-2 antibody responses in children with MIS-C and mild and severe COVID-19. *medRxiv* 2020. doi:10.1101/2020.08.17.20176552.

220 Bodansky A, Mettelman RC, Sabatino JJ, Vazquez SE, Chou J, Novak T *et al.* Molecular mimicry in multisystem inflammatory syndrome in children. *Nature 2024 632:8025* 2024; **632**: 622–629.

221 Franchitti E, Bottino P, Sidoti F, Carpino A, Pruccoli G, Ramenghi U *et al.* Investigating the Role of Gut Microbiota in Pediatric Patients with Severe COVID-19 or MIS-C. *Microorganisms* 2025; **13**: 83.

222 Holm M, Espenhain L, Glenthøj J, Schmidt LS, Nordly SB, Hartling UB *et al.* Risk and Phenotype of Multisystem Inflammatory Syndrome in Vaccinated and Unvaccinated Danish Children Before and During the Omicron Wave. *JAMA Pediatr* 2022; **176**: 821–823.

223 Sharma C, Ganigara M, Galeotti C, Burns J, Berganza FM, Hayes DA *et al.* Multisystem inflammatory syndrome in children and Kawasaki disease: a critical comparison. *Nat Rev Rheumatol* 2021; **17**: 731.

224 Rodriguez-Smith JJ, Verweyen EL, Clay GM, Esteban YM, de Loizaga SR, Baker EJ *et al.* Inflammatory biomarkers in COVID-19-associated multisystem inflammatory syndrome in children, Kawasaki disease, and macrophage activation syndrome: a cohort study. *Lancet Rheumatol* 2021; **3**: e574–e584.

225 Otar Yener G, Paç Kısaarslan A, Ulu K, Atalay E, Haşlak F, Özdel S *et al.* Differences and similarities of multisystem inflammatory syndrome in children, Kawasaki disease and macrophage activating syndrome due to systemic juvenile idiopathic arthritis: a comparative study. *Rheumatol Int* 2021; **42**: 879.

226 McCrindle BW, Rowley AH, Newburger JW, Burns JC, Bolger AF, Gewitz M *et al.* Diagnosis, Treatment, and Long-Term Management of Kawasaki Disease: A Scientific Statement for Health Professionals From the American Heart Association. *Circulation* 2017; **135**: e927–e999.

227 Systemic Juvenile Idiopathic Arthritis | Arthritis Foundation. https://www.arthritis.org/diseases/systemic-juvenile-idiopathic-arthritis (accessed 30 Apr2026).

228 Fautrel B, Mitrovic S, De Matteis A, Bindoli S, Antón J, Belot A *et al.* EULAR/PReS recommendations for the diagnosis and management of Still's disease, comprising systemic juvenile idiopathic arthritis and adult-onset Still's disease. *Ann Rheum Dis* 2024; **83**: 1614–1627.

229 Onel KB, Horton DB, Lovell DJ, Shenoi S, Cuello CA, Angeles-Han ST *et al.* 2021 American College of Rheumatology Guideline for the Treatment of Juvenile Idiopathic Arthritis: Therapeutic Approaches for Oligoarthritis, Temporomandibular Joint Arthritis, and Systemic Juvenile Idiopathic Arthritis. *Arthritis Care Res (Hoboken)* 2022; **74**: 521–537.

230 Update on Pediatric Rheumatology: Growth Spurt in the Knowledge Base | Consultant360. https://www.consultant360.com/articles/update-pediatric-rheumatology-growth-spurt-knowledge-base (accessed 12 May2026).

231 Juvenile Idiopathic Arthritis - Rheumatology for Primary Care. https://rheumforprimarycare.org/jia/# (accessed 12 May2026).

232 Henderson LA, Canna SW, Friedman KG, Gorelik M, Lapidus SK, Bassiri H *et al.* American College of Rheumatology Clinical Guidance for Multisystem Inflammatory Syndrome in Children Associated With SARS–CoV-2 and Hyperinflammation in Pediatric COVID-19: Version 3. *Arthritis and Rheumatology* 2022; **74**: e1–e20.

233 Jone PN, Tremoulet A, Choueiter N, Dominguez SR, Harahsheh AS, Mitani Y *et al.* Update on Diagnosis and Management of Kawasaki Disease: A Scientific Statement From the American Heart Association. *Circulation* 2024; **150**: e481–e500.

234 Esteve-Sole A, Anton J, Pino-Ramirez RM, Sanchez-Manubens J, Fumadó V, Fortuny C *et al.* Similarities and differences between the immunopathogenesis of COVID-19-related pediatric multisystem inflammatory syndrome and Kawasaki disease. *J Clin Invest* 2021; **131**. doi:10.1172/JCI144554.

235 Ravelli A. MIS-C and Kawasaki disease: Different illnesses or part of the same spectrum? *Global Pediatrics* 2024; **8**: 100150.

236 Gámez-González LB, Murata C, García-Silva J, Ulloa-Gutierrez R, Márquez-Aguirre M, Ríos-Olivares I *et al.* Macrophage Activation Syndrome in MIS-C. *Pediatrics* 2024; **154**. doi:10.1542/PEDS.2024-066780/199878.

237 Harwood R, Allin B, Jones CE, Whittaker E, Ramnarayan P, Ramanan A V. *et al.* A national consensus management pathway for paediatric inflammatory multisystem syndrome temporally associated with COVID-19 (PIMS-TS): results of a national Delphi process. *Lancet Child Adolesc Health* 2021; **5**: 133–141.

238 Burns JC, Franco A. The immunomodulatory effects of intravenous immunoglobulin therapy in Kawasaki disease. *Expert Rev Clin Immunol* 2015; **11**: 819.

239 Negi VS, Elluru S, Sibéril S, Graff-Dubois S, Mouthon L, Kazatchkine MD *et al.* Intravenous Immunoglobulin: An Update on the Clinical Use and Mechanisms of Action. *Journal of Clinical Immunology 2007 27:3* 2007; **27**: 233–245.

240 Zhu YP, Shamie I, Lee JC, Nowell CJ, Peng W, Angulo S *et al.* Immune response to intravenous immunoglobulin in patients with Kawasaki disease and MIS-C. *J Clin Invest* 2021; **131**. doi:10.1172/JCI147076.

241 Harahsheh AS, Portman MA, Khoury M, Elias MD, Lee S, Lin J *et al.* Management of Multisystem Inflammatory Syndrome in Children: Decision-Making Regarding a New Condition in the Absence of Clinical Trial Data. *Canadian Journal of Cardiology* 2023; **39**: 803–814.

242 Ouldali N, Toubiana J, Antona D, Javouhey E, Madhi F, Lorrot M *et al.* Association of Intravenous Immunoglobulins Plus Methylprednisolone vs Immunoglobulins Alone With Course of Fever in Multisystem Inflammatory Syndrome in Children. *JAMA* 2021; **325**: 1.

243 Trinité B, Tarrés-Freixas F, Rodon J, Pradenas E, Urrea V, Marfil S *et al.* SARS-CoV-2 infection elicits a rapid neutralizing antibody response that correlates with disease severity. *Scientific Reports 2021 11:1* 2021; **11**: 2608-.

244 Pradenas E, Trinité B, Urrea V, Marfil S, Ávila-Nieto C, Rodríguez de la Concepción ML *et al.* Stable neutralizing antibody levels 6 months after mild and severe COVID-19 episodes. *Med (N Y)* 2021; **2**: 313.

245 Dobaño C, Vidal M, Santano R, Jiménez A, Chi J, Barrios D *et al.* Highly sensitive and specific multiplex antibody assays to quantify immunoglobulins M, A, and G against SARS-CoV-2 antigens. *J Clin Microbiol* 2021; **59**. doi:10.1128/JCM.01731-20;REQUESTEDJOURNAL:JOURNAL:JCM;JOURNAL:JOURNAL:JCM;WGROUP:STRING:PUBLICATION.

246 Ortega N, Ribes M, Vidal M, Rubio R, Aguilar R, Williams S *et al.* Seven-month kinetics of SARS-CoV-2 antibodies and role of pre-existing antibodies to human coronaviruses. *Nature Communications 2021 12:1* 2021; **12**: 4740-.

247 Aguilar R, Casabonne D, O'Callaghan-Gordo C, Vidal M, Campo JJ, Mutalima N *et al.* Assessment of the combined effect of epstein-barr virus and plasmodium falciparum infections on endemic burkitt lymphoma using a multiplex serological approach. *Front Immunol* 2017; **8**: 1284.

248 Olink® Target 96 User Manual. .

249 Olink Target 96 — Olink®. https://olink.com/products/olink-target-96 (accessed 18 May2026).

250 Ravelli A, Minoia F, Davì S, Horne A, Bovis F, Pistorio A *et al.* 2016 Classification Criteria for Macrophage Activation Syndrome Complicating Systemic Juvenile Idiopathic Arthritis: A European League Against Rheumatism/American College of Rheumatology/Paediatric Rheumatology International Trials Organisation Collaborative Initiative. *Arthritis and Rheumatology* 2016; **68**: 566–576.

251 Pradenas E, Trinité B, Urrea V, Marfil S, Tarrés-Freixas F, Ortiz R *et al.* Clinical course impacts early kinetics,magnitude, and amplitude of SARS-CoV-2 neutralizing antibodies beyond 1 year after infection. *Cell Rep Med* 2022; **3**: 100523.

252 van der Straten K, Guerra D, van Gils MJ, Bontjer I, Caniels TG, van Willigen HDG *et al.* Antigenic cartography using sera from sequence-confirmed SARS-CoV-2 variants of concern infections reveals antigenic divergence of Omicron. *Immunity* 2022; **55**: 1725.

253 Goetzke CC, Massoud M, Frischbutter S, Guerra GM, Ferreira-Gomes M, Heinrich F *et al.* TGFβ links EBV to multisystem inflammatory syndrome in children. *Nature 2025 640:8059* 2025; **640**: 762–771.

254 Burgner D, Harnden A. Kawasaki disease: What is the epidemiology telling us about the etiology? *International Journal of Infectious Diseases* 2005; **9**: 185.

255 Rosenfeld N, Tasher D, Ovadia A, Abiri S, Dalal I. Kawasaki disease with a concomitant primary Epstein - Barr virus infection. *Pediatr Rheumatol Online J* 2020; **18**: 65.

256 Esper F, Shapiro ED, Weibel C, Ferguson D, Landry ML, Kahn JS. Association between a Novel Human Coronavirus and Kawasaki Disease. *J Infect Dis* 2005; **191**: 499.

257 Shahbaz FF, Martins RS, Umair A, Ukrani RD, Jabeen K, Sohail MR *et al.* A Review of Coronaviruses Associated With Kawasaki Disease: Possible Implications for Pathogenesis of the Multisystem Inflammatory Syndrome Associated With COVID-19. *Clin Med Insights Pediatr* 2022; **16**: 11795565221075320.

258 Lapp SA, Abrams J, Lu AT, Hussaini L, Kao CM, Hunstad DA *et al.* Serologic and Cytokine Signatures in Children With Multisystem Inflammatory Syndrome and Coronavirus Disease 2019. *Open Forum Infect Dis* 2022; **9**. doi:10.1093/OFID/OFAC070.

259 Lawrence DA, Jadhav A, Mondal TK, Carson K, Lee WT, Hogan AH *et al.* Inflammatory and Autoimmune Aspects of Multisystem Inflammatory Syndrome in Children (MIS-C): A Prospective Cohort Study. *Viruses 2024, Vol 16,* 2024; **16**. doi:10.3390/V16060950.

260 Thiriard A, Meyer B, Eberhardt CS, Loevy N, Grazioli S, Adouan W *et al.* Antibody response in children with multisystem inflammatory syndrome related to COVID-19 (MIS-C) compared to children with uncomplicated COVID-19. *Front Immunol* 2023; **14**: 1107156.

261 Sananez I, Raiden SC, Algieri SC, Uranga M, Grisolía NA, Filippo D *et al.* A poor and delayed anti-SARS-CoV2 IgG response is associated to severe COVID-19 in children. *EBioMedicine* 2021; **72**: 103615.

262 Zhang A, Stacey HD, D'Agostino MR, Tugg Y, Marzok A, Miller MS. Beyond neutralization: Fc-dependent antibody effector functions in SARS-CoV-2 infection. *Nature Reviews Immunology 2022 23:6* 2022; **23**: 381–396.

263 Pantaleo G, Correia B, Fenwick C, Joo VS, Perez L. Antibodies to combat viral infections: development strategies and progress. *Nature Reviews Drug Discovery 2022 21:9* 2022; **21**: 676–696.

264 Alqahtani SAM. Mucosal immunity in COVID-19: a comprehensive review. *Front Immunol* 2024; **15**: 1433452.

265 Li Y, Jin L, Chen T, Pirozzi CJ. The Effects of Secretory IgA in the Mucosal Immune System. *Biomed Res Int* 2020; **2020**: 2032057.

266 Sterlin D, Mathian A, Miyara M, Mohr A, Anna F, Claër L *et al.* IgA dominates the early neutralizing antibody response to SARS-CoV-2. *Sci Transl Med* 2021; **13**: 2223.

267 Damelang T, Brinkhaus M, van Osch TLJ, Schuurman J, Labrijn AF, Rispens T *et al.* Impact of structural modifications of IgG antibodies on effector functions. *Front Immunol* 2023; **14**: 1304365.

268 Bruhns P, Iannascoli B, England P, Mancardi DA, Fernandez N, Jorieux S *et al.* Specificity and affinity of human Fcγ receptors and their polymorphic variants for human IgG subclasses. *Blood* 2009; **113**: 3716–3725.

269 Andualem H, Kiros M, Getu S, Hailemichael W. Immunoglobulin G2 Antibody as a Potential Target for COVID-19 Vaccine. *Immunotargets Ther* 2020; **9**: 143.

270 Yates JL, Ehrbar DJ, Hunt DT, Girardin RC, Dupuis AP, Payne AF *et al.* Serological analysis reveals an imbalanced IgG subclass composition associated with COVID-19 disease severity. *Cell Rep Med* 2021; **2**: 100329.

271 Burns MD, Bartsch YC, Davis JP, Boribong BP, Loiselle M, Kang J *et al.* Long-term humoral signatures following acute pediatric COVID-19 and Multisystem Inflammatory Syndrome in Children. *Pediatr Res* 2023; **94**: 1327–1334.

272 Irrgang P, Gerling J, Kocher K, Lapuente D, Steininger P, Habenicht K *et al.* Class switch toward noninflammatory, spike-specific IgG4 antibodies after repeated SARS-CoV-2 mRNA vaccination. *Sci Immunol* 2023; **8**.

doi:10.1126/SCIIMMUNOL.ADE2798;REQUESTEDJOURNAL:JOURNAL:SCIIMMUNOL;PAGEGROUP:STRING:PUBLICATION.

273 Rispens T, Huijbers MG. The unique properties of IgG4 and its roles in health and disease. *Nat Rev Immunol* 2023; **23**: 1.

274 Sermet-Gaudelus I, Temmam S, Huon C, Behillil S, Gajdos V, Bigot T *et al.* Prior infection by seasonal coronaviruses, as assessed by serology, does not prevent SARS-CoV-2 infection and disease in children, France, April to June 2020. *Eurosurveillance* 2021; **26**: 2001782.

275 Choe S-A, Soon An H, June Choe Y, Young June Choe C. No temporal association between human coronavirus and Kawasaki disease: National data from South Korea. *J Med Virol* 2021; **93**: 585–587.

276 Chang LY, Lu CY, Shao PL, Lee PI, Lin MT, Fan TY *et al.* Viral infections associated with Kawasaki disease. *Journal of the Formosan Medical Association* 2014; **113**: 148–154.

277 Robinson WH, Younis S, Love ZZ, Steinman L, Lanz T V. Epstein–Barr virus as a potentiator of autoimmune diseases. *Nat Rev Rheumatol* 2024; **20**: 729–740.

278 Mahajan S, Mahajan S, Patgiri S. Association and Interaction of Epstein–Barr Virus with SARS-CoV-2 Infection—A Review. *Viruses* 2025; **17**: 903.

279 Chen T, Song J, Liu H, Zheng H, Chen C. Positive Epstein–Barr virus detection in coronavirus disease 2019 (COVID-19) patients. *Scientific Reports 2021 11:1* 2021; **11**: 10902-.

280 Paolucci S, Cassaniti I, Novazzi F, Fiorina L, Piralla A, Comolli G *et al.* EBV DNA increase in COVID-19 patients with impaired lymphocyte subpopulation count. *International Journal of Infectious Diseases* 2021; **104**: 315–319.

281 Habib M, Buisson M, Lupo J, Agbalika F, Socié G, Germi R *et al.* Lytic EBV infection investigated by detection of Soluble Epstein-Barr virus ZEBRA in the serum of patients with PTLD. *Scientific Reports 2017 7:1* 2017; **7**: 10479-.

282 Nagata K, Kumata K, Nakayama Y, Satoh Y, Sugihara H, Hara S *et al.* Epstein–Barr Virus Lytic Reactivation Activates B Cells Polyclonally and Induces Activation-Induced Cytidine Deaminase Expression: A Mechanism Underlying Autoimmunity and Its Contribution to Graves' Disease. *Viral Immunol* 2017; **30**: 240.

283 Reiter A, Verweyen EL, Queste E, Fuehner S, Jakob A, Masjosthusmann K *et al.* Proteomic mapping identifies serum marker signatures associated with MIS-C specific hyperinflammation and cardiovascular manifestation. *Clinical Immunology* 2024; **264**: 110237.

284 Tulling AJ, Holierhoek MG, Jansen-Hoogendijk AM, Hoste L, Haerynck F, Tavernier SJ *et al.* Serum proteomics reveals hemophagocytic lymphohistiocytosis-like phenotype in a subset of patients with multisystem inflammatory syndrome in children. *Clinical Immunology* 2024; **264**: 110252.

285 Gurlevik SL, Ozsurekci Y, Sağ E, Derin Oygar P, Kesici S, Akca ÜK *et al.* The difference of the inflammatory milieu in MIS-C and severe COVID-19. *Pediatr Res* 2022; **92**: 1805.

286 Chalin A, Lefevre B, Devisme C, Pronier C, Carrière V, Thibault V *et al.* Serum CXCL10, CXCL11, CXCL12, and CXCL14 chemokine patterns in patients with acute liver injury. *Cytokine* 2018; **111**: 500–504.

287 Poulsen KL, Ross CKC-D, Chaney JK, Nagy LE. Role of the chemokine system in liver fibrosis: a narrative review. *Dig Med Res* 2022; **5**: 30–30.

288 Altara R, Manca M, Hessel MH, Gu Y, van Vark LC, Akkerhuis KM *et al.* CXCL10 Is a Circulating Inflammatory Marker in Patients with Advanced Heart Failure: a Pilot Study. *J Cardiovasc Transl Res* 2016; **9**: 302–314.

289 Altara R, Gu YM, Struijker-Boudier HAJ, Thijs L, Staessen JA, Blankesteijn WM. Left Ventricular Dysfunction and CXCR3 Ligands in Hypertension: From Animal Experiments to a Population-Based Pilot Study. *PLoS One* 2015; **10**: e0141394.

290 Gudowska-Sawczuk M, Mroczko B. What Is Currently Known about the Role of CXCL10 in SARS-CoV-2 Infection? *International Journal of Molecular Sciences 2022, Vol 23, Page 3673* 2022; **23**: 3673.

291 Allam O, Samarani S, Marzouk R, Ahmad A. Human platelets produce and constitute the main source of IL-18 in the circulation (44.25). *The Journal of Immunology* 2012; **188**: 44.25-44.25.

292 Zhu M, Rong X, Li M, Wang S. IL-18 and IL-35 in the serum of patients with sepsis thrombocytopenia and the clinical significance. *Exp Ther Med* 2019; **19**: 1251.

293 Glez-Vaz J, Azpilikueta A, Olivera I, Cirella A, Teijeira A, Ochoa MC *et al.* Soluble CD137 as a dynamic biomarker to monitor agonist CD137 immunotherapies. *J Immunother Cancer* 2022; **10**: e003532.

294 Tomkinson BE, Brown MC, Ip SH, Carrabis S, Sullivan JL. Soluble CD8 during T cell activation. *The Journal of Immunology* 1989; **142**: 2230–2236.

295 Morgan CL, Price CP, Cohen SBA, Madrigal JA, Newman DJ. Soluble CD8 stabilizes the HLA class I molecule by promoting β2M exchange: Analysis in real-time. *Hum Immunol* 1999; **60**: 442–449.

296 Kachapati K, Bednar KJ, Adams DE, Wu Y, Mittler RS, Jordan MB *et al.* Recombinant soluble CD137 prevents type one diabetes in nonobese diabetic mice. *J Autoimmun* 2013; **47**: 94–103.

297 Marques M de O, Abdo A, Silva PB, Silva Junior A, Alves LB de O, Costa JVG *et al.* Soluble CD137 as a potential biomarker for severe COVID-19. *Immunol Lett* 2022; **248**: 119.

298 Brunner TM, Serve S, Marx A-F, Fadejeva J, Saikali P, Dzamukova M *et al.* A type 1 immunity-restricted promoter of the IL−33 receptor gene directs antiviral T-cell responses. *Nat Immunol* 2024; **25**: 256–267.

299 Wang H, Hosakote YM, Boor PJ, Yang J, Zhang Y, Yu X *et al.* The alarmin IL-33 exacerbates pulmonary inflammation and immune dysfunction in SARS-CoV-2 infection. *iScience* 2024; **27**: 110117.

300 Russi AE, Ebel ME, Yang Y, Brown MA. Male-specific IL-33 expression regulates sex-dimorphic EAE susceptibility. *Proc Natl Acad Sci U S A* 2018; **115**: E1520–E1529.

301 DeBiasi RL, Harahsheh AS, Srinivasalu H, Krishnan A, Sharron MP, Parikh K *et al.* Multisystem Inflammatory Syndrome of Children: Subphenotypes, Risk Factors, Biomarkers, Cytokine Profiles, and Viral Sequencing. *Journal of Pediatrics* 2021; **237**: 125-135.e18.

302 Patel H, Carter MJ, Jackson H, Powell O, Fish M, Terranova-Barberio M *et al.* Shared neutrophil and T cell dysfunction is accompanied by a distinct interferon signature during severe febrile illnesses in children. *Nature Communications 2024 15:1* 2024; **15**: 1–16.

303 Le Marchand C, Singson JRC, Clark A, Shah D, Wong M, Chavez S *et al.* Multisystem inflammatory syndrome in children (MIS-C) cases by vaccination status in California. *Vaccine* 2025; **43**. doi:10.1016/J.VACCINE.2024.126499.

304 Rybkina K, Bell JN, Bradley MC, Wohlbold T, Scafuro M, Meng W *et al.* SARS-CoV-2 infection and recovery in children: Distinct T cell responses in MIS-C compared to COVID-19. *Journal of Experimental Medicine* 2023; **220**. doi:10.1084/jem.20221518.

305 McArdle AJ, Vito O, Patel H, Seaby EG, Shah P, Wilson C *et al.* Treatment of Multisystem Inflammatory Syndrome in Children. *New England Journal of Medicine* 2021; **385**: 11–22.

306 Yasuhara J, Masuda K, Watanabe K, Shirasu T, Takagi H, Sumitomo N *et al.* Longitudinal Cardiac Outcomes of Multisystem Inflammatory Syndrome in Children: A Systematic Review and Meta-Analysis. *Pediatr Cardiol* 2023; **44**: 892–907.

307 de Melo Oliveira RH, Patil A, Annex BH, Pathak AP, Popel AS. A mechanistic computational model of HGF-VEGF-mediated endothelial cell proliferation and vascular permeability. *iScience* 2025; **28**: 113199.

308 Molnarfi N, Benkhoucha M, Funakoshi H, Nakamura T, Lalive PH. Hepatocyte growth factor: A regulator of inflammation and autoimmunity. Autoimmun. Rev. 2015; **14**: 293–303.

309 Hao W, Liu Q, Li X, Xu Y, Guan W, Zhang L *et al.* CCL23 is a potential biomarker for antineutrophil cytoplasmic antibody–associated vasculitis. *Arthritis Res Ther* 2025; **27**: 83.

310 Ong SWX, Fong SW, Young BE, Chan YH, Lee B, Amrun SN *et al.* Persistent Symptoms and Association With Inflammatory Cytokine Signatures in Recovered Coronavirus Disease 2019 Patients. *Open Forum Infect Dis* 2021; **8**. doi:10.1093/ofid/ofab156.

311 Rao L, Liao J, Guo X, Miu Q, Zheng Y, Xun W. The diagnostic accuracy of CC chemokine ligand 23 for Kawasaki disease. *Front Immunol* 2026; **17**: 1758367.

312 Qu H, Sundberg E, Aulin C, Neog M, Palmblad K, Horne AC *et al.* Immunoprofiling of active and inactive systemic juvenile idiopathic arthritis reveals distinct biomarkers: a single-center study. *Pediatr Rheumatol Online J* 2021; **19**: 173.

313 Heredia M, Charrout M, Klomberg RCW, Aardoom MA, Jongsma MME, Kemos P *et al.* Combined plasma protein and memory T cell profiling discern IBD-patient-immunotypes related to intestinal disease and treatment outcomes. *Mucosal Immunol* 2025; **18**: 76–89.

314 Ricaño-Ponce I, Riza AL, de Nooijer AH, Pirvu A, Dorobantu S, Dragos A *et al.* Characterization of sepsis inflammatory endotypes using circulatory proteins in patients with severe infection: a prospective cohort study. *BMC Infect Dis* 2022; **22**: 778.

315 Matsumiya T, Ota K, Imaizumi T, Yoshida H, Kimura H, Satoh K. Characterization of Synergistic Induction of CX3CL1/Fractalkine by TNF-α and IFN-γ in Vascular Endothelial Cells: An Essential Role for TNF-α in Post-Transcriptional Regulation of CX3CL1. *The Journal of Immunology* 2010; **184**: 4205–4214.

316 Volin M V., Huynh N, Klosowska K, Chong KK, Woods JM. Fractalkine is a novel chemoattractant for rheumatoid arthritis fibroblast-like synoviocyte signaling through MAP kinases and Akt. *Arthritis Rheum* 2007; **56**: 2512–2522.

317 Lv Y, Yang Z, Hai L, Chen X, Wang J, Hu S *et al.* Differential alterations of CXCR3, CXCR5 and CX3CR1 in patients with immune thrombocytopenia. *Cytokine* 2024; **181**: 156684.

318 Postea O, Vasina EM, Cauwenberghs S, Projahn D, Liehn EA, Lievens D *et al.* Contribution of platelet CX3CR1 to platelet-monocyte complex formation and vascular recruitment during hyperlipidemia. *Arterioscler Thromb Vasc Biol* 2012; **32**: 1186–1193.

319 Funken D, Brüggemann A, Mende K, Lerchenberger M, Rentsch M, Khandoga A. Blockage of CX3CL1 Attenuates Platelet and Leukocyte Recruitment in Murine Hepatic I/R. *European Surgical Research* 2022; **63**: 244.

320 Schäfer A, Schulz C, Eigenthaler M, Fraccarollo D, Kobsar A, Gawaz M *et al.* Novel role of the membrane-bound chemokine fractalkine in platelet activation and adhesion. *Blood* 2004; **103**: 407–412.

321 Tian F, Ma L, Zhao R, Ji L, Wang X, Sun W *et al.* Correlation Between Matrix Metalloproteinases With Coronary Artery Lesion Caused by Kawasaki Disease. *Front Pediatr* 2022; **10**: 802217.

322 Senzaki H, Masutani S, Kobayashi J, Kobayashi T, Nakano H, Nagasaka H *et al.* Circulating Matrix Metalloproteinases and Their Inhibitors in Patients with Kawasaki Disease. *Circulation* 2001; **104**: 860–863.

323 Brodeur KE, Liu M, Ibanez D, de Groot MJ, Chen L, Du Y *et al.* Elevation of IL-17 cytokines distinguishes Kawasaki disease from other pediatric inflammatory disorders. *Arthritis Rheumatol* 2023; **76**: 285.

324 Yasin S, Fall N, Brown RA, Henderlight M, Canna SW, Girard-Guyonvarc'h C *et al.* IL-18 as a biomarker linking systemic juvenile idiopathic arthritis and macrophage activation syndrome. *Rheumatology (Oxford)* 2019; **59**: 361.

325 Rosário C, Zandman-Goddard G, Meyron-Holtz EG, D'Cruz DP, Shoenfeld Y. The Hyperferritinemic Syndrome: macrophage activation syndrome, Still's disease, septic shock and catastrophic antiphospholipid syndrome. *BMC Med* 2013; **11**: 185.

326 Eloseily E, Riordan ME, Mahmoud I, Clark A, Chang M, Russell A *et al.* Baseline Clinical Features and Biomarker Profiles of the Childhood Arthritis and Rheumatology Research

Alliance Systemic Juvenile Idiopathic Arthritis- Associated Lung Disease Cohort. *Arthritis Care Res (Hoboken)* 2025. doi:10.1002/ACR.70015;PAGE:STRING:ARTICLE/CHAPTER.

327 Chen G, Deutsch GH, Schulert GS, Zheng H, Jang SR, Trapnell B *et al.* Identification of Distinct Inflammatory Programs and Biomarkers in Systemic Juvenile Idiopathic Arthritis and Related Lung Disease by Serum Proteome Analysis. *Arthritis and Rheumatology* 2022; **74**: 1271–1283.

328 Truong DT, Trachtenberg FL, Hu C, Pearson GD, Friedman K, Sabati AA *et al.* Six-Month Outcomes in the Long-Term Outcomes After the Multisystem Inflammatory Syndrome in Children Study. *JAMA Pediatr* 2025; **179**: 293–301.

329 Khrongsrattha S, Vijarnsorn C, Santimahakullert K, Hongkan W, Petarwut N, Srivichean A *et al.* Midterm cardiovascular outcomes in children with MIS-C compared to Kawasaki disease: a multicenter prospective cohort study. *Scientific Reports 2025 16:1* 2025; **16**: 1199-.

ANNEX

1. Articles derived from this thesis project

- **Pidkova, T.,** Pino-Ramirez, R. M., Urrea, V., Vidal, M., Aguilar, R., Moncunill, G., Antón, J., Clotet, B., Dobaño, C., Fortuny, C., Blanco, J., & Trinité, B. (2025). Tracking the soluble biomarkers of MIS-C and their association with clinical parameters and severity. Pediatric Research 2025. https://doi.org/10.1038/s41390-025-04542-8

2. Publications related to other projects

- Pradenas, E., Marfil, S., Urrea, V., Trigueros, M., **Pidkova, T.,** Pons-Grífols, A., Ortiz, R., Rovirosa, C., Tarrés-Freixas, F., Aguilar-Gurrieri, C., Toledo, R., Chamorro, A., Noguera-Julian, M., Mateu, L., Blanco, I., Grau, E., Massanella, M., Carrillo, J., Clotet, B., ... Blanco, J. (2023). Impact of hybrid immunity booster vaccination and Omicron breakthrough infection on SARS-CoV-2 VOCs cross-neutralization. iScience 2023 26:4, 26(4), 106457. https://doi.org/10.1016/j.isci.2023.106457

- Pradenas, E., Urrea, V., Marfil, S., **Pidkova, T.,** Aguilar-Gurrieri, C., Abancó, F., Mateu, L., Chamorro, A., Grau, E., Trigueros, M., Carrillo, J., Massanella, M., Trinité, B., Clotet, B., & Blanco, J. (2025). Recurrent waning of anti-SARS-CoV-2 neutralizing antibodies despite multiple antigen encounters. Journal of Translational Medicine 2025 23:1, 23(1), 783. https://doi.org/10.1186/s12967-025-06837-0

- Izquierdo-Pujol, J., Pedreño-López, N., **Pidkova, T**., Nevot, M., Urrea, V., Laguía, F., Muñoz-López, F., Dalmau, J., Gonzalez-Aumatell, A., Carreras-Abad, C., Mendez, M., Rodrigo, C., Massanella, M., Blanco, J., Carrillo, J., Trinité, B., Martinez-Picado, J., & Morón-López, S. (2026). Pediatric long COVID is characterized by myeloid CCR6 suppression and immune dysregulation. JCI Insight 2026 11:7, 11(7), e201111. https://doi.org/10.1172/jci.insight.201111

3. Dissemination

Poster presentations

1. Key Inflammatory Biomarkers Differentiate MIS-C from Convalescent COVID-19 and Kawasaki Disease.

o Conference on Retroviruses and Opportunistic Infections 2025 (CROI 2025). San Francisco, California, USA.

2. Differential Inflammatory Signatures Across MIS-C, Kawasaki Disease, and Still Disease

o European Alliance of Associations for Rheumatology Congress 2026 (EULAR 2026). London, United Kingdom.